UNIVERSITÀ DEGLI STUDI DI NAPOLI
"FEDERICO II"
CHEMICAL ENGINEERING DEPARTMENT

# ***Rheological study of interactions between MHEC and superplasticizers in aqueous solutions for applications in cement industry***

Chemical Engineering PhD course

*Tutor*

Prof. Nino Grizzuti (tutor)

*Candidate:*

dott. Fabio Nicodemi

*Scientific committee:*

Dott.ssa Roberta Alfani (CTG-Italcementi Group)

Prof. Giovanni Ianniruberto

# Table of contents

## Acknowledgments

The financial and logistic support of Italcementi Group is gratefully acknowledged.

# *Introduction*

# INTRODUCTION

## 1.1 *The cement and the clinker*

A cement is a binder, a substance that sets and hardens independently, and can bind other materials together. The most important use of cement is the production of mortar and concrete to form strong building materials that are durable to normal environmental effects.

It is uncertain where cement was first discovered, also if there are proofs that Egyptians and Assyrians made many buildings using very fine powders. Almost certainly, concrete made from such mixtures was first used on a large scale by Roman engineers. From that moment, cement and its by-products were extensively used in the realisation of an enormous number of buildings, infrastructures and facilities.

The main component of cement is a product made by heating of some natural materials called *clinker*. The clinker, in combination with other components, gives many kinds of cement. The most common cement is the Portland cement (so called because it has a great similarity with the rock of Portland, an island in Dorset, UK) and its clinker is obtained by heating, in some predefined proportions, lime, silica, alumina, calcium and iron oxides, and in small amount also magnesia, lead oxides, phosphates and alkalis. In particular, lime comes from chalky stones; it has alkaline nature and it is the main component of a Portland clinker because it is present by about 65% of the total. Silica instead comes from shale and clayey sands and it is characterized by an acid chemical nature; it is present by about 25%. The rest of the components comes from other inorganic materials.

The production of clinker begins always with a first milling of raw materials. The so obtained powder, technically called “flour”, is introduced in a rotating oven, composed by a lightly inclined cylinder which is internally coated with a refractory material, and it moves forward against heat flow (produced by combustion of fuels and other). During the advance of the flour, the latter is subjected to a series of chemical transformations which consist essentially in a free-water ejection, followed by a bind-water ejection which occurs at a temperature between 100°C and 750°C. At a higher temperature, the decarbonation of the limestone occurs, followed by a partial fusion of the mixture (*clinkerization*) which is responsible for the formation of calcium silicates. When the mix begin to get colder (at about 1350°C) a partial crystallization is visible with the formation of

calcium aluminates. The material is then cooled and further milled to obtain particles with size less than 100 μm.

From the clinker of Portland cement is then possible to obtain other cements. Cement kinds regulated by the normative systems are for example:

- **Sulfoaluminate cement**: obtained by mixing calcium sulfoaluminate clinker with calcium sulphate and Portland cement;
- **Portland blast furnace cement**: it contains up to 70% ground granulated blast furnace slag, Portland clinker and chalk. All compositions produce high ultimate strength, but as slag content is increased, early strength is reduced, while sulphate resistance increases and heat evolution diminishes. Used as an economic alternative to Portland sulphate-resisting and low-heat cements;
- **Portland pozzolan cement:** it includes fly ash cement, since fly ash is a pozzolan, but also includes cements made from other natural or artificial pozzolans. In the countries where volcanic ashes are available (e.g. Italy, Chile, Mexico, the Philippines) these cements are often the most common form in use;
- **Portland fly ash cement**: it contains up to 30% fly ash. The fly ash is pozzolanic, so that ultimate strength is maintained. Because fly ash addition allows a lower concrete water content, early strength can also be maintained. Where good quality cheap fly ash is available, this can be an economic alternative to ordinary Portland cement;
- **Portland silica fume cement**: obtained with addition of silica fume which can yield exceptionally high strengths. Cements containing 5-20% silica fume are occasionally produced;
- **Masonry cements:** they are used for preparing bricklaying mortars and stuccos, and must not be used in concrete. They are usually complex proprietary formulations containing Portland clinker and a number of other ingredients that may include limestone, hydrated lime, retarders, waterproofers and colouring agents. They are formulated to yield workable mortars that allow rapid and consistent masonry work;
- **White blended cements:** may be made using white clinker and white supplementary materials such as high-purity metakaolin.

In addition to these kinds of cements there are also some other cements which are not obtained from Portland cement.

The main mineralogical constituents of a Portland cement are essentially four: tricalcium silicate ($C_3S$), bicalcium silicate ($C_2S$), tricalcium aluminate ($C_3A$) and tetracalcium alumino-ferrite ($C_4AF$). These constituents never exist in the pure form; for example, $C_3S$ is essentially a solid solution containing Mg and Al called *"Alite"*. The $C_2S$ instead contains elements like Al, Mg and potassium oxides and it is called *"Belite"*, while the ferric phase is a solid solution of variable composition made up of $C_2F$, $C_6A_2F$ and other iron-based compounds, generally indicated as $C_4AF$. A rough illustration of cement composition is reported in the figure 1.1.

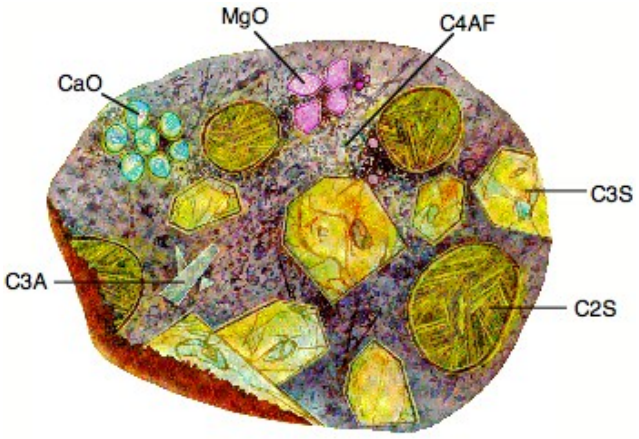


*Figure 1.1: Main cement compounds*

It is important to note that in the cement chemistry symbols have different meaning from classical chemistry: *C* is for CaO, *S* is $SiO_2$ *A* is $Al_2O_3$ and *F* is for $Fe_2O_3$.

The $C_3S$ is probably the most important constituent because reacting with water it gives high mechanical resistance; for this reason, generally high concentrations of $C_3S$ are preferred in the cement fabrication. An high dosage of lime is so used but it is not enough to have high $C_3S$ content in the cement. A rapid formation of this compound is obtained by keeping the temperature between 1350-1500°C, when the liquid phase is present in the oven. $C_3S$ is stable only above a temperature of 1250°C and for this reason, after cooking, a quench is required.

The $C_2S$ is present in the clinker with the β crystalline form. It can hydrate in a long time, so the development of mechanical resistance due to this material is visible after very long maturing times.

The $C_3A$ is the compound with the highest hydration velocity but it does not contribute to the development of the mechanical resistance. From this point of view, it should be preferred to avoid the presence of this compound in the clinker, but practically it is very useful to keep a low melting temperature thus reducing the energetic cost.

As described above, the formula $C_4AF$ normally indicates a ternary solid solution which is able to give a modest contribution to the mechanical resistance after hydration, especially after 15 days annealing. As the $C_3A$, $C_4AF$ has also an important rule on the melting temperature drop.

In addition to the main compounds, some other impurities can be found in the clinker. One of these is certainly the magnesium oxide (MgO), which must be present in a maximum amount of 2-2.5% due to its expansive behaviour.

Other impurities are alkaline oxides, phosphates and fluorides which can also contribute to keep low melting point[1].

## 1.2 *The most common uses of the cement*

Cement mixed with water is virtually a plastic stone, and it can be used for many purposes in place of stone with economy in shaping to the form required, and advantage in securing a hard, fire-proof material. It may be used for shop floors, buildings, foundations for heavy machinery, bridge piers, walks, waterworks dams, reservoirs, walls, dry-docks, culverts, etc. A concrete casing will protect iron or timber structures from corrosion in air or in water, and will protect exposed iron work of structures from effects of conflagration. *Concrete* is a composite construction material, composed of cement (commonly Portland cement) and other cementitious materials such as fly ash and slag cement, aggregates (generally a coarse aggregate made of gravels or crushed rocks such as limestone, or granite, plus a fine aggregate such as sand), water, and chemical admixtures.
The word concrete comes from the Latin word "concretus" (meaning compact or condensed); it was in fact extensively used by Roman engineers, who used a mix of quicklime, pozzolana and an aggregate of pumice.

Strengthened with iron bars, or meshed wire, placed in it when it is being moulded to shape, cement is known as *reinforced concrete*, and will thus form bridge floors, bridge spans, and the upper floors of buildings which must support great weight. In fact, typical concrete mixes have high resistance to compressive stresses (about 4,000 psi (28MPa)). However, any appreciable tension (*e.g.,* due to bending) will break the microscopic rigid lattice, resulting in cracking and separation of the concrete. For this reason, typical non-reinforced concrete must be well supported to prevent the development of tension. If a material with high strength in tension, such as steel, is placed in concrete, then the composite material resists to both compression and bending and other direct tensile actions. A reinforced concrete section where the concrete resists the compression and steel resists the tension can be made into almost any shape and size for the construction industry.
In marine use, concrete is limited because of its weight. It may be used as permanent ballast in the bilges of steel ships, and is an effective protection from corrosion when applied to absolutely clean iron or to iron surfaces covered with closely adhering red rust. When so used, cement may be mixed with water and applied with a brush, or it may be mixed in the proportion of about two parts sand and one part cement and applied wet, with a trowel, in a layer varying from 1/4 inch to any desired thickness. In this way ship tanks, bunkers, and bilges are protected, as the mixture forms a close bond with iron. In no case will this bond form if the iron is oil coated[2,3].

## 1.3 *The hydration of cement*

The most important mineralogical constituents of a cement are certainly the silicates, which are directly responsible for the mechanical properties of hardened cement.

The hydration reaction for $C_3S$ is:

$$C_3S + H_x \rightarrow C_y \cdot S \cdot H_{(x+y-3)} + CH_{(3-y)} \quad (1.1)$$

where *H* is for $H_2O$. The stoichiometry of this reaction is approximate because the coefficients depend on the temperature and the presence of additives and they change during the reaction. In the same way the reaction for hydration of $C_2S$ is the following:

$$2\,C_2S + H_5 \;\rightarrow\; C_3 \cdot S_2 \cdot H_4 + CH \qquad (1.2)$$

Also for the reaction 1.2 the stoichiometry is not very strict but depends on several factors. As visible, the hydration reaction of $C_2S$ is different from the reaction of $C_3S$ especially for the minor content of calcium hydroxide produced after hydration.

The $C_3A$, although present in the clinker in a very small amount, strongly influences the hydration kinetics of the other compounds, as it suddenly reacts with water to give:

$$2\,C_3A + 21\,H \;\rightarrow\; C_4AH_{13} + C_2\,AH_8 \qquad (1.3)$$

These phases are so thermodynamically unstable that they suddenly transform in other compounds as shown in the reaction 1.4:

$$C_4AH_{13} + C_2AH_8 \;\rightarrow\; 2\,C_3AH_6 + 9\,H \qquad (1.4)$$

The fast hydration of $C_3A$ is generally not very convenient in the production of mortars and concrete, because it increases the temperature of the mix too fast and it greatly accelerates the hydration of the other phases, giving a material which hardens and loses workability too rapidly.

For this reason, generally a certain amount of chalk is added to the clinker to give the reaction 1.5:

$$2\,C_3A + 3(CaSO_4 \cdot 2H) + 26\,H \;\rightarrow\; C_3A \cdot 3CaSO_4 \cdot H_{32} \qquad (1.5)$$

The formation of the quaternary salt (called *ettringite*) is responsible for the reaction time prolongation.

The hydration of $C_4AF$, present in the clinker with an amount of about 8-13%, was always not very studied just because it is assumed as very similar to the hydration process of $C_3A$. The main difference from this latter is in the reaction rate which is certainly slower and becomes even slower with the addition of chalk.

After mixing with water, the fine powder of cement becomes a plastic dough where the calcium hydroxide generally represents the 18-25% of the total. The rest of the material is essentially composed of variable percentages of other materials such as the hydrated phase CSH (characterized by needle-like crystals) and the ettringitic phases (also called Aft phase, to indicate that they are composed of aluminium and ferric compounds). The monosulphate is formed after the disappearance of the ettringitic phases; it normally constitutes the 10% of the solid mass and it is characterized by hexagonal crystals of submicron size.

The hydration reactions are accompanied by a considerable heat production; the representation of the heat production vs. time in figure 1.2 gives an idea of the kinetic of cement hydration.

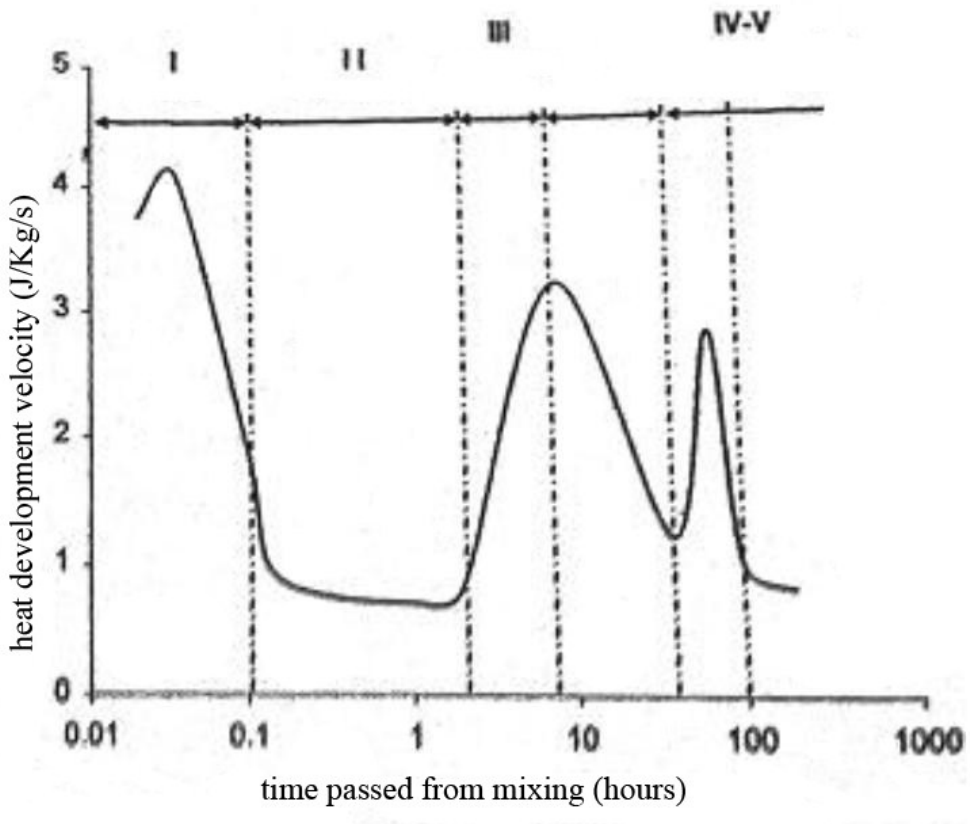


*Figure 1.2: Hydration kinetic of cement phases*

The first stage is characterised by a heat production due to the hydration of $C_3A$ which causes the formation of ettringitic phases that cover the anhydrous $C_3A$ preventing its hydration. This results in a sharp decrease of the reaction rate which is in turn responsible of a heat production decrease. This phenomenon is then followed by a so-called "dormant period", where the ettringitic phases thickening almost completely stops the hydration of anhydrous compounds. This stage can last few hours, then a third period occurs which is characterised by a strong heat development. This is essentially due to two phenomena: one is the break of ettringite film and continuation of aluminates hydration, the other is the conversion of the CSH in hydrated phase which becomes more permeable to the ionic species in solution. This phase coincides with the so-called "initial setting time" and with the subsequent loss of plasticity. Then the setting process continue for some hours and it concludes with the so-called "final setting time" which coincides with the beginning of the hardening process.

The third peak in the graph is finally due to the transformation of the ettringitic phase in monosolfoaluminate.

## 1.4 *Modified cement and the water/cement ratio*

The technological content of the cement and of its derivatives has been considerably increased in the last century because of the growing interest for these materials and for their incredible potential development. This interest have led to a large number of studies having the purpose to increase the performances and quality especially of concrete and mortars.

The production of *"High Performance Concrete"* (HPC) is now a current practice in nations like Japan, France, Norway and others. The HPC is characterised by a compression resistance in the range of 60-100 $N/mm^2$ thanks to:

1. a minor water/cement ratio (0.40-0.30) due to the use of additives;
2. addition of minerals with elevated surface area;
3. high-quality chipping aggregates (granite, basalt, etc.…).

Recently, a further evolution of these materials has led to the so-called *"Reactive Powder Concrete"* (RPC) with incredibly high performance (very elevated with respect to the HPC), generally obtained with the employment of polymeric fibres. The RPC are still in the project stage and so they are not already extensively used, but some applications have been already proposed, such as the achievement of tunnels or building in areas where can be very much stressed (i.e. seismic areas).

On the other side of the HPC and RPC, which together are classified as DSP (*Densified with Small Particles*), there is another class of high performance cement-based materials; they are classified as MDF (*Macro Defect Free*) and are different from DSP because the increase of performance is generally reached by adding some particular additives. They are generally some water-soluble polymers which modify the water/cement ratio and the mix rheology allowing to use some peculiar manufacturing processes such as calendering or extrusion.

One of the most common solutions to increase the compression resistance ($R_c$) is to reduce the capillary porosity of the cement ($V_p$). To achieve this target, two parameters can be modified:

- the cement hydration rate $\alpha$;
- the water/cement ratio $a/c$.

The theory developed by Powell[4] allows to correlate these two parameters with $R_c$ and $V_p$. This theory, validated by a great number of experimental evidences, is based on the equations 1.6 and 1.7.

$$V_P = 100\ a/c - 36.15\ \alpha \tag{1.6}$$

$$R_c = K\ [\frac{0.679\ \alpha}{0.3175\alpha + a/c}]^n \tag{1.7}$$

It is easily deducible from equations that an increase of $\alpha$ and a decrease of $a/c$ leads to a reduction of porosity $V_p$ and so finally to an increase of $R_c$. To modify $\alpha$ and the ratio $a/c$, the addition of some particular additives is necessary.

## 1.5 *The additives of the cement*

As seen in the previous section, in recent years the composition of cement formulations have radically changed and this is essentially due to the introduction of a large variety of additives.

Today, in the cement field there are practically additives for every use:

- **water reducers**: they increase the workability of the cement formulations allowing a partial water reduction;
- **setting accelerators**: substances able to change the initial and final setting time;
- **setting retardants**: they delay the initial reaction between water and cement compounds;
- **hardening accelerators:** they improve the hydration rate of the concrete to favour a faster development of compression resistance;
- **aerants**: chemicals able to increase the air content in the formulation improving the workability and reducing the freezing effect on the concrete;
- **water proofers**; they provide resistance to water;
- **water retention additives**: they prevent a rapid evaporation of the water in the mix;
- **rheology modifiers**: able to modify the flow properties of the slurry.

These additives are generally chemicals of organic nature (commonly used in liquid form) added to the cement mix in a variable percentage between 0.1% and 3%, producing a relevant effect on the features of the formulation, both in fresh stage and after hardening.

Each additive usually also presents some secondary effects (sometimes also slightly negative) on the slurry. For example, some water reducers are also able to delay the initial reaction between water and cement compounds, practically acting also like a setting retardant.

The use of these substances is so common that about 80% of concrete is generally made using additives. Only in Italy, their consumption is estimated to be about 250000 ton/year and expected to increase in the next years.

The world of additives is so wide that there are dedicated books just for this subject; here we will analyse in particular two categories of additives: the rheology modifiers and the fluidificants.

## 1.6 *The rheology modifiers*

Rheology modifiers (RMs) are a class of chemical substances extensively employed in many fields, from food to cosmetics, in the realisation of some inks, paints and also explosives and many other chemical products. They are generally substances that, when added to an aqueous mixture, increase its viscosity without substantially modifying its other properties. They provide body, increase stability, and improve suspension of added ingredients. Thickening agents are often used as food additives and in personal hygiene products. Some thickening agents are gelling agents, forming a gel. The agents are materials used to thicken and stabilize liquid solutions, emulsions, and suspensions. RMs dissolve in the liquid phase as a colloid mixture that forms a weakly cohesive internal structure.

In the cement field, RMs are more correctly called "water retention and rheology modifier" (WRRM), because their very hydrophilic structure allows for an high hydration of molecules. This effect is of primary importance when WRRMs are added to the cement, because they control the hydration process of cement constituents. This is the reason why the WRRMs, even if they are present in small amounts, significantly influence the rheological properties of the solutions.

It is possible to find commercial WRRMs with molecular weight on between 10000 and more than $10^6$ Dalton and of different kind. Consequently, the properties of the solution can be tuned by several parameters such as concentration, molecular weight, degree of substitutions and so on[5,6].

Most commercial WRRMs are cellulose derivates obtained by alchilation and alcossilation of the cellulose chain. One of the principal cellulose derivatives used in cement industry is methylhydroxyiethylcellulose (MHEC).

The cellulose is a linear homopolymeric polysaccharide, made up of glucose with β-1.4 bonds (figure 1.3).

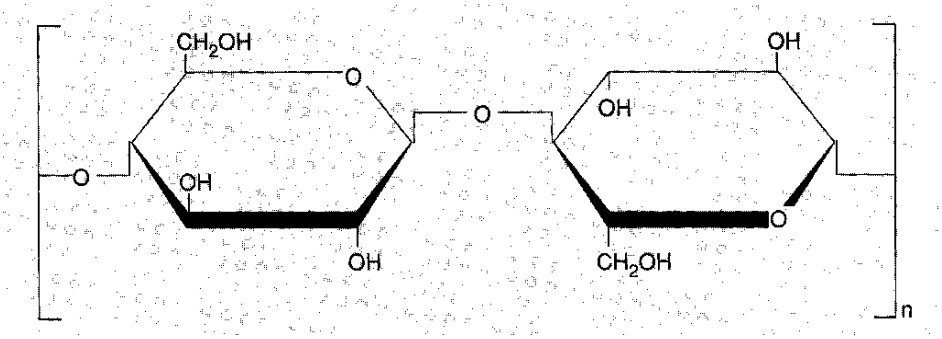


*Figure 1.3: Molecular structure of cellulose*

As strong intermolecular interactions due to H-bonds are established, the pure cellulose is insoluble in water. The substitution of functional groups –OH by C2, C3 and C4 of monomeric unit make the cellulose soluble in water. These substitutions can be operated by etherification. The most frequent substitutions are made with ($OCH_3$), hydroxypropylic (POOH) and hydroxyethylic groups (EOOH). MHEC is obtained through etossilation and metilation of cellulose (figure 1.4).

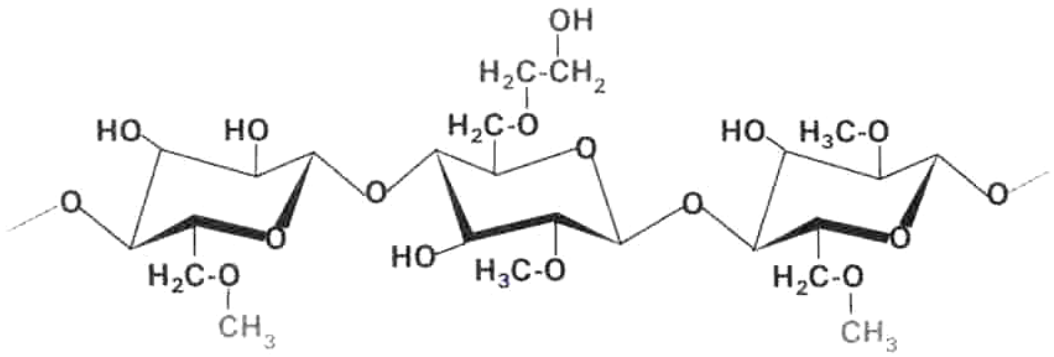


*Figure 1.4: Molecular structure of MHEC*

## 1.7 *The fluidificants*

In modern cement technology, water reducer additives have greatly contributed to the improvement of high performance concretes. These polymeric compounds confer high flowability to concrete pastes, keeping low the water content, improving the workability, and ensuring high mechanical strength, shrinkage, and durability of the hardened material[7]. The relevant effects obtained on the cement mixtures with these additives are partially shown in the figures 1.5.

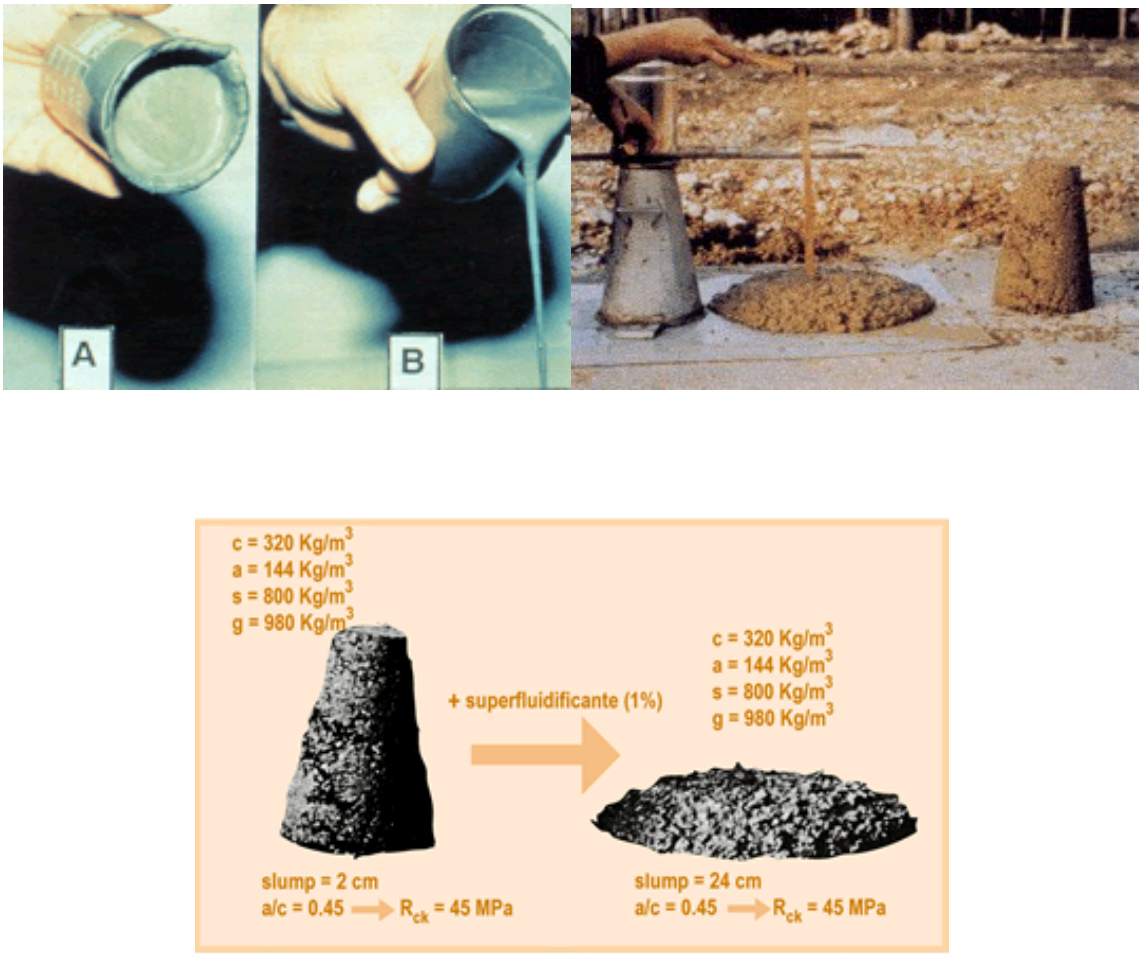


*Figures 1.5: Differences in the rheological behaviour of some mixtures without (A) and with fluidificants (B)*

Before the introduction of these additives, paste workability during mixing and casting processes was gained using a high water excess but at the end of the hydration process of cement, the unreacted water remained trapped inside the cement matrix and, as it evaporated, an undesired increase of porosity was developed thus compromising the composite performances, such as mechanical strength and resistance to external agents. With water reducers, pastes can be produced with a limited amount of water to perform the hydration reaction. As a result, the structure of the composite is more compact and presents higher durability and resistance.

Water reducer additives are distinguished in three categories: fluidificants (P), superfluidificants (SP) and iperfluidificants (IP). They substantially differ for the efficacy in water reduction but the action mechanism is the same: they adsorb on cement grains creating a sort of barrier around them (figures 1.6, 1.7).

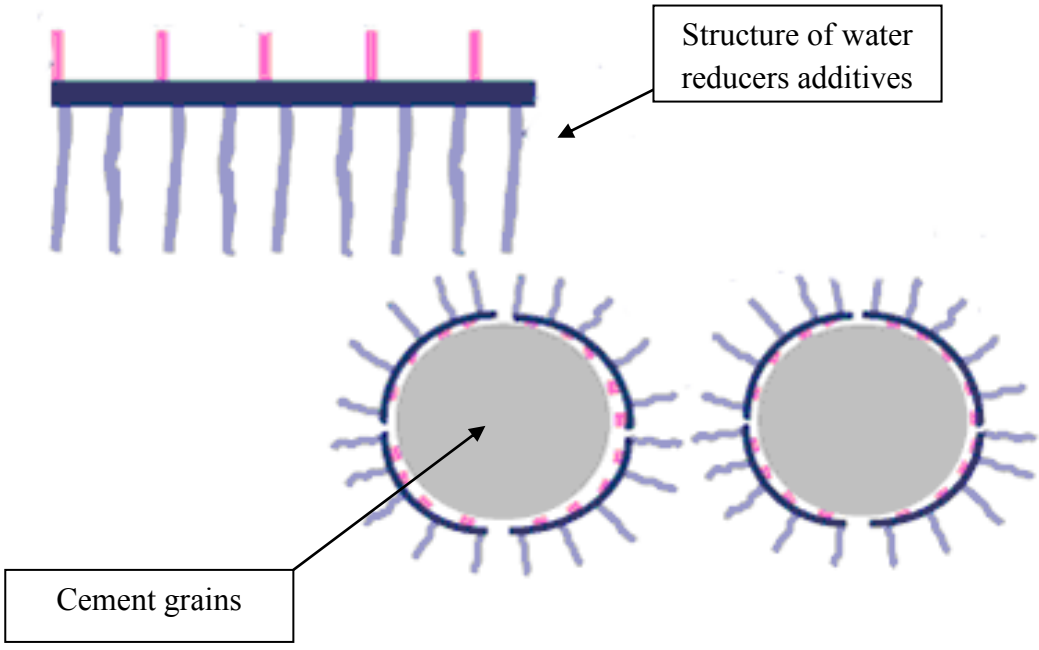


*Figure 1.6: Mechanism of hindrance of the SPs*

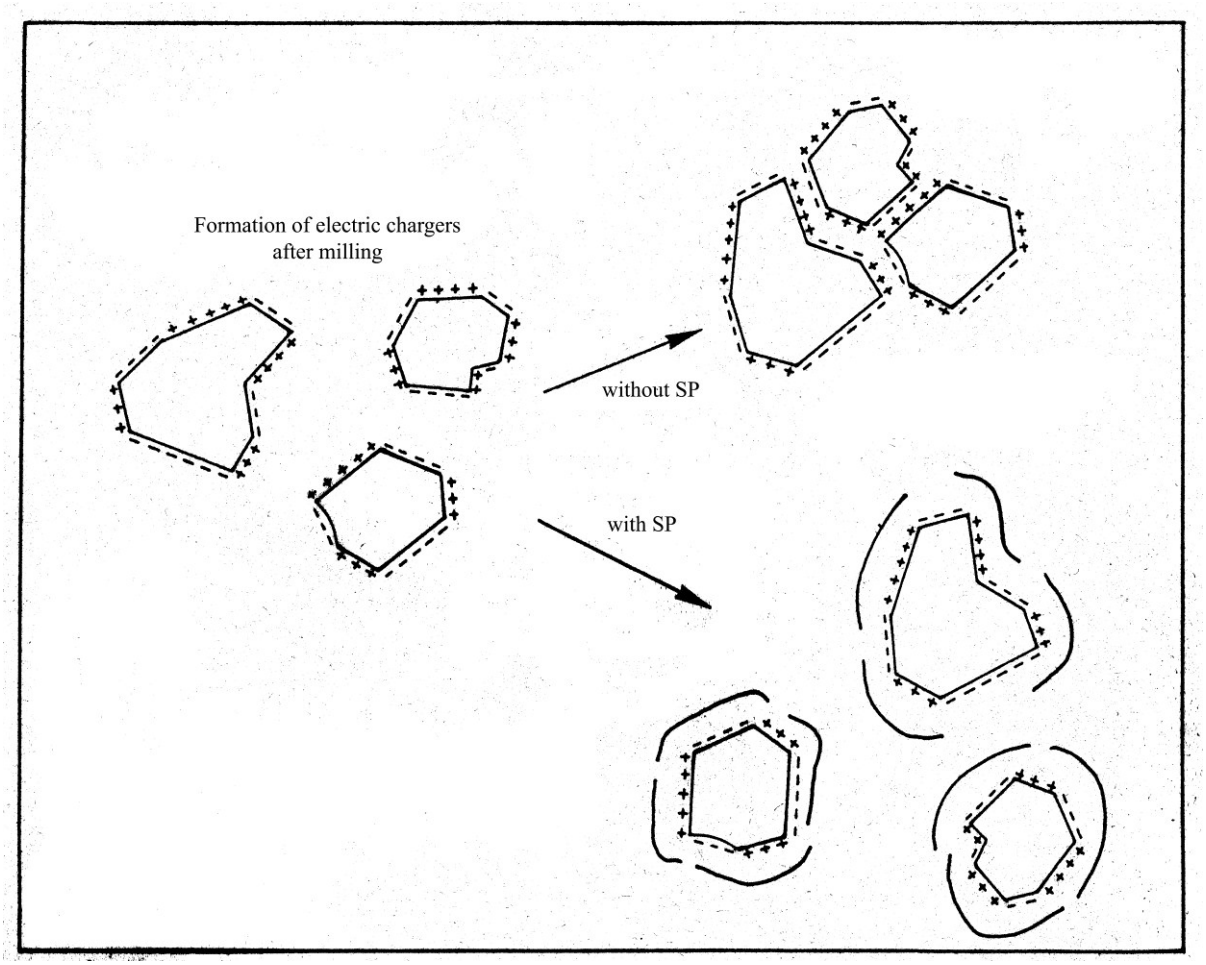


*Figure 1.7:Difference between system with and without SP*

In fact, during milling opposite sign charges are formed on the cement grain surface and due to attraction forces the grains tend to stay together.

Some water reducers have also negatively charged groups which stretch out of the particle surface and provide electric hindrance to grain surfaces. Some experiments have confirmed that the influence of steric hindrance is higher than the influence of electric hindrance[8].

There are several types of water reducers: the main ones are CAE (an acrylic ester copolymer), SPS (polystyrene sulphonate), SMF (melamminesulphonate), G (gluconate), SNF (naphthalene sulphonate), LSG (ligninsulphonate), PG (glucosidal polymer). They are enumerated in figure 1.8.

One of the most important parameter linked to the use of the fluidificants is the dosage. These additives are between the most expensive components of a slurry, so finding a good compromise between cost and efficiency is of fundamental importance. Furthermore, an excessive amount of fluidificants in a mixture can alter the mechanical properties of cement and lead to a negative result.

The dosage varies mainly according to the kind of fluidificant used for the specific application. While for an iperfluidificant the average dosage is between 1.5-2.5% wt., it is certainly lower for a superfluidificant (0.8-1.4%) and for a simple fluidificant (0.2-0.7%).

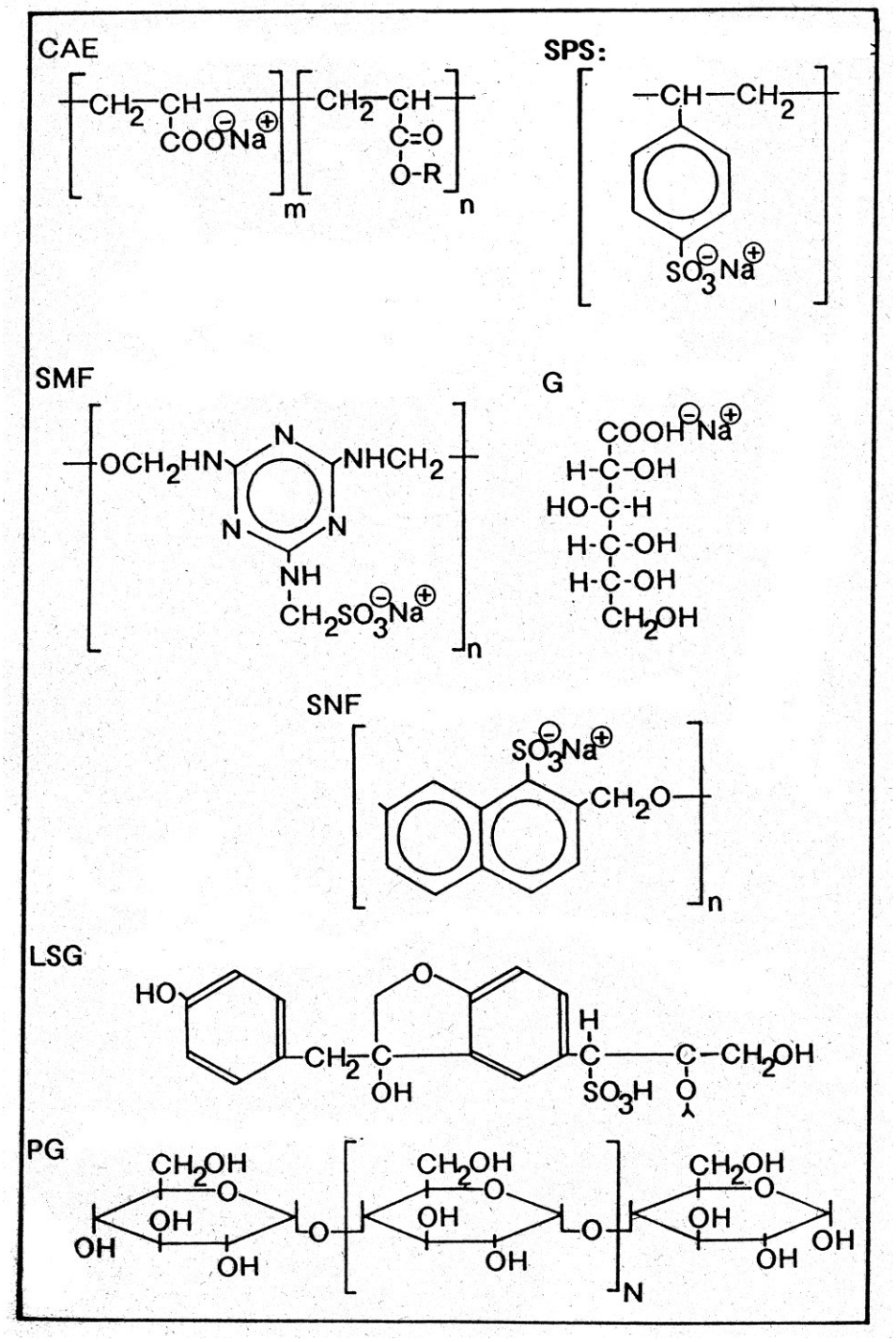


*Figure 1.8: Main fluidificant categories*

There is no optimal dosage for all applications and all conditions. Dosage is generally identified in an empirical way, trying to reproduce the operative conditions of the system as better as possible. This can be achieved by studying the performance curves obtained for several periods of time. In figures 1.9 and 1.10, the 1-day and the 28-day resistances are respectively shown.

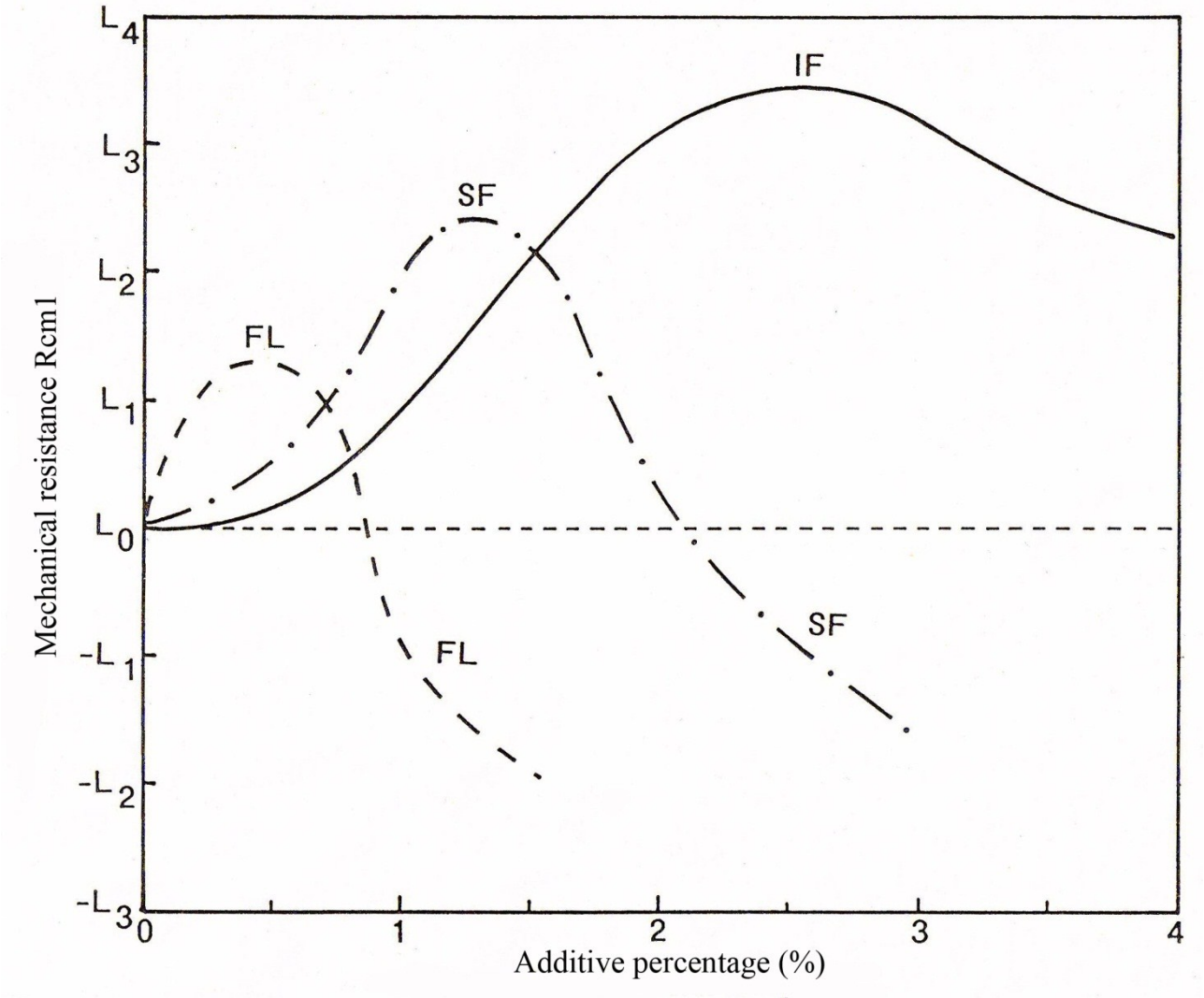


*Figure 1.9: Mechanical resistance of a standard concrete after 1 day as a function of the percentage for different fluidificants*

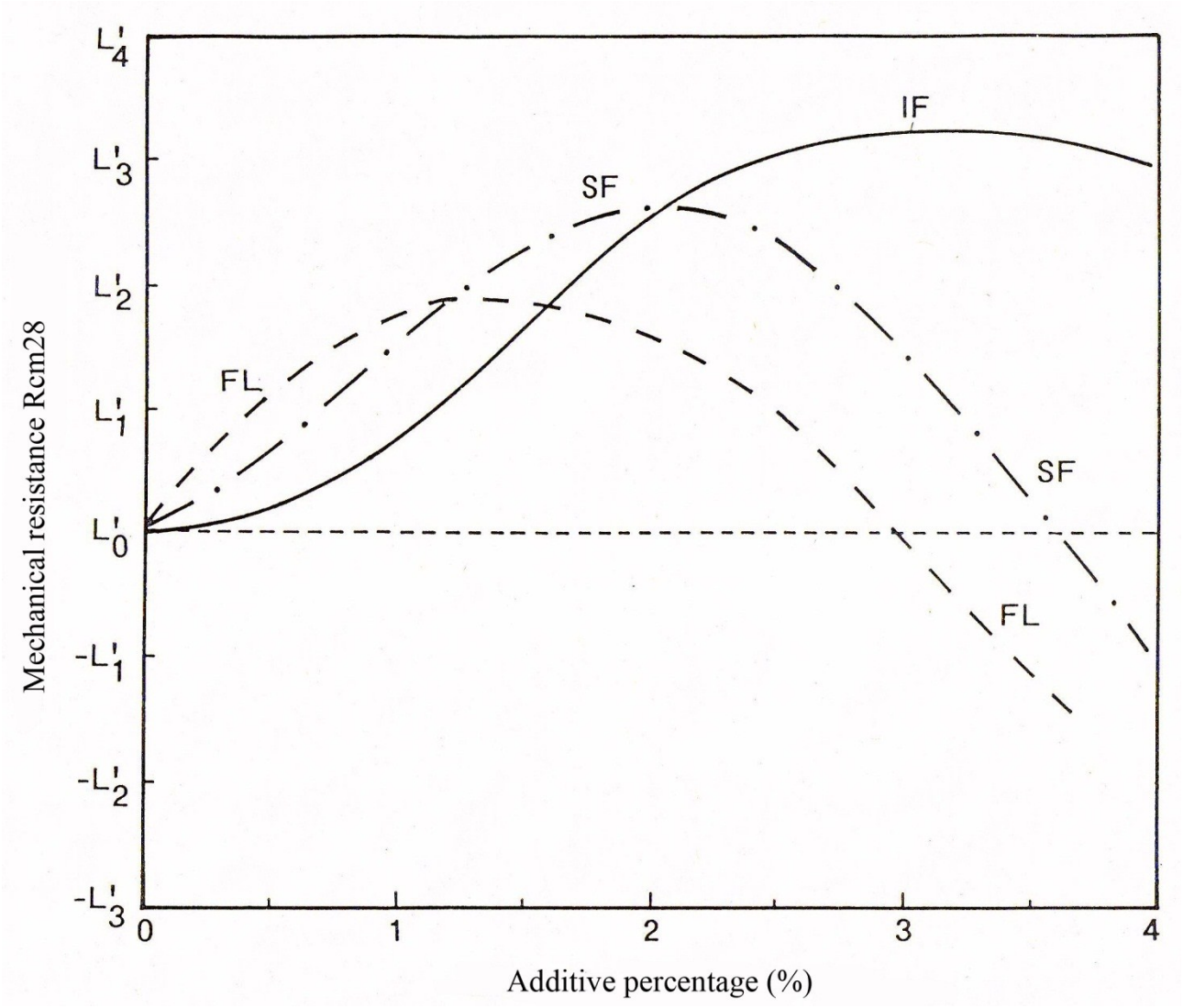


*Figure 1.10: Mechanical resistance of a standard concrete after 28 days as a function of percentage for different fluidificants*

The predominance of the stabilization mechanism (electrostatic repulsion vs. the steric repulsion) depends on either the chemical nature or the molecular weight of the additive; for example, in the polymers of ligninsulphonate, naphthalene sulphonate and melamine the prevailing effect is the electrostatic repulsion for the presence of negatively charged groups in the chain, while in the acrylic fluidificants the main effect is due to the long lateral chains that create steric hindrance.

Beyond the dispersing effect, all the polymers used to produce fluidificant additives inhibit the nucleation and growing of the hydration products. They basically are incorporated in the compounds that forms during the first minutes after hydration (prevalently aluminic phases) and

they reduce the creation of bonds between hydrated cement particles. This results in a prolonged workability time. On the other hand, some fluidificants lead to the formation of some instable organic-mineral phases which are more permeable to water thus shortening the dormant period, decreasing the initial setting time.

In summary, the effect of fluidificant addition is very complex. Even a small change in the composition of cement can lead to a large change of slurry properties in presence of these additives. For this reason and also because water reducers cover about 90% of the additives market, numerous studies are centred on the chemical and rheological behaviour of cement mixture in presence of these substances.

## 1.8 *A new application for cement with additives: the extrusion process*

The employment of additives in the cement field has given the possibility to use cement and its mixtures for some particular applications, like extrusion process. The use of extrudable cement-based pastes is an important subject in the modern concrete industry. The process of extrusion is one of most used processing employed in plastics, metals and clay industry. It consists essentially in forcing the material, in the melt state, through a die that reproduces the form of the desired manufact. Generally the compression of the material is made with a rotating endless screw in rotation; the screw can be also thermally controlled, either to heat and melt the material or to cool it when the friction developed by the process produces overheating effects. The points of strength of this technique are:

- high velocity of production;
- low costs;
- high reproducibility of manufactured parts.

In the case of cement pastes one important issue is related to the fact that these formulations do not have rheological properties suitable for extrusion. For this reason the material must be necessarily additivated with appropriate rheology modifiers. The price paid for this formulation effort is compensated by the possibility to use the economically convenient and fast extrusion process as a substitute for more time consuming and more expensive processes. The cement, in fact, unlike other ceramic materials, has the great advantage of hardening by simple hydration, without requiring cooking at high temperature. Furthermore, extruded cement manufacts possess improved mechanical properties due to the introduction of synthetic fibres in the formulation[9,10]. Fibres can be also obtained by recycle of plastic materials, with obvious positive consequences. This kind of product satisfies the need of a low environmental impact (low energy consumption) and high recyclability, factors that are more and more important in the choice of structural materials for massive production. Some examples of the obtainable manufacts are given in figure 1.11.

*Figure 1.11: Example of cement extruded products (Ultrapanel process)*

A necessary condition to obtain pastes for extrusion is the use of one or more chemicals able to work as adhesives for the powders, possibly under elevated strengths, such as those reached during the extrusion process. The products that have demonstrated more efficiency from this point of view

are certainly the cellulose derivates. These substances can have different viscosity, kind and rate of substitution, water retention, etc. To characterize extruded pastes it is necessary to develop methods of analysis different from those used for conventional cement. In determining the best formulations to use in industrial extrusion, particular attention must be paid to rheology.

## 1.9 *Cement-based paints for coating*

Another interesting application for cement formulations with controlled rheology is that of cement paints for coating. Cement-based paints are an innovative product under development by CTG-Italcementi Group of Bergamo. The importance of these formulations is based on the property of some cements to resist to the attack of very aggressive chemical agents like those normally used in some industrial pipelines. Obviously, to make a whole pipe in cement requires too high costs, certainly more expensive than making the same pipe, for example, in plastic or metal. For this reason it is more convenient to coat pipes made of cheaper materials with cement paints. In figures 1.12 some examples of coated pipes are shown.

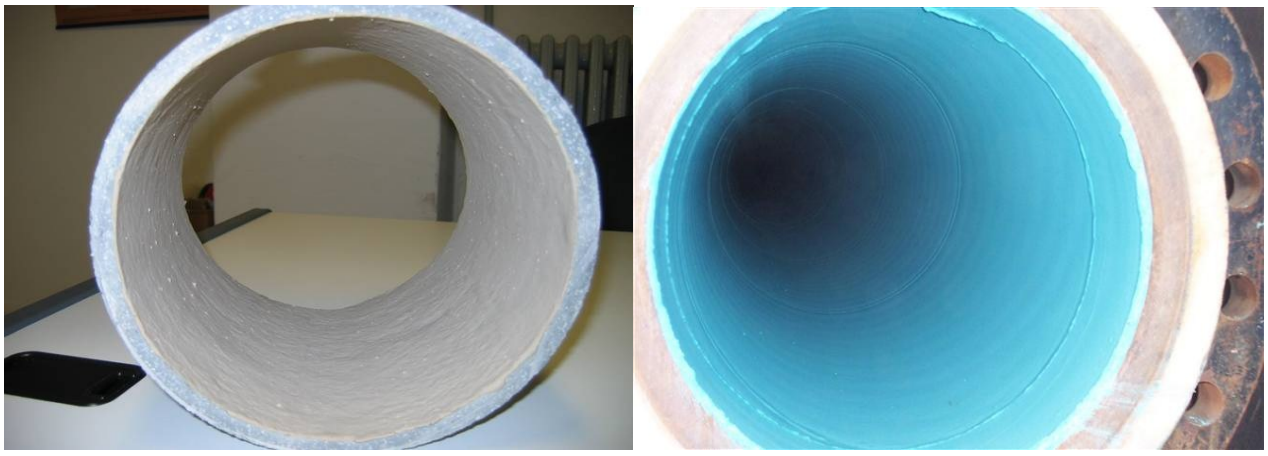

*Figure 1.12: Examples of coated pipes*

The control of the rheology of these systems is of primary importance, as it is also for all commercial paints. Paints, in general, must respect some specific rheological requirements. Figure 1.13 shows the typical viscous behaviour of the commercial paint used to compare the rheological behaviour of our system (in this case "litosil" from Boero).

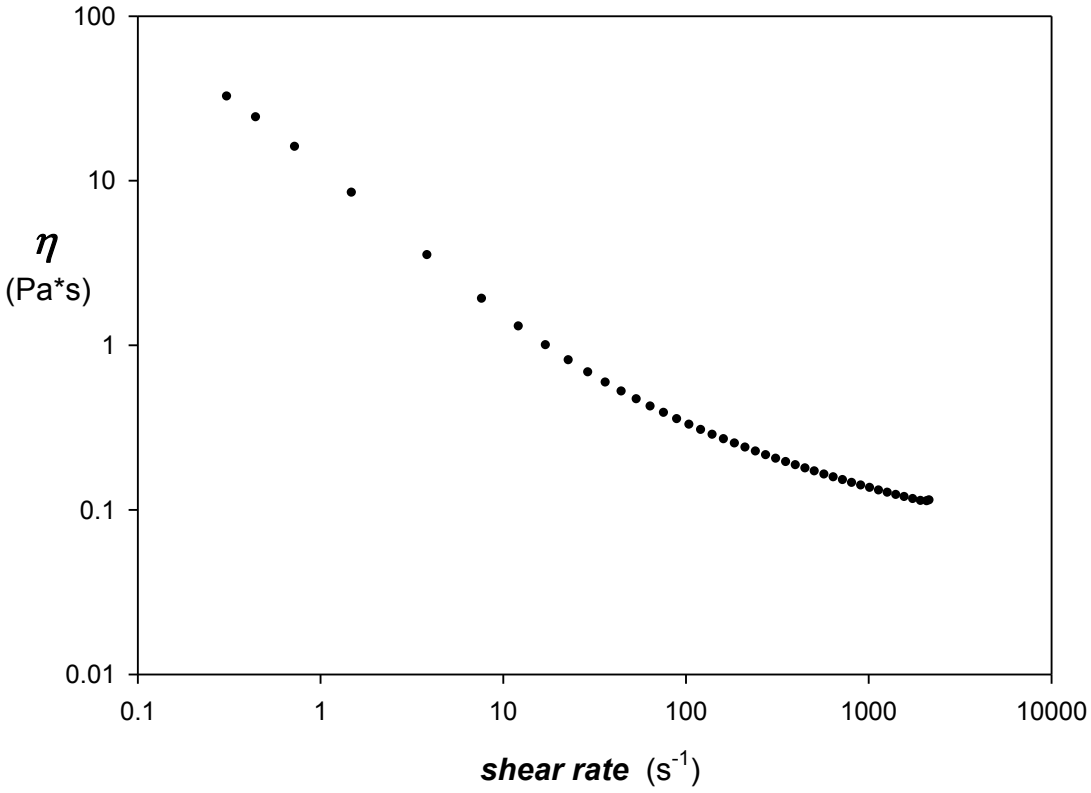


*Figure 1.13: Viscous behaviour of a commercial paint*

The low shear rate region corresponds to the absence of external stresses, that is when the paint is just applied or when it remains steady in the bin. If the formulation is not correct in this zone of shear rates it is possible to see three different negative phenomena:

- sagging: the liquid paint applied on a wall tends to drip, originating blemishes, variations of depth, etc. To avoid or at least to limit this problem the paint must show a high viscosity. The rheology in this region approaches that of a Bingham fluid where, under a typical value of yield stress, no flow is present.

- settling (sedimentation): in steady paints combined phenomena of coagulation, aggregation and sedimentation of the solid phase are possible. The paint regains its original fluidity only after a vigorous mixing. Settling is an undesired phenomenon for which sufficiently high viscosity is required.

- levelling: it is the phenomenon that allows to the layer of paint to take on a thickness as uniform as possible; the driving force for the flow is given by surface tension, which tends to minimize the paint surface, while the resisting force is obviously the viscous friction. To obtain a good levelling it is necessary to find a "rheological compromise" by an appropriate tuning of the formulation.

The intermediate shear rate zone usually corresponds to those of the production process of paints; during this phase a low viscosity is certainly to be preferred. This involves the necessity to formulate a paint characterized by shear thinning behaviour.

The shear thinning behaviour must continue also in the high shear rate zone because this zone corresponds to the typical regime of paint application. In these conditions a low viscosity is to prefer because it allows for a simpler application or the utilization of low pump pressures.[11-12]

The rheological behaviour of the paints is an important parameter to control also when a special application technique is required. For instance, if a blow application is very convenient in a particularly context for a paint, its rheology can be modified accordingly. In particular, the viscosity at high shear rates must be very low but the paint must not drip suddenly after application, when the only active force on paint is the weight force, and so the viscosity must rapidly increase.

## 1.10 *Rheology and its importance*

In the two applications above described the importance to study the flow properties of the mixtures clearly emerges.

The *rheology* is the branch of Physics that studies the flow and deformation of a body that is subjected to the action of external forces. The word "rheology" comes from the Greek verb *ρεω*, which means "to flow, to stream". Rheology is a relatively new science. The foundation of The

Rheology Society dates back to April 29 1929, when some important scientists such as Bingham, Prandtl and Ostwald met in Columbus (Ohio).

One of the most important concept of the rheology is certainly that of *viscosity*; from an intuitive point of view viscosity represents the resistance of a body to flow. Quantitatively, it can be defined as the measure of flow capability of a fluid under the influence of shear stresses. The higher the fluid viscosity (with the same applied force), the lower the shear rate of the fluid. Otherwise, with the same shear rate, a fluid with a higher viscosity needs a higher shear stress to flow at the same rate.

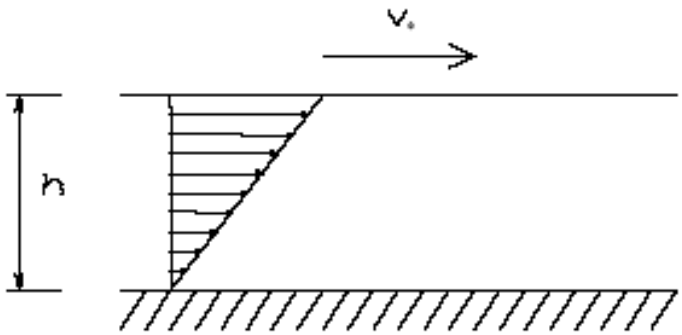


*Figure 1.14: Ideal experiment with two parallel plates*

Figure 1.14 represents the classical ideal parallel plates experiment. A tangential force F which is able to move the plate To is applied to the upper plate with area A. In stationary conditions, a triangular profile is established in the fluid, with a maximum velocity $v_0$ at the upper plate. In this case, the stress is given by:

$$\sigma = \frac{F}{A} \tag{1.8}$$

The shear rate is given by:

$$\dot{\gamma} = \frac{dv}{dy} = \frac{v_0}{h} \tag{1.9}$$

The viscosity is then defined as the ratio between the shear stress and the shear rate:

$$\eta = \frac{\sigma}{\dot{\gamma}} \tag{1.10}$$

The viscosity has dimensions of a force on a surface multiplied by a time. In the International System the unit of measurement of the viscosity is:

$$[\eta] = \left[\frac{Kg\frac{m}{s^2}}{m^2}\, s\right] = \left[\frac{N}{m^2}\, s\right] = [Pa\, s] \tag{1.11}$$

In the CGS system instead the unit of measurement of the viscosity is the *poise*:

$$[\eta] = \left[\frac{g\frac{cm}{s^2}}{cm^2}\, s\right] = \left[\frac{erg}{cm^2}\, s\right] = [P] \tag{1.12}$$

The unit Pa·s is numerically ten times smaller than the poise.

Apart from being a definition, equation 1.10 represents a *constitutive equation*, a relationship between the stress and the conditions of flow. In fact, a very convenient graphic representation in rheology is the plot of stress vs. shear rate. If the curve obtained is practically a straight line (for a given temperature), the fluid is called *Newtonian* and represents the simplest rheological behaviour.

With the expression "*non-Newtonian*" is possible to define all fluids which are characterised by a non-linear relation between stress and shear rate. The constitutive equation then becomes:

$$\sigma = f(\dot{\gamma}) \tag{1.13}$$

which can be also written as

$$\sigma = \eta(\dot{\gamma}) \cdot \dot{\gamma} \tag{1.14}$$

The main non-Newtonian behaviours are shown in figure 1.15.

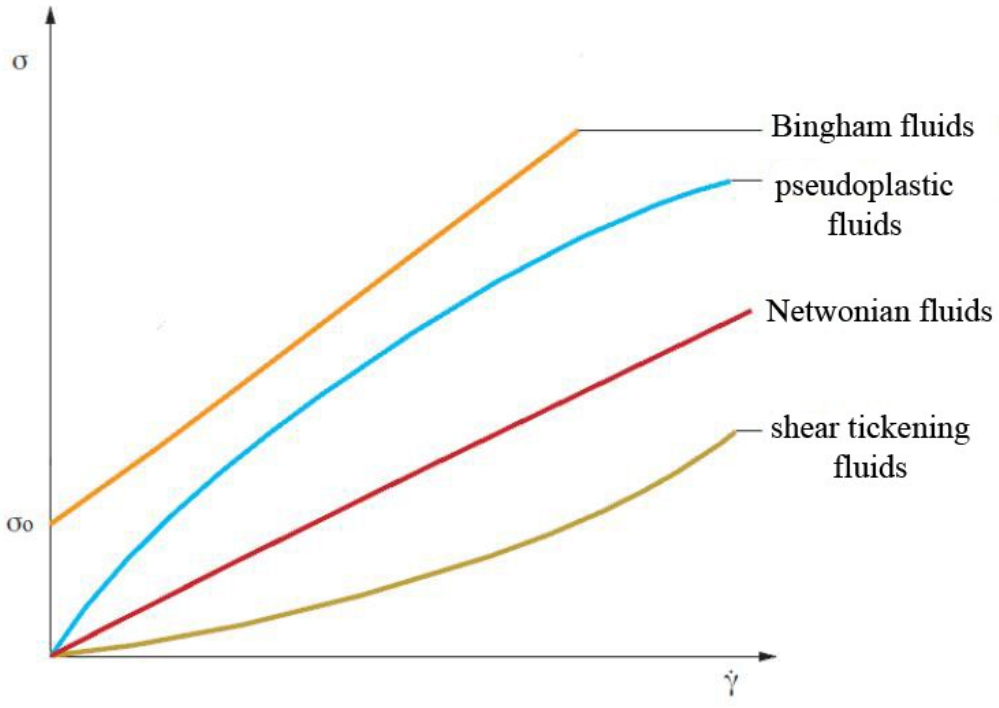


*Figure 1.15: Difference between Newtonian and main non Newtonian rheological behaviours*

The first category is represented by the *pseudo-plastic* (or *shear thinning*) fluids, which show a decreasing viscosity when the stress is increased. The *shear thickening* fluids have instead the opposite behaviour.

Another particular rheological behaviour is represented by the *Bingham fluids*: they behave as a rigid body at low stresses but flows as a viscous fluid at high stress[13-15].

The quantitative determination of the rheological behaviour represents one of the main aspects of the applied rheology. An analytical relation able to a priori determine the viscosity of the fluid for a given value of stress or shear rate is very useful from a practical point of view. Literature is full of mathematical models with the purpose of calculating the viscosity of a fluid as a function of shear rate. The most popular models are the following[16]:

- **Power law fluids**: this expression is given by the observation that the viscosity of a large number of fluids shows a linear trend for high shear rates when a log-log representation is used. This rheological behaviour is described by equation 1.15:

$$\sigma = K\dot{\gamma}^{n} \tag{1.15}$$

  where *K* is defined "*consistency*" and *n* represents the *"flow index"*.
  The viscosity of the fluid is obtained from equation: 1.16:

$$\eta = K\dot{\gamma}^{n-1} \tag{1.16}$$

  This representation is extensively used in many applicative areas, because it is the most simple constitutive relation for a non-Newtonian fluid.

- **Ellis model**: it satisfies the need of representing the viscosity curve in a large shear rate range:

$$\eta = \frac{\eta_0}{1 + (\tau\dot{\gamma})^{1-n}} \tag{1.17}$$

This model contains three parameters and its behaviour is of simple understanding. For low values of $\dot{\gamma}$, the denominator tends to 1 and the viscosity tends to the value of the Newtonian plateau $\eta_0$. For $\tau\dot{\gamma}$ >>1 the behaviour of the fluid approaches a power law behaviour.

- **Cross model**: sometimes the power law region is followed by a second plateau in the high shear rate zone and it is possible to describe this behaviour with equation 1.18:

$$\eta = \eta_\infty + \frac{(\eta_0 - \eta_\infty)}{1 + (\tau\dot{\gamma})^{1-n}} \tag{1.18}$$

where $\eta_\infty$ is the value of the viscosity at high shear rates.

- **Carreau model**: used to better describe the transition region between Newtonian and non-Newtonian behaviour and it represents a more complex version of the Cross model; the equation becomes

$$\eta = \eta_\infty + \frac{(\eta_0 - \eta_\infty)}{[1 + (\tau\dot{\gamma})^{1-n}]^{\frac{1-n}{a}}} \tag{1.19}$$

- **Yasuda model**: this model is also used to better describe the transition region but it considers $\eta_\infty$= 0

$$\eta = \frac{\eta_0}{[1 + (\tau\dot{\gamma})^{1-n}]^{\frac{1-n}{a}}} \tag{1.20}$$

As visible, in these last two models a parameter *a* is introduced with the purpose to describe the transition between Newtonian and non-Newtonian behaviour.

The knowledge of the rheological behaviour of a fluid and the study of its constitutive equation is today possible thanks to some particular instruments, called *rheometers*.

Another important concept in rheology is the viscoelasticity. The viscoelasticity is a peculiar rheological behaviour of some particular materials which present a behaviour between that of an elastic solid and that of a viscous fluid. In particular if the material is subjected to an oscillatory periodic deformation of amplitude $\gamma_0$ and frequency $\boldsymbol{\omega}$, the stress response can be put in the form:

$$\frac{\sigma}{\gamma_0} = G' \sin(\omega t) + G'' \cos(\omega t) \tag{1.21}$$

where G' is the *storage modulus* and G'' is the *loss modulus*. This relation has origin from the observation that purely elastic materials have stress and strain in phase. In purely viscous materials, strain lags stress by a 90 degree phase lag. So viscoelastic materials exhibit behaviours in between these two limits, presenting an intermediate lag in strain. The dynamic complex modulus G can be used to represent the relations between the oscillating stress and strain according to the equation 1.22.

$$G = G' + i\, G'' \tag{1.22}$$

where

$$G' = \frac{\sigma_0}{\gamma_0} \cos \delta \tag{1.23}$$

and

$$G'' = \frac{\sigma_0}{\gamma_0} \sin\, \delta \tag{1.24}$$

In equations 1.23 and 1.24 $\sigma_0$ is the stress amplitude and $\delta$ is the phase lag. The two parameters G'(also called elastic modulus) and G''(also called viscous modulus) are both achievable from oscillatory experiments.

## 1.11 *Purpose of this work*

The purpose of my work of PhD is the rheological study of the interactions between rheology modifiers (in particular based on methylhydroxyetilcellulose, MHEC) and superfluidificants in aqueous solutions.

This PhD project, in collaboration with CTG-Italcementi Group of Bergamo, has the final purpose of gaining a deep understanding of the rheological behaviour of cement-based aqueous formulations containing the above mentioned additives for use in technologically advanced applications in the cement industry, such as the extrusion of cement-based pastes and the formulation of cement-based paints.

The rheology of a cement-based formulation, that is one including all the additives and the materials used as inerts, is practically very difficult to study mostly because of the great number of constituents and of their different chemical nature. For this reason, one main stage of this work will concern the study of solutions of additives alone, followed by the determination of the correlations between the behaviour of the simplified model system (in this case water + RM + SP) and the rheological behaviour of the complete formulations. This study is therefore aimed to a better understanding of the cement mixture rheology and to the forecasting of the behaviours modifying the operational parameters.

## 1.12 *State of the art*

Literature is full of works about rheology and chemical behaviour of classical cementitiuos formulations[17-36] and common paints[37-60]. On the other side, works about the rheological behaviour of cement additives like MHEC and superplasticizers are not very numerous because this kind of study is relatively new and because MHEC is a material recently introduced in the cement field. Most studies concern other cellulosic rheology modifiers such as HEC, HPC, MHPC, etc. Moreover, most of these works concern chemical aspects of these substances, while just few are about rheological studies and even less are about interactions between cellulosic rheology modifiers and SPs.

Thermo-reversible gelation of aqueous solutions of macromolecules has been recognised as being a highly important phenomenon, with implications for several practical applications of these materials. Of particular interest is the behaviour of non-ionic water soluble cellulose derivatives, whereby aqueous solutions have been shown to gel reversibly at elevated temperatures[61-66]. However, the study of this process is complicated by the possibility of a range of further phenomena during the heating cycle. In particular, precipitation from aqueous solution may take place as a result of the inverse temperature-solubility relationship of these polymers. The onset of precipitation may be detected via light transmission measurements; as the temperature is increased the transmission remains unchanged until, at the initial precipitation (IPT), a decrease is seen which becomes more marked with increasing temperature[67]. This is closely related to the cloud point of the solution, whereby the system becomes opaque over a narrow temperature range due to the presence of particulate matter. The interrelationship between gelation, clouding and precipitation remains relatively poorly understood and indeed the definitions used for these processes have not been assigned to universal agreement.

Sarkar has suggested that the IPT may be considered to be the point of 97.5% light transmission and the cloud point as the temperature of 50% transition, while the same author described the incipient gelation temperature (IGT) as the temperature of maximum viscosity[68]. In practice, however the terms are arguably used fairly loosely and indeed often interchangeably. It must be also outlined cloud point measurement, which is derived from the surfactant field, is only generally used for dilute solutions as a means of quality control. Similarly, the working definition of the temperature of gelation varies in the literature, bearing in mind that gelation must be considered in terms of the viscoelastic properties of the system rather than the viscosity alone. Some authors consider the gelation concentration or temperature to be the point at which the elastic modulus exceeds the viscous modulus (which may of course depend on the frequency of measurement), while others consider it to be the point at which a macroscopically discernible increase in stiffness is apparent.

All the above points are further complicated by the possibility of a heating rate dependence of the observed transitions.

Hussain S. et al. have investigated the thermo-rheological behaviour of some hydroxypropyl methylcellulose (HPMC) aqueous systems to determine the concentration and substitution dependence of the gelation process[69]. Solutions containing up to 20% w/v HPMC were prepared using three grades of material, all provided by the Dow Chemical Company. Temperature ramps

were performed using a rate of 2°C/min between 20 and 90°C at 1.0 Hz and at 4.7Pa and a low viscosity silicon oil was used to avoid evaporation.

Figure 1.16 shows the thermograms of a 2% w/v HPMC E4M system. At 20°C G" is greater than G', indicating a viscoelastic system dominated by the liquid (viscous) component. As the temperature is increased G' decreases gradually, until the temperature reaches 55°C where a minimum is observed. The minimum persists until approximately 70°C at which point an increase is seen. G" follows a similar trend on heating with a sharp decrease at 55°C and an increase at 75°C. On cooling a two-step increase is observed for both G" and G', but is more prominent for the latter. The two steps are observed at 65 and 50°C.

The behaviour pattern of a minimum followed by recovery on heating with an increase in moduli with one or more steps on cooling was seen at all concentrations; figure 1.17 shows the thermogram of the 20% w/v HPMC E4M system.

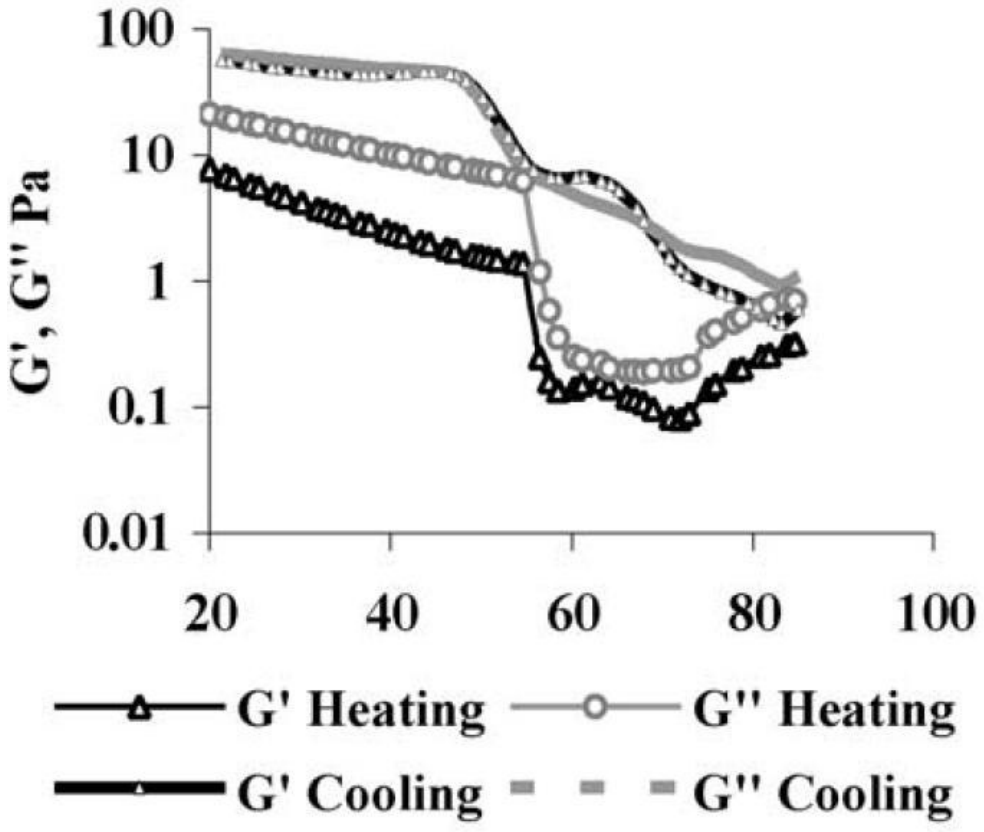


*Figure 1.16: Thermogram of a 2% w/v HPMC E4M system*

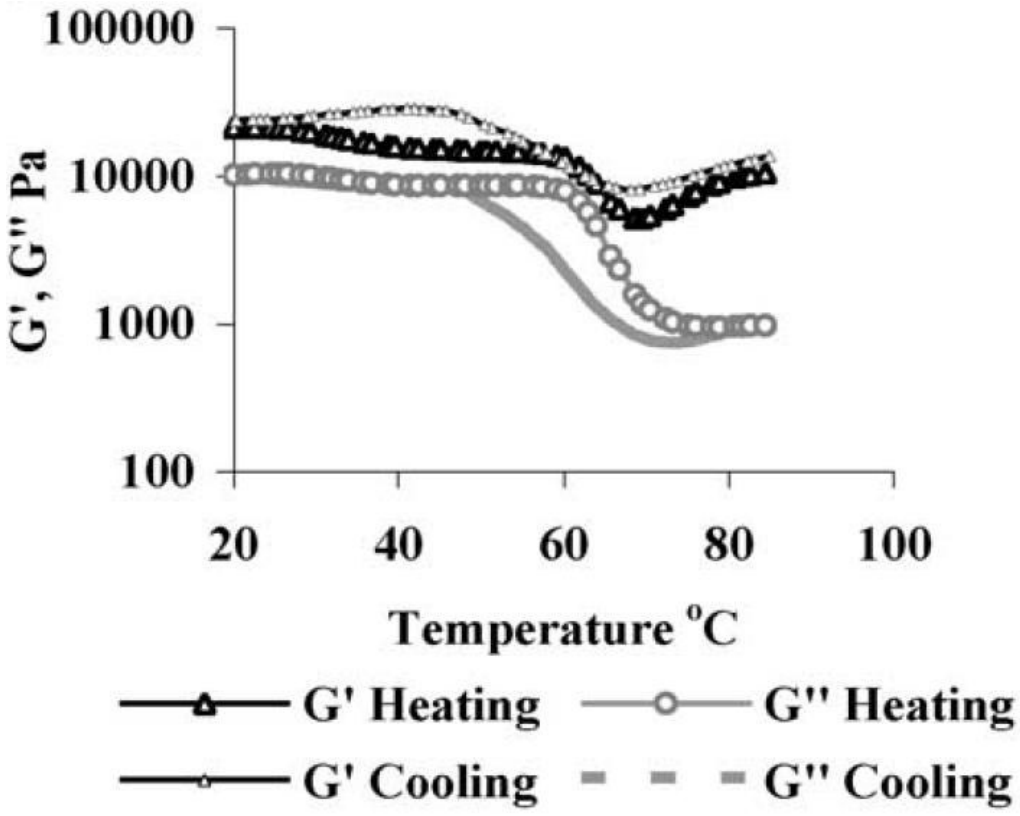


*Figure 1.17: Thermogram of a 20% w/v HPMC E4M system*

On heating G' falls sharply at 60 °C and rises at 65°C, while G" falls sharply at 60°C and levels off at 65°C. On cooling G' increases below 65°C and levels off to the original value at 50°C. G" rises sharply below 70°C and levels off below 50°C. The absolute values of the moduli are considerably greater for the more concentrated systems, but it is interesting to note that the general temperature dependence remains similar. This similarity is exemplified by the figures 1.18 and 1.19, showing the G' and G" thermograms for various different concentrations of E4M studied on heating. The sharp decrease in G' is observed at 55-60°C in all cases. However, it was noted that changes in both G' and G" varied from a two-step to a single step increase on cooling at increased concentrations.

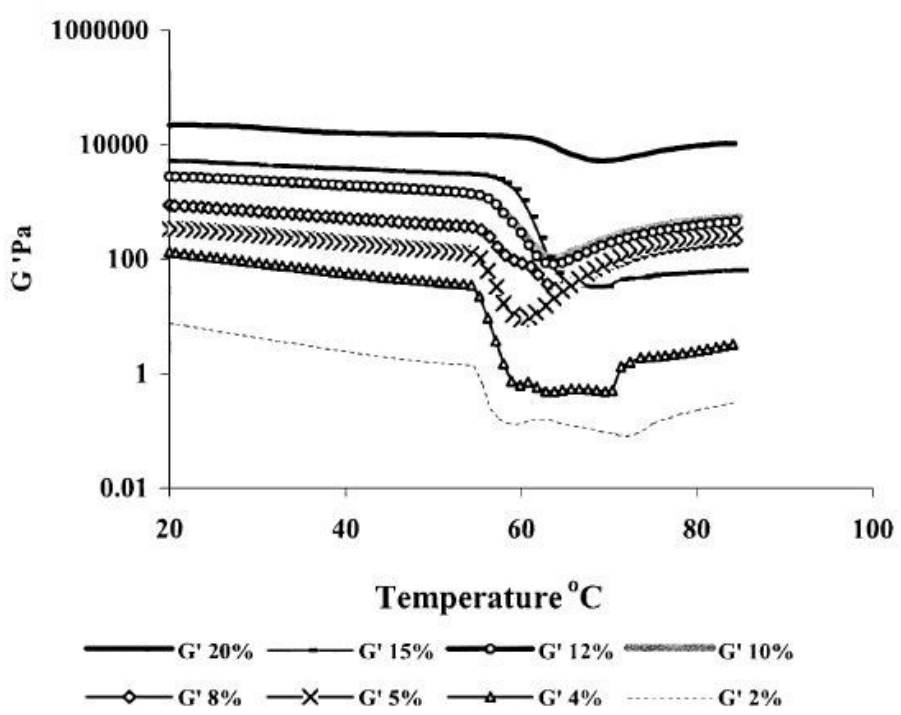


*Figure 1.18: Thermogram showing the change in the storage modulus G'*

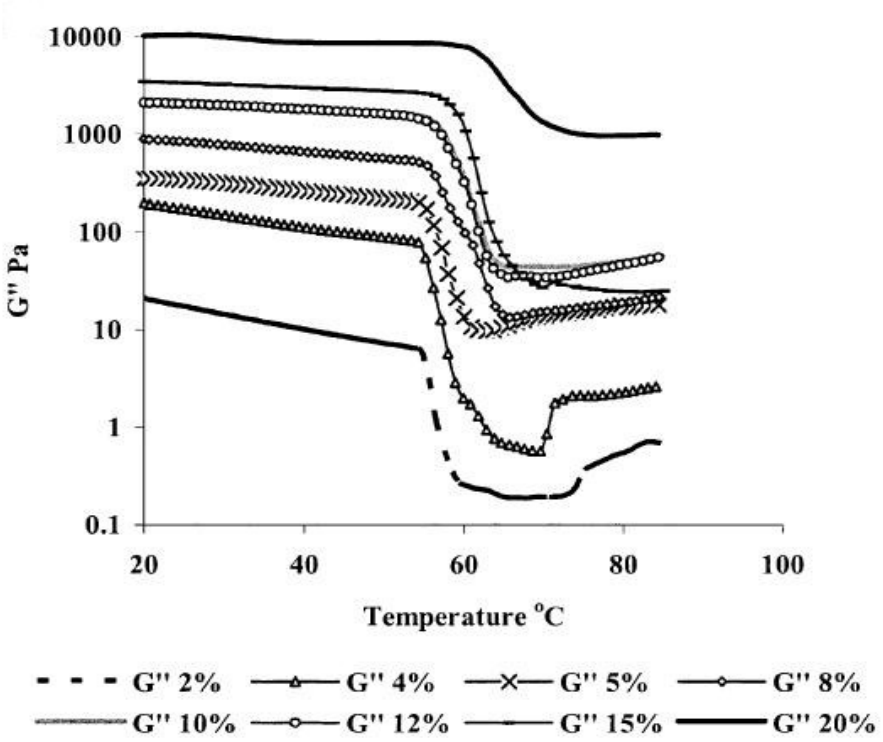


*Figure 1.19: Thermogram showing the change in the storage modulus G"*

The thermorheological behaviour of other two HPMCs (F4M and K4M) solutions were similar, although the temperatures at which the events occurred differed for K4M.

In order to correlate, the observed transitions with visual clouding, corresponding solutions were also heated and their behaviour observed visually (figure 1.20).

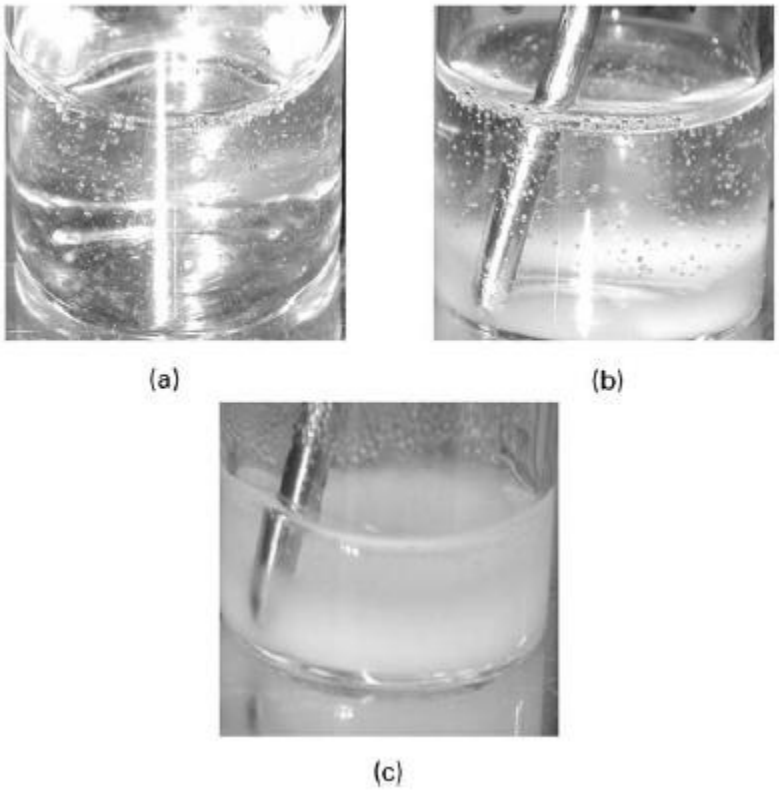


*Figure 1.20: Photographs of 2% w/v E4M solutions at 25°C (a) showing an isotropic solution, (b) 42°C showing the onset of clouding and 51°C (c) showing phase separation.*

It was interesting to note that clouding was apparent for the 2% E4M systems, starting at about 42°C which is lower than the temperature at which the rheo-thermal transition was observed. As the temperature was increased the system started to phase separate into two layers at approximately 51°C, which is close to the transition temperature seen during the temperature sweeps. It was noted that on further increasing the temperature, the polymer rich (cloudy) layer appeared to increase in

stiffness at approximately 75°C. On stirring the solution, the watery phase acted as a lubricant for the polymer rich phase making it easy to move around the beaker. This lubrication effect was also observed on the rheometer plate. On cooling the phase separation process reserved giving a clear single phase below 50°C.

A recent work of J. Pourchez et al.[70] investigates the influence of HPMC and HEMC on cement hydration. In this study a particular technique of characterization is exploited: since water retention is defined as the ability of a mortar to retain water, it can be measured with a standardized apparatus composed of a perforated dish attached to a vacuum assembly by a funnel. The perforated dish is filled with the mortar and vacuum is applied. As the initial mixing water mass in the plastic mortar is known, its mass loss is easily determined after the suction period. Water retention capacity is defined by the 1.25:

$$R(\%) = \frac{E - e}{E}\ x\ 100 \qquad (1.25)$$

with *E* the initial mass of mixing water and *e* loss of mass after suction. In the experiments several HEMCs and HPMCs of different molecular weight have been used. Experimental results show an increase of water retention capacity by comparison with non-admixed mortar. A significant influence of the molecular weight is also revealed; for a given class of chemical structure, water retention increases with $M_w$. The results allow to demonstrate that the methoxyl content is the key parameter concerning the portlandite precipitation delay induced by HPMCs and HEMCs.

A more recent work of J. Pourchez[71] concerns HEC influence on cement hydration measured by conductometry. According to this study, the conductometry is a powerful tool for monitoring the hydration kinetics because this technique provides rather detailed information on the different steps of the hydration reaction. The quantification of the hydration delay uses the CH precipitation time as a benchmark, which corresponds to a drop in conductivity. Also for these tests HECs of different molecular weight are used. Results show that hydration delay induced by HECs is always higher than delay induced by other rheology modifiers such as HEMC and HPMC. Also the pH of solution has a primary importance: hydration retardation in limewater is higher than the one in neutral water, as shown in figure 1.21:

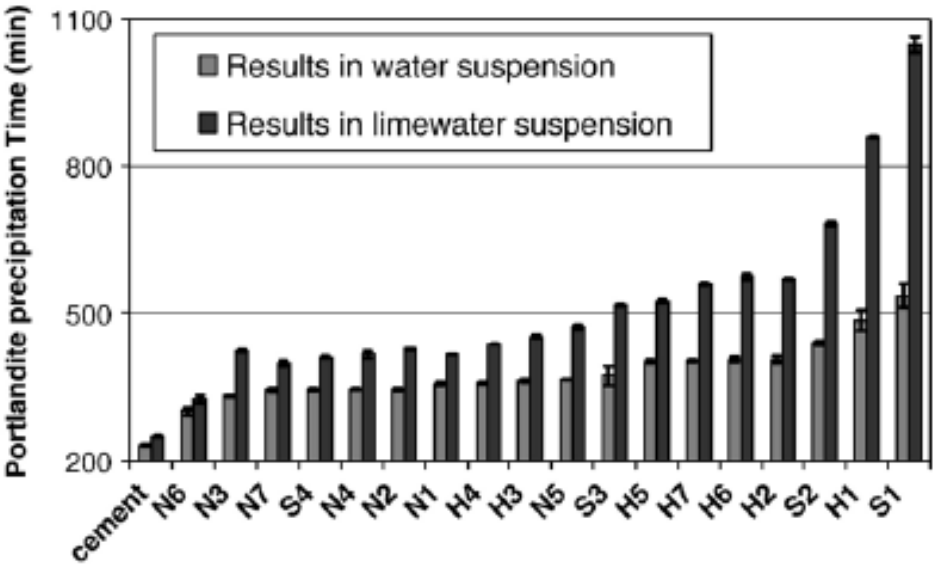


*Figure 1.21: Cement hydration in presence of several additives*

An interesting study on performance characteristics and rheological behaviour of cement grouts with combinations of high range water reducer and cellulose-based viscosity modifier is the object of a research promoted by M. Saric-Coric and collaborators[72]. The performance of grouts made with 0,40 water/cement ratio containing an hydroxypropyl methylcellulose (HPMC) as rheology modifier was investigated for mixtures made with polynaphtalene sulphonate (PNS) and polymelamine sulphonate (PMS). Grouts were tested for consistency using the minislump and Marsh cone 5 min after the initial contact of cement with water. Rheological properties were then evaluated followed by forced bleeding and washout testing. The loss of consistency was also determined by evaluating the minislump and 60 min Marsh cone flow time. Between 5 and 60 min, the grouts were poured into a sealed container to prevent evaporation. The results obtained for these tests led to the following conclusions: for the same consistency, the incorporation of the cellulose-based rheology modifier is shown to increase the superfluidificant demand between 10 and 40% with either PNS- or PMS-based water reducer; the slump loss at 60 min is higher for grouts prepared with PMS than those with PNS; mortars containing the rheology modifier develop 6% to 16% lower compressive strength than those without any rheology modifier.

The effect of SPs on the hydration of Portland cement paste has been extensively studied; in particular the effect of the side chains length, molecular weight and side chain density on workability and on the early hydration characteristics was investigated in great detail[73-80]. The workability, in particular, was found to strongly depend on the PEO side chain density, while the side chain length and the molecular weight had a minor influence. Nevertheless, one of the intrinsic complications to understand the SPs influence on the cement hydration is the difficulty to have monodisperse polymers: often their chemical formula is uncertain and their interaction vary along with the considered dry phases, leading usually to contradictory results. Besides, it has been clearly shown that the interaction of this class of polymers with the aluminate-rich phase is not a simple adsorption but a more complex intercalation phenomenon which can result in the formation of a layered organo-mineral composite and in a drastic decrease of the amount of available active polymer[81-83].

The study of interactions between rheology modifiers and superfluidificants in aqueous solutions has been the object of some investigations by the research group of P. Baglioni and co-workers at the university of Florence in collaboration with Italcementi Group. The study of the group has concerned a chemical-physical aspect of the problem using instruments like differential scanning calorimetry (DSC), magnetic nuclear resonance (NMR), scanning electronic microscopy (SEM), X-ray diffraction, etc. A new method of investigation with DSC has been tweaked which makes possible to know the quantity of water linked to the additives or reacted with constituents of cement causing the hydration and subsequent hardening[84]. The DSC analysis has been performed using some particular pans sealed with a neoprene O-ring to avoid water leaking and carrying out each measurement with the following temperature program: from room temperature down to -30°C at 40°C/min, isothermal regime at -30°C for four minutes from -30°C to -12°C, at 20°C/min, and from -12°C to 14°C at 4°C/min. The isothermal step at -30°C was performed to ensure free water to freeze despite possible super cooling effects. Each sample was previously maintained in a thermostatic bath at constant temperature (10, 20, 30 and 40°C). Each DSC curve showed a peak relative to water freezing and a peak due to its melting. The enthalpy variation of the water melting makes it possible to calculate a Free Water Index (FWI) as:

$$FWI = \frac{\Delta H_{exp}}{x\,\Delta H_{init}} \tag{1.26}$$

where $\Delta H_{exp}$ is the enthalpy change of the water melting determined by the DSC experimental curve, x is the average weight fraction of water in the cement paste and $\Delta H_{init}$ is the theoretical value of the specific enthalpy of fusion of water at 0°C in the paste determined considering that at the beginning of the hydration reaction FWI = 1.

This approach has been used to study the influence of additives on the hydration process of $C_3S$ and other constituents of cement. The effect of superplasticizers has been studied comparing the addition of three different superplasticizers to a $C_3S$/water paste: a naphthalene-sulfonic, a polyacrilate and a polycarboxylate. In figure 1.22 data are shown for the pure water solution and in the figures 1.23-1.25 for the solutions with additives.

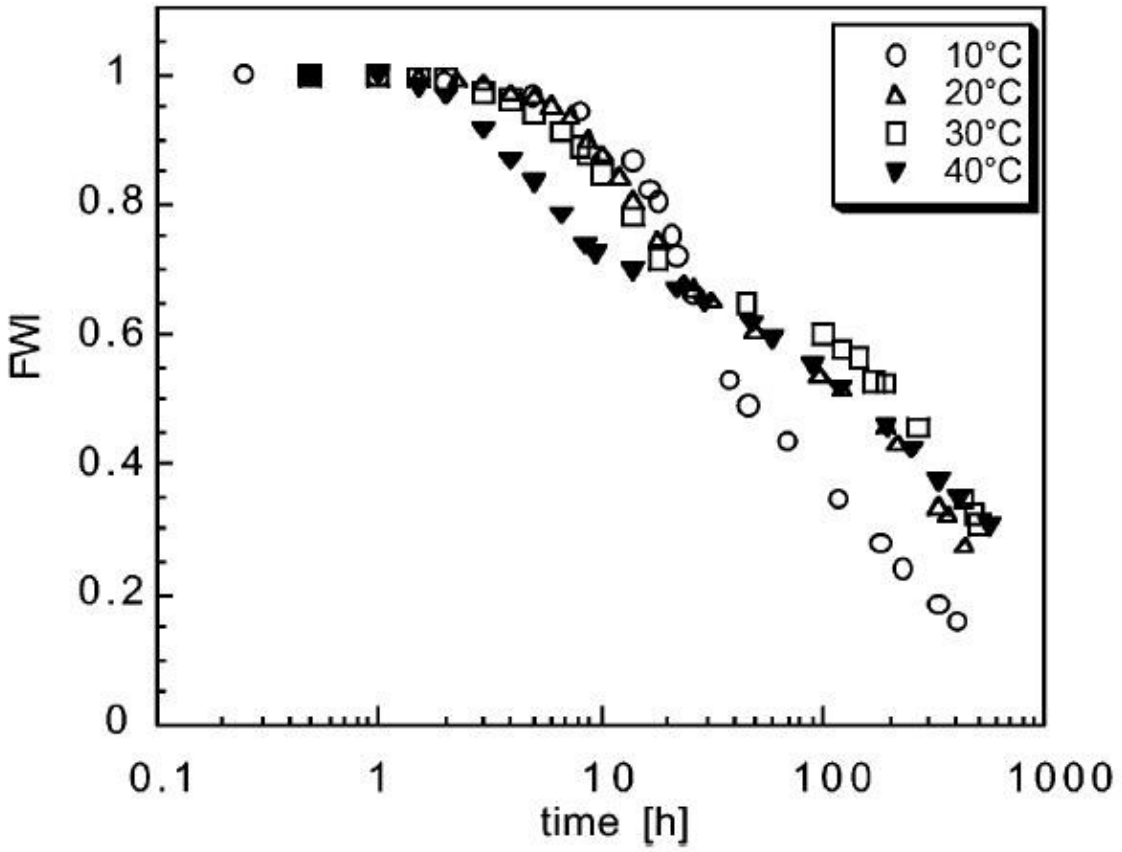


*Figure 1.22: FWI versus time for a $C_3S$ paste cured in pure water (w/c =0.4) at 10, 20, 30 and 40°C*

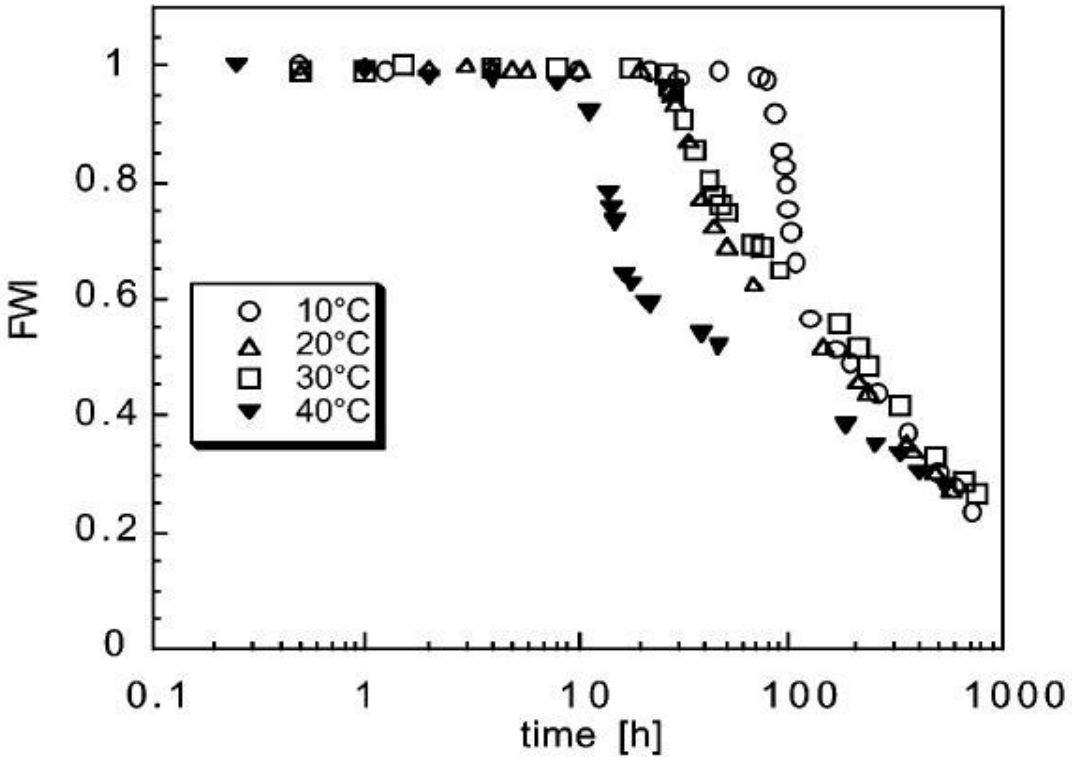


*Figure 1.23: FWI versus time for a $C_3S$ paste cured in water with NSF at 10, 20, 30 and 40°C*

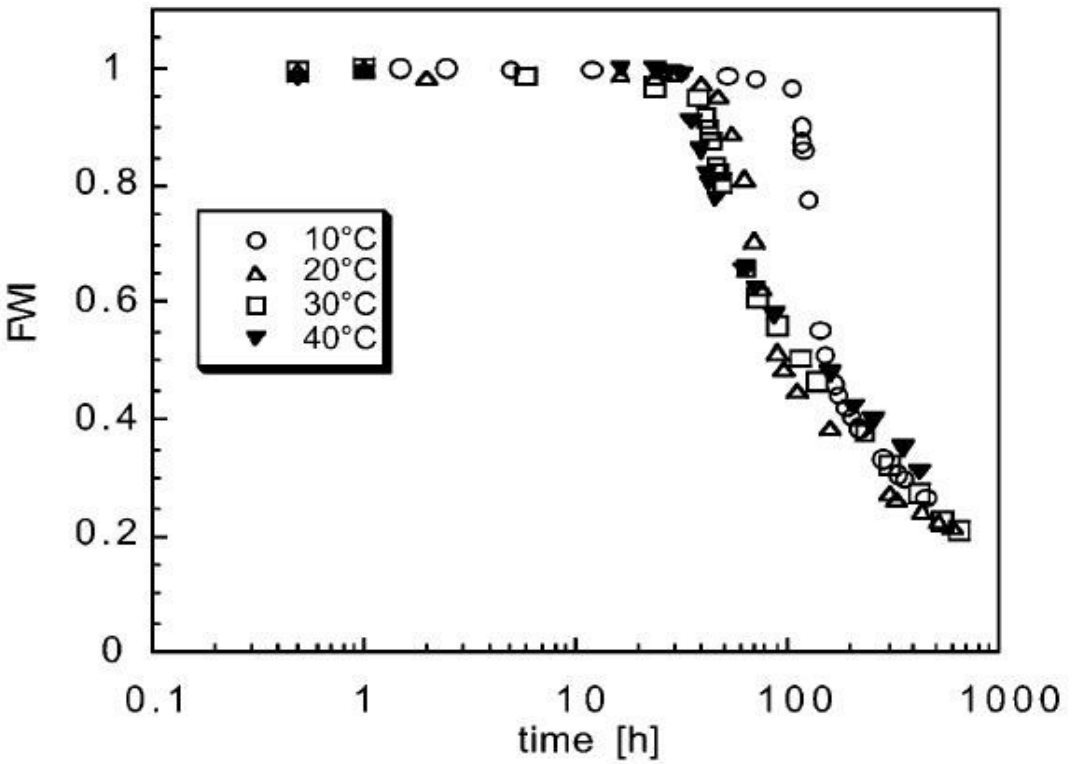


*Figure 1.24: FWI versus time for a $C_3S$ paste cured in water with HSP111 at 10, 20, 30 and 40°C*

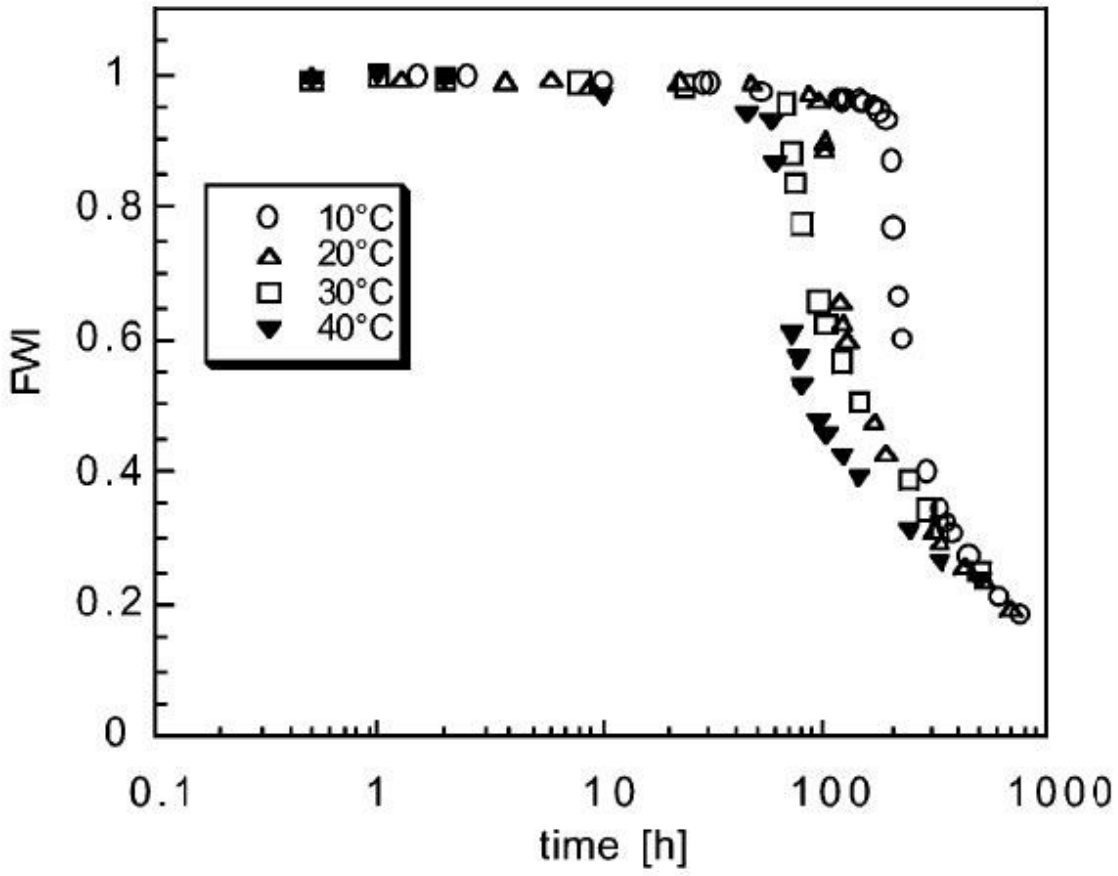


*Figure 1.25: FWI versus time for a $C_3S$ paste cured in water with HSP 114 at 10, 20, 30 and 40°C*

In this case the $C_3S$ hydration proceeds according to three steps: induction, acceleration and deceleration period. For the description of the acceleration period an Avrami-Erofeev law was used, while the final part of the FWI curve follows a three-dimensional diffusion equation. With this technique it was also possible to obtain the activation energies for the induction period and for nucleation-and-growth process of the hydrated phase, the M parameter (related to the morphological characteristics of the growing crystals), and the diffusional constants for pastes cured with and without superplasticizers. The presence of additives gives rise to a dramatic increment of the activation energy for the acceleration period, while the M parameter remains roughly constant. These results strongly suggests a modification in the hydration mechanism, maybe related to the morphology of the hydrated phase. To confirm this theory, SEM investigation was performed on diluted suspensions of $C_3S$ in pure water and in superplasticizers solutions. Figure 1.26 shows the

SEM image of $C_3S$ in pure water: the grain surface is covered by a fibre-like hydrated phase. In presence of SP the fibrillar structures are not visible, also after long incubation periods, while the formation of some other regular structures around the main grains is enhanced.

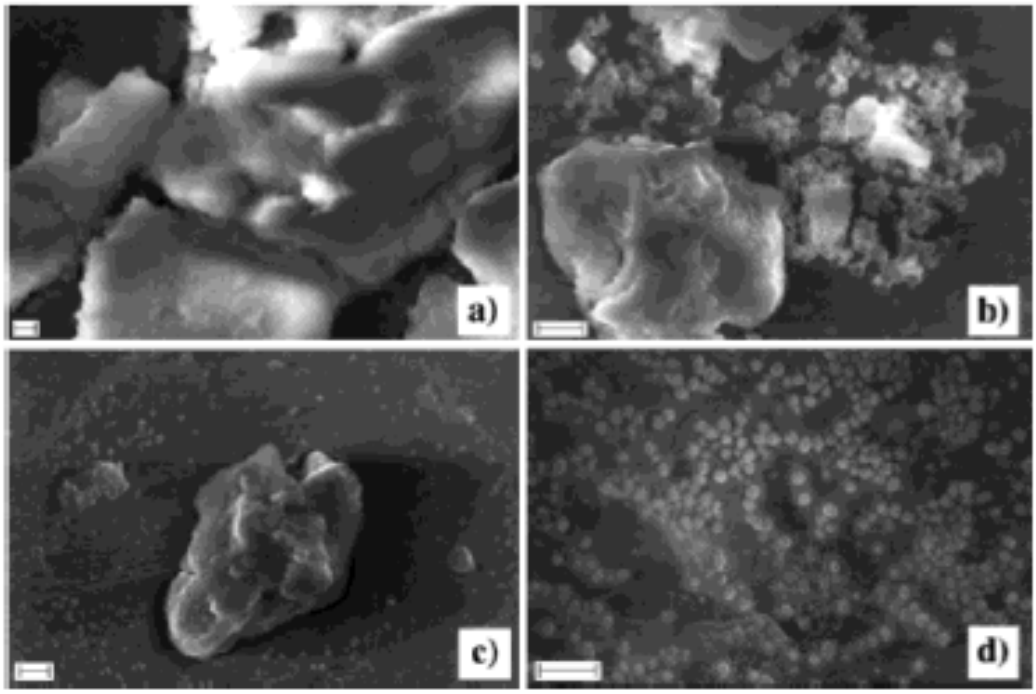


*Figure 1.26: SEM images of $C_3S$ suspensions (w/c = 50), cured at 25°C for 24 h: (a) $C_3S$ in pure water, (b) $C_3S$ in water with NSF, (c) $C_3S$ in water with HSP111, (d) $C_3S$ in water with HSP114*

The same experiments have been conducted also on cement pastes in the presence of a cellulosic additive (MHEC): the presence of cellulose ether does not significantly alter the activation energy for the acceleration period, and also, the parameter M remains roughly constant. Therefore no modifications in the $C_3S$ hydration mechanism occur in the presence of cellulose ether, but the FWI evolution shows that there is a strong increment of the water availability during the acceleration period: the additive, due to its highly hydrophilic chemical structure, interacts with the aqueous phase, making it homogeneously distributed over the paste. As a consequence, water does not need to diffuse to reach the anhydrous phase and it is available to the hydration in a shorter period of time[85-88].

Thermogravimetry-differential thermal analysis (TG-DTA), XRD measurements and other experiments confirm that the presence of the additive does not change the chemical nature of the hydration products; nevertheless, a slight retardation is recorded when the MHEC is added to the paste [89].

In another work of the group of P. Baglioni, in collaboration with a research group at the university "La Sapienza" of Rome, a study of the influence of superplasticizers on the first steps of tricalcium silicate hydration by NMR is proposed[90]. It deals with the analysis by $^{1}H$ nuclear magnetic resonance relaxation of water in pure tricalcium silicate ($C_3S$) pastes and $C_3S$ pastes with sulphonated naphthalene formaldehyde (SNF) condensate. A series of $^{1}H$ spin-spin relaxation time experiments on cement samples following the hydration kinetics has been performed in order to study the dependence of relaxation times on the hydration time. Spin lattice relaxation times have been measured by means of a standard inversion recovery pulse sequence, with 54 values of the inversion time in the range 50 ms – 10 s. The experimental data have been fitted both with a monoexponential and a biexponential function in order to evaluate the contributions from water in different environments. The results show that the main effect of the SNF superplasticizer is to increase the dormant stages of hydration and to enhance the distinction among the dormant, acceleration and diffusion periods in the samples without the superplasticizer.

In summary, despite their extensive utilization in the cement industry, the understanding of the physico-chemical mechanisms of interaction between these additives and the cement is far from being complete and further study is necessary to understand these phenomena[91].

The works present in literature about the rheology of the cement-including formulations are also not very numerous, especially those about the applications that the present work is aimed to investigate. While for extrusion of cement there are some papers because it is a relatively new topic, to find works about coating with cement is not possible.

One of the groups who have best investigated the rheological properties of cement-based extrudates is that of Zongjin Li and Bin Mu. In one of their works[92], the researchers present some results on the study of the rheology field of short fibre-reinforced cementitious extrudate. The work started with an analysis of cement flows in a shallow flight extruder in which the height of the flight to the width of the channel ratio is small. The fresh cementitious flow inside was considered as a 2D steady shear flow with nonlinear viscoelastic properties. By the fact that the Deborah number is small for the cementitious flow in an extruder, the constitutive equation of "retarded-motion-

expansion" was adopted and the formula of the flow volume rate for a shallow flight screw extruder was derived and numerically solved by the finite-difference method. A correction factor was also used to modify the obtained results for the case of the deep flight screw extruder. Using a pressure sensor installed at the front end of the extruder to measure the pressure change, the group has reached the results summarized in figure 1.27.

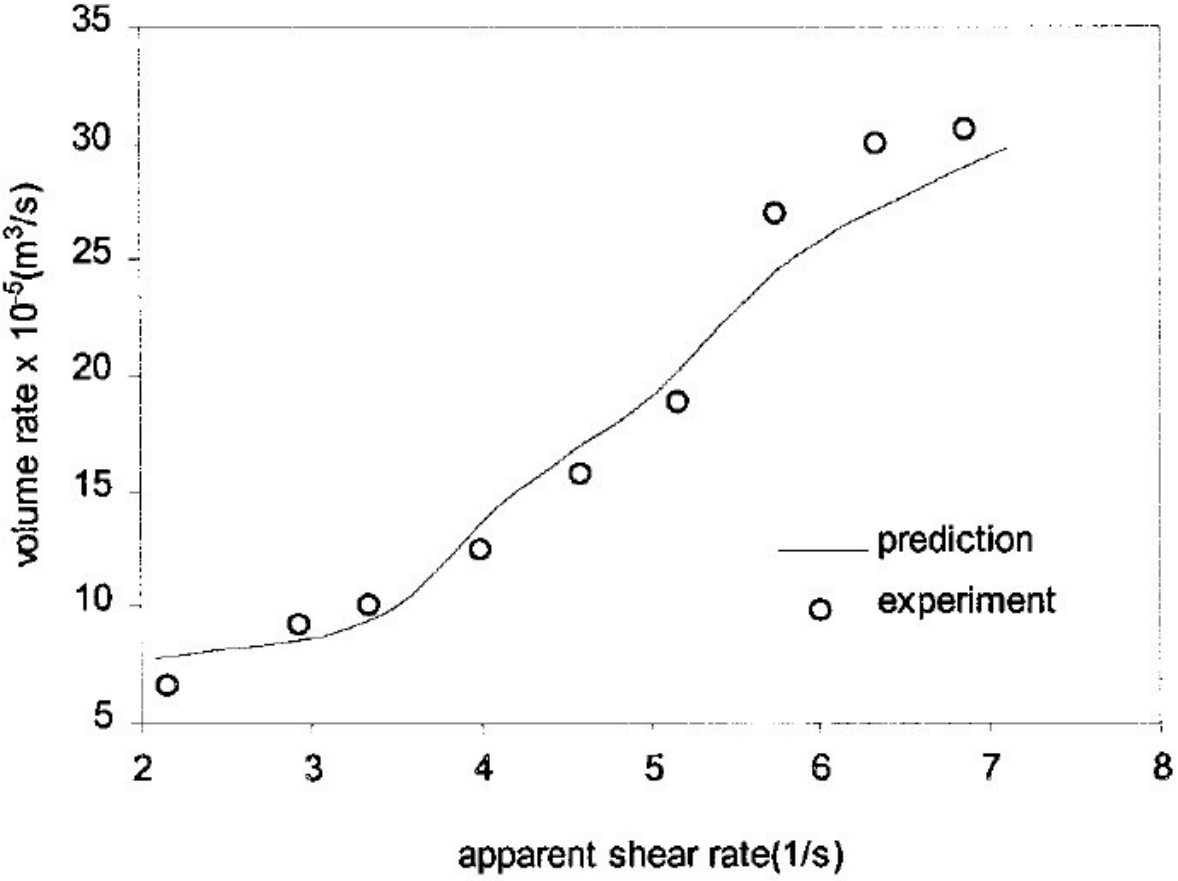


*Figure 1.27: Theoretical predictions and corresponding experimental data*

As visible, there is a good agreement between the theoretical predictions and the experimental results. The system behave as a non-Newtonian fluid with a reduction in viscosity as the shear rate increases (shear thinning). At low shear rates, the nonlinearity between the shear stress and shear rate of the cementitiuos flow is small; however, it becomes quite large at high shear rates and the retarded-motion expansion model can describe this behaviour reliably. During their experiments, the scientists have also concluded that: a) the numerical scheme is quite straightforward and with the suitable initial estimates it is sufficient to predict experimental results; b) at high shear rates, both the down channel and the cross channel velocity profiles are unstable and the numerical scheme needs more iteration steps to achieve the convergent solution; c) generally, the prediction of

the flow volume rate in a deep flight extruder based on the viscoelastic assumptions is significantly different from that based on the Newtonian assumptions but this difference is relatively small at the low shear rate range.

In a more recent work, the group of Zongjin Li has published other results gathered during a collaboration between the Hong Kong University of Science and Technology and the Columbia University. In this work[93], the fresh cementitious extrudate was modelled as a viscoelastic material moving in a three-dimensional extruder channel. The viscosity-related and the elasticity-related material were obtained using a homemade rheometer (see the figure 1.28). In this way, the governing equations were linearized and solved numerically by the finite-difference method, using the suitable velocity and stress boundary conditions.

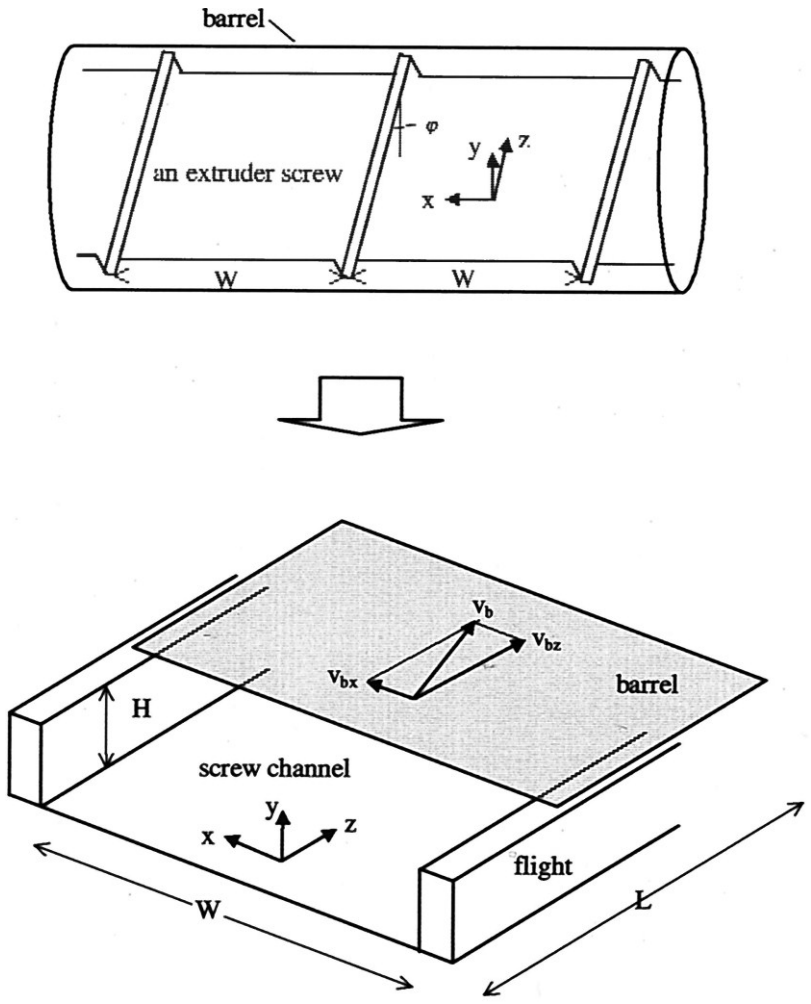


*Figure 1.28: Simplified geometry of a single-screw extruder*

In this system the screw and the barrel are unrolled into a plane with the coordinate system fixed to the screw root. The barrel is considered to move at a velocity $v_b$ in a direction opposite to the screw rotation and the velocity $v$ is assumed not to change significantly along the down-channel z-direction. The equations of motion become

$$\begin{cases} 0 = \dfrac{\partial^2 \tau_{xx}}{\partial x \partial y} + \dfrac{\partial^2 \tau_{xy}}{\partial y^2} - \dfrac{\partial^2 \tau_{xy}}{\partial x^2} - \dfrac{\partial^2 \tau_{yy}}{\partial x \partial y} \\ 0 = -\dfrac{\partial p}{\partial z} - \dfrac{\partial \tau_{xz}}{\partial x} - \dfrac{\partial \tau_{yz}}{\partial y} \end{cases} \tag{1.27}$$

where $\tau$ is the stress tensor and $\partial p/\partial z$ is the prescribed pressure gradient in the z-direction. The authors use a viscoelastic constitutive model described[94] by the equation 1.28.

$$\boldsymbol{\tau} = -\eta(\dot{\gamma})\left(\boldsymbol{\gamma}_{(1)} + \frac{1}{G}\boldsymbol{\tau}_{(1)}\right) \tag{1.28}$$

where G is an elastic modulus and $\eta$ $(\dot{\gamma})$ is an arbitrary function for describing the shear-rate dependent viscosity. $\tau$ and $\gamma_{(1)}$ are the stress tensor and the rate-of-strain tensor respectively. The boundary conditions are determined by the constitutive equation and the equation of continuity, using the appropriate velocity components and their derivatives, but all these elements are omitted for brevity. The 3-D model has been used to predict the rheological behaviour of an extrudate. The mixing proportions of the extrudate has been cement:slag:sand1:sand2:water = 1:1:0,39:0,26:0,60, where sand1 and sand2 denote silica with different diameters. A cone-plate apparatus based on a rotatable was used to measure the elasticity-related material constant G. A trial-and-error method has been used to design the extruder die. The research has given the following results: a) the short-fibre-reinforced cement-based composites show shear-thinning behaviour. The viscosity decreases as the shear rate increases; b) materials with less elasticity or viscosity lead to a more uniform and

more symmetrical down-channel and cross-channel velocity profile, which is essential to a cementitious extrudate; c) at both low and high apparent shear rates, the elasticity of the material has a positive effect on the flow-volume rate while in the range of moderate apparent shear rates the effect is negative.

# *Materials and Methods of preparation*

# MATERIALS AND METHODS OF PREPARATION

The tests performed in this work have required a great assortment of different materials and different methods of preparation in order to well understand the mechanisms at the basis of some peculiar dynamics. In particular, two radically opposite ways of sample preparation have been adopted. One is used for the simplified systems which require a smaller variety of materials but a great care to be sure of the complete dissolution of all the ingredients. The second one is used for the real systems which require a great variety of substances, and it is certainly more immediate and less reproducible.

For the simplified systems the necessary materials are primarily the chemicals used as additives, in addition to those used to simulate different physico-chemical environment.

For the real systems (cement formulations) all the materials traditionally used for cement applications are considered (cement, limestone, aggregates and other inerts) apart from all the additives used in small amount.

## 2.1 *Rheology modifiers*

The rheology modifiers (RMs) tested are all provided by CTG-Italcementi Group. They appear as a white fine powder difficult to solubilize in water. Most of them are methylhydroxyethylcelluloses (MHEC) with the addition of very small amounts of other additives used to control the effect of rheology modification and water retention.

## 2.2 *Superplasticizers*

The superplasticizers (SPs) used are all provided by CTG-Italcementi Group. They can appear as concentrated aqueous solutions or dry powders according to the synthesis method.

The SPs tested are of two kinds: acrylics or methacrylics.

## 2.3 *Calcium hydroxide*

The calcium hydroxide ($Ca(OH)_2$), provided by AppliChem GmbH, has been used to simulate the alkaline environment in the aqueous solution giving a pH=12 under saturated conditions.

## 2.4 *Sodium sulphate*

The sodium sulphate ($Na_2SO_4$), provided by AppliChem GmbH, has been dissolved in some aqueous solutions and used to simulate a chemical environment closer to that typical of cement mixtures.

## 2.5 *Portland cement*

Two kinds of cement have been used for the preliminary tests: 52,5R and 42,5R. The 52,5R is a class of Portland cement formulated to give compression resistance after 2 days of setting ≥ 30 MPa and a compression resistance after 28 days ≥ 52,5 MPa. The 42,5R, obtained from rough milling and with a higher percentage of $C_2S$ to give a cheaper material, is a class of cement formulated to give compression resistance after 2 days ≥ 20 MPa and a compression resistance after 28 days ≥ 42,5 MPa. Both the cements are provided by CTG-Italcementi Group and produced by Italcementi.

## 2.6 *Calcium-sulfoaluminate binder*

The calcium-sulfoaluminate binder (CSB) is a special cement-based binder produced by Italcementi obtained from a clinker of solfoaluminate of calcium. The CSB is rapidly replacing the Portland cement in numerous applications mainly because it is considered a more eco-compatible material.

The calcium-sulfoaluminate cement is provided by CTG-Italcementi Group.

## 2.7 Photocatalytic binder

The photocatalytic binder is a new cement-based binder developed by CTG Italcementi Group which is able to dull the polluting organic and inorganic chemicals present in the air with a patented system.

## 2.8 Inerts

All the inert materials have been provided by CTG Italcementi Group. In this definition are included materials such as sands, bigger aggregates, calcium carbonate and other similars.

## 2.9 Preparation of the aqueous solutions

The preparation of the aqueous solution is complicated by the fact that the RM powder is not very easy to dissolve. Nevertheless, a high viscosity is generally suddenly achieved when this substance is added to the aqueous solution. For this reason, especially when the concentration of RM is higher, as in the case of systems for extrusion, a particular method of preparation is required. If the SP must be present in the solution, a preliminary dissolution of it in neutral (or alkaline) water is necessary. After the dissolution of the SP, the RM fine powder must be added under active mixing and waiting for a week is essential to be sure of the complete dissolution of it.

At the end of this procedure, a centrifugation is required to avoid the presence of air bubbles in the sample which can alter the measurements with the rheometer.

For the dilute solution (used to simulate the systems for coating) the procedure above described is optional because the viscosity of the system is not so high to hinder the dissolution of the remaining RM, so a normal stirring work is enough to have a good dissolution of the additives in water.

## 2.10 *Preparation of the cement-based systems*

The preparation of the cement formulations is, as imaginable, very different from the preparation of the aqueous solution. First of all, these systems require a very active mixing essentially because the dry powder of cement tends to easily form lumps. Lump formation must be avoided to ensure a good homogeneity of the material, especially when it must be tested and so it must give results as reproducible as possible. Anyway two different methods of preparation have been used:

- *Preparation with the planetary mixer Hobart (for the paints)*:

The dry elements are first mixed for a prefixed time and added to water under mixing in another bowl. The mixture is then manually mixed to check that lumps are not present. In figure 2.1 the Hobart mixer is illustrated.


*Figure 2.1: Illustration of the Hobart mixer*

- *Preparation with the intensive mixer Eirich and high shear mixer (for extrudates)*:

In this way of preparation the dry elements are first energically mixed in an intensive mixer (Eirich) and the water is then added to give a wet powder. Subsequently this wet powder is kneaded in a

calander-like mixer able to impose a high shear strain. The dough so formed assumes the form of a pastry-like plastic material. It can so be used in an extruder or in a die rheometer. In figures 2.2 the phases of preparation are illustrated.


*Figures 2.2: Illustration of the preparation with Eirich mixer (1-2) and high shear mixer (3-4-5-6). (Images achieved in the laboratories of CTG-Italcementi Group)*

# *Instrumentation*

# INSTRUMENTATION

## 3.1 *Rotational rheometer*

A rheometer is a laboratory device used to measure the way in which a liquid, suspension or slurry flows in response to applied forces. It is used for those fluids which cannot be defined by a single value of viscosity and therefore require more parameters to be set and measured than is the case for a viscometer. It measures the rheology of the fluid.

The ideal parallel plate rheometer is practically impossible to use because of its kinematic conditions: in fact the plates translate one to each other and after time they completely separate. Moreover the stress applied to the sample continuously decreases because of the decreasing of the surface of application. The best way to reduce these undesired effects is to force the movement of the fluid along a close trajectory, repeatable in the time. This is the principle exploited in rotational rheometers: the instrument is made up of two plates, one is fixed and the other is in movement. The fluid is positioned between the plates. A motor provides the torque necessary to put the moving plate in rotation while a second device (transducer) is responsible to measure the torque necessary to move the plate. From the torque, with some calculations it is possible to obtain the value of the stress and also the value of the viscosity.

There are two kinds of commercial rotational rheometers: *controlled-stress rheometers* and *controlled-strain rheometers*. In the first ones the torque-transducer is the same motor used to put in rotation the plate while the shear rate is derived from the measure. They have recently been introduced on the market but, for the rapid development of the technology, they have competitive prices and they are presently the most employed rheometers.

The strain-controlled rheometers are older than the first ones; in this case the movement is produced by an independent motor to impose the shear rate while the torque is directly measured by a transducer positioned in correspondence of the fixed plate.

The strain-controlled rheometers are the less diffused but they are particularly convenient for some tests useful in the study of viscoelastic systems. Besides the motor of these rheometers is generally more powerful, allowing for the achievement of high torques, and so they are particular suitable for experiments on polymer melts.

Independently from the kind of rotational rheometer employed, some geometries are available; they change on the basis of the fluid tested and of the test performed. In the following, the main geometries for polymer melts are reported.

*Cone and plate geometry*

The viscosity of polymer melts in low shear rate is generally studied with the help of rotational rheometers using the cone-plate geometry illustrated in figure 3.1.

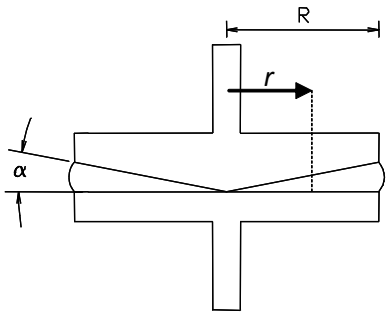


*Figure 3.1: Illustration of the cone-plate geometry*

In this geometry, the material is inserted between a cone and a plate and one of them is set in rotation. For each *r* the shear rate is given by the ratio between the velocity of the plate and the gap between them.

For small angles it is possible to write the equation 3.1:

$$\dot{\gamma} = \frac{\Omega r}{h} \cong \frac{\Omega r}{r\alpha} = \frac{\Omega}{\alpha} \tag{3.1}$$

where α is the angle of the cone. As clearly visible, the shear rate is uniform in the whole sample. This makes it possible the determination of the non-Newtonian viscosity. The tangential strain is also uniform (equation 3.2).

$$\sigma = \frac{3M}{2\pi R^3} \tag{3.2}$$

and the viscosity is given by equation 3.3

$$\eta = \frac{3M\alpha}{2\pi R^3 \Omega} \tag{3.3}$$

Equation 3.3 gives accurate results under the condition that the cone angle is small enough.

*Parallel plates geometry*

As seen above, the cone-plate geometry has the property to generate an uniform shear rate. In this way the material is equally deformed in all its points. In some cases and for different reasons other geometries are employed. One of these is the parallel plates geometry (shown in figure 3.2).

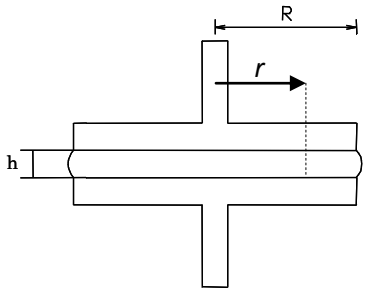


*Figure 3.2: Illustration of the plate-plate geometry*

The shear rate is easily determined by equation 3.4

$$\dot{\gamma} = \frac{\Omega r}{h} \tag{3.4}$$

$\dot{\gamma}$ is clearly variable with the radius. It means that the real viscosity can be measured only for a Newtonian fluid. The Newtonian analysis gives the same expression for the stress used for the cone-plate geometry (equation 3.5).

$$\eta = \frac{2Mh}{\pi R^4 \Omega} \tag{3.5}$$

For non-Newtonian fluids on 3.5 can be also used but it gives an approximate result. In this case, the apparent viscosity is plotted with respect to the maximum shear rate, obtainable from 3.4 imposing r=R (equation 3.6).

$$\dot{\gamma} = \frac{\Omega R}{h} \tag{3.6}$$

For its features, the parallel plates geometry is rarely used for viscosity evaluations while it is preferred for viscoelasticity measures and it can represent a first tool for a rotational rheometer if the budget is limited.

## 3.2 *Viskomat NT*

The rheology characterization of cement mixtures with a conventional rotational rheometer is not a very simple operation. The configuration of a conventional rheometer is in fact not appropriate for several reasons. The main problem is represented by settling, the sedimentation of solid particles on the bottom especially when long times are required to perform the measures To study the rheology of cement and other similar materials particular rheometers have been introduced, like the one illustrated in figure 3.3.

*Figure 3.3: Picture of Viskomat NT*

The Schleibinger Viskomat NT is the rheometer present in the CTG-Italcementi Group laboratories used to perform our experiments. The standard measuring system consists of a stationary probe which is mounted concentrically in a rotating cylindrical sample container (figure 3.4). As the sample flows around the paddle the shear resistance generates a torque which is continuously monitored electronically. The paddle is mounted on a measuring head, which runs up and down automatically to allow for easy filling, emptying and cleaning of the sample container.

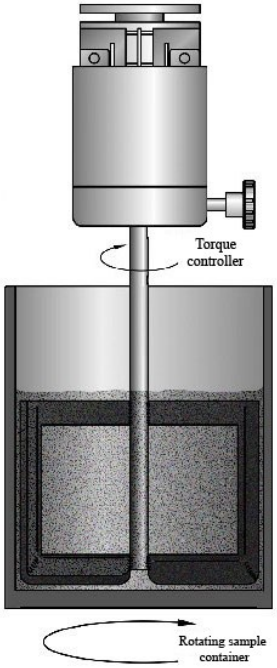


*Figure 3.4: Picture of the cylindrical sample container*

The rheometer uses particular geometries such as vane, screw, anchors, etc. In figures 3.2 some examples have been reported.

*Figure 3.5: Examples of Viskomat NT geometries*

The geometry used for our experiments was a special modified vane geometry (figure 3.6), designed in the CTG-Italcementi Group laboratories and chosen for its particular mixing capacity and the ability to avoid sedimentation.

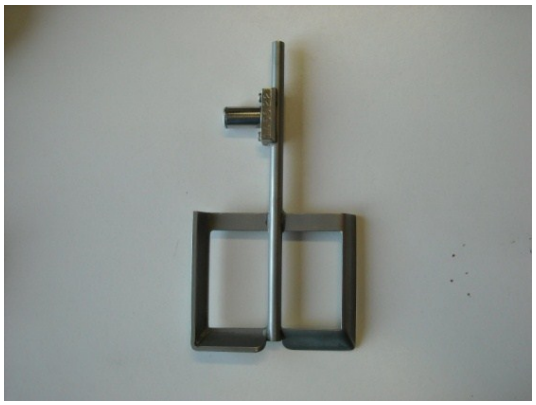

*Figure 3.6: Viskomat NT special geometry*

The torque values can be transformed in viscosity values opportunely modelling the geometry.

## 3.3 Die rheometer

The die rheometer used for the experiments is actually a rheometer derived from an Instron press in order to work with the same principles of a capillary rheometer[95,96]. The capillary rheometer cannot be directly used to measure the viscosity of cement mixtures because of several practical problems, such as their very narrow dies, with a cross-section characteristic dimension in the order of 1 mm, whereas the highly heterogeneous nature of the materials, the dimensions of some components (fibers, fine aggregates) coupled to their high viscosity, require much larger dies. For the above-cited reasons, the experimental rheological study of cement pastes has been recently approached by making use of the so-called ram extrusion methodology. This experimental technique is based on the same principles of the standard capillary rheometers, the main difference being in the use of dies of much larger transversal dimension, in the order of magnitude of 1 cm.

The capillary rheometer is, together with the cone-plate rotational rheometer, the most used rheological instrumentation for the viscosity evaluation of materials. The straight trajectories and the lack of edge effect allow the achievement of extremely elevated shear rates (greater than to 100000 $s^{-1}$). Besides, the possibility to impose high shear rates allows also the characterization of very viscous fluids. The working principle is illustrated in figure 3.7. The fluid is pushed by a piston through the channel of the rheometer and the pressure variation between the entrance and the exit (where generally the pressure is the atmospheric pressure) is measured. If the advancement velocity is known, it is possible to calculate the viscosity of the fluid. The section of the pipe can be of different kinds: circular (the most used), slit die, etc. The equation of the most classical circular section (figure 3.8) are shown in the following.

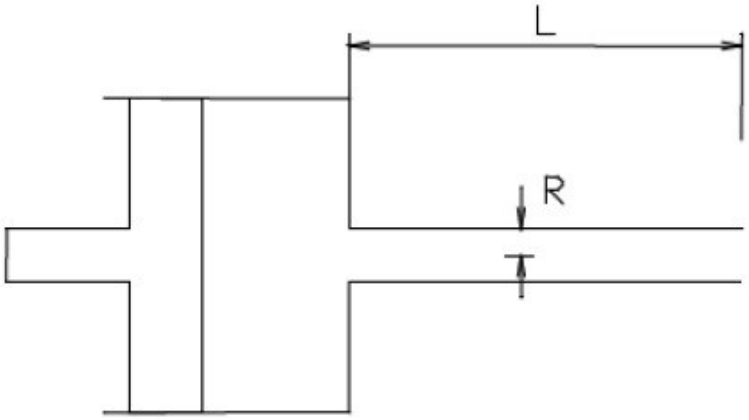


*Figure 3.7: Scheme of a capillary rheometer*

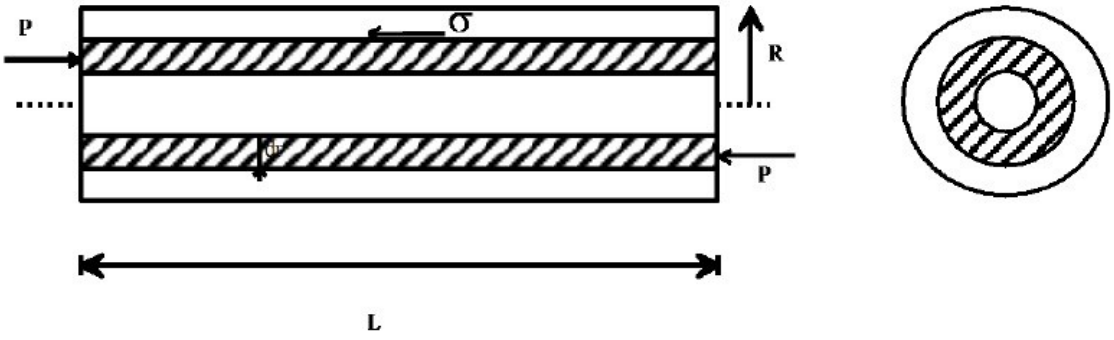


*Figure 3.8: Scheme of a capillary rheometer with circular section*

In a capillary rheometer with a circular section, the surfaces of the flow are concentric cylinders which move in a telescope fashion. Neglecting the entrance effects, in stationary conditions it is possible to make a force balance on a volume delimited by two cylinders of length L and radius, respectively *r* and *r*+*dr*. The only forces acting on this volume along the axial direction are that of pressure and of shear stress. From the force balance along the z direction, a direct link between the pressure difference P and the shear stress on the wall can be easily found (equation 3.7).

$$\sigma_p = \frac{\Delta P}{L}\frac{R}{2} \tag{3.7}$$

where $\Delta P/L$ is the pressure loss for unit length. The following step in this analysis consists in the determination of the radial velocity profile which is easily achievable just for the Newtonian case. In this case, in fact, the equation 3.8 is valid.

$$\dot{\gamma}_{p,N} = \frac{4Q}{\pi R^3} \tag{3.8}$$

Combining equations 3.7 and 3.8, the equation of the rheometer is obtained (equation 3.9).

$$\eta_n = \frac{\pi R^4}{8L}\frac{\Delta P}{Q} \tag{3.9}$$

In the case of non-Newtonian fluids, this kind of rheometer can still be used but the experimental data need a further elaboration, also known as "Mooney-Rabinowitsch correlation". The logic of this correlation is the following: for a non-constant viscosity fluid equation 3.7 is still valid, instead the shear rate on the wall must be corrected to consider the non-Newtonian effects. In the case of a shear-thinning fluid, for example, the velocity profile results to be flatter in the middle and steeper near the wall. The opposite situation is observable for a shear thickening fluid. The correlation of Mooney-Rabinowitsch (the mathematical details are reported in the Appendix I) is reported in equation 3.10.

$$\dot{\gamma}_p = \dot{\gamma}_{p,N}\frac{3n+1}{4n} \tag{3.10}$$

where *n* is

$$n = \frac{dlog\tau_p}{dlog\dot{\gamma}_{p,N}} \tag{3.11}$$

The parameter *n* is in fact the slope of the double-logarithmic scale graph where the shear stress at the wall is reported as a function of the Newtonian shear rate, also called "apparent shear rate". Summarizing, the determination of a non-Newtonian fluid viscosity with the capillary rheometer (the same procedure is also valid for the die rheometer) is the following:

- For different flows several measurements of pressure loss are obtained; this allows to obtain the shear stress on the wall and the correspondent apparent shear rate.
- The calculated values of $\boldsymbol{\sigma}_p$ are reported in graph as a function of $\dot{\gamma}_{p,N}$. In this way, the parameter n is achievable from the slope of this graph.
- The viscosity value is calculated from the ratio $\sigma_p/\dot{\gamma}_p$.

The viscosity curve is easily obtainable repeating the last two steps for different values of $\dot{\gamma}_{p,N}$.

The capillary rheometers present on the market belong to two kinds: imposed-flow rheometers and pressure-imposed rheometers. In the first, the fluid flow through the pipe is controlled for example pushing a piston with a fixed velocity. In the second, instead, an assigned pressure is applied in several ways to the fluid from the entrance. In both cases, generally, the exit pressure is the atmospheric pressure and the pressure difference **Δ**P is measured by a transducer. The membrane of the transducer is flat and cannot be hosted on the curve surface without disturbing the flow and the measurements of the pressure is influenced by the complex flow which has origin in the entrance zone. The lines of the flow are reported in the figure 3.9.

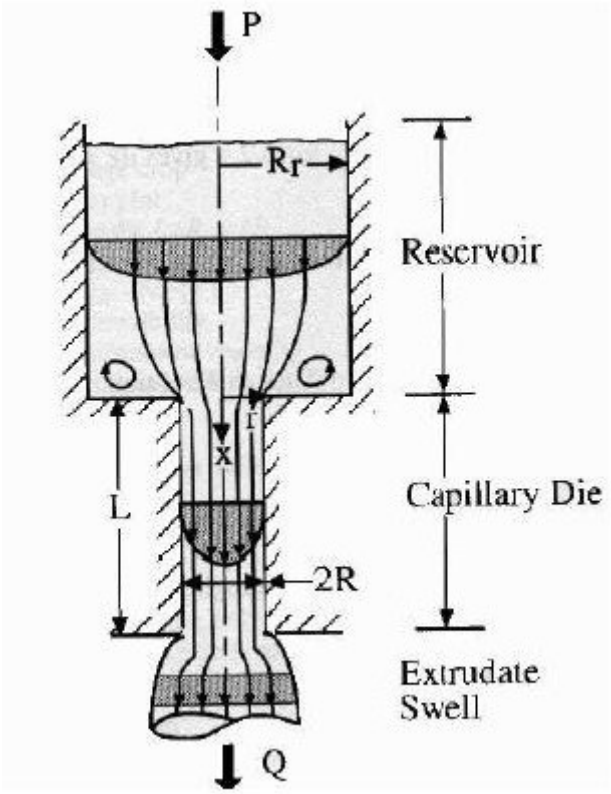


*Figure 3.9: Flow lines in the entrance zone of the capillary rheometer*

As visible, in the entrance zone a strong component of extensional flow is present and this situation determines a further energy dissipation. Consequently, the pressure measured before the contraction is given by the sum of the pressure losses along the capillary and those of the entrance zone. To determine these contribution and to obtain a correct viscosity value, a special procedure must be

adopted. This procedure is called “Bagley correction” and it is also illustrated on details of the Appendix I.

# *Experimental results: systems for coating*

# EXPERIMENTAL RESULTS: SYSTEMS FOR COATING

The experimental procedure has followed two parallel ways, each one centred on a specific kind of system. The systems for coating are in fact very different from the systems used for extrusion: in the first the main ingredient is, as imaginable, water while in the second the quantity of the liquid phase is much smaller respect to the solid content. As a consequence, the rheology of these systems differs very deeply, not only because of the difference in water /cement ratio (or better water /solid ratio) but mainly because the additives, which are the major responsible for the viscosity change, are present in various proportions. Also the preparation protocol of the samples radically differs from one system to another.

In the following pages, the experimental results of the work are reported, going from the systems for coating ( less concentrated) to the systems for extrusion (more concentrated).

## *4.1 Rheological study of a commercial paint*

As seen above, cement is a very complex mixture of inorganic phases. For this and other reasons, a cement-based paint is very different from a classical paint. The latter is generally a suspension of polymers and other organic and inorganic compounds. In the case of cement-based paints the solvent is water, while in the case of classical paints it can be also an organic volatile solvent. The rheology of the cementitiuos system is different to study and to predict, and the only rheological standard reference available for this purpose is represented by the classical commercial paints. For these reasons, a preliminary study of a common paint has been performed.

The paint, a commercial paint produced by Boero (Litosil), has been diluted, as indicated by the producer, with a 15% wt. of water. As discussed above, the choice of this picture is not arbitrary but the result of some considerations on its composition and its applicability. The first test performed is a stress sweep test, which gives the response of the viscosity to an increasing or decreasing stress. In particular an increasing stress from 1 to 300 Pa was applied; the resulting viscosity curve is reported in the figure 4.1.

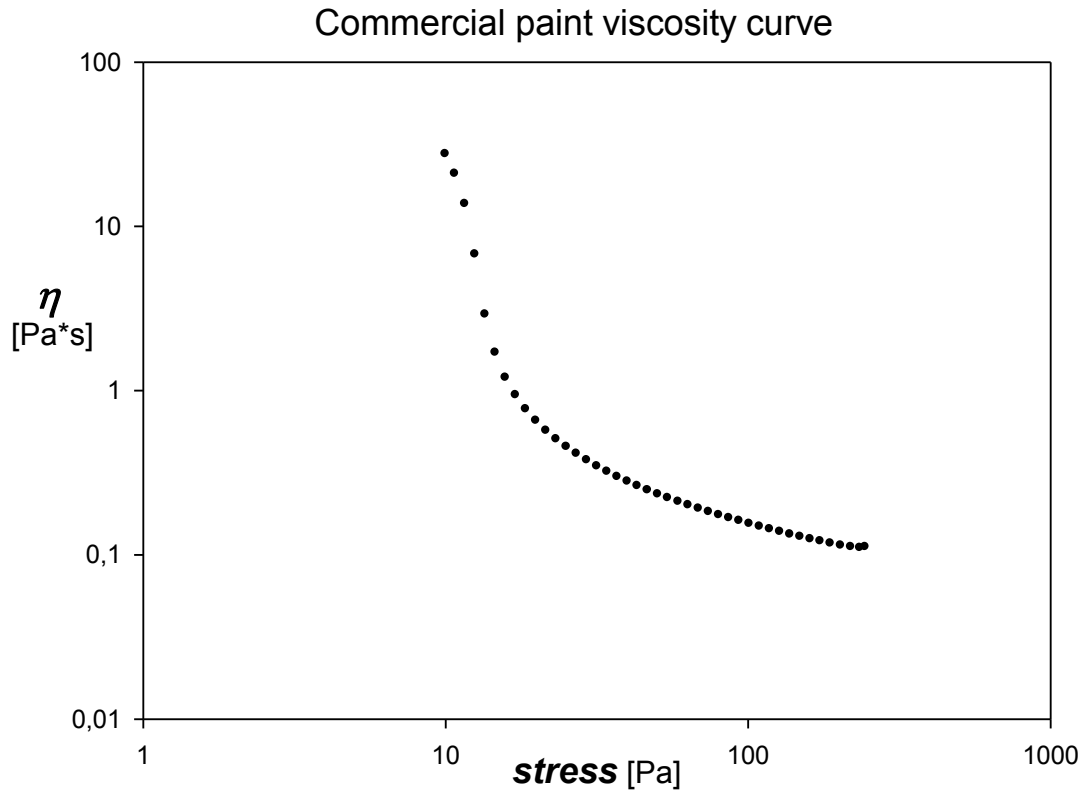


*Figure 4.1: Viscosity curve of the commercial paint*

The viscosity starts from very high values, passing through a short plateau for a stress of about 10 Pa. A sharp decrease of viscosity of about two orders of magnitude follows at high stresses. In the high shear stress zone the decreasing of viscosity continues but in a less marked way. Overall the paint presents a shear thinning behaviour. The sudden increase of viscosity for stress values less than 1 Pa suggests a Bingham-fluid behaviour. This is confirmed by plotting the stress as a function of the shear rate, as shows figure 4.2. The fluid presents high viscosity values in the region of stress between 1 and 10 Pa; passing this zone, it begins to flow with a roughly linear trend.

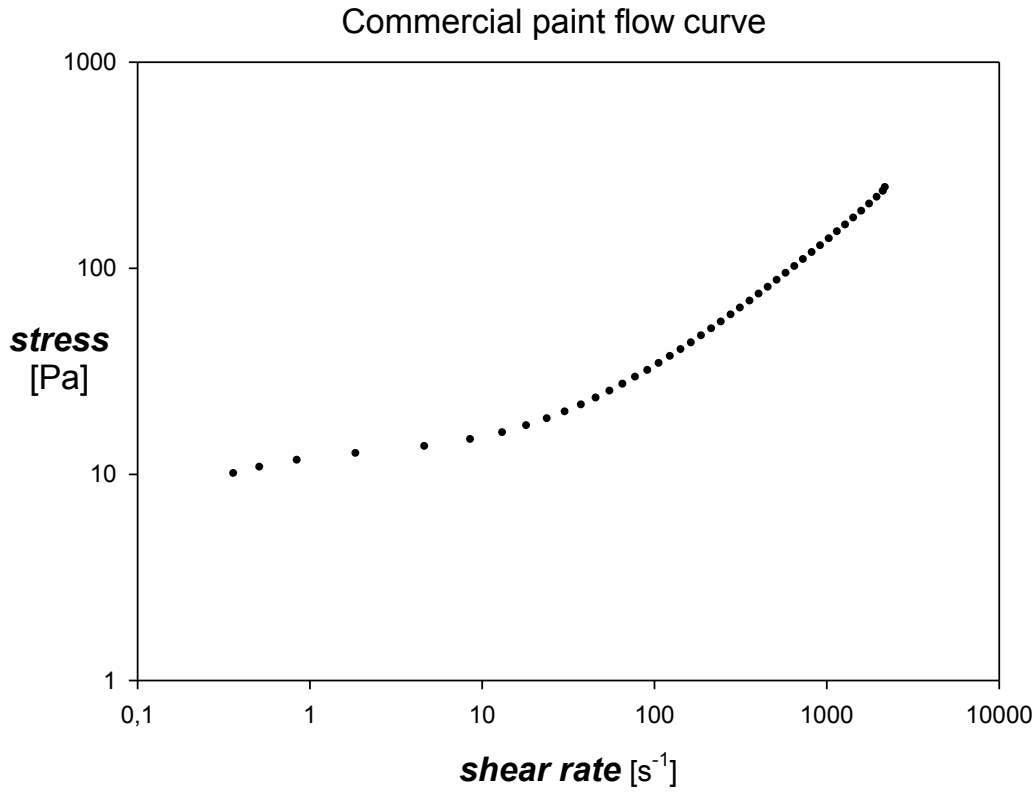


*Figure 4.2: Flow curve of the commercial paint*

A frequency sweep test at 100 Pa with an increasing frequency has been also performed with the paint sample to analyse the viscoelastic behaviour of this material. As it is clear from figure 4.3, the paint presents a viscous component that prevails on the viscous component (G" is always higher than G').

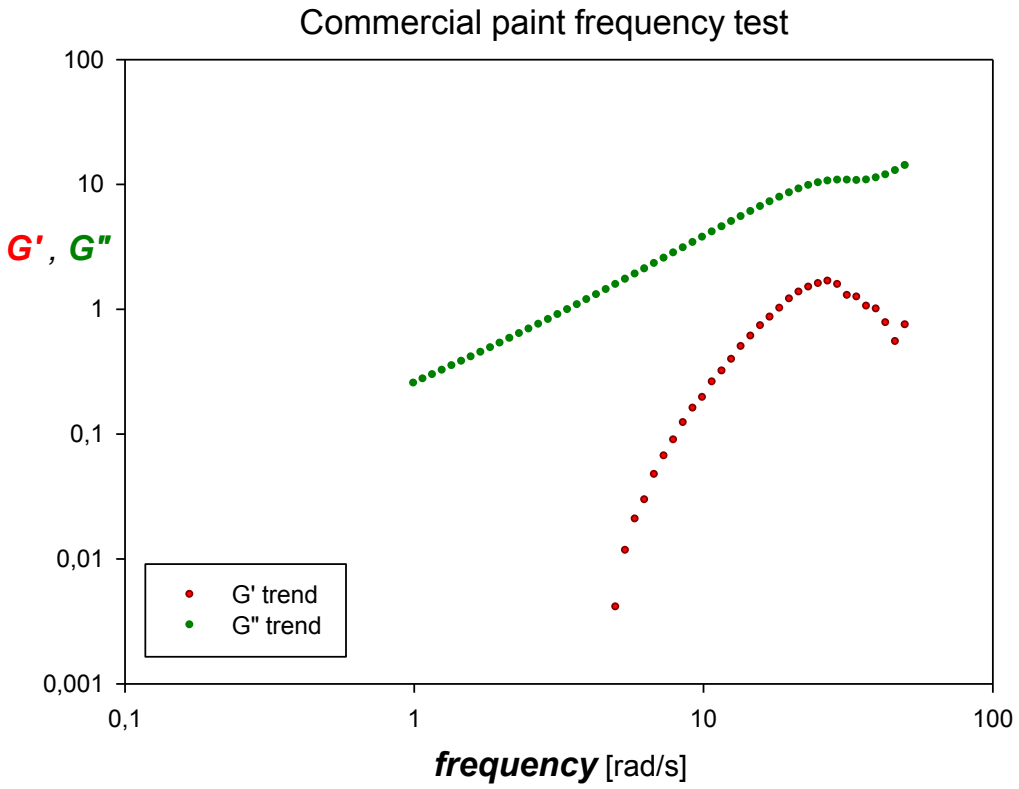


*Figure 4.3: Frequency analysis of the commercial paint*

To analyse the behaviour of a fluid under a constant stress action, the creep experiments are generally employed.; in this case the fluid deformation is put in relation to the value of the imposed stress. To perform a creep experiment, following a well-defined protocol is very important. With this aim the first creep experiment has been performed with a 300 Pa stress imposed for a time of 30 s to completely destroy the original microstructure of the material, then the fluid has been kept at rest for 180 s. Then, on the same sample a test with a 2 Pa stress has been launched for 120 s followed by a resting time of 180 s once again. The initial test to destroy the microstructure has been then performed followed by a resting time of 180s, and so on, testing the same sample with the following stress values: 2 Pa, 4 Pa, 8 Pa, 16 Pa, 32 Pa, 64 Pa, 128 Pa. Figure 4.4 shows results of the creep experiments.

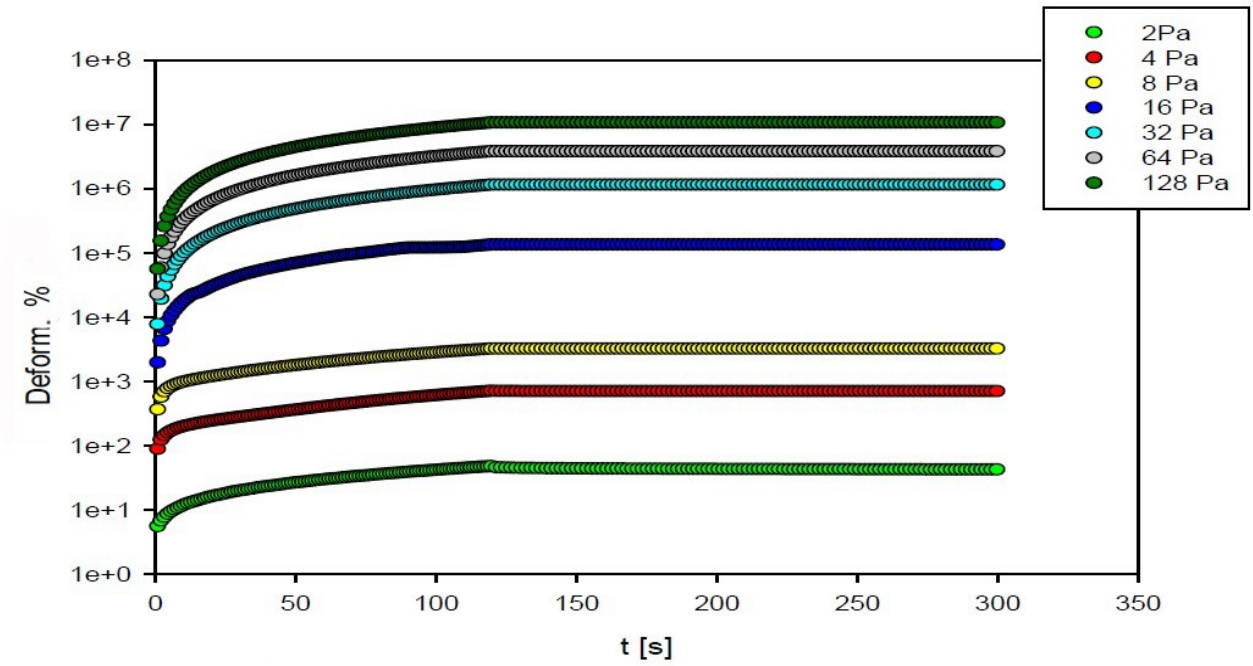


*Figure 4.4: Creep experiments of the commercial paint*

The experiments evidence that the paint has a sort of transition in the rheological behaviour which occurs around the 10 Pa stress zone. In this point, in fact, the paint passes from a viscoelastic behaviour (visible at low stress values) to a viscous behaviour (visible at high stress values).

A final test has been performed on the paint evaluating the presence of thixotropy. Thixotropy is the property of certain gels or fluids that are thick (viscous) under normal conditions, but become thin (less viscous) over time when shaken, agitated or otherwise stressed. To evaluate the presence of this particular feature, a common test generally performed consists in increasing the stress applied to the sample from zero to a fixed value according to a well-defined ramp, then decreasing the stress back to zero. The presence of hysteresis will give the proof of a thixotropic behaviour. In figure 4.5 the results of this experiment are reported.

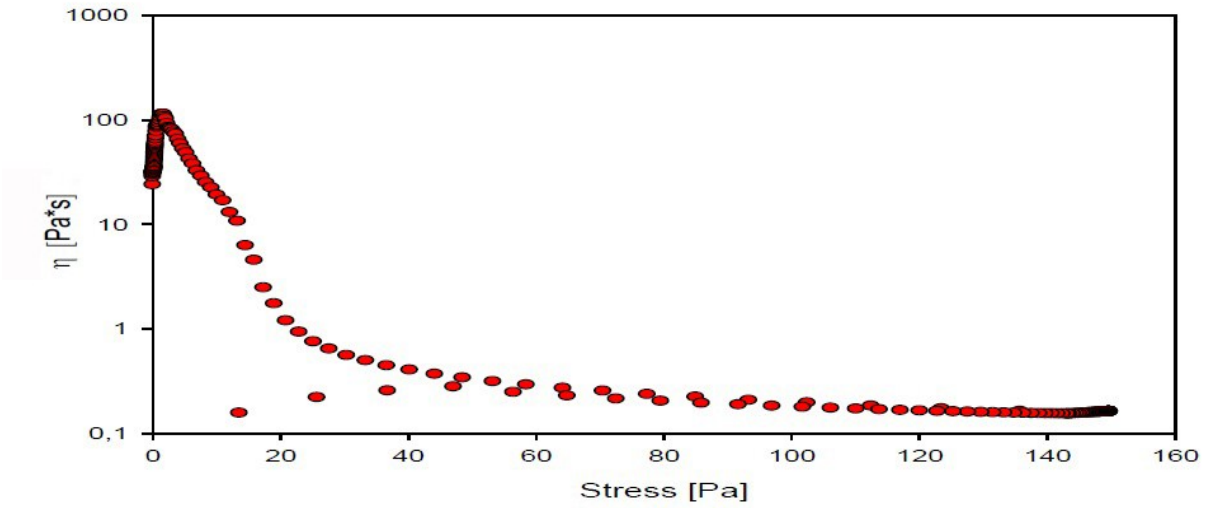


*Figure 4.5: Test to evaluate the presence of thixotropy in the commercial paint*

The paint clearly presents a thixotropic behaviour. The latter is very common for paints and this is the reason why generally painters have to mix the paint to allow for an easier application.

## *4.2 Rheological study of different RMs solutions*

As the RMs are the substances directly involved in the change of viscosity, a preliminary study of the viscosity curve of several rheology modifiers of different chemical nature and different molecular weights has been necessary. With this aim, seven RMs with different molecular weight and different substitution typology have been analysed with two concentrations (0.37% and 0.75%wt.) in limewater. Limewater was used to have a chemical matrix as close as possible to the chemical environment of cement-based formulations and it was prepared by dissolving $Ca(OH)_2$ on saturation in bidistilled water; the correct alkalinity of the solution (about 12 pH points) was checked with a standard pHmeter. The curves obtained are reported respectively in figures 4.6 and 4.7.

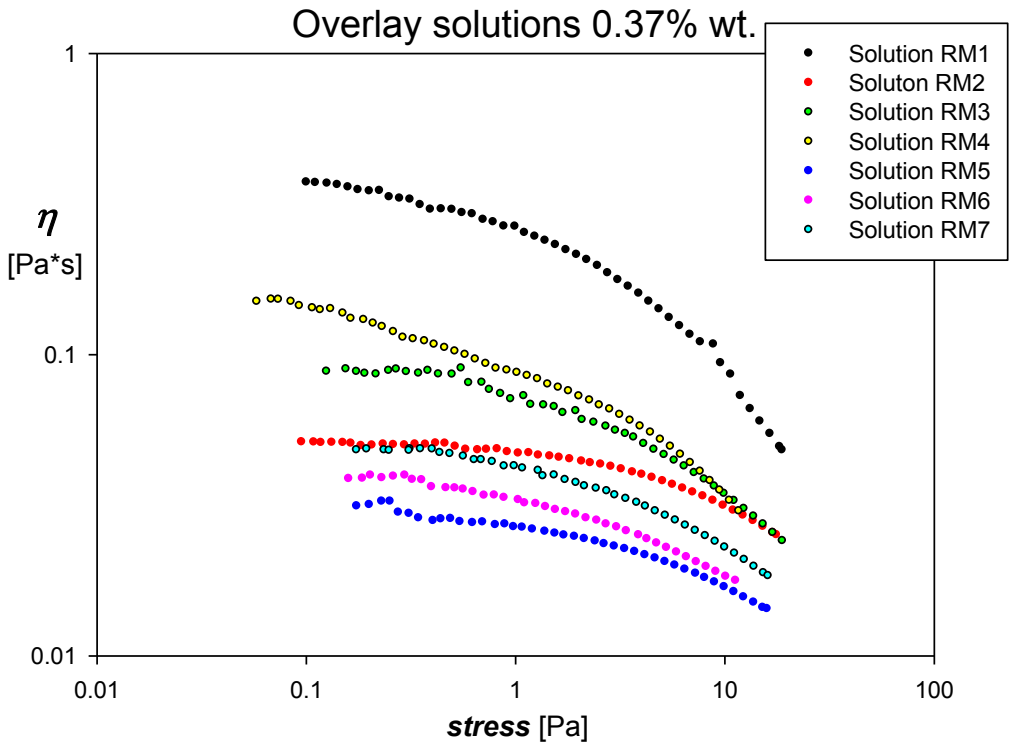


*Figure 4.6: Overlay of the viscosity curves of 0,37%wt. RMs solutions*

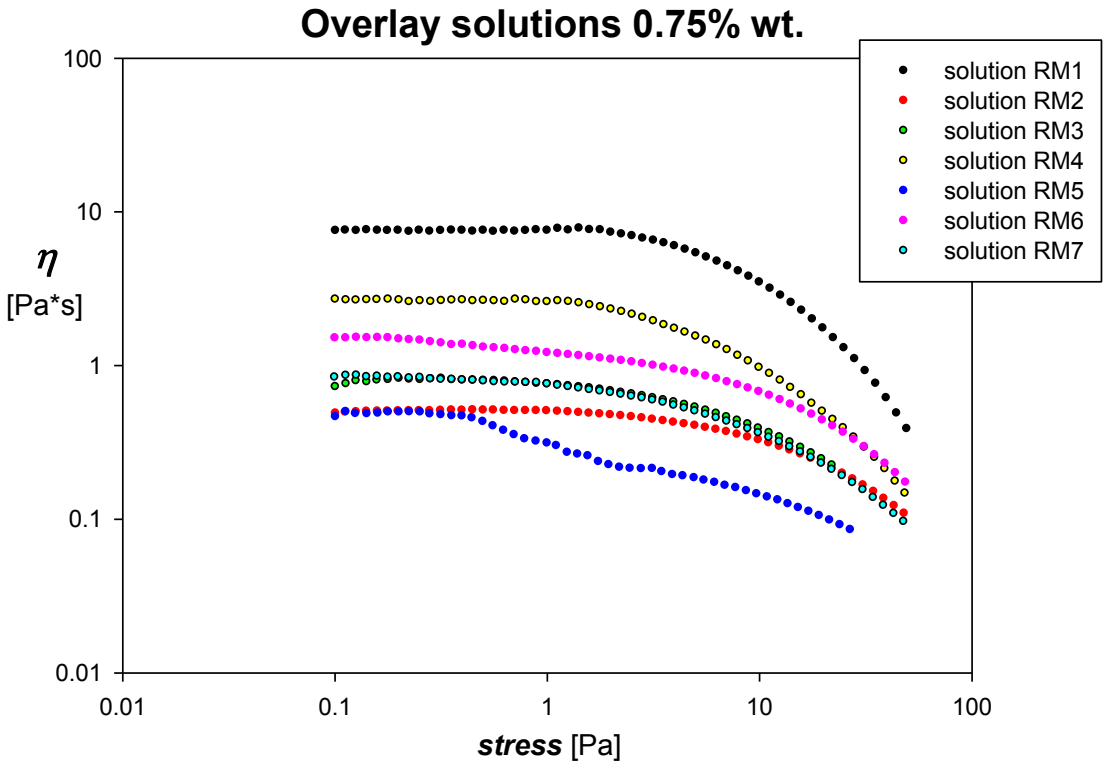


*Figure 4.7: Overlay of the viscosity curves of 0,75%wt. RMs solutions*

The viscosity of the curves are different depending both on the molecular weight and also on the water affinity, which is directly dictated by the chemical nature of the RMs. This is also an explanation for the different order visible between the curves represented in the two graphs. All the curves present a typical shear-thinning behaviour which is very common for many polymeric solutions; this effect is enhanced with the increase of concentration.

To understand the role of the SP in the rheological behaviour of these aqueous solutions, other experiments have been performed on the RM alkaline solutions containing also this kind of additives; in figures 4.8-4.11 the comparison between the viscosity curves of the samples with and without SPs are proposed.

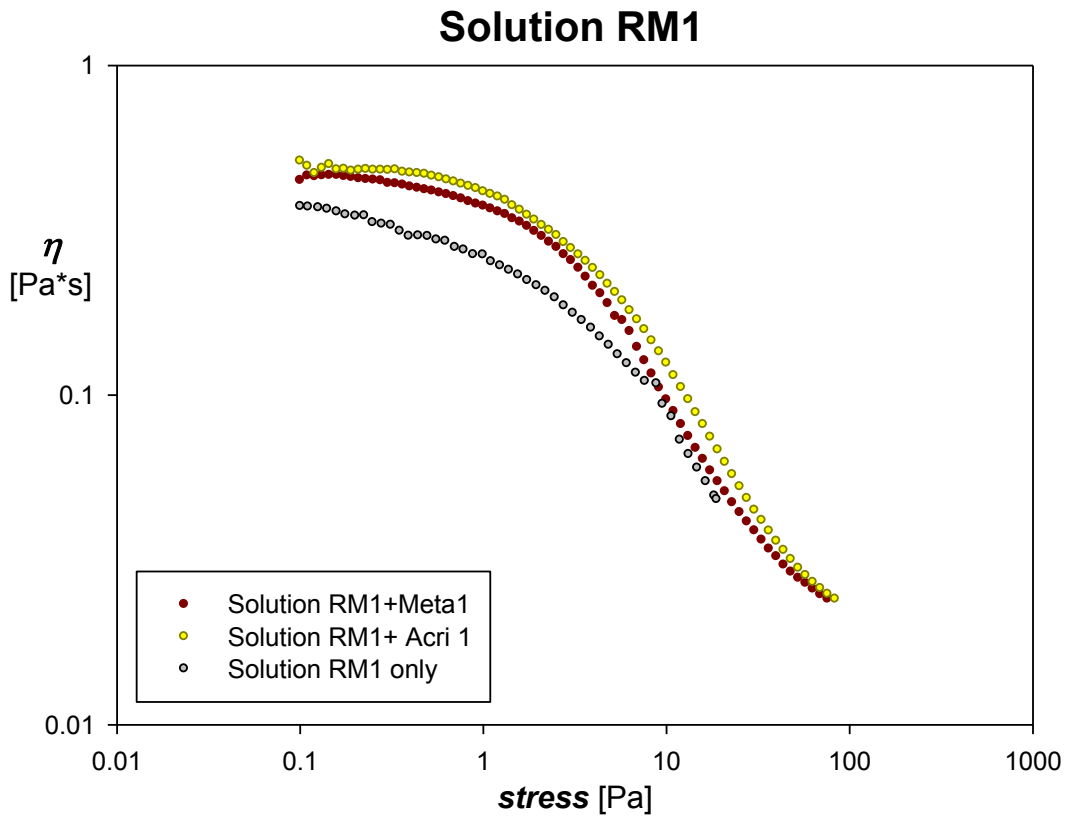


*Figure 4.8: Comparison between the viscosity curves of RM1 solutions with and without SPs*

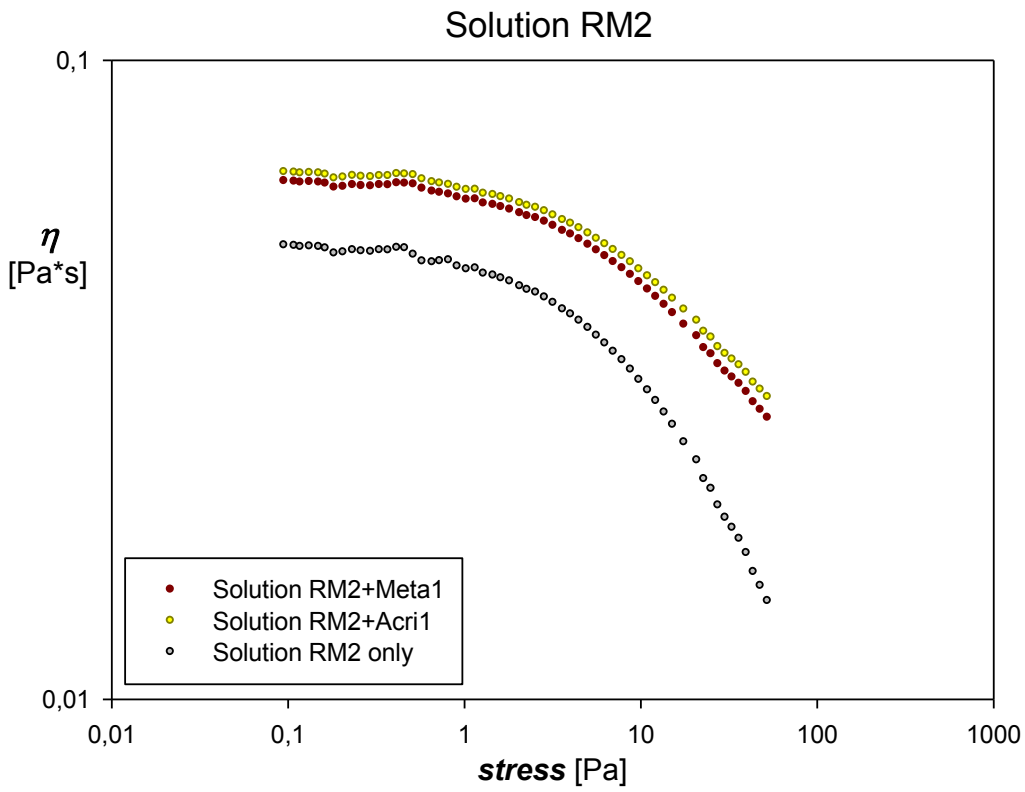


*Figure 4.9: Comparison between the viscosity curves of RM2 solutions with and without SPs*

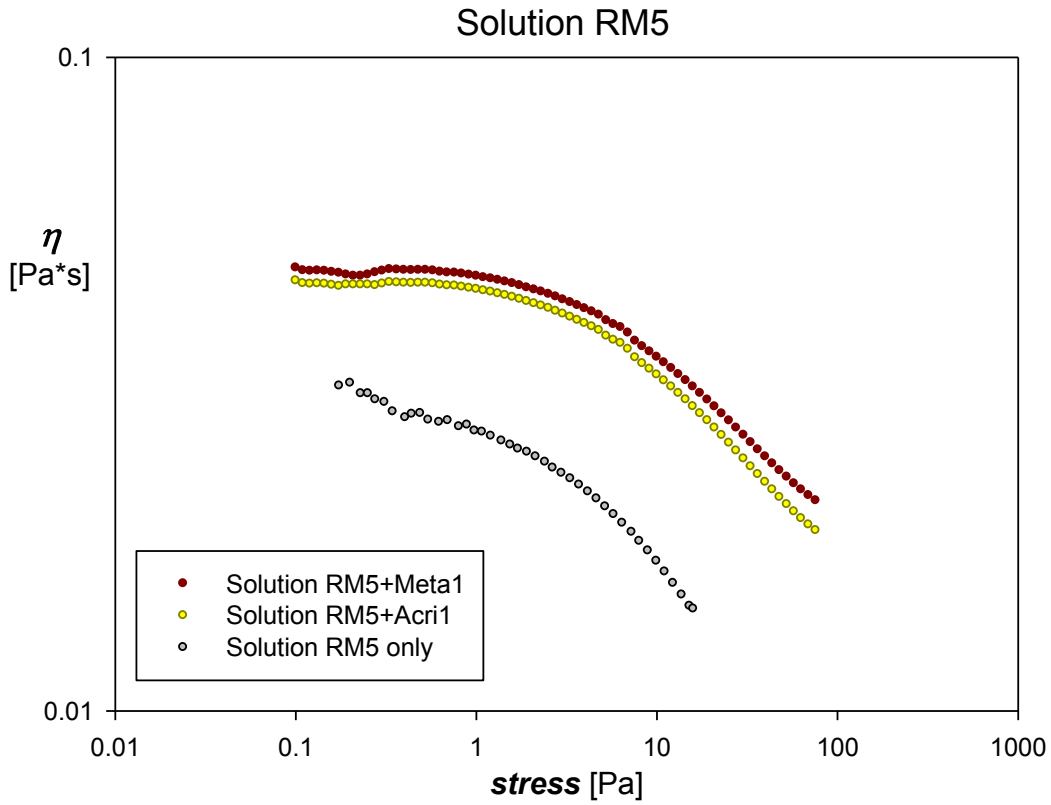


*Figure 4.10: Comparison between the viscosity curves of RM5 solutions with and without SPs*

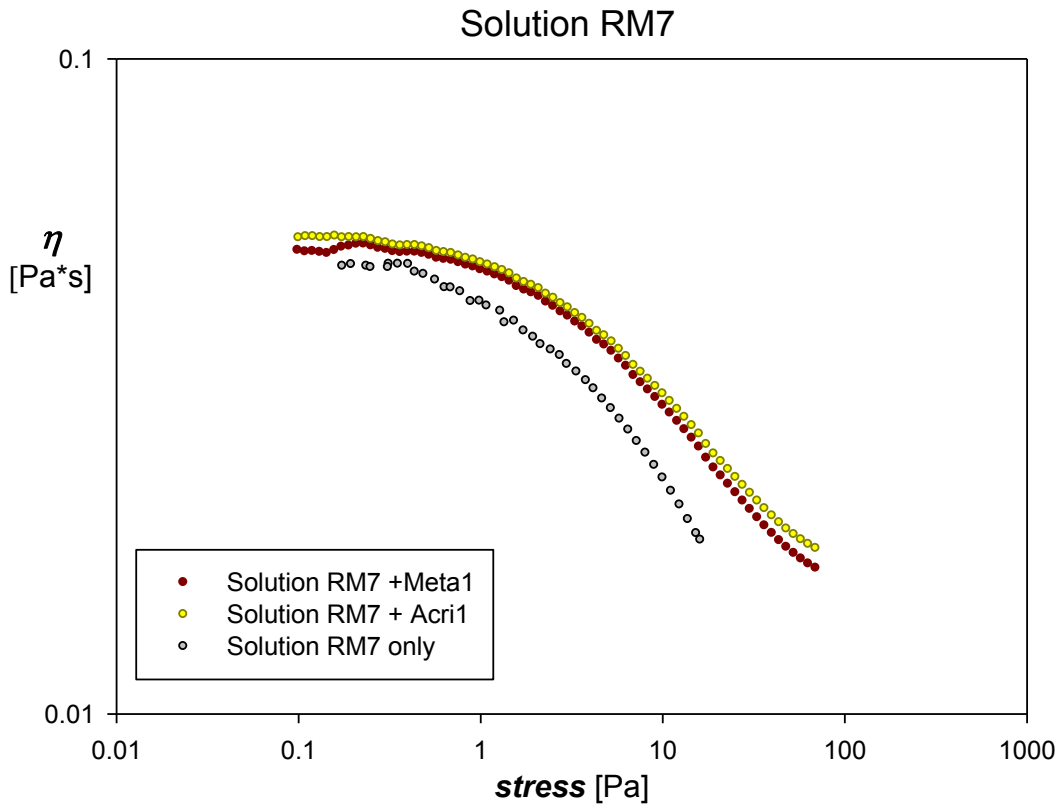


*Figure 4.11: Comparison between the viscosity curves of RM7 solutions with and without SPs*

The four graphs evidence that there is an interaction between RM and SP which leads to an increase of the viscosity of the solutions, but no great differences are visible between the solutions containing the SP Meta1 and the solutions containing SP Acri1.

## 4.3 Rheological study of experimental cement-based paints

In order to understand the possible correlations between the rheological behaviour of the simplified systems (represented by the aqueous solutions of the additives) and the real systems (represented by the formulations containing cement and all the other "ingredients") some experimental Portland cement-based paints have been prepared using the same additives in the same proportions used for the solutions (the complete formulations are confidential). The analysis of these paints have been performed on the Viskomat NT rheometer in the laboratories of CTG-Italcementi Group, according

to the experimental procedure extensively described in the Appendix II. The results are reported in the figures 4.12 and 4.13.

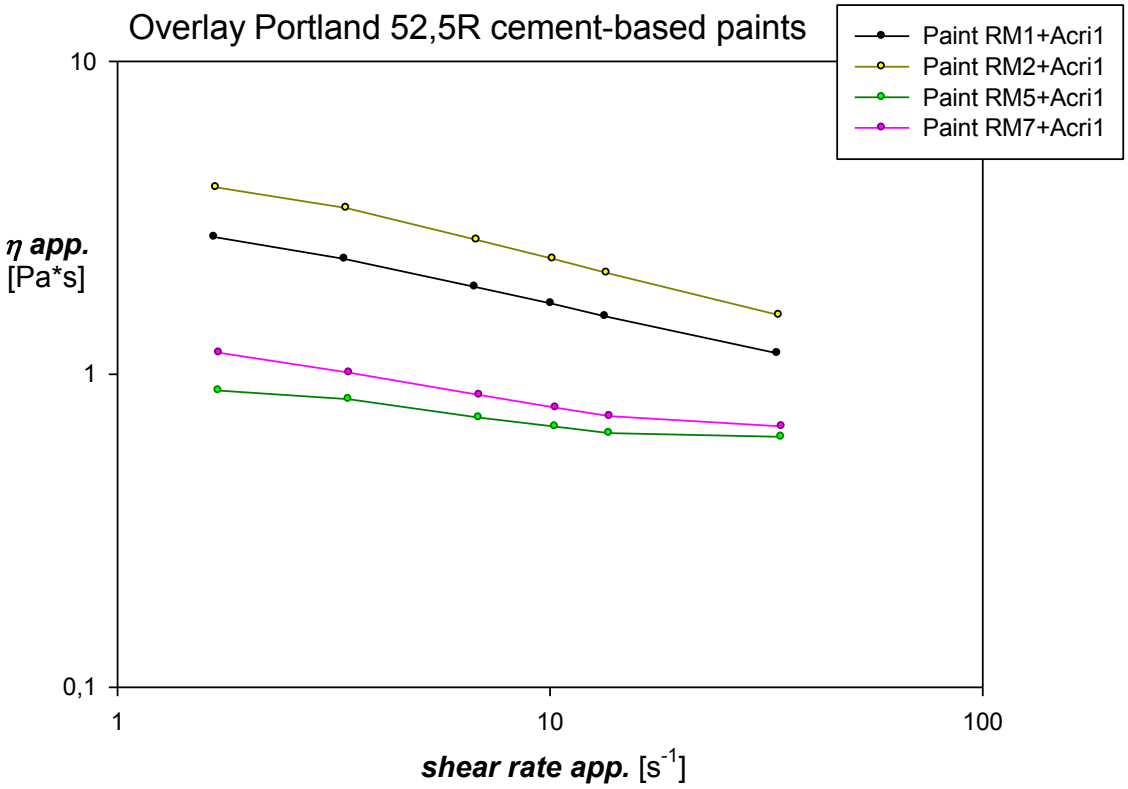


*Figure 4.12: Overlay between the viscosity curves of cement-based paints with Acri1*

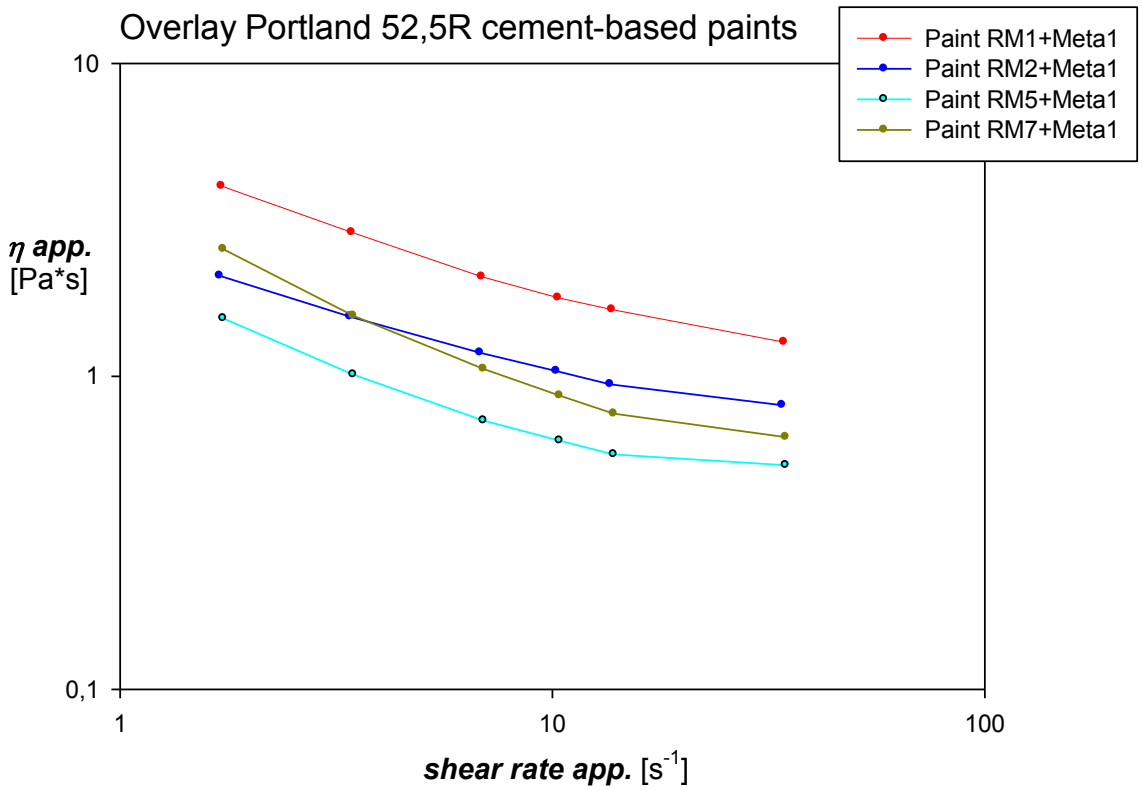


*Figure 4.13: Overlay between the viscosity curves of cement-based paints with Meta1*

The curves reported show two different behaviours: the paints prepared with the metacrylic SP change their viscosity very rapidly with increasing shear rate. The slope of their curves is also more marked. In any case, the behaviour of both kinds of paints is shear thinning, as desirable in all paints. A further observation suggests that the difference of viscosity is not so accentuated as in the case of the aqueous solutions prepared with RM and SP. This effect is very probably due to rheological effects introduced by the addition of cement and other dry materials to the aqueous components. In figures 4.14-4.21 the comparisons between the solutions and the relative paints are reported.

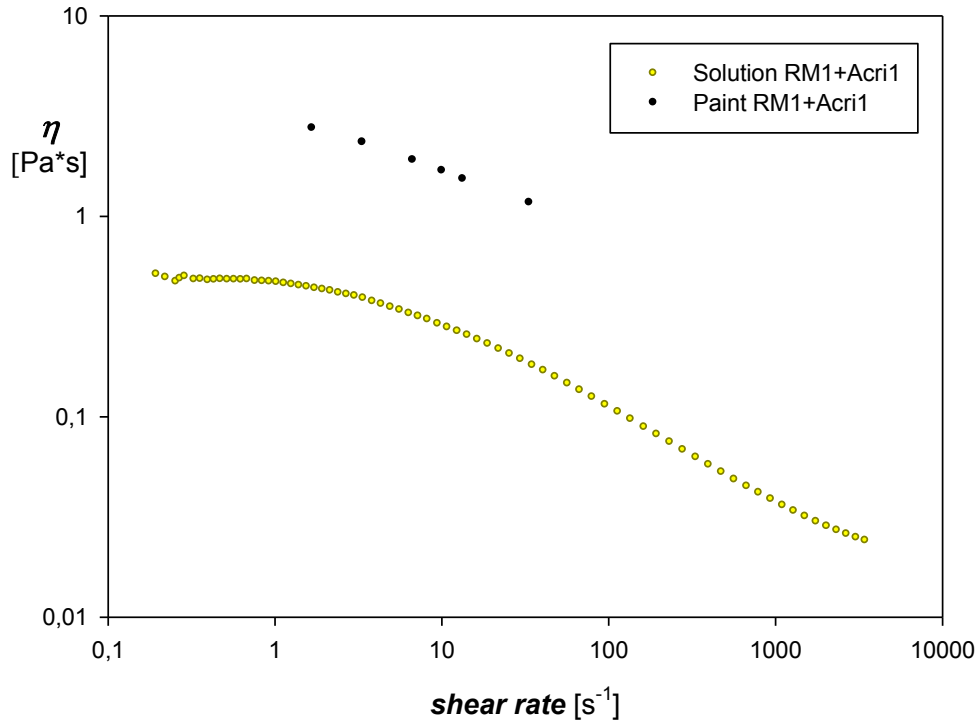


*Figure 4.14: Comparison between solution and paints (RM1+Acri1)*

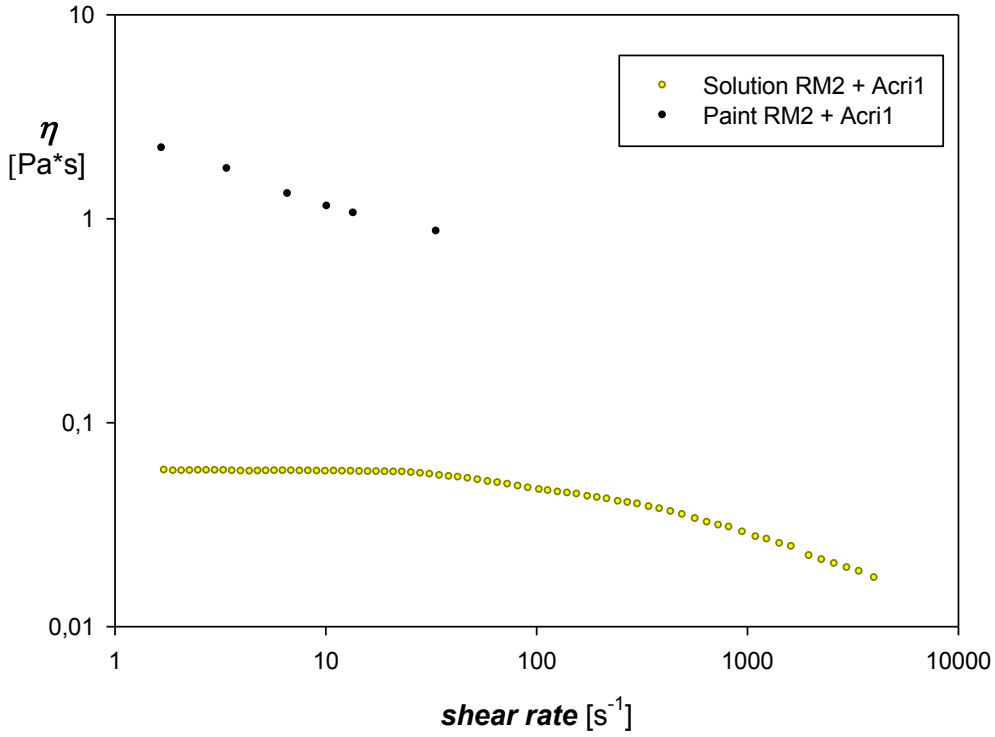


*Figure 4.15: Comparison between solution and paints (RM2+Acri1)*

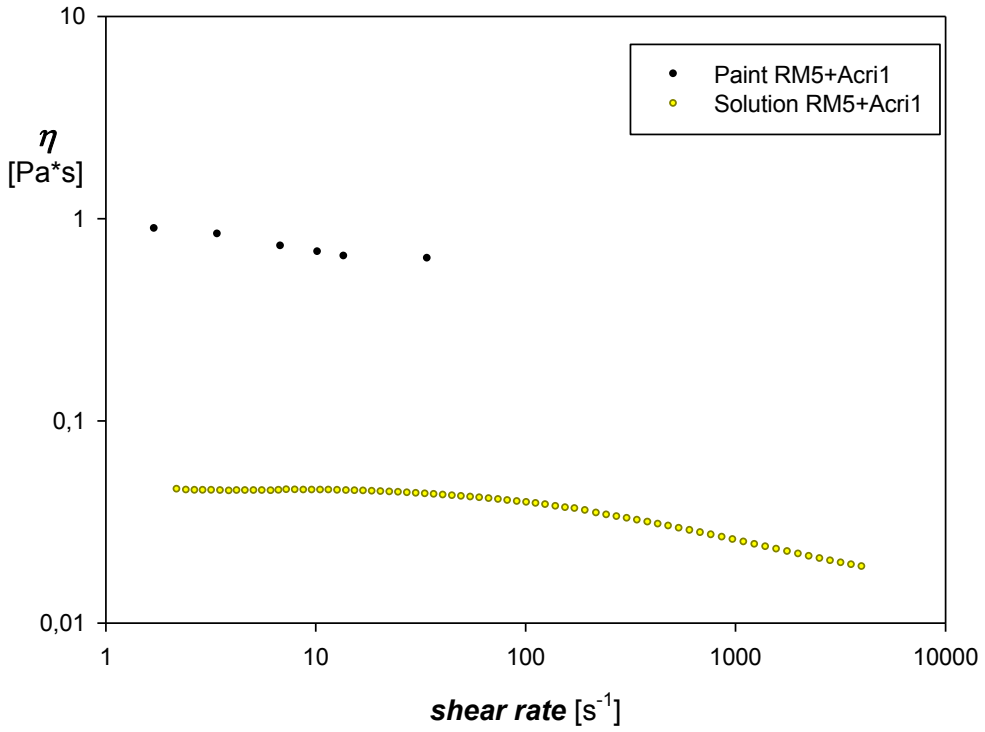


*Figure 4.16: Comparison between solution and paints (RM5+Acri1)*

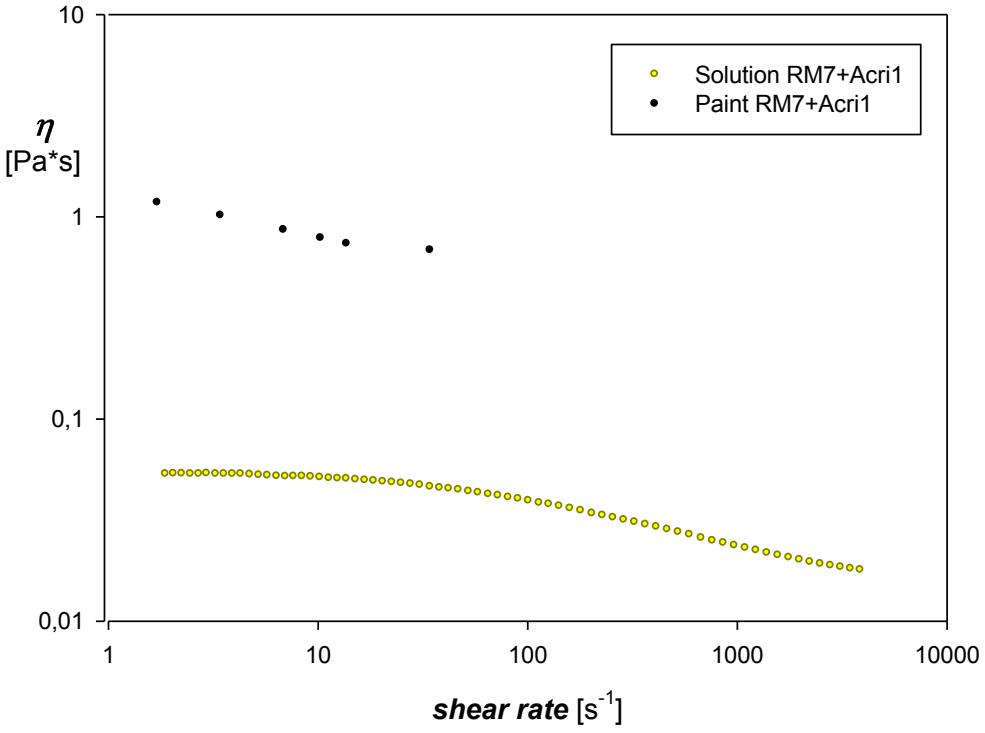


*Figure 4.17: Comparison between solution and paints (RM7+Acri1)*

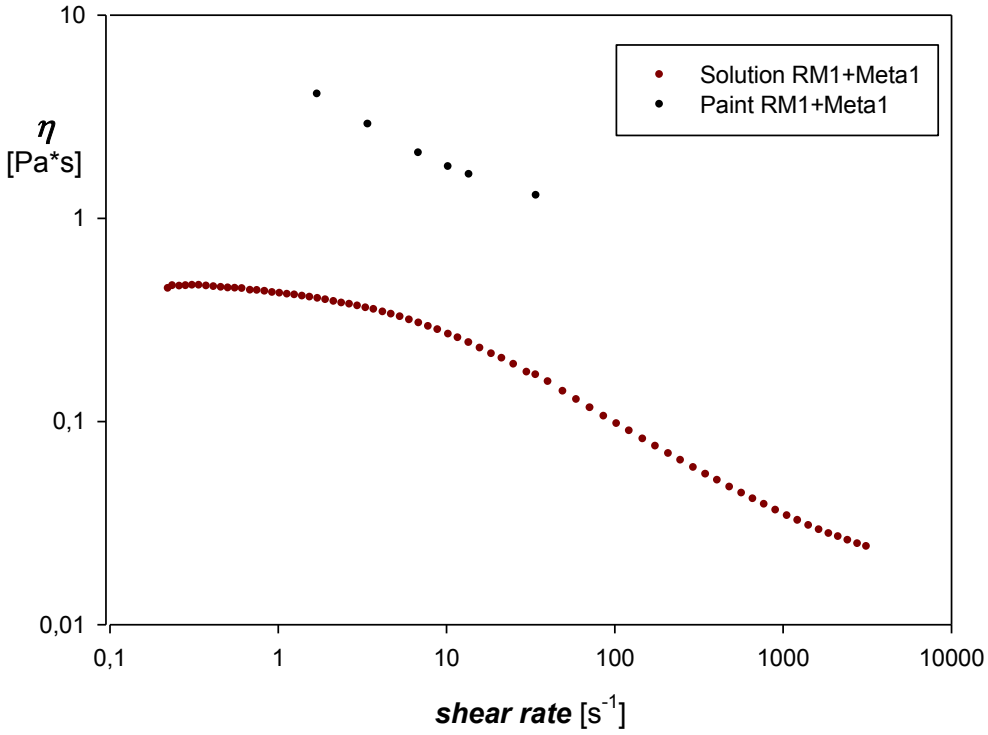


*Figure 4.18: Comparison between solution and paints (RM1+Meta1)*

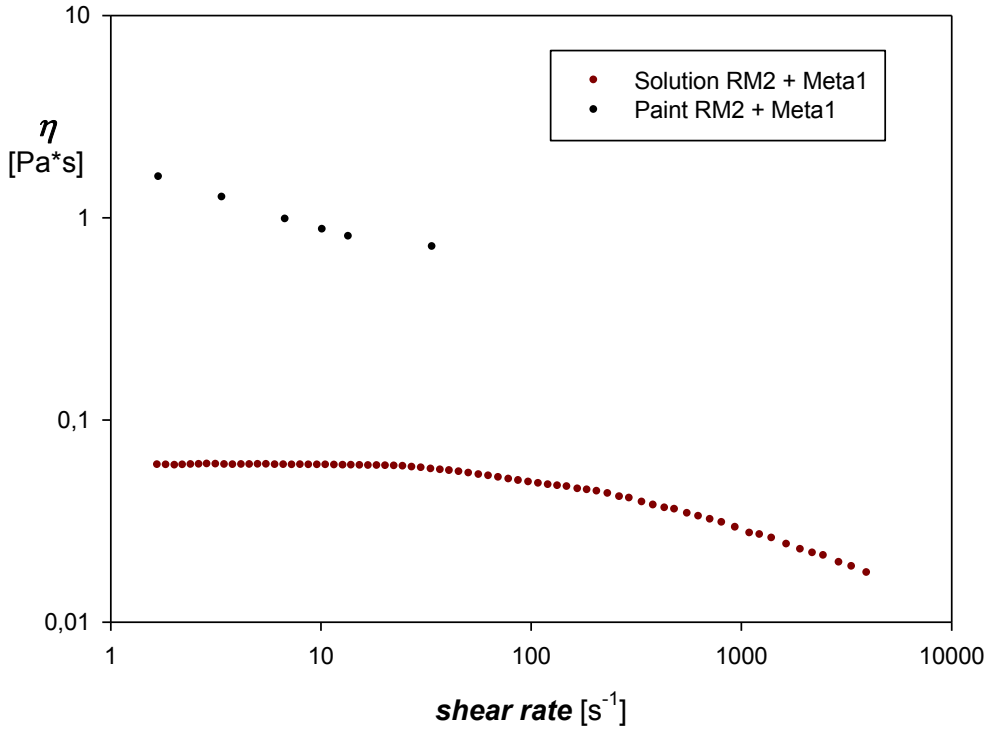


*Figure 4.19: Comparison between solution and paints (RM2+Meta1)*

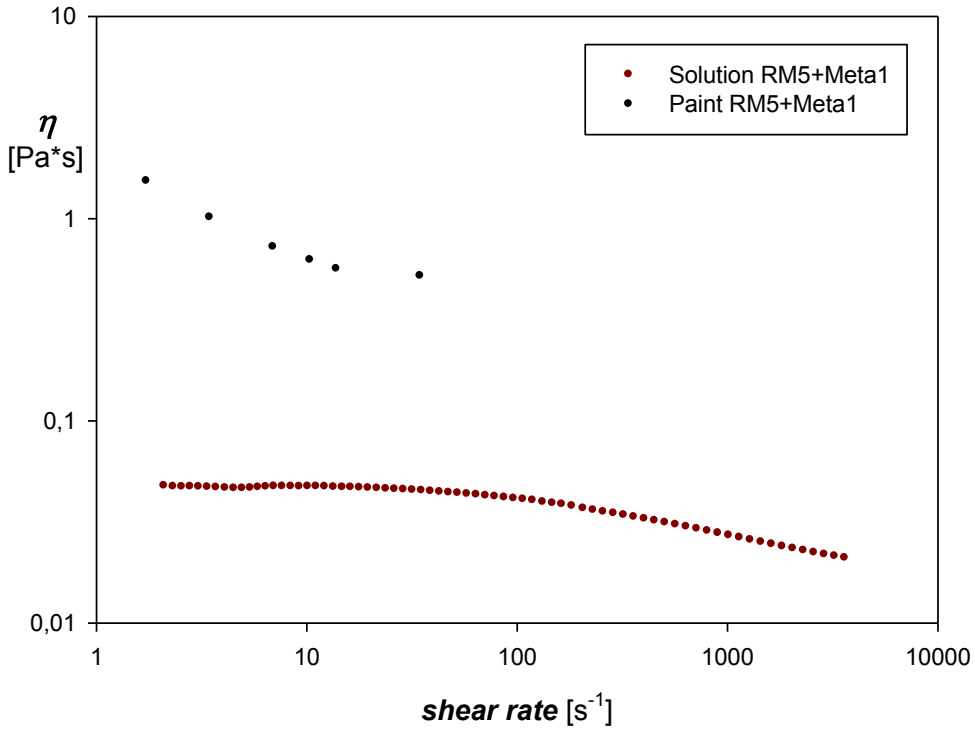


*Figure 4.20: Comparison between solution and paints (RM5+Meta1)*

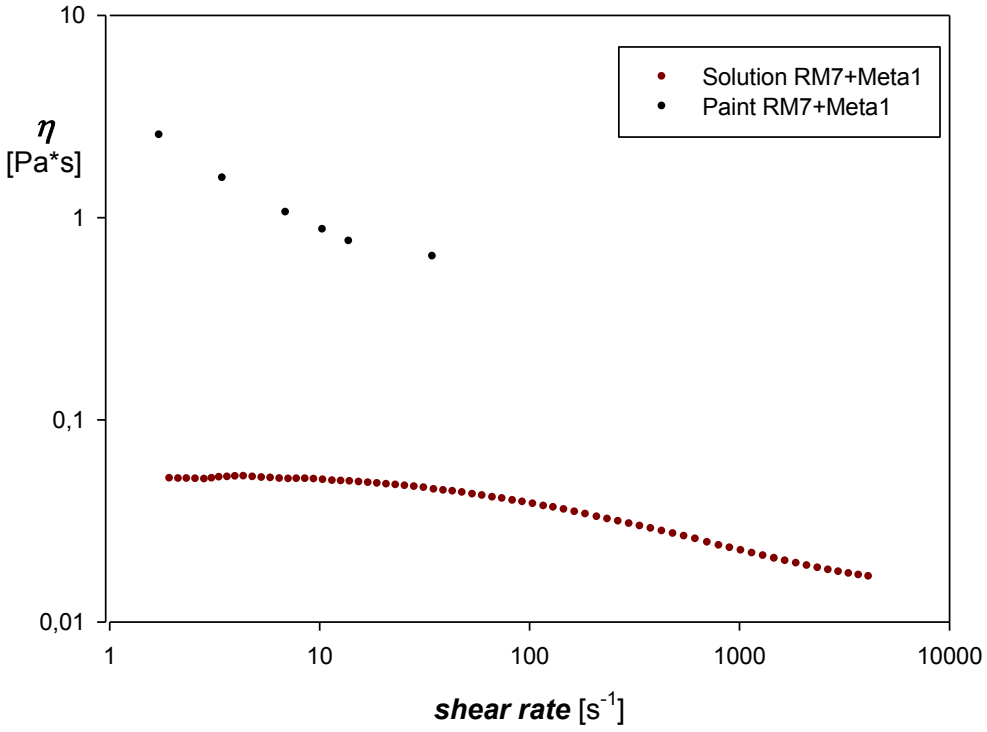


*Figure 4.21: Comparison between solution and paints (RM7+Meta1)*

A clear comparison between the aqueous solutions and the paints seems not possible, in the sense that to make a forecast of the rheological behaviour of a paint does not seem possible starting from the rheological behaviour of the aqueous solution prepared with the same RM and the same SP. This problem is of great practical importance because the equipment to prepare and to test the cement-based paint is not conventional and requires specialised laboratories. In spite of that, the order of viscosity is well respected in both sequences (paints and solutions): the most viscous aqueous solution give the most viscous paint and this can be a good starting point for the realisation of a new paint.

In figures 4.22 and 4.23 the viscosity vs. stress curves are reported for a complete description of the phenomena.

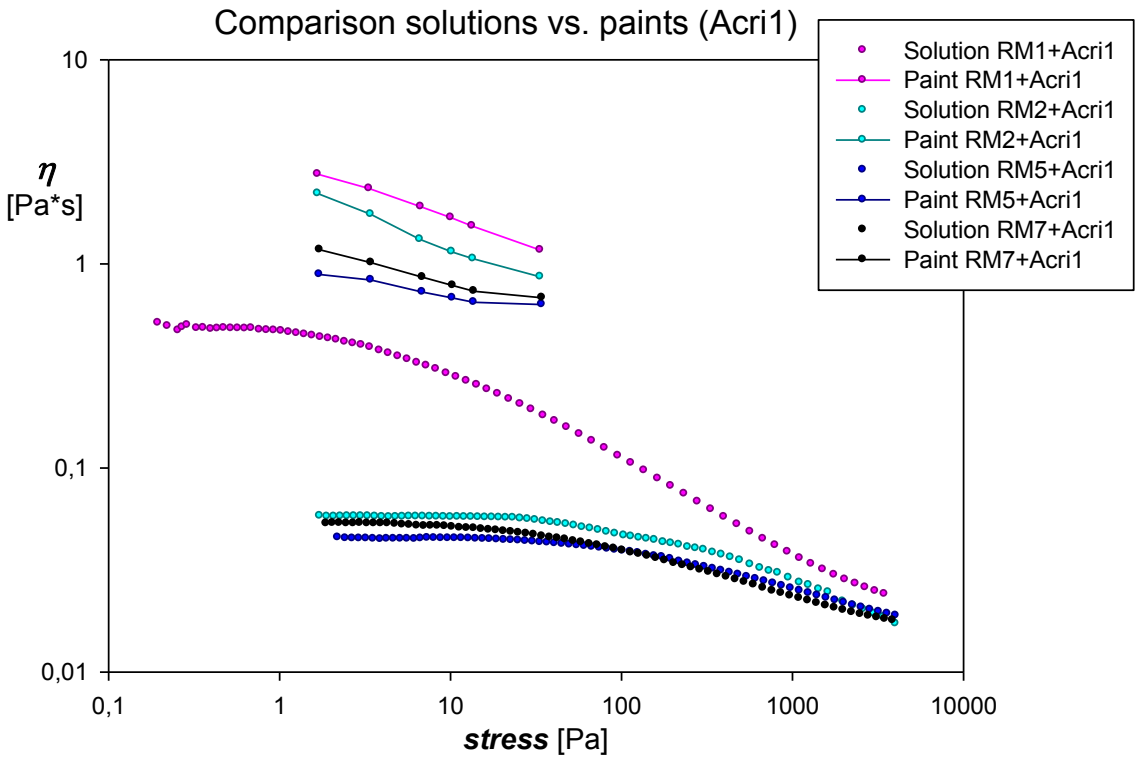


*Figure 4.22: Overlay of the viscosity vs. stress curves of the aqueous solution and paints prepared with SP Acri1*

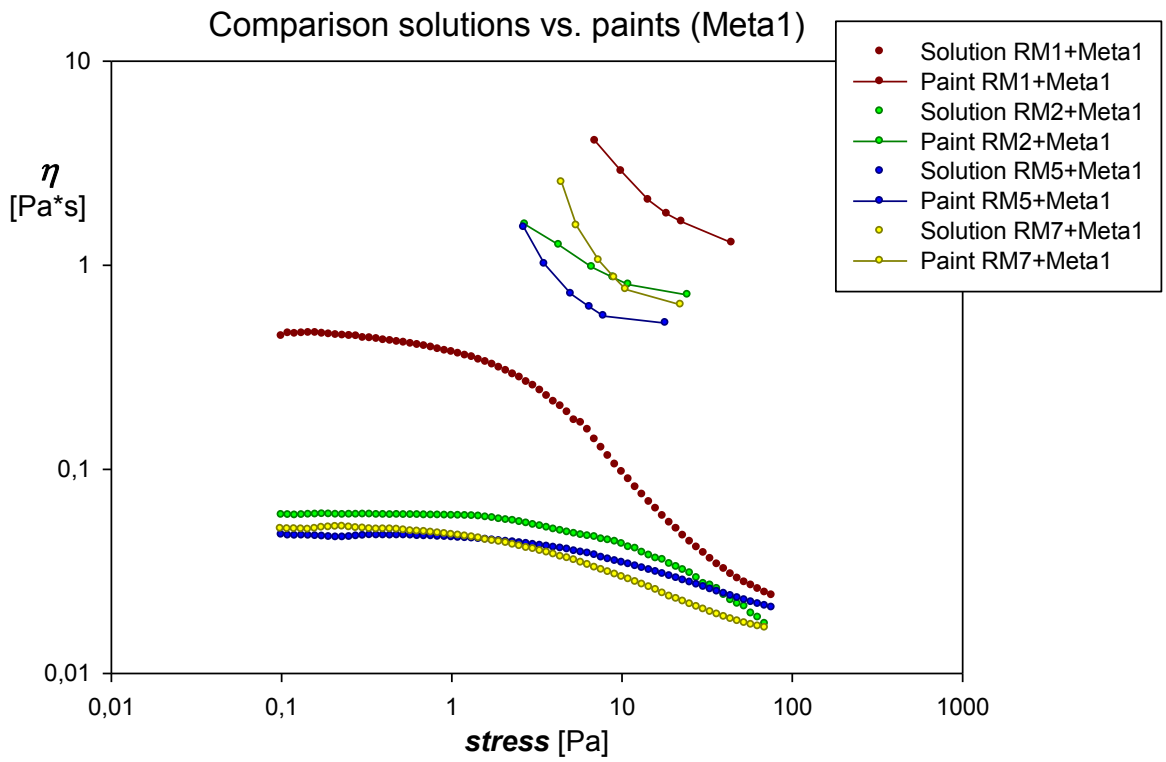


*Figure 4.23: Overlay of the viscosity vs. stress curves of the aqueous solution and paints prepared with SP Meta1*

The procedure used to measure the viscosity of the experimental paints have given good results, so the entire experimental methodology can be easily applied to other cementitious paints and similar materials, such as grouts. In the following pages, some applications of this measurement methodology will be shown.

## 4.4 Characterization of experimental calcium-sulfoaluminate paints

To understand the real technological importance of cement-based paints, a first issue to be faced is that of the potential applications of cement. Cement is a versatile material that can be tuned to have some peculiar properties. As discussed before, the CTG-Italcementi Group laboratories have been developed an innovative cement-based formulation which is able to resist to very acid environments. To check the possibility to use this cement in the formulation of paints able to coat specific surfaces and so to protect these surfaces from the acid attack, some tests have been performed on experimental paints containing this cement. For this purpose, the viscosity

measurement of a commercial paint was first required; the commercial paint works as a reference standard.

For the characterisation of the experimental paints, two different RM concentrations have been tested according to table 4.1.

| | **0,37%** | **0,75%** |
|---|---|---|
| **RM1** | *Paint 1* | *Paint 2* |
| **RM2** | *Paint 3* | *Paint 4* |
| **RM3** | *Paint 5* | *Paint 6* |
| **RM4** | *Paint 7* | *Paint 8* |

*Table 4.1*

For all these particular formulations, a special acrylic SP in powder form (AcriP1) has been used to make the mixing easier. The results are reported in figures 4.24 and 4.25.

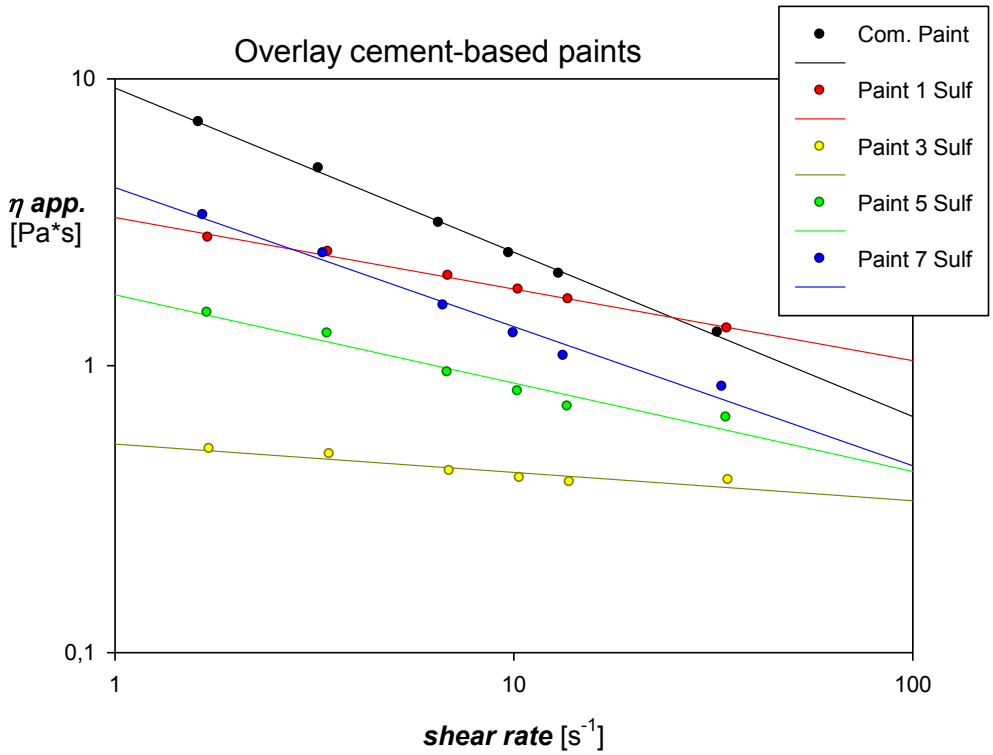


*Figure 4.24: Viscosity curves of few experimental calcium-sulfoaluminate cement-based paints* (RM 0,37%wt)

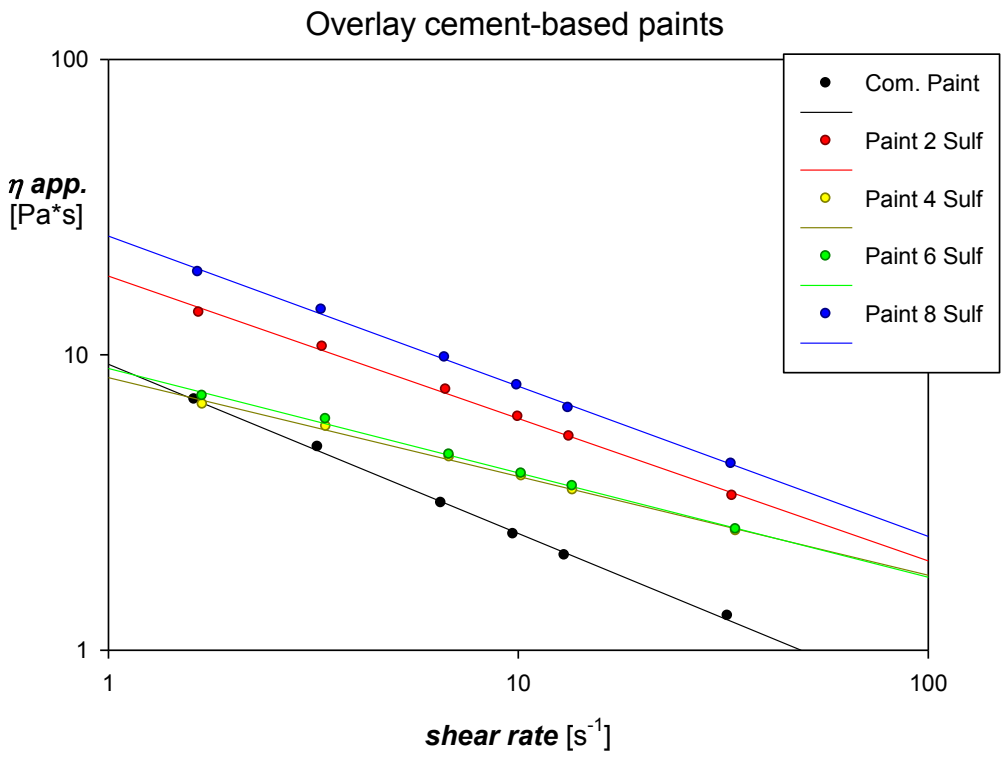


*Figure 4.25: Viscosity curves of few experimental calcium-sulfoaluminate cement-based paints* (RM 0,75%wt)

The first apparent fact is that the viscosity changes radically with the increase of the RM content. If the RM amount is 0,37% of the total, all the paints have a lower viscosity with respect to the commercial paint in the whole range of the shear rate applied, except Paint 1 at high shear rates. If the RM amount is 0,75% of the total, all the paints have a higher viscosity with respect to the commercial paint. This means that very probably the correct viscosity level can be reached with a concentration between 0,37% and 0,75%. Another important parameter to consider is the slope of the curves. As visible, in the graph concerning the paints prepared with RMs 0,37%wt., the curves present completely different behaviours and the blue curve (representing the rheological behaviour of Paint 7) has a slope which is very close to that of the curve representing the commercial paint. Instead, in the graph relative to the paints prepared with RMs 0,75%wt. two different behaviours are visible: the slopes of the red line and of the blue line (respectively Paint 2 and Paint 8) are very close and the same effect is visible for Paints 4 and 6. These latter formulations have almost the same identical behaviour and this is probably due to the fact that different kinds of cellulose derivates can have different water affinity with the increase of cellulose content and so they can give unexpected viscosity levels. All these conclusions lead to the fact that a good paint (at least from a rheological point of view) can be made for example using the RM4 with a correct dosage

without changing other parameters or ingredients in the formulations. The same effect can be very probably achieved also opportunely tuning the water content, as demonstrated in the following paragraph for a photo-catalytic cement-based paint.

## *4.5 Characterization of an experimental photo-catalytic cement-based paint*

To realise a new paint is not an easy task, in particular with a material like cement. In any case, the procedure above described can be very helpful for this purpose.

To avoid the possible differences in the rheological behaviour introduced by the different kind of cement, a first set of measurements has been performed using a conventional Portland cement 52,5R. In these formulations, two different acrylic SPs (AcriP1 and AcriP2) and two different RMs (RM1 and RM5) have been used in concentration of 0,37%wt, for a total of 4 possible combinations.

As a reference standard, the viscosity curve of the commercial paint used in the previous experiment has been considered. The comparison between the experimental paints and the commercial paint is proposed in figure 4.26.

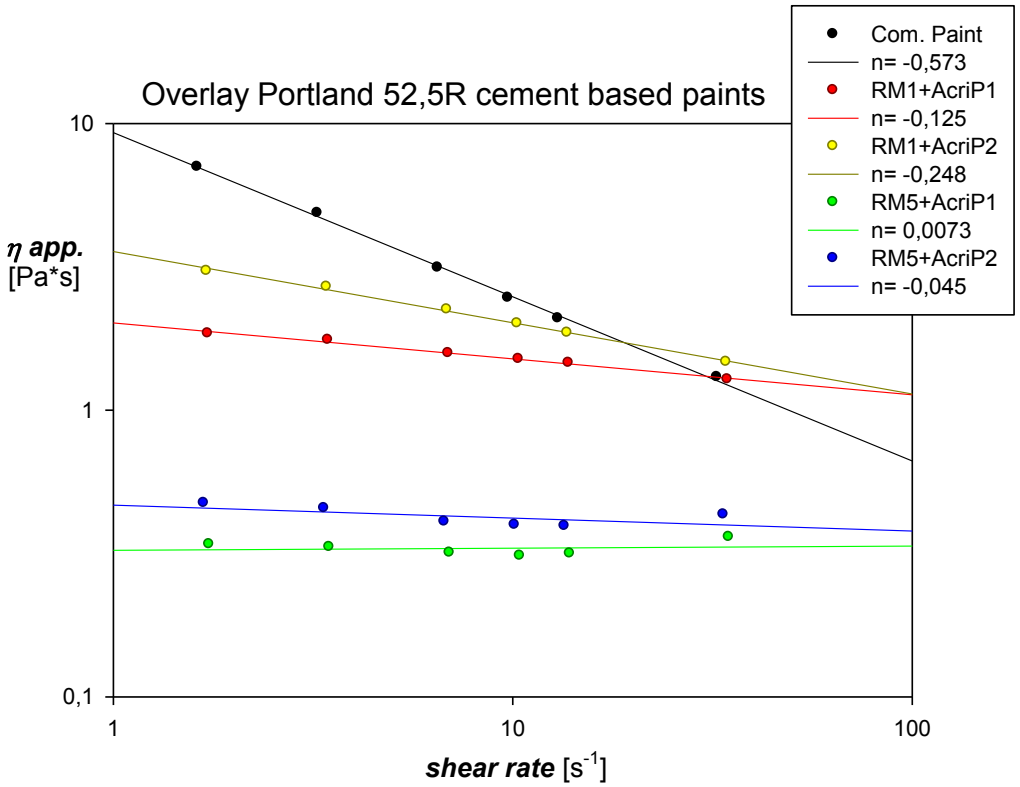


*Figure 4.26: Viscosity curves of few experimental Portland cement-based paints* (RM 0,37%wt)

A clear difference between the paints prepared with RM1 and RM5 is visible once again as expected. The action of the SP on the rheological behaviour of the paints seems also important: in both the case, the SP AcriP2 seems to determine a higher viscosity. The slope of the curves of the experimental paints is always very different from the slope of the black curve (commercial paint). This is certainly a sign of a non-correct formulation and these paints cannot avoid dripping because the viscosity at low shear rate is not sufficiently high.

To check if some important differences are introduced by the change of cement kind, other tests have been performed with the same composition but substituting the Portland cement 52,5R with the cement 42,5R. The graph reported in figure 4.27 shows the obtained results.

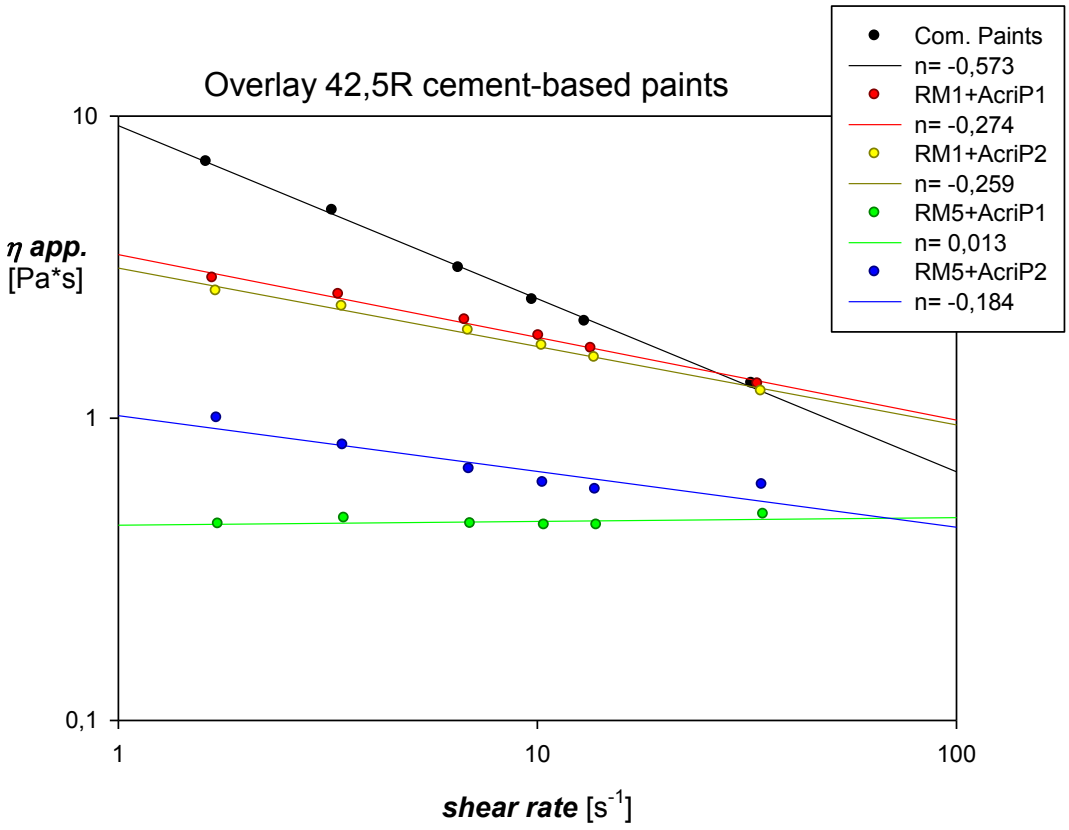


*Figure 4.27: Viscosity curves of few experimental Portland cement-based paints* (RM 0,37%wt)

As visible, there are not great differences between paints containing Portland 52,5R and those containing 42,5R, except for the fact that in the second graph (figure 4.27) the rheological behaviours of the paints containing RM1 are very similar to each other. This effect is probably due to a different action of the SP on the new cement, effect that in each case is apparently not visible in the paints containing RM5.

In the following tests another possibility has been considered: the inversion between the amount of filler and the amount of cement to have cheaper and more eco-compatible formulations. With this purpose a test on the paint RM1+AcriP1 has been performed changing the ratio cement/filler in its composition (figure 4.28).

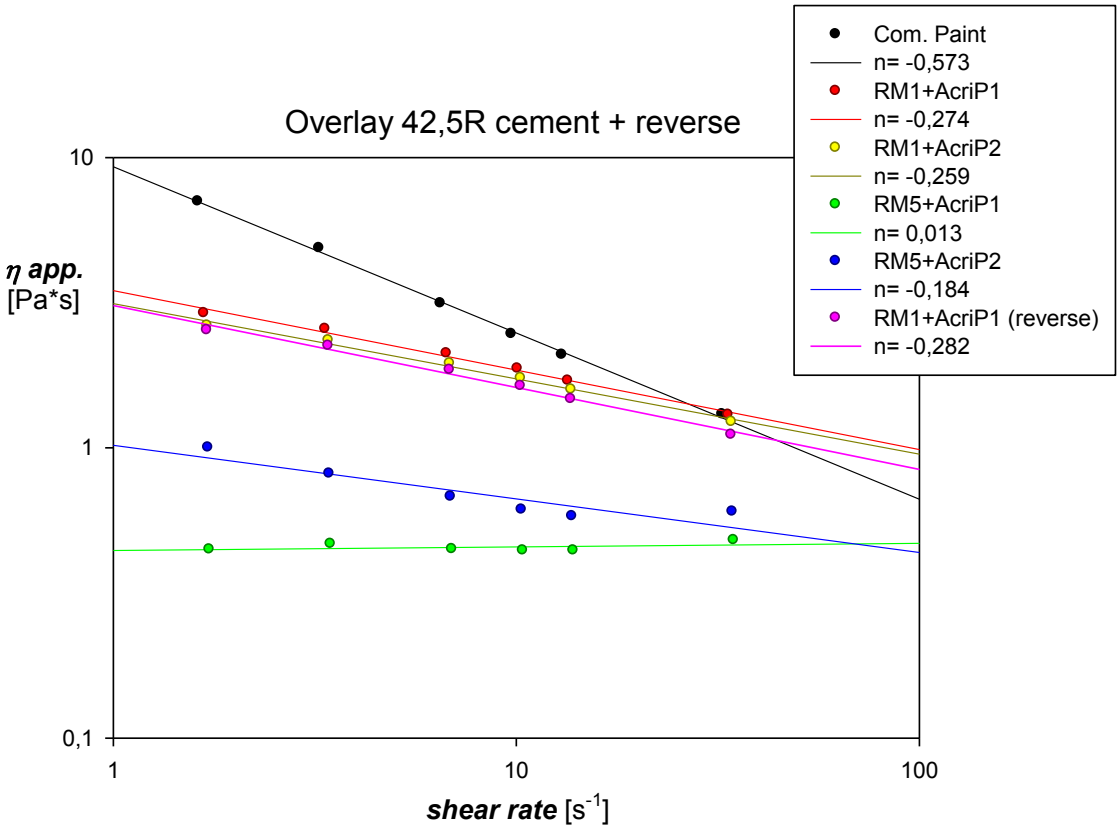


*Figure 4.28: Viscosity curves of few experimental 42,5R cement-based paints* (RM 0,37%wt) *and an experimental paint containing an inverted ratio cement/filler*

It appears very clear that the inversion does not change the rheological behaviour of the paint; the reason is very probably to be found in the very close granulometry of the two compounds and in the fact that the amount of cement in both the cases is not enough to determine a fast hardening of the mixture. So the next step has been to test the experimental paints containing the cement for photo-catalytic action. A paint with the same proportions has been prepared substituting the amount of cement 42,5R with a limestone cement with photocatalytic activity (PHC) and then tested as the previous paints (figure 4.29). The inversion of cement and filler amount has been kept. The number of SP has been reduced to one (Acri2) since they give similar effects and the same has been done for the RM (only RM1 is employed in the next experiment).

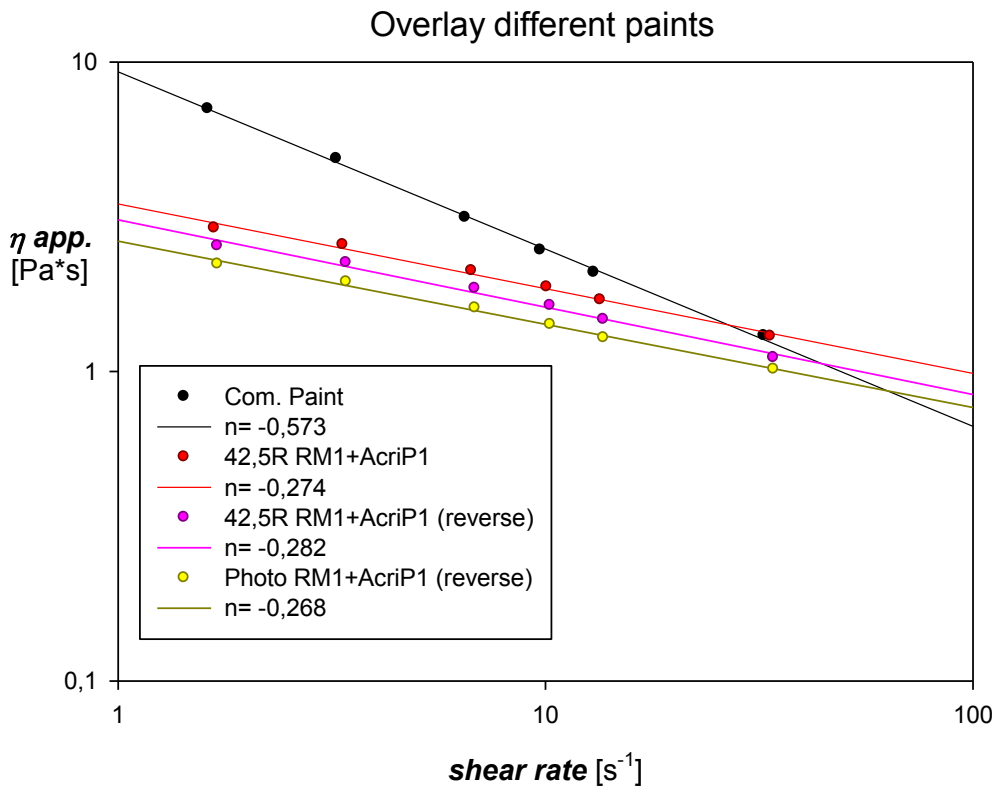


*Figure 4.29: Viscosity curves of an experimental 42,5R cement-based paints* (red line), *an experimental paint containing an inverted ratio cement 42,5R/filler* (purple line) *and another paint containing photo-catalytic cement* (yellow line)

Also in this case no great changes have occurred: also the paint prepared with the PHC cement has shown a behaviour very similar to those seen before. It is clear that the change of slope suitable for a better rheological behaviour of the paint is possible by just changing the cement kind, so a modification in the formulation of the original paint is required.

A modification in the RM amount is not very useful, because it changes very drastically the viscosity level without changing the slope of the curve. Moreover the level viscosity can be also gradually tuned by decreasing the amount of water. So the next tests have been concentrated on the evaluation of the SP reduction effect. With this aim, further tests have been performed on formulations with a reduced amount of water (to increase the viscosity) and with a reduced amount of SP (-50%). The viscosity curves are reported in the figure 4.30.

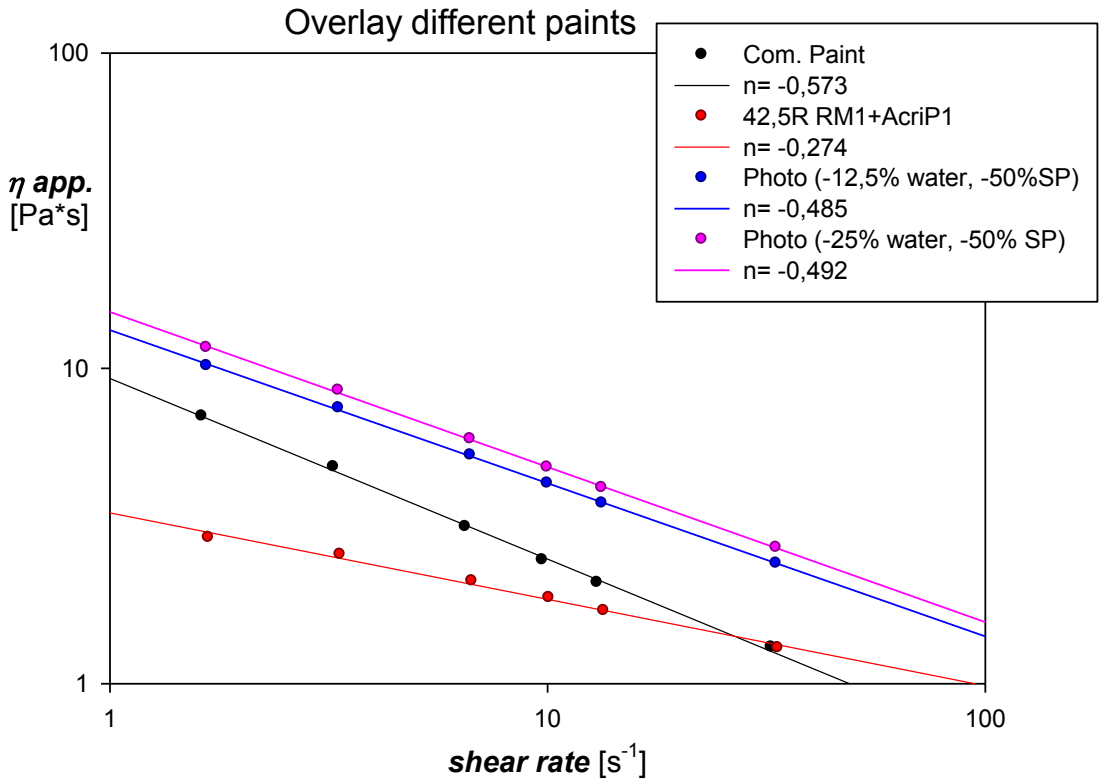


*Figure 4.30: Viscosity curves of few experimental cement-based paints:42,5R* (red line), *photo-catalytic with reduced water and reduced SP* (blue line and purple line)

The two curves relative to the new paints (blue and purple) show a viscosity which is higher than the viscosity of the reference paint (black line). This is however not a great problem because during the application the painter can decide to correct the thickness by adding more water, as it normally happens with the commercial paints, or it is also possible to slightly reduce the amount of cellulose derivatives in order to further reduce the cost of the formulation. The most important note regards the slope change of these curves which are now much closer to that of the commercial paint. In some wall application tests these two paints have given very good results because they are easy to apply and they do not give visible dripping.

Table 4.2 resumes the quantitative parameters k and n for the paints according to a power law fitting model.

| | ***k*** | ***n*** |
|---|---|---|
| *Commercial paint* | 9,33 | -0,573 |
| *RM1+AcriP1 cem 52,5R paint* | 2,01 | -0,125 |
| *RM1+AcriP2 cem 52,5 R paint* | 3,57 | -0,248 |
| *RM5+AcriP1 cem 52,5R paint* | 0,47 | 0,0073 |
| *RM5+AcriP2 cem 52,5R paint* | 0,32 | -0,045 |
| *RM1+AcriP1 cem 42,5R paint* | 3,46 | -0,274 |
| *RM1+AcriP2 cem 42,5 R paint* | 3,14 | -0,259 |
| *RM5+AcriP1 cem 42,5R paint* | 1,02 | 0,013 |
| *RM5+AcriP2 cem 42,5R paint* | 0,44 | -0,0184 |
| *RM1+AcriP1 reverse cem 42,5 R paint* | 3,09 | -0,282 |
| *RM1+AcriP1 reverse Photo paint* | 2,63 | -0,268 |
| *Photo -12,5% water paint* | 13,18 | -0,485 |
| *Photo -25% water paint* | 15,10 | -0,492 |

*Table 4.2*

## *4.6 Conclusions*

In this study several limewater solutions of RMs and SPs have been tested. During the experiments, a strong interaction between RM and SP has been observed, which leads to an increase of the viscosity of the solutions. Anyway, no great differences are visible between the solutions containing the SP Meta1 and the solutions containing SP Acri1. Few comparisons between these solutions and the experimental cement-based paints prepared with the same additives have been evaluated, but they have not given a precise methodology to predict with enough reliability the rheological behaviour of the paints starting from the study of the solutions rheological properties.

This study has allowed to setup a new measurement methodology which allows to use the Viskomat NT to define with great accuracy the viscosity of cement-based paints and other cement-based

formulations by minimizing the effect of sedimentation. Using this method, several cement-based (Portland cement, calcium-sulfoaluminate and cement with photocatalytic activity) paints have been tested and their rheological properties have been tuned to give behaviours very similar to the ones of the commercial formulations.

# *Experimental results: systems for extrusion*

# EXPERIMENTAL RESULTS: SYSTEMS FOR EXTRUSION

The systems for extrusion represent the last category analysed in this work. As discussed before, they are the most concentrated systems. In these systems, the additives are present in a smaller amount with respect to the other materials of the formulations (cement, inerts, etc.) but in an enough quantity to determine relevant changes in their rheological behaviour and processability. The following paragraphs describe all the results obtained during the experiments, in the case of the aqueous solutions and in the case of the cement-based formulations. A comparison between these two kinds of systems and a further investigation on the cement formulations are then also reported.

## 5.1 *Rheological study of the RM neutral and limewater solutions*

Similarly to the previous experimental paths, a preliminary study of the viscosity curve of solutions containing only RM has been adopted. For this tests, the only RM1 was chosen due to its sufficiently high molecular weight. This cellulose derivative was firstly dissolved in water (6,36%wt) according to the protocol described in section 2.9; after complete dissolution the sample appears like an opaque sticky solution. It has been studied in a stationary stress sweep test to obtain the viscosity trend with an increasing stress from 100 to 1000 Pa, as illustrated in figure 5.1. The rheometer tool configuration used in this experiment was a 25 mm cone-plate with an angle of 0.1 rad. The experiment has been performed with a controlled temperature of 20°C.

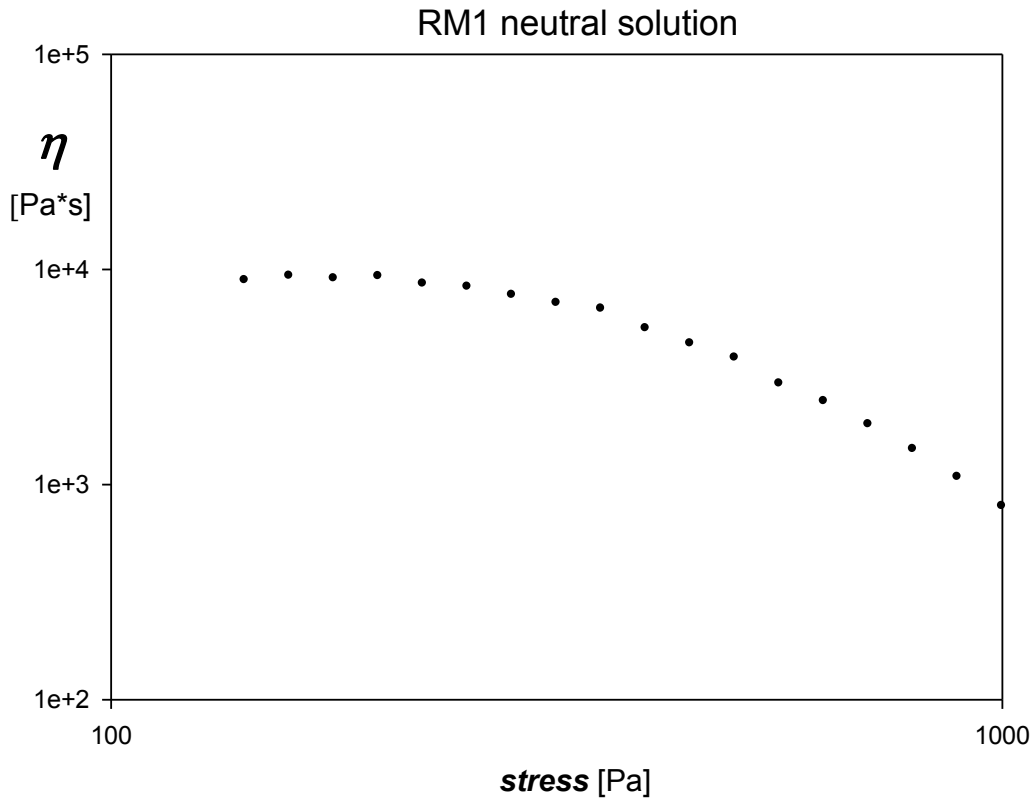


*Figure 5.1: Viscosity curve of the RM1 water solution* (RM 6,36%wt)

The viscosity curve represent a classical shear-thinning behaviour, with a moderate viscosity fall after the 200 Pa stress zone following a Newtonian plateau. During the experiments, no macroscopic changes have been noted for the tested sample.

To study the viscoelastic properties of this material with respect to changes in temperature, the sample has been also submitted to a temperature ramp test (figure 5.2). The settings of this experiment are the following: a temperature increase from 20°C to 70°C with a rate of 3°C/min, a cone-plate geometry 25 mm, 10 Pa of stress applied, frequency 1 rad/s. An anti-evaporation system was applied to the lower plate of the rheometer.

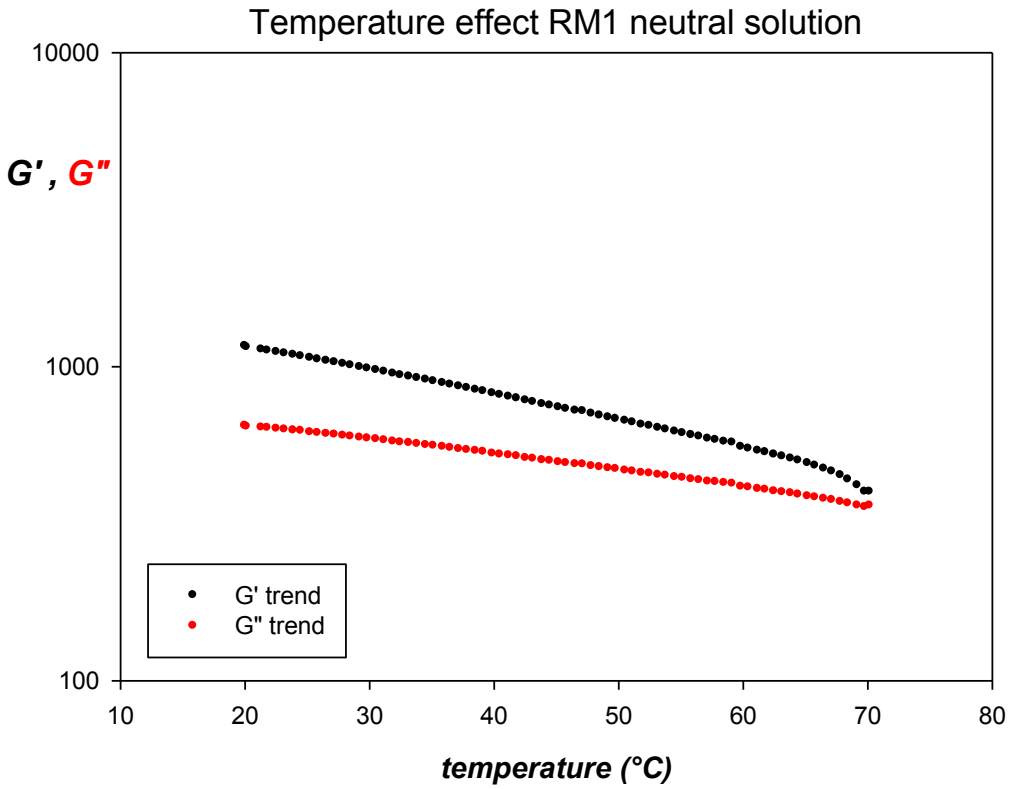


*Figure 5.2: Viscoelastic moduli behaviour in the temperature ramp test* (RM 6,36%wt)

As predictable, a decreasing of both the viscoelastic moduli has been noticed with the increase of temperature. In figures 5.3 and 5.4, the G' and G" behaviours during the cooling ramp (performed with the same velocity of 3°C/min) are also respectively reported. No relevant differences are visible in both the graphs between the moduli behaviours in the heating phase and in the cooling phase: the initial properties of the material are regained at the end of the thermal cycle.

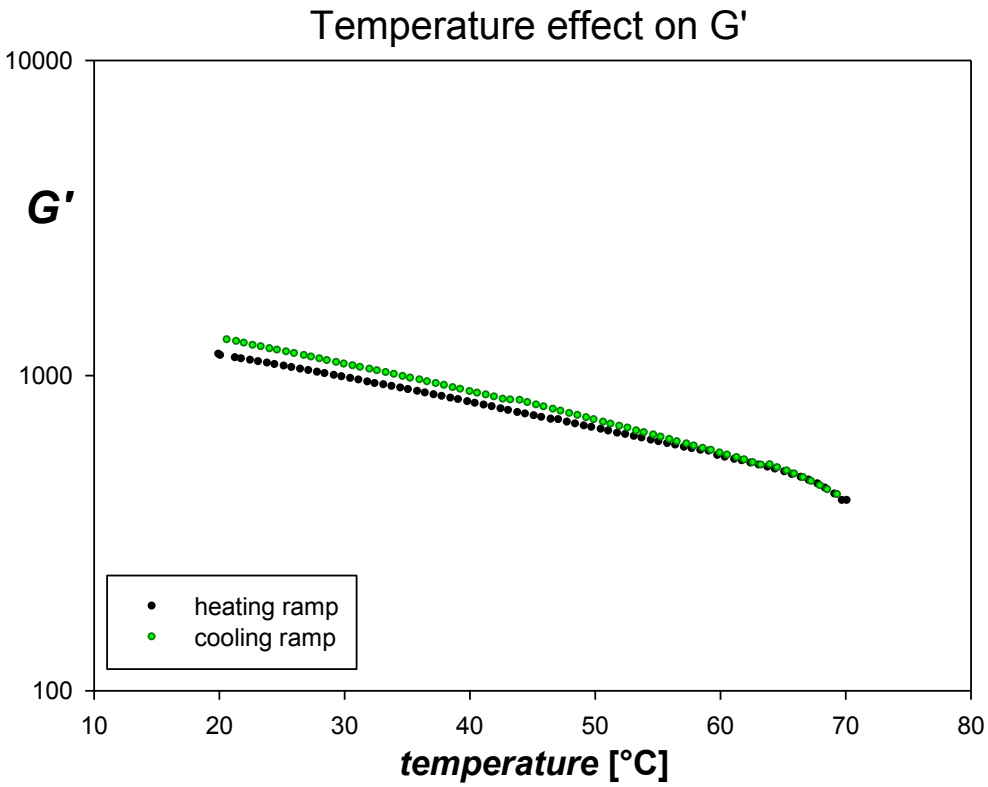


*Figure 5.3:Storage modulus behaviour in the temperature ramp test*

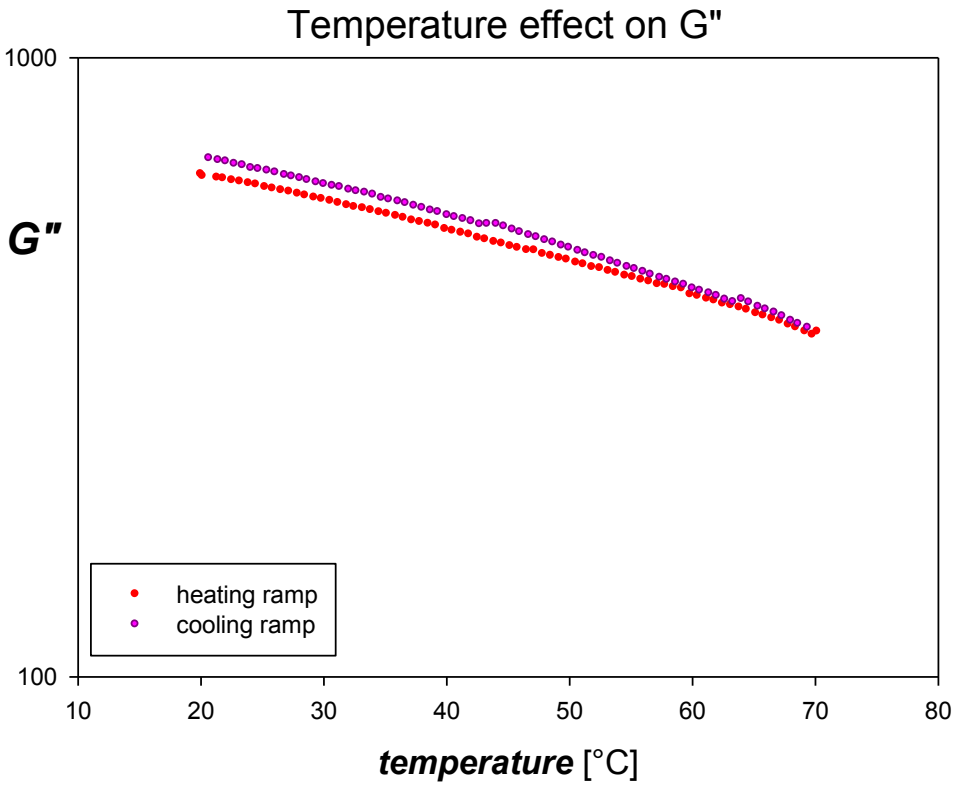


*Figure 5.4:Loss modulus behaviour in the temperature ramp test*

To evaluate the possible change of rheological behaviour of the cellulose in the alkaline environments (as in the cement formulation chemical environment), a sample of RM solution prepared with limewater (the details are exposed in the chapter 2) has been tested. The results of the stationary sweep test are shown in figure 5.5.

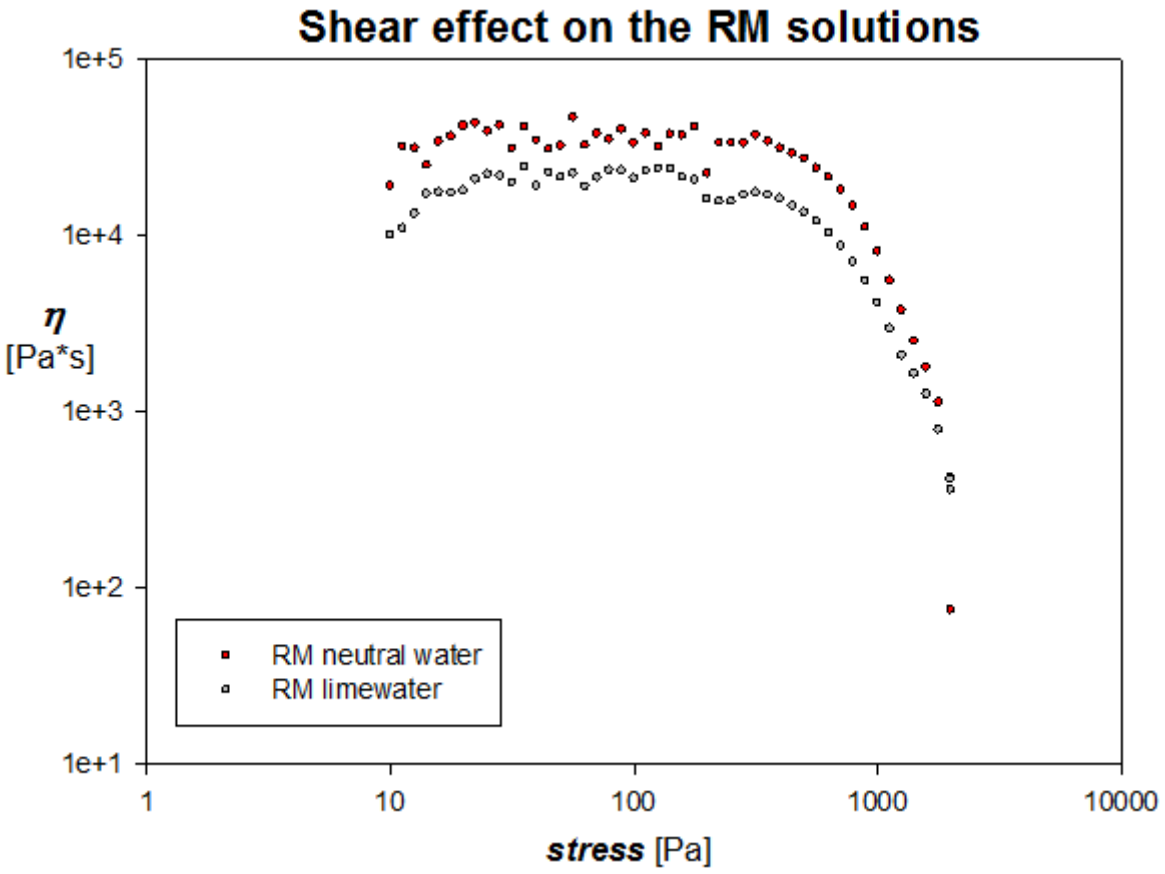


*Figure 5.5:Comparison between the RM neutral water solution and the RM limewater solution (stress sweep test)*

The graph shows a great similarity between the two kinds of solutions: both present shear thinning behaviour and the viscosity curve tends to converge in the high stress zone. The sample has then been tested also with the temperature ramp experiment (figure 5.6).

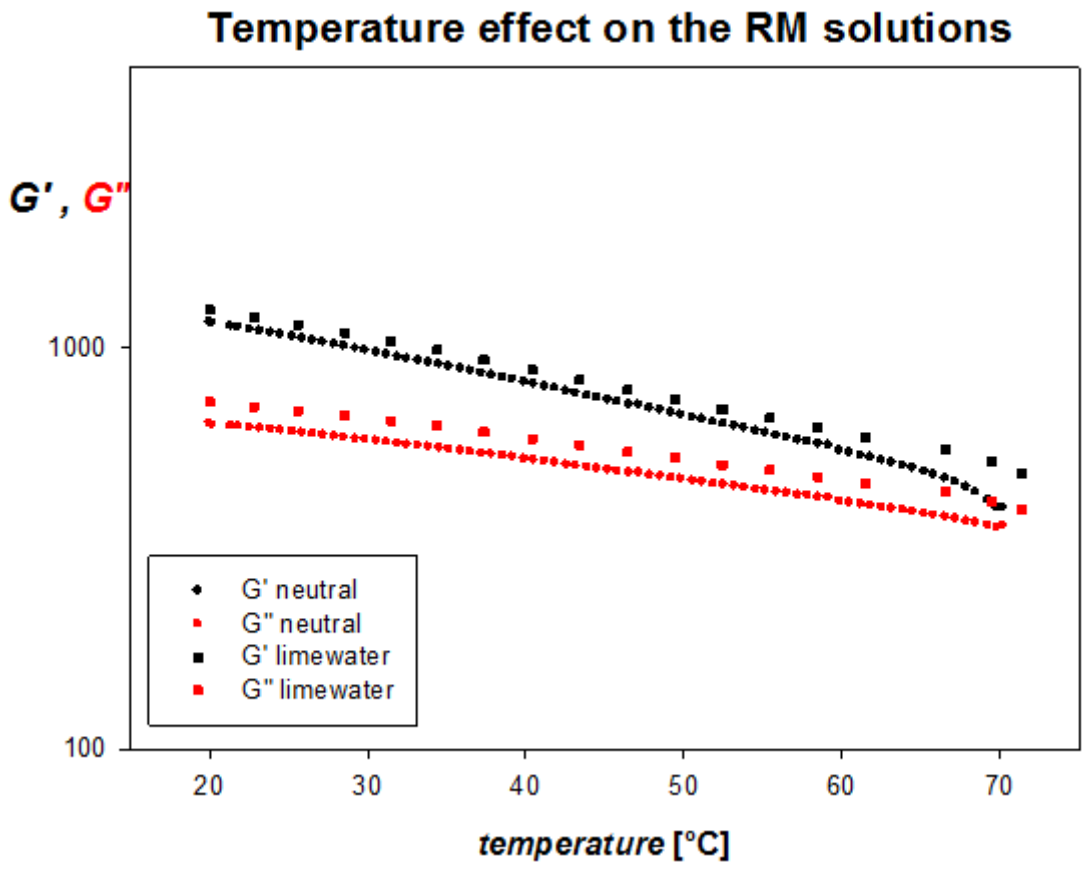


*Figure 5.6:Comparison between the RM neutral water solution and the RM limewater solution (dynamic temperature ramp test)*

The dynamic temperature ramp test has not evidenced great differences between the two solutions. Also in this case the storage modulus and the loss modulus trends are very similar in the two cases and further dynamical experiments have confirmed that the initial properties of the limewater solution are completely recovered after a heating/cooling cycle.

## 5.2 *Effect of superplasticizers addition*

To study the influence of the SP addition on the rheological behaviour of these solutions, the same tests have been also performed on neutral and limewater solutions also containing few acrylic and methacrylic SPs. The addition of these substances does not apparently change the aspect of these concentrated solutions. The settings of these experiments are the same used for the previous

samples. Four different acrylic SPs and three different methacrylic SPs have been used for the preparation of the solutions. Figures 5.7 and 5.8 show respectively the results obtained for the acrylic solutions and for the methacrylic solutions.

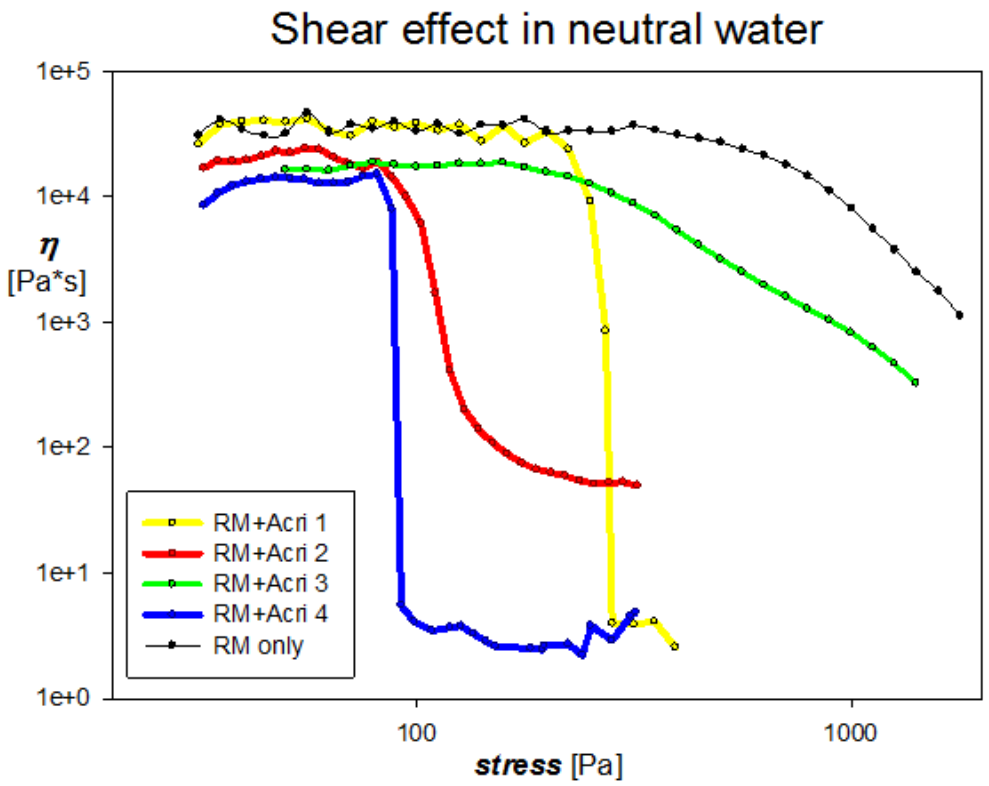


*Figure 5.7:Comparison between the solutions prepared with RM1 and four different acrylic SPs*

In the low stress zone, all solutions show Newtonian behaviour. But, unlike the pure RM system, whose viscosity remains high even at large value of stress, a four-decade drop in the viscosity is observed for the solutions containing also acrylic SPs. The slope change is sharp and takes place at a critical value of the stress which depends on the type of SP. The only exception to this trend is given by the solution prepared with Acri3, in which there is no a sharp decrease in viscosity, on the contrary it shows a rheological behaviour which is quite similar to that of the RM only solution. An analogous consideration can be made also for the addition of methacrylic SPs. Also in this case the addition of the superplasticizer leads to a sudden and drastic decrease of viscosity and also in this case the stress threshold for the observation of this particular effect is in the same window. In figures 5.9 and 5.10 the same data are reported as stress vs. shear rate: it is possible to observe that high shear rates are reachable only by solutions containing the SP.

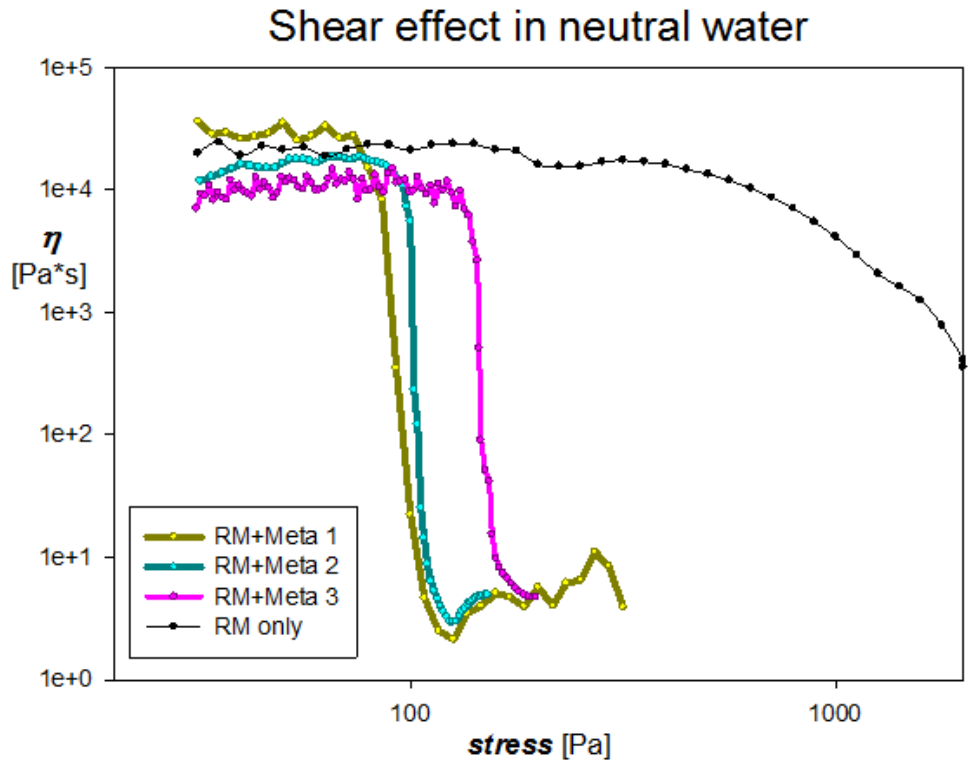


*Figure 5.8:Comparison between the solutions prepared with RM1 and four different methacrylic SPs*

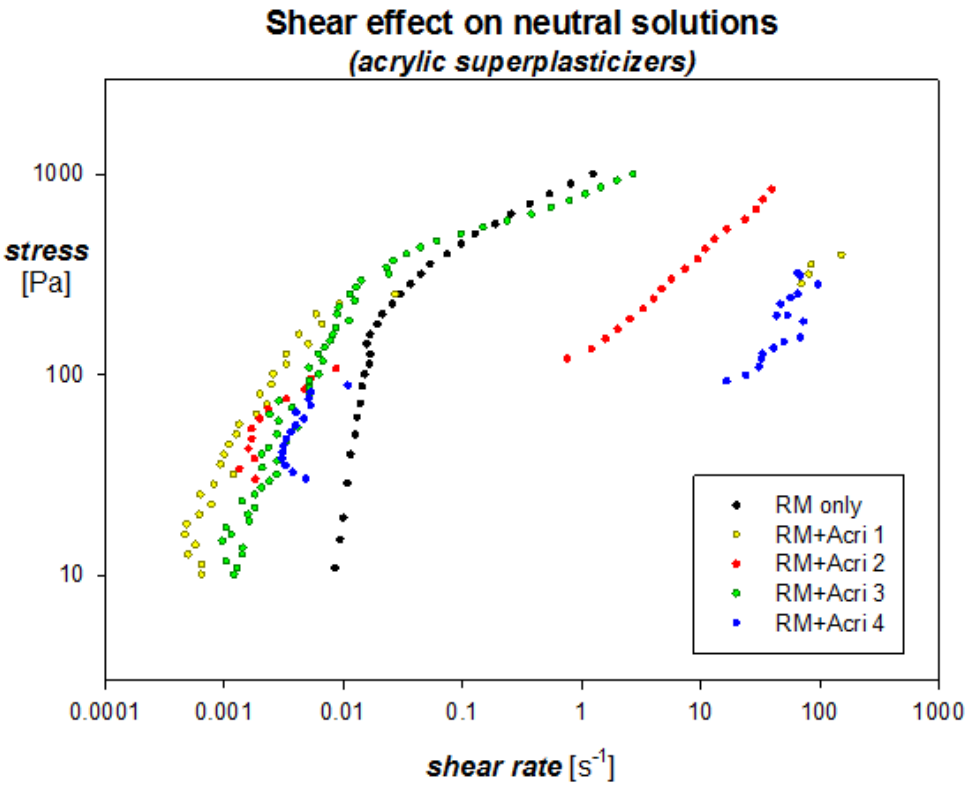


*Figure 5.9: Flow curves of the solutions containing the acrylic SPs*

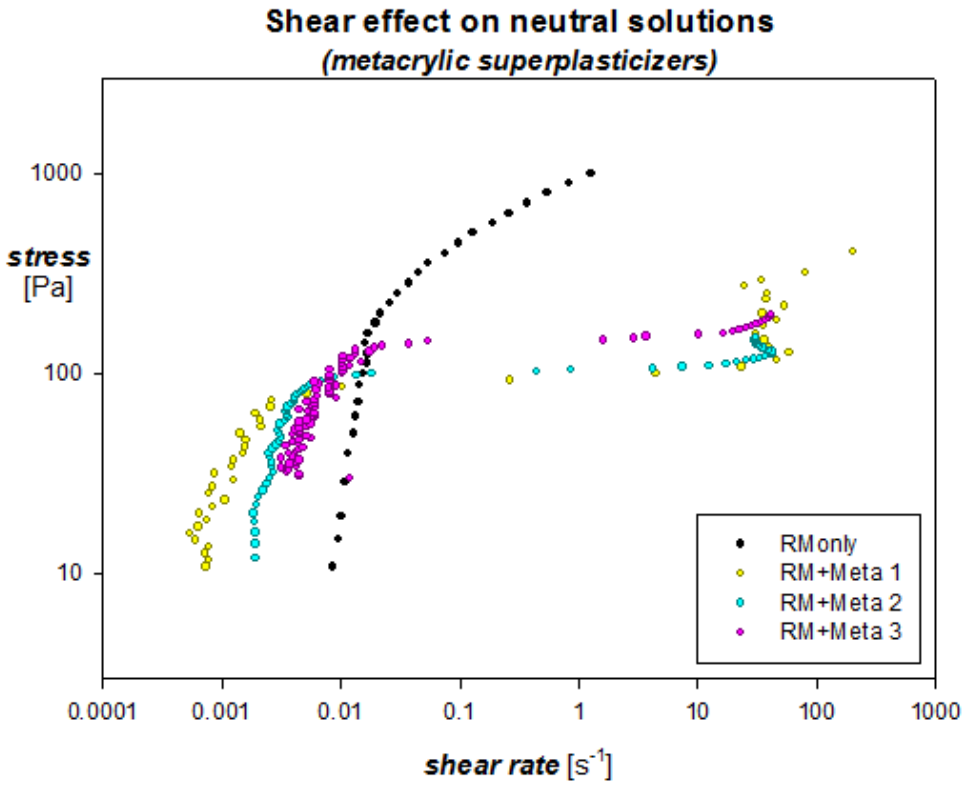


*Figure 5.10: Flow curves of the solutions containing the methacrylic SPs*

The slope in the intermediate shear rate region for the solutions containing also the SP is again an indication of a flow-induced change in the rheological behaviour. It can be inferred that a strong interaction between the two kinds of additives is present. This kind of behaviour is very probably due to some instability established in the solutions by the presence of cumbersome chains of SP, which have also a great quantity of negatively charged terminals that disturb further on the interactions between water and MHEC.

In order to better simulate the cement environment and to better understand the interactions between the RM and the SPs, also in a different chemical matrix, the same tests have been performed on limewater solutions. In figures 5.11 and 5.12, shear effects on alkaline solutions with acrylics and methacrylics are respectively shown.

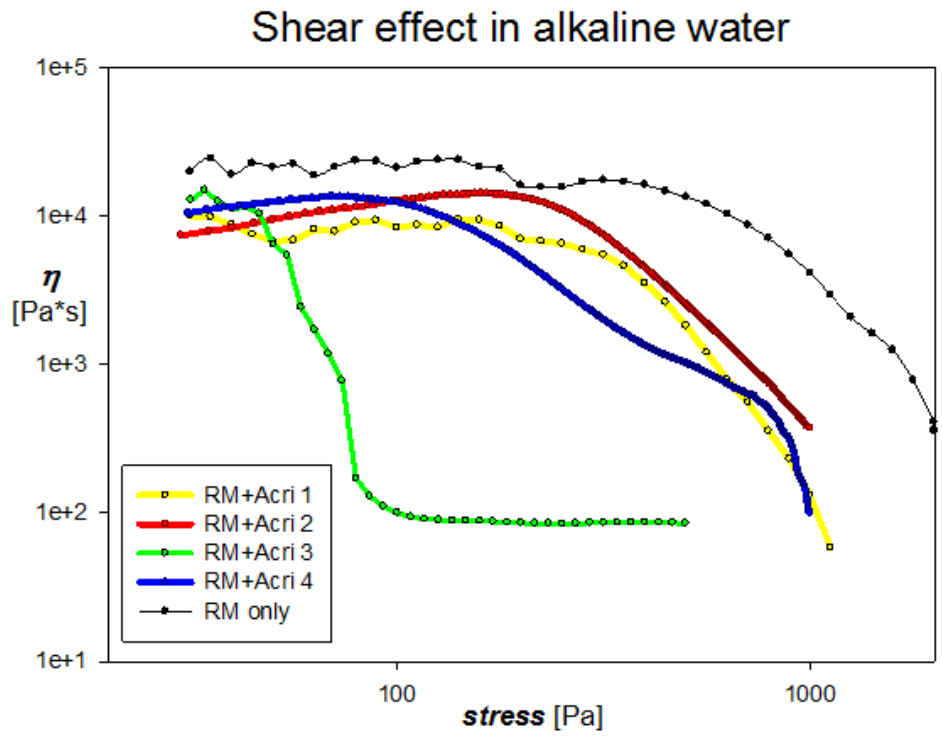


*Figure 5.11:Comparison between the limewater solutions prepared with RM1 and four different acrylic SPs*

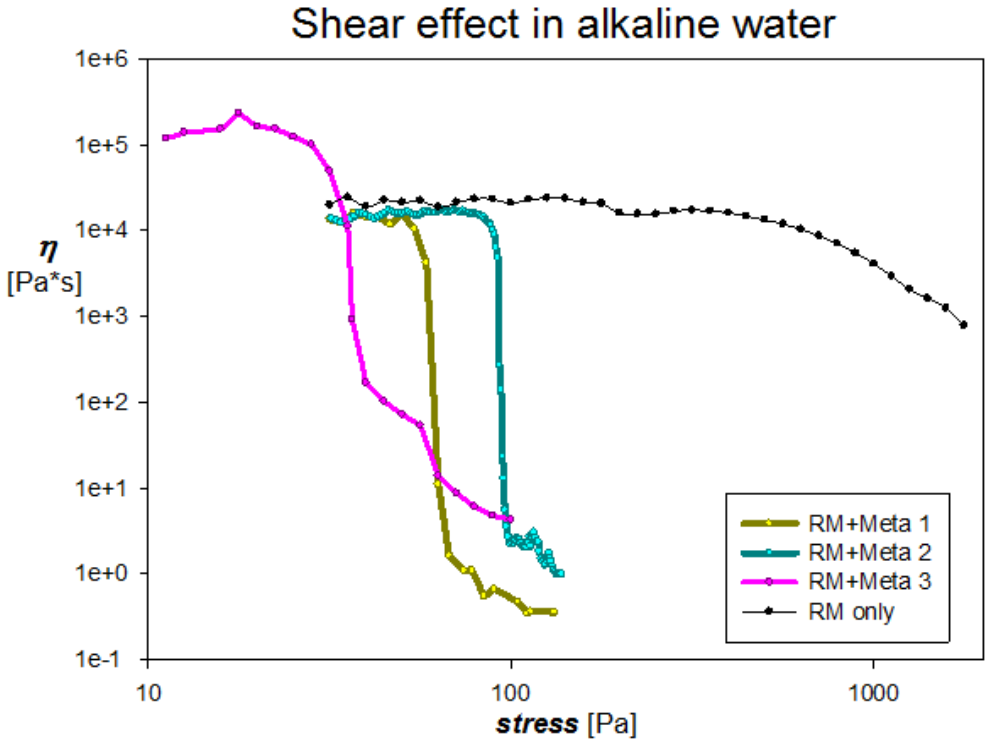


*Figure 5.12:Comparison between the limewater solutions prepared with RM1 and four different methacrylic SPs*

Two different effects are visible with SP addition in the limewater solutions. The acrylic SPs lead to a kind of stabilization of the solution to the shear effect. In fact their behaviour is now more similar to the behaviour of RM solution than to that of the same solutions prepared in neutral water. The only exception to this trend is once again the solution containing the SP Acri3; its behaviour can be considered particular because it is exactly the opposite of that of other acrylic SPs. The methacrylic SPs addition in limewater environment seems instead not to alter the previous situation: the sharp decrease of viscosity is clearly visible also in this case for all solutions. Probably this effect is due to the pH change and the acrylic SPs are more sensitive to this change than methacrylic SPs for some reasons or a particular interaction between some ions present in solution, like $Ca^{2+}$, and the carboxylic groups of acrylic SPs has been established. In fact the acrylic COOH groups are more acid than methacrylic COOH groups, so they present an higher proton dissociation in limewater than these latter. As a further proof of this hypothesis, a pH decrease effect has been observed after the preparation of sample. Such an effect is more visible for all the solutions prepared with acrylic SPs (measures with the pHmeter are shown in figures 5.13-5.16). The higher proton dissociation probably leads to an higher neutralization of alkaline environment. This could means that the effect of "stabilization" of the solution is not due to the pH conditions but probably to the presence of a particular interaction between calcium hydroxide and one or both the additives.

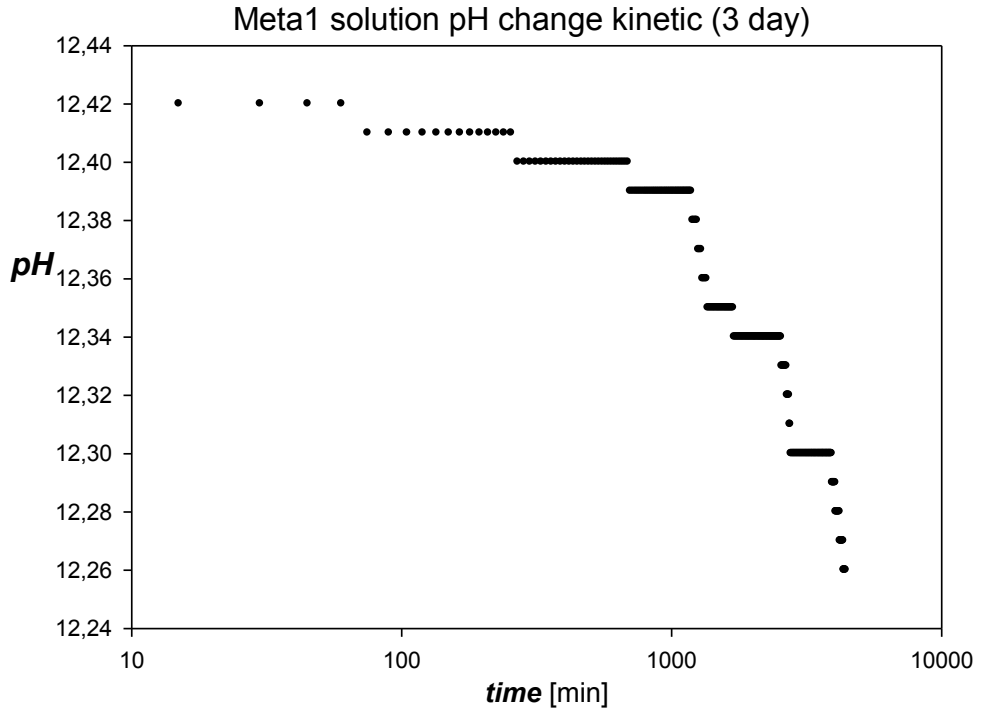


*Figure 5.13: pH change kinetic of the solution containing SP Meta1 (3 day after preparation)*

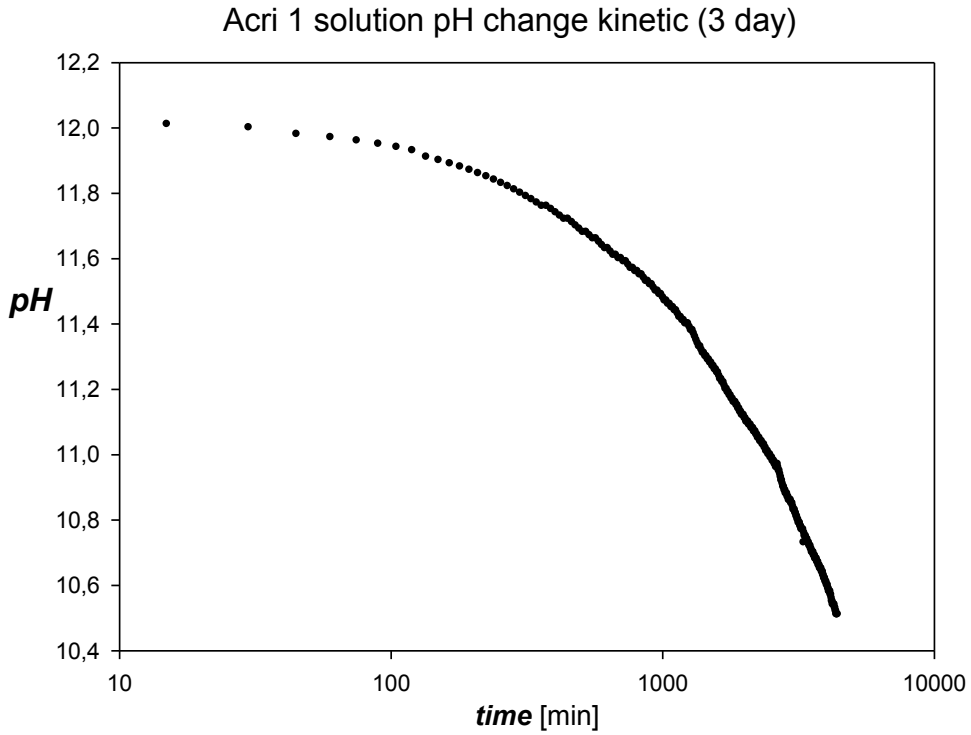


*Figure 5.14: pH change kinetic of the solution containing SP Acri1 (3 day after preparation)*

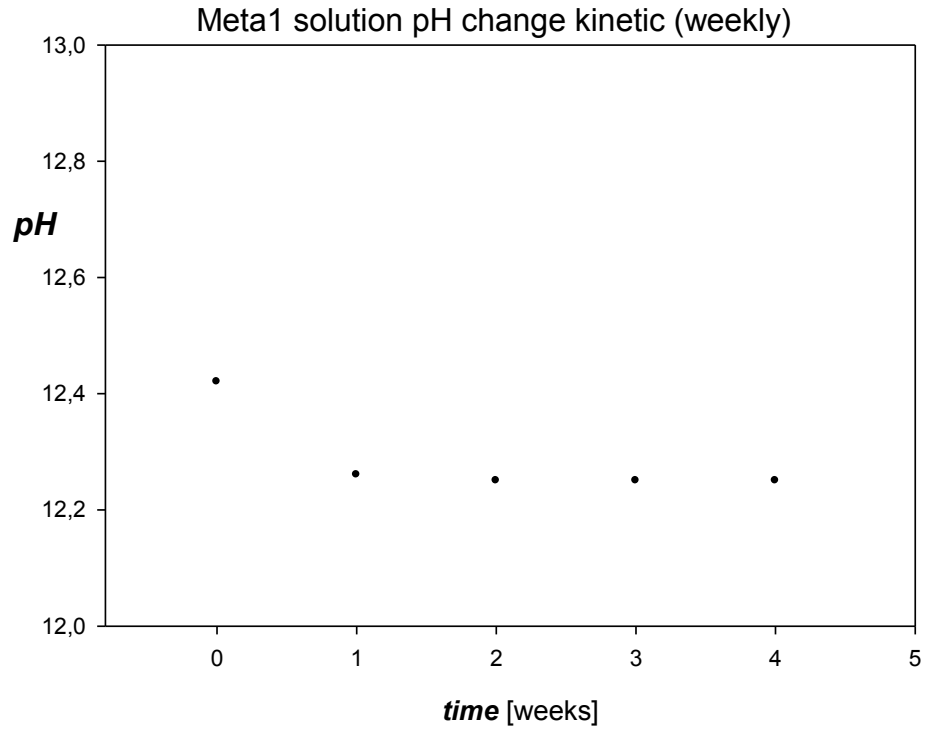


*Figure 5.15: pH change kinetic of the solution containing SP Meta1 after 28 days from preparation*

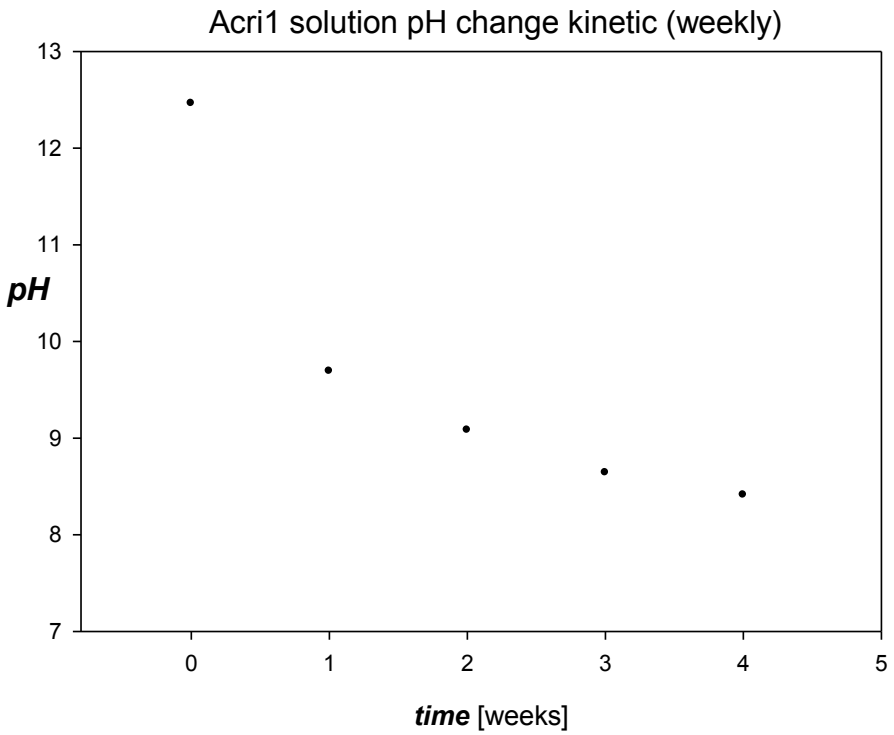


*Figure 5.16: pH change kinetic of the solution containing SP Acri1 after 28 days from preparation*

All samples have been also tested with oscillatory stresses under a temperature increase to study the behaviour of the viscoelastic moduli G' and G" with a temperature change. The oscillatory mode has been performed imposing a constant stress of 10 Pa with a fixed frequency (1 rad/s) while the temperature increases from 20° to 70°C with a rate of 3°C/min. The results obtained for the neutral solution are reported in figures 5.17-5.23. Also for these tests interesting results have been obtained. A sharp decrease of the viscoelastic moduli values is visible trespassing a temperature threshold. This characteristic temperature is variable with the superfluidificant employed. At higher temperatures the behaviour of the solutions is prevalently viscous as confirmed by the fact that G" is much longer than G'. Moreover, some of these solutions definitively lose the initial properties or, at least, there is a very slow recovery.

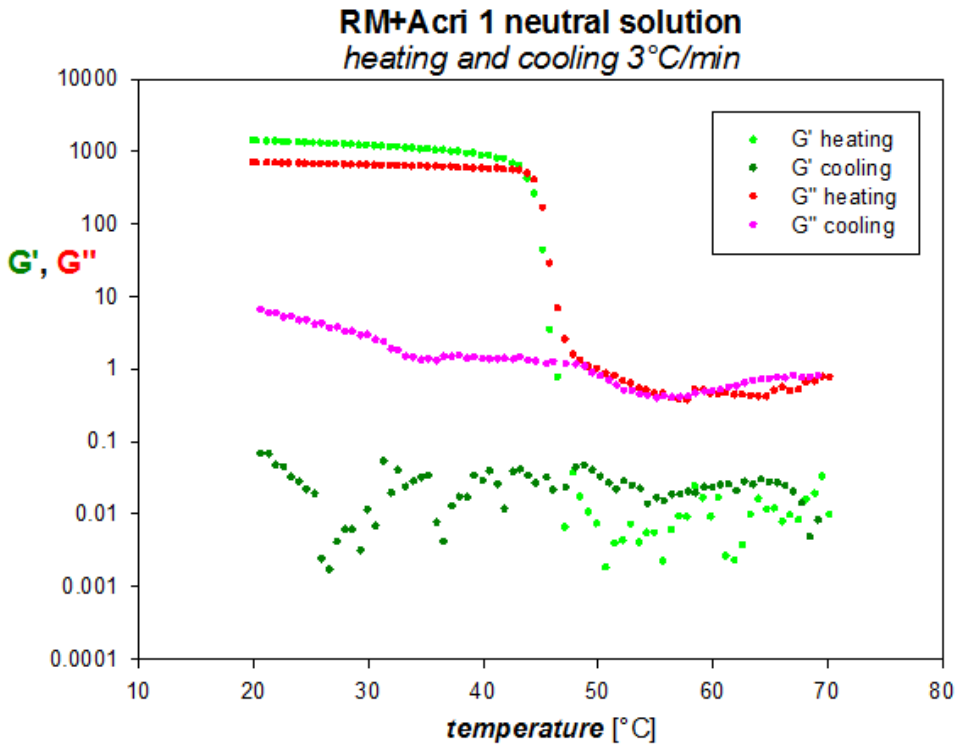


*Figure 5.17: Heating and cooling cycle in a temp ramp test (RM+Acri1 sample)*

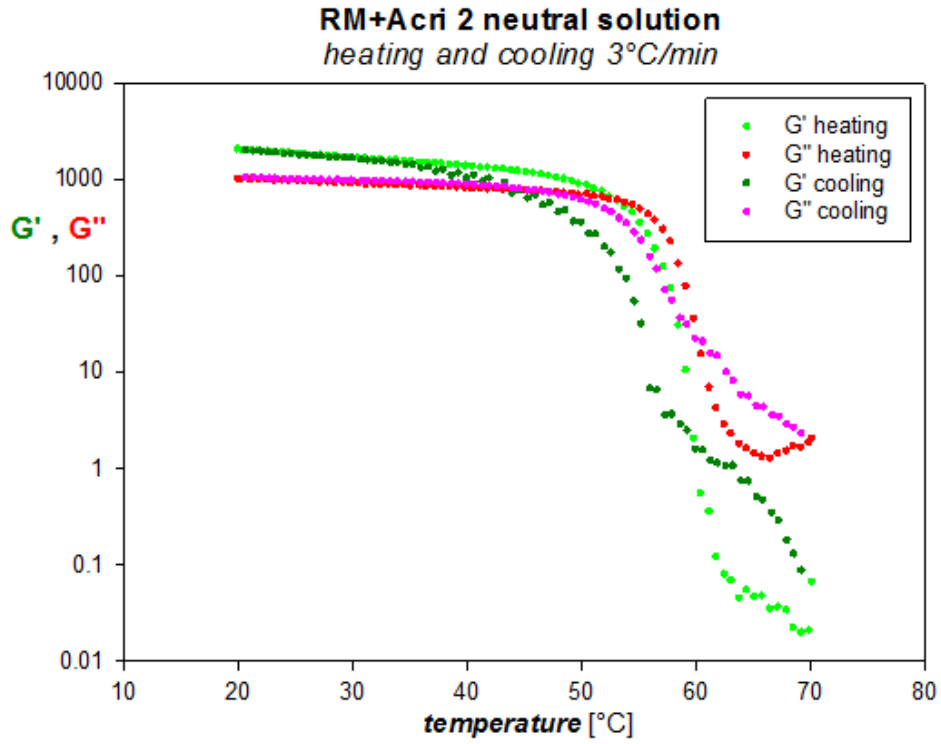


*Figure 5.18: Heating and cooling cycle in a temp ramp test (RM+Acri2 sample)*

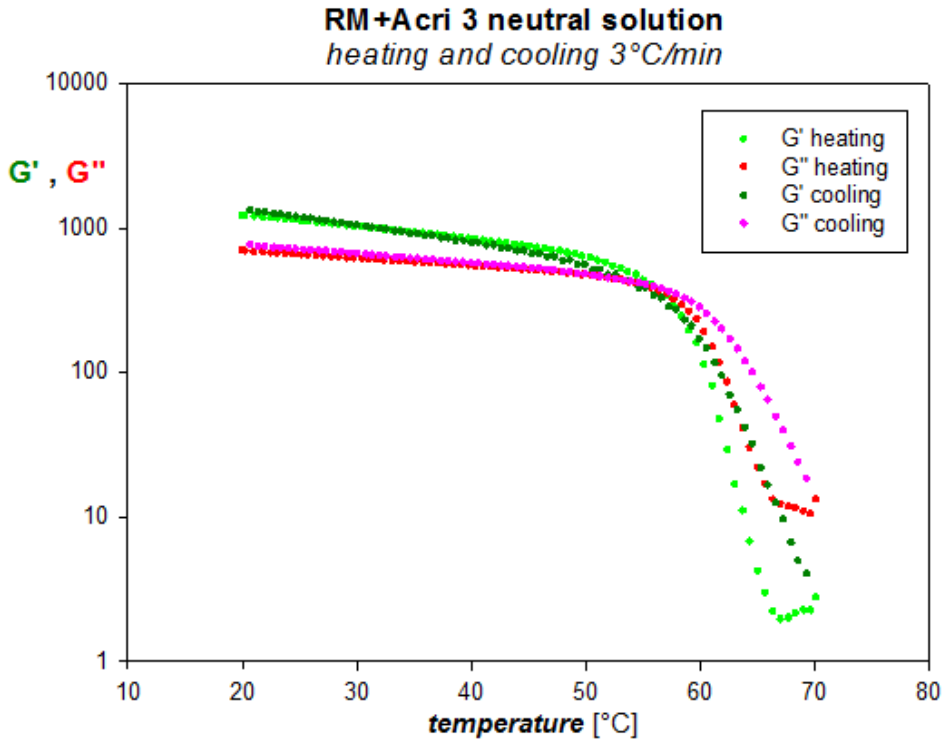


*Figure 5.19: Heating and cooling cycle in a temp ramp test (RM+Acri3 sample)*

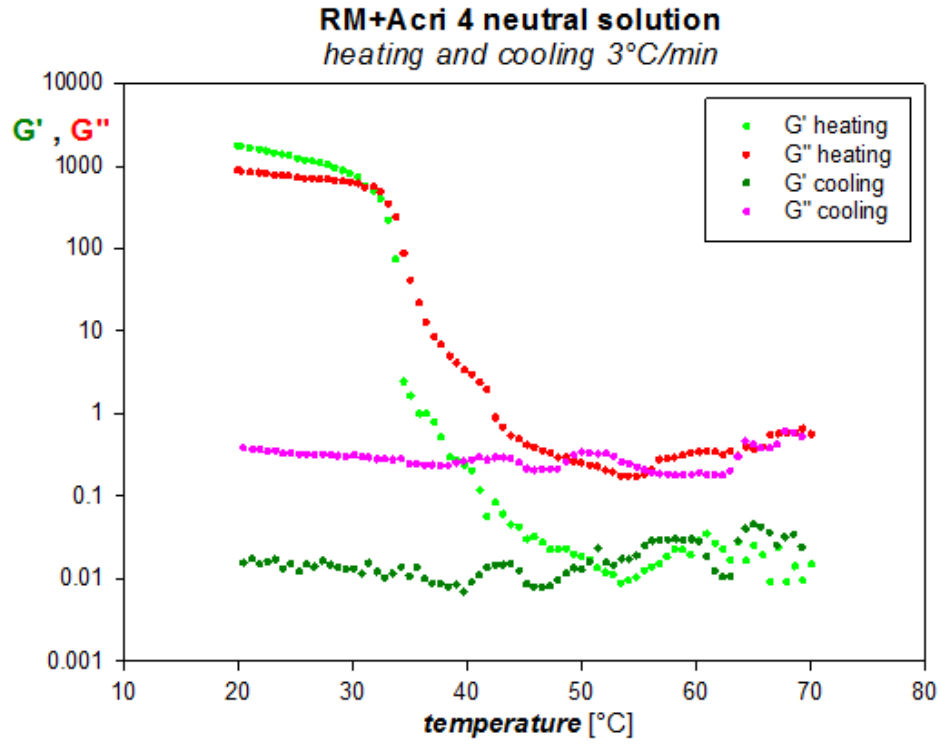


*Figure 5.20: Heating and cooling cycle in a temp ramp test (RM+Acri4 sample)*

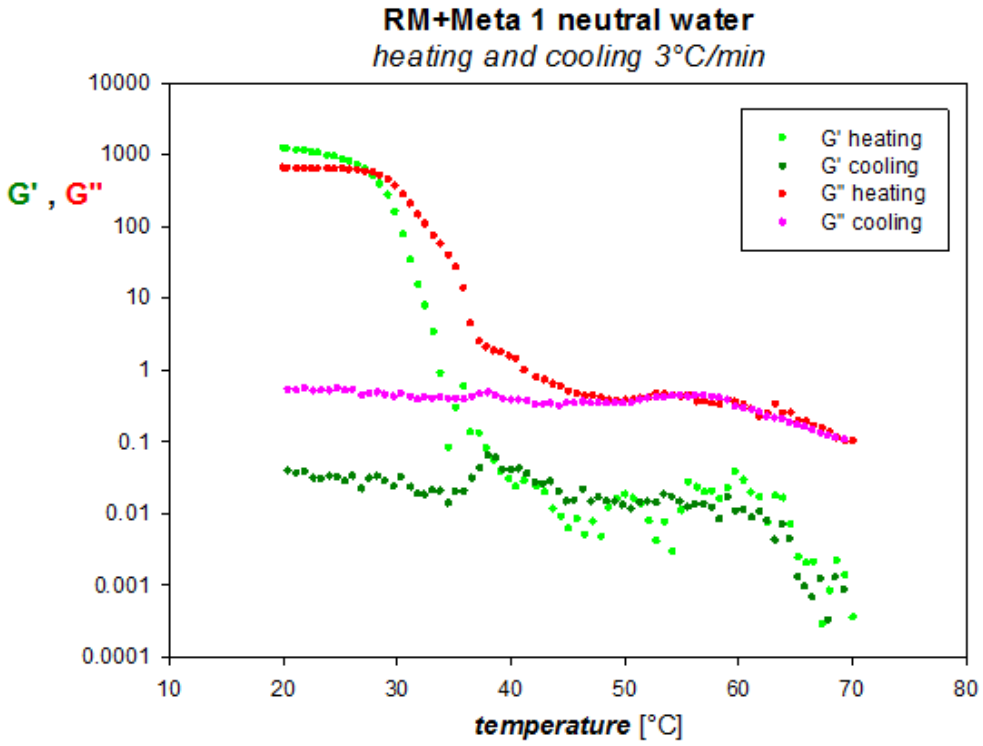


*Figure 5.21: Heating and cooling cycle in a temp ramp test (RM+Meta1 sample)*

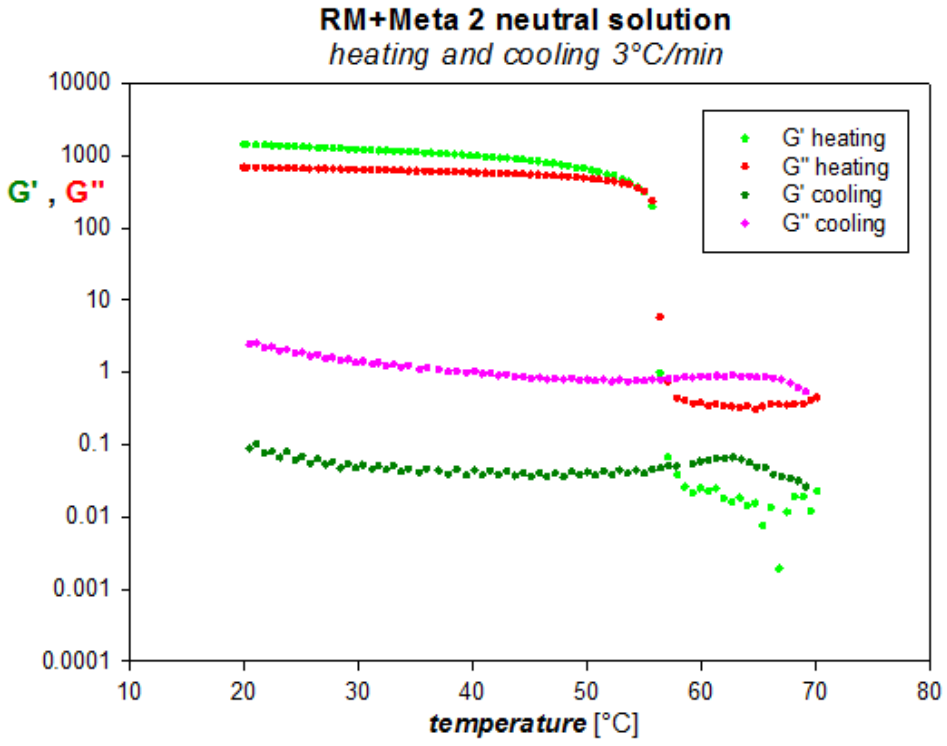


*Figure 5.22: Heating and cooling cycle in a temp ramp test (RM+Meta2 sample)*

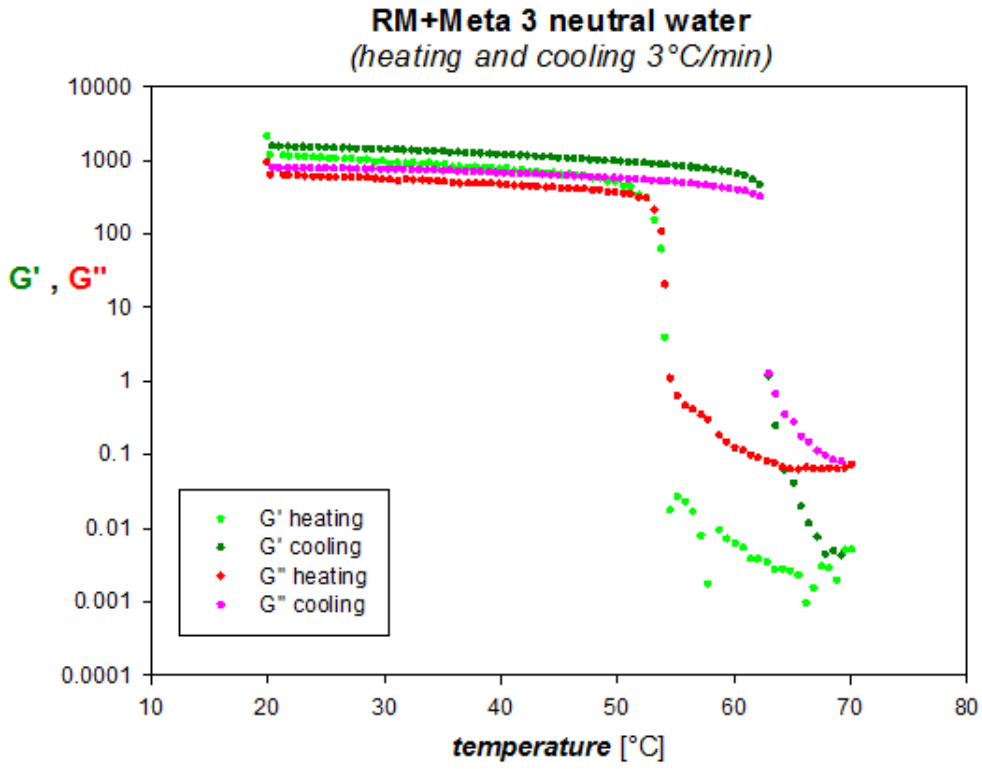


*Figure 5.23: Heating and cooling cycle in a temp ramp test (RM+Meta3 sample)*

As the stress-induced phenomena described above, also this kind of behaviour is probably due to the onset of some instability of these systems and micro-precipitation of MHEC because its interaction with water get worse with temperature increase. The micro-precipitation can explain the drastic viscoelastic moduli decrease; in any case the ability of some samples to recover the initial values is not still clear. It is important to note that no attention in these analysis has been paid to operate in a linearity regime because the purpose of these tests is to underline the peculiar macroscopic effect visible increasing the temperature of the system. Other tests could be certainly very useful but they do not fit the real aims of this work.

To evaluate in a quantitative way the effect above described several parameters have been introduced. They are reported below:

- *precipitation stress value* ($\tau_p$): the stress value in correspondence of the drastic decrease of viscosity; it has been obtained from the intersection between the tangential line of the curve in the initial linear part and the tangential line of the curve during fall;

- *initial average viscosity* ($\bar{\eta}_i$): obtained calculating the average of the viscosity values before drastic precipitation of the curve;
- $\frac{\eta_s}{\eta_c}$ *ratio*: it is simply the ratio between the initial viscosity of the aqueous solutions containing SP and RM and the initial viscosity of the solution containing the only RM in water;
- *precipitation temperature value ($T_p$)*: the value of temperature in correspondence of the drastic decrease of G' and G" value; it has been obtained from the intersection between the tangential line of the curve in the initial linear part and the tangential line of the curves in the sharp decrease zone;
- $\dot{\gamma}_{cr,i}$ *and* $\dot{\gamma}_{cr,s}$ : they represent the lower and the higher critical values relative to the beginning of a shear banding-like effect;
- *G' and G" initial values* ($\overline{G'}_i$ *e* $\overline{G''}_i$): calculated as the average of G' and G" values before sharp precipitation.

The table 5:1 resume all parameters for the solutions prepared with neutral water.

| **Parameters** | Acri1 + RM | Acri2 + RM | Acri3 + RM | Acri4 + RM | Meta1 + RM | Meta2 + RM | Meta3 + RM |
|---|---|---|---|---|---|---|---|
| $\boldsymbol{\tau_p}$ [Pa] | 224 | 88 | 300 | 88 | 79 | 87 | 122 |
| $\boldsymbol{\bar{\eta}_i}$ [Pa*s] | $\mathbf{3.2 \cdot 10^4}$ | $\mathbf{2.2 \cdot 10^4}$ | $\mathbf{1.75 \cdot 10^4}$ | $\mathbf{1.4 \cdot 10^4}$ | $\mathbf{3.3 \cdot 10^4}$ | $\mathbf{2.9 \cdot 10^4}$ | $\mathbf{2.5 \cdot 10^4}$ |
| $\boldsymbol{\frac{\eta_s}{\eta_c}}$ | 0.91 | 0.63 | 0.51 | 0.4 | 0.96 | 0.85 | 0.71 |
| $\dot{\gamma}_{cr,i}$<br>$\dot{\gamma}_{cr,s}$<br>$[\boldsymbol{s^{-1}}]$ | 0.027<br>60 | 0.017<br>0.06 | -<br>- | $10^{-2}$<br>10 | 0.02<br>30 | 0.016<br>0.05 | 0.01<br>0.2 |
| $\boldsymbol{T_p}$ [°C] | 44 | 56 | 55 | 35 | 27 | 56 | 56 |
| $\boldsymbol{\overline{G'}_i}$ [Pa] | 1100 | 1423 | 860 | 986 | 982 | 1083 | 1001 |
| $\boldsymbol{\overline{G''}_i}$ [Pa] | 624 | 840 | 550 | 767 | 875 | 886 | 820 |

*Table 5.1*

The results obtained for limewater solutions are reported in figures 5.24-5.30. A partial stabilization seems to be given by the limewater environment to the solutions containing acrylic SPs; also in this case the solution with Acri3 seems the only exception. Instead the behaviour of solutions where a methacrylic SP is present seems not to change in limewater as compared to neutral water.

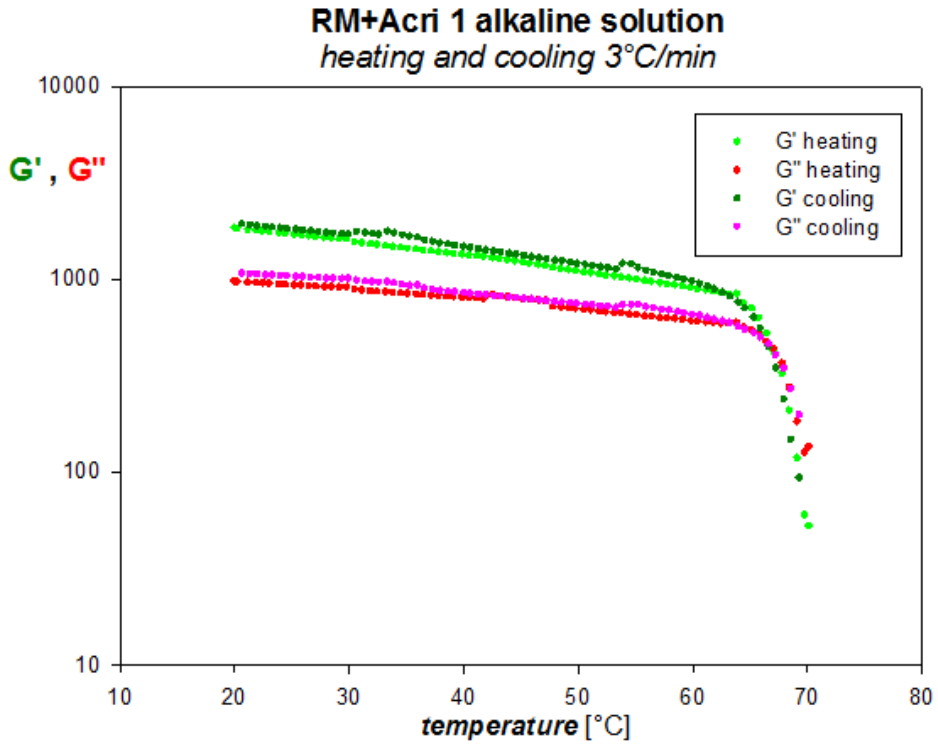


*Figure 5.24: Heating and cooling cycle in a temp ramp test (RM+Acri1 sample)*

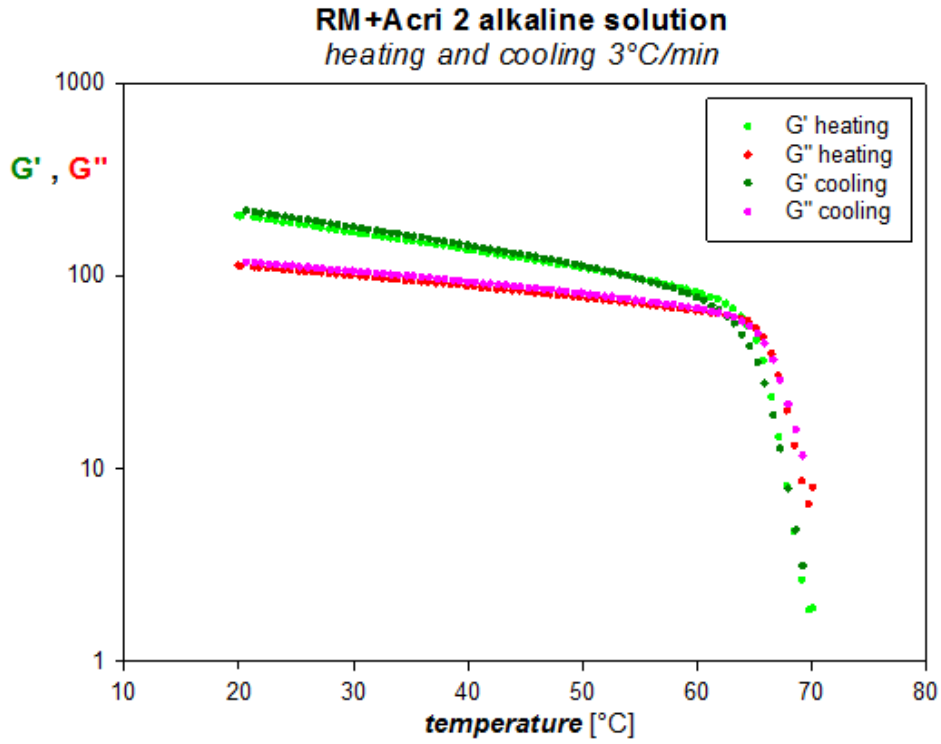


*Figure 5.25: Heating and cooling cycle in a temp ramp test (RM+Acri2 sample)*

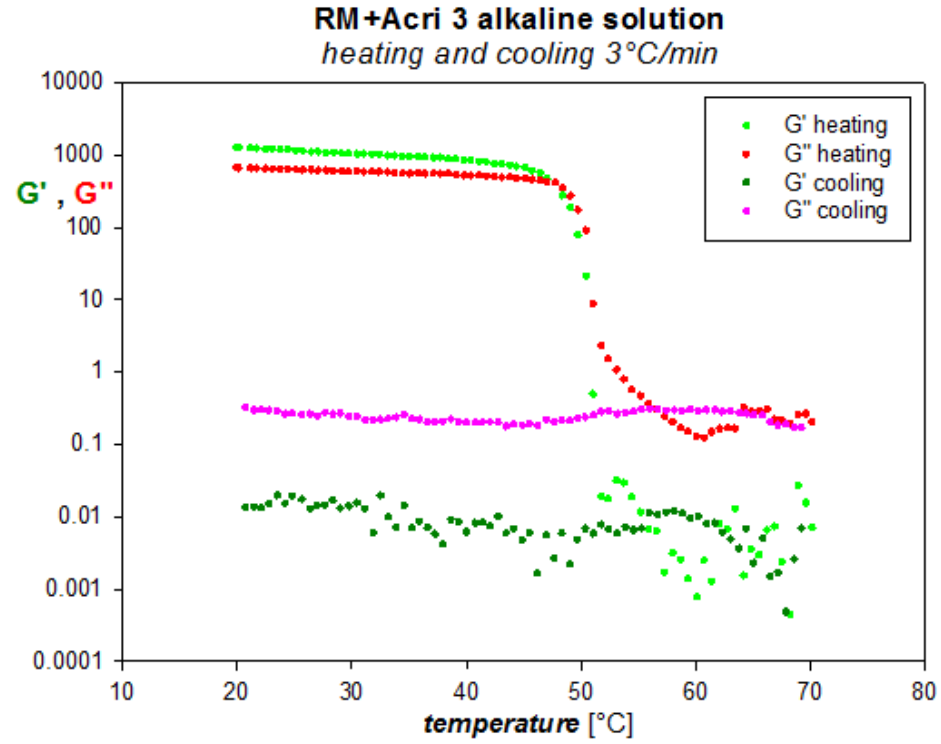


*Figure 5.26: Heating and cooling cycle in a temp ramp test (RM+Acri3 sample)*

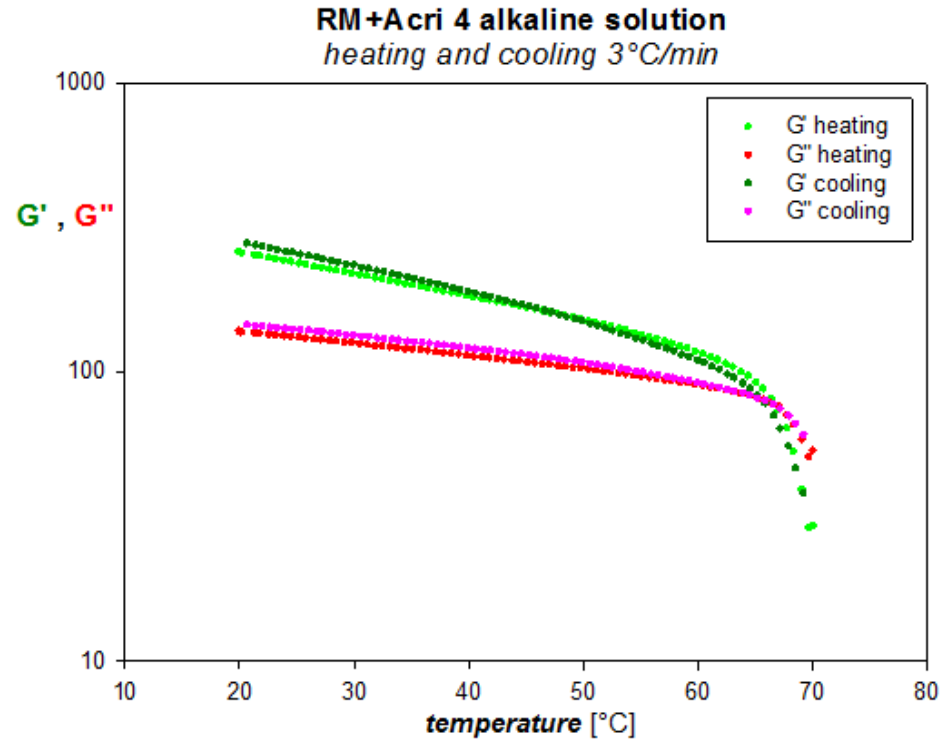


*Figure 5.27: Heating and cooling cycle in a temp ramp test (RM+Acri4 sample)*

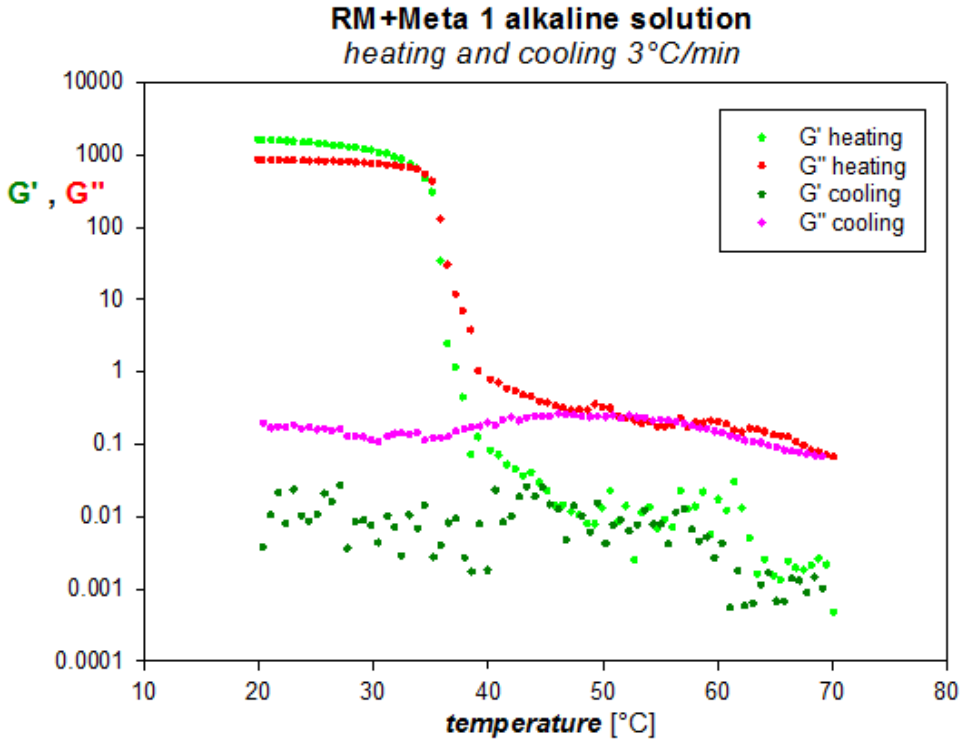


*Figure 5.28: Heating and cooling cycle in a temp ramp test (RM+Meta1 sample)*

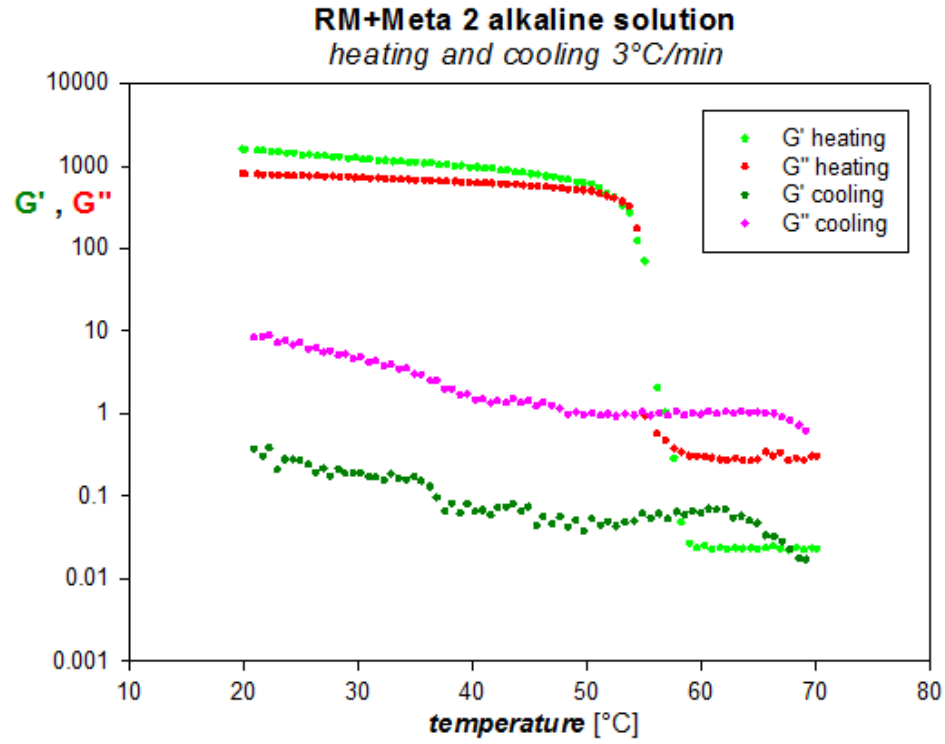


*Figure 5.29: Heating and cooling cycle in a temp ramp test (RM+Meta2 sample)*

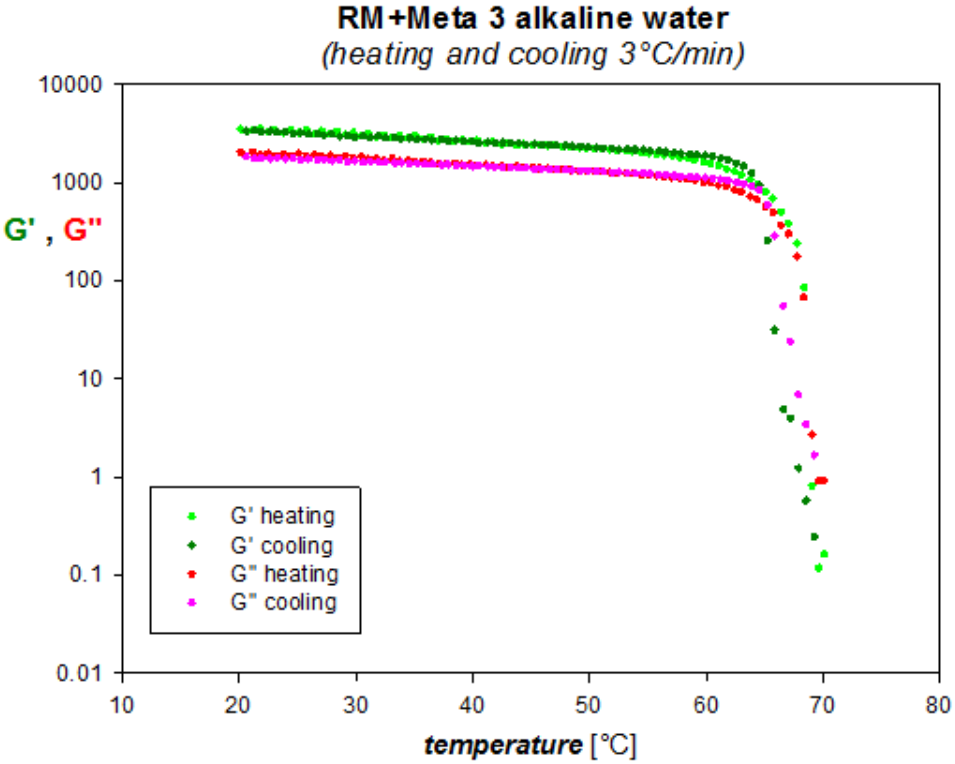


*Figure 5.30: Heating and cooling cycle in a temp ramp test (RM+Meta3 sample)*

Analysing these preliminary results it is clear that the two kinds of additives have a synergic effect on the rheology of the solutions. However these tests do not give a complete explanation of the phenomena and other tests have been performed on these systems. They are reported in the following pages.

Table 5.2 resume all quantitative parameters.

| **Parameters** | Acri1 + RM (limewater) | Acri2 + RM (limewater) | Acri3 + RM (limewater) | Acri4 + RM (limewater) | Meta1 + RM (limewater) | Meta2 + RM (limewater) | Meta3 + RM (limewater) |
|---|---|---|---|---|---|---|---|
| $\boldsymbol{\tau_p}$ [Pa] | 230 | 317 | 40 | 253 | 79 | 92 | 35 |
| $\boldsymbol{\bar{\eta}_i}$ [Pa*s] | $\mathbf{1.4 \cdot 10^4}$ | $\mathbf{1.5 \cdot 10^4}$ | $\mathbf{2 \cdot 10^4}$ | $\mathbf{3.3 \cdot 10^4}$ | $\mathbf{2 \cdot 10^4}$ | $\mathbf{2 \cdot 10^4}$ | $\mathbf{1.1 \cdot 10^5}$ |
| $\frac{\boldsymbol{\eta_s}}{\boldsymbol{\eta_c}}$ | 0.7 | 0.75 | 1 | 1.65 | 1 | 1 | 5.5 |
| $\dot{\gamma}_{cr,i}$<br>$\dot{\gamma}_{cr,s}$<br>$[\boldsymbol{s^{-1}}]$ | -<br>- | -<br>- | 0.04<br>0.4 | -<br>- | 0.006<br>40 | 0.016<br>0.05 | 0.005<br>9 |
| $\boldsymbol{T_p}$ [°C] | 64 | 63 | 47 | 65 | 37 | 55 | 66 |
| $\boldsymbol{\bar{G}'_i}$ [Pa]<br>$\boldsymbol{\bar{G}''_i}$ [Pa] | 170<br>50 | 130<br>85 | 965<br>570 | 165<br>118 | 1011<br>887 | 1079<br>856 | 2156<br>1746 |

*Table 5.2*

## 5.3 *Effect of the sulphates addition*

An aqueous solution more similar to the cement-based formulation can be obtained adding to the limewater solutions a certain amount of sulphates. The cement chemical matrix in fact is characterised by the presence of these ions which are mainly introduced with lime addition after the clinker production to improve the cement characteristics.

Some water solutions of SP and RM containing also sulphates have been prepared following the protocol illustrated in the paragraph 2.9. Three different concentrations (30 mM, 100 mM and 200 mM have been used to simulate, respectively, low sulphated cements, medium sulphated cements and high sulphated cements. As above, the first experiments have been performed on the limewater solutions containing the RM without SP addition (figures 5.31-5.34).

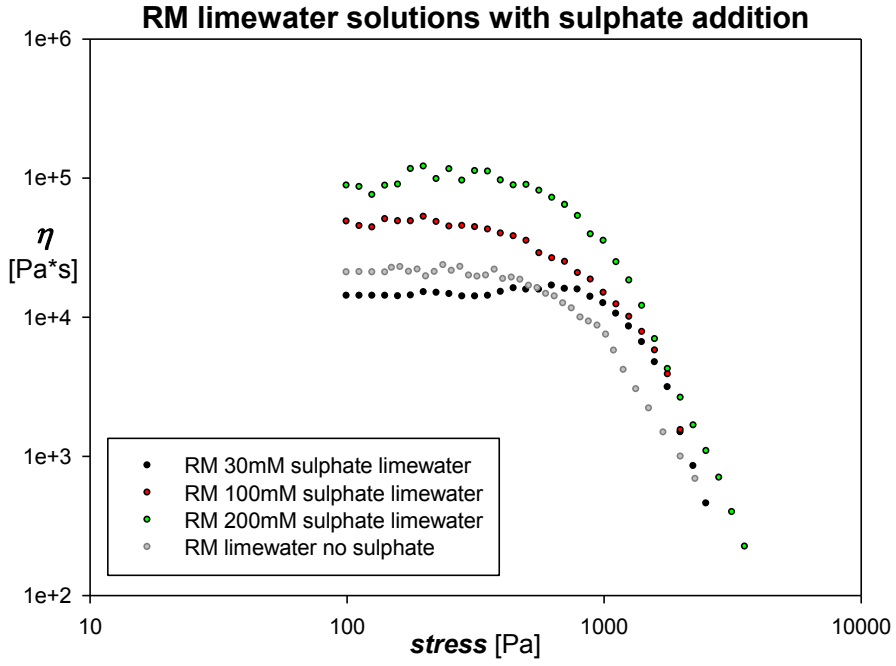


*Figure 5.31: Comparison between RM limewater solution with three different sulphate concentrations (stress sweep test)*

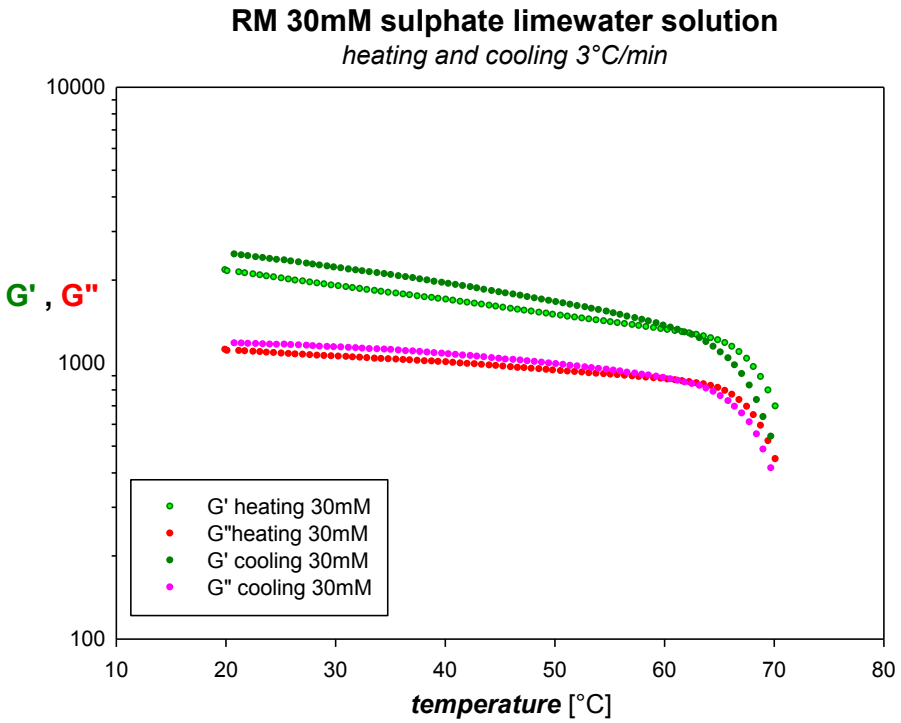


*Figure 5.32: Heating and cooling cycle in the temperature ramp test (30mM)*

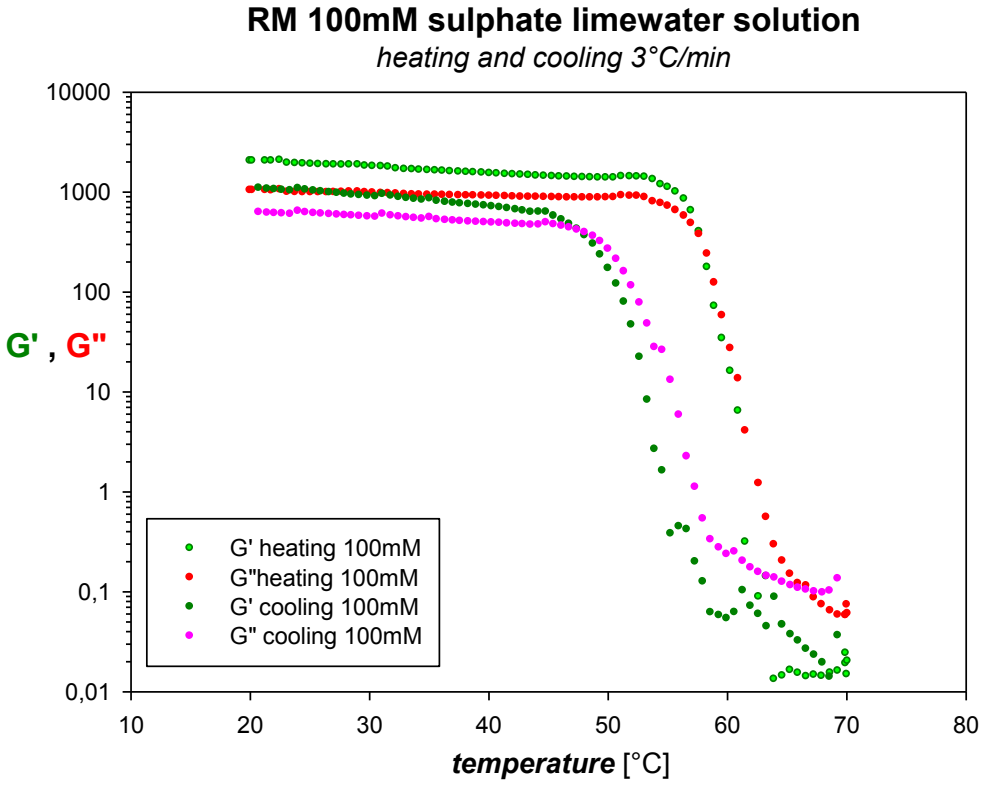


*Figure 5.33: Heating and cooling cycle in the temperature ramp test (100mM)*

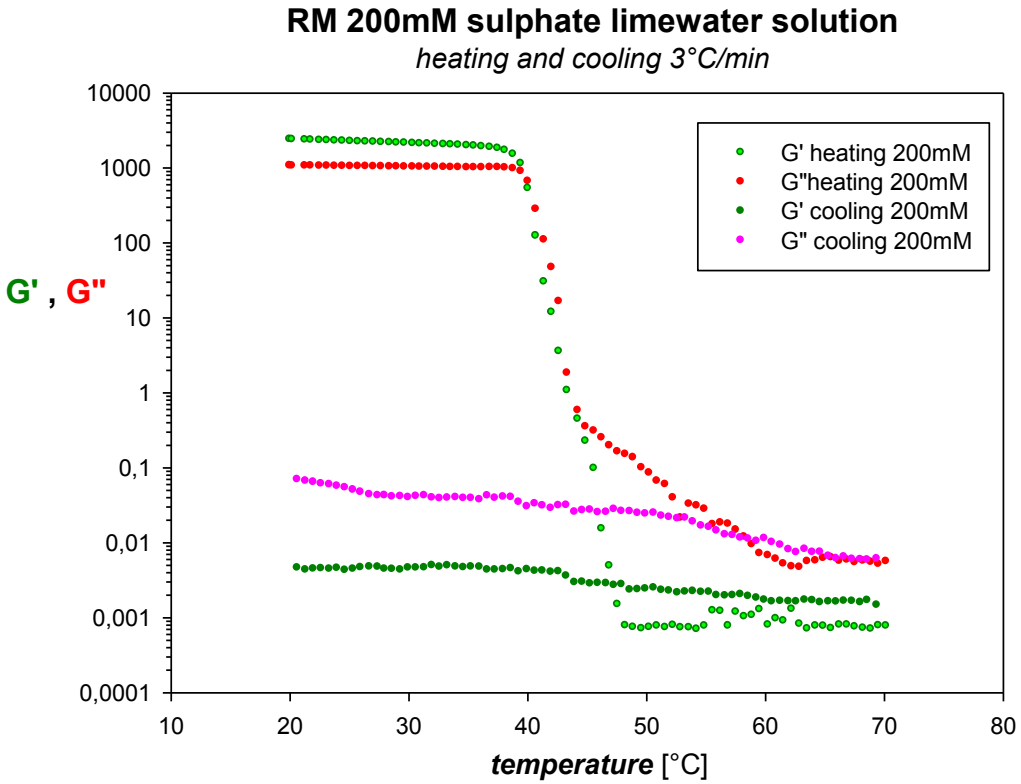


*Figure 5.34: Heating and cooling cycle in the temperature ramp test (200mM)*

The stress sweep test has evidenced the differences between viscosity curves of the four solutions: the solution with 30 mM of sulphate concentration is the only solution to be characterised by a lower viscosity respect to the RM solution without sulphates and this occurs just for stress values higher than 550-560 Pa. Apart from this effect, the initial viscosity value increases with the concentration of sulphate and this is probably due to a structuring effect introduced by the sulphate ions on the aqueous solution which is not visible under a certain sulphate concentration. The four curves tends to converge in the high shear stress zone. No sharp viscosity decreases are visible also for these solutions. The dynamic tests have evidenced a further difference between the solution 30 mM and the other two sulphate solutions: these latters present the typical sudden decrease of G' and G" observed in the neutral and limewater solutions containing also the SP. The explanation of this phenomenon is probably to research in the electronic interactions between the cellulose and ions present in the solution which lead to a worse interaction between water environment and cellulose ether, inducing a lower temperature microprecipitation.

A further sophistication of the complexity of these systems comes from the addition of SPs to the sulphate solutions in order to understand the effect of sulphate ions presence on the SP behaviour.

With this aim, two different acrylic SPs (Acri1 and Acri2) and two different methacrylic SPs (Meta1 and Meta2) were added to three different concentrations of sulphate (once again 30 mM, 100 mM and 200 mM). The results obtained from the stationary tests are plotted in the following graphs (figures 5.35-5.38). For comparison the curves of the correspondent limewater solutions without the sulphate addition are also reported.

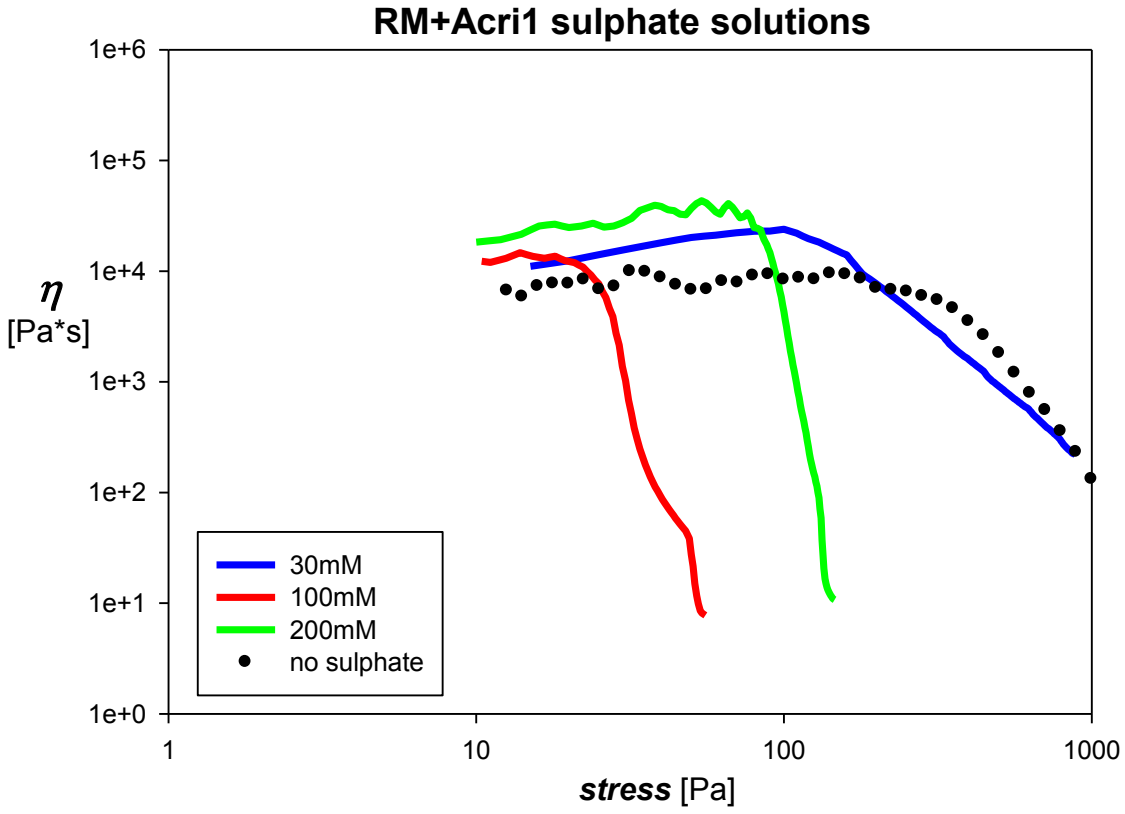


*Figure 5.35: Viscosity curves of the sulphate solutions with SP Acri1*

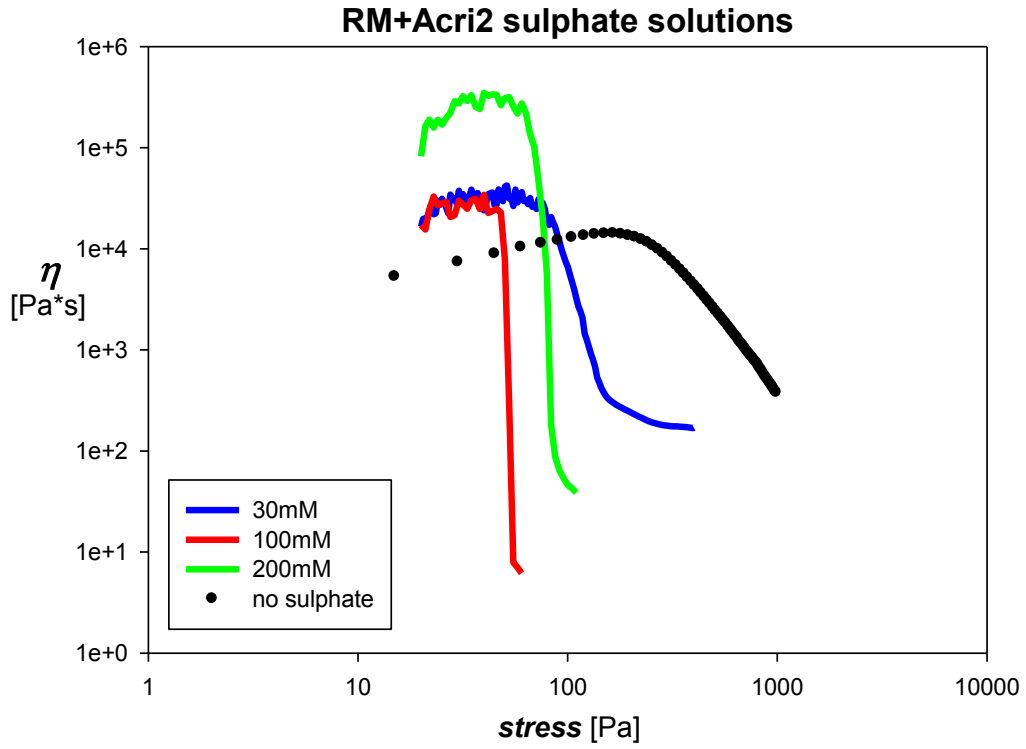


*Figure 5.36: Viscosity curves of the sulphate solutions with SP Acri2*

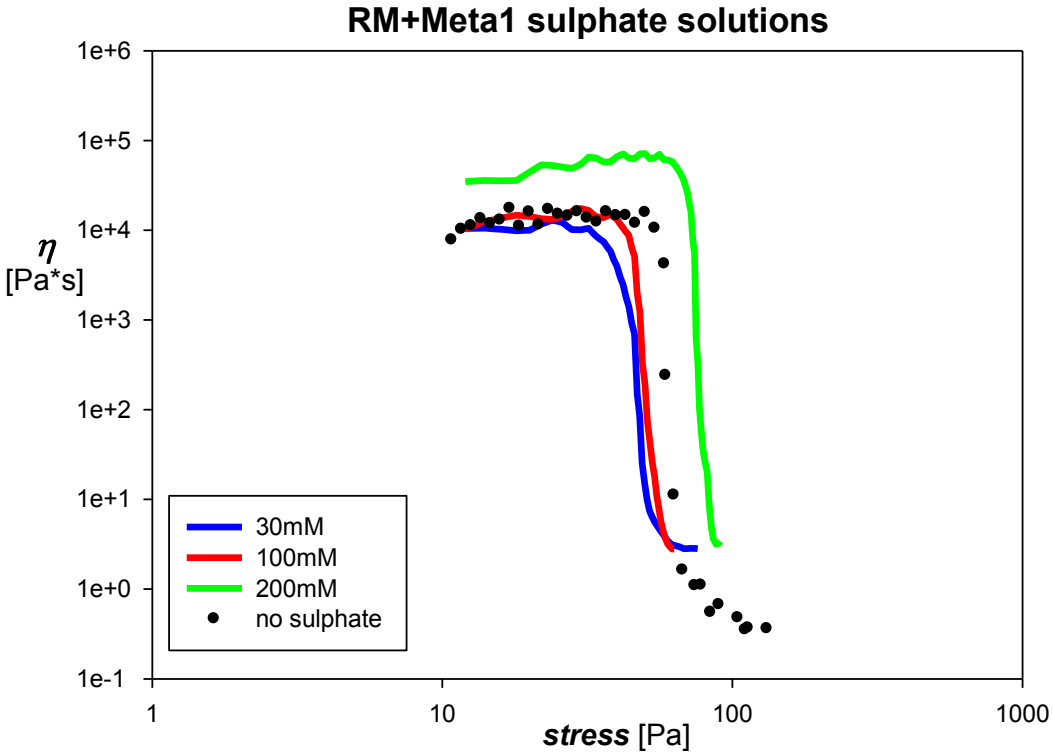


*Figure 5.37: Viscosity curves of the sulphate solutions with SP Meta1*

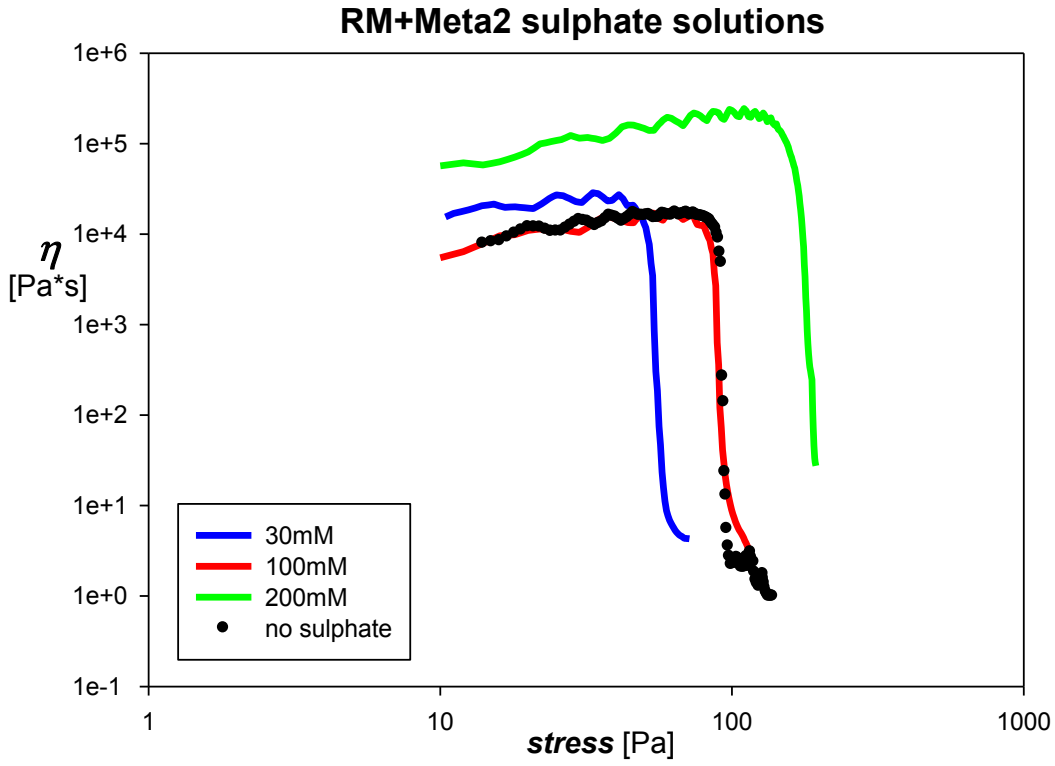


*Figure 5.38: Viscosity curves of the sulphate solutions with SP Meta2*

As clearly visible, the destabilization effect induced by the SP addition is present also for these samples; the only exception seems to be represented by the 30 mM sulphate solution containing the SP Acri1. An important observation can be done about the viscosity fall order (considering an increasing stress) of the solution: as more clearly shown in table 5.3, the fall order is 30→100→200 for both solutions containing the methacrylic SPs and it is instead 100→200→30 for the solutions containing the acrylic SPs.

| **SP** | Viscosity fall order |
|---|---|
| ***Acri1*** | 100mM→200mM→30mM |
| ***Acri2*** | 100mM→200mM→30mM |
| ***Meta1*** | 30mM→100mM→200mM |
| ***Meta2*** | 30mM→100mM→200mM |

*Table 5.3*

The linear trend which characterises the solutions with methacrylics can be probably explained with a particular effect introduced by the sulphate ions addition. This effect increases with the sulphate content of the solution. The particular order visible for the acrylics reminds in a certain way) the strange effect seen in the sulphate solutions with RM only (see figure 5.31). In particular, the viscosity of the 30 mM solution (without SP) presented an initial viscosity lower than the viscosity of the solution without sulphates but, with respect to this latter, the 100mM and the 200mM had an initial viscosity which was respectively higher and higher. Probably the two phenomena are connected but the results of these experiment are not sufficient to deeply investigate on the possible link.

To complete the description the flow curves are illustrated in figures 5.39-5.42.

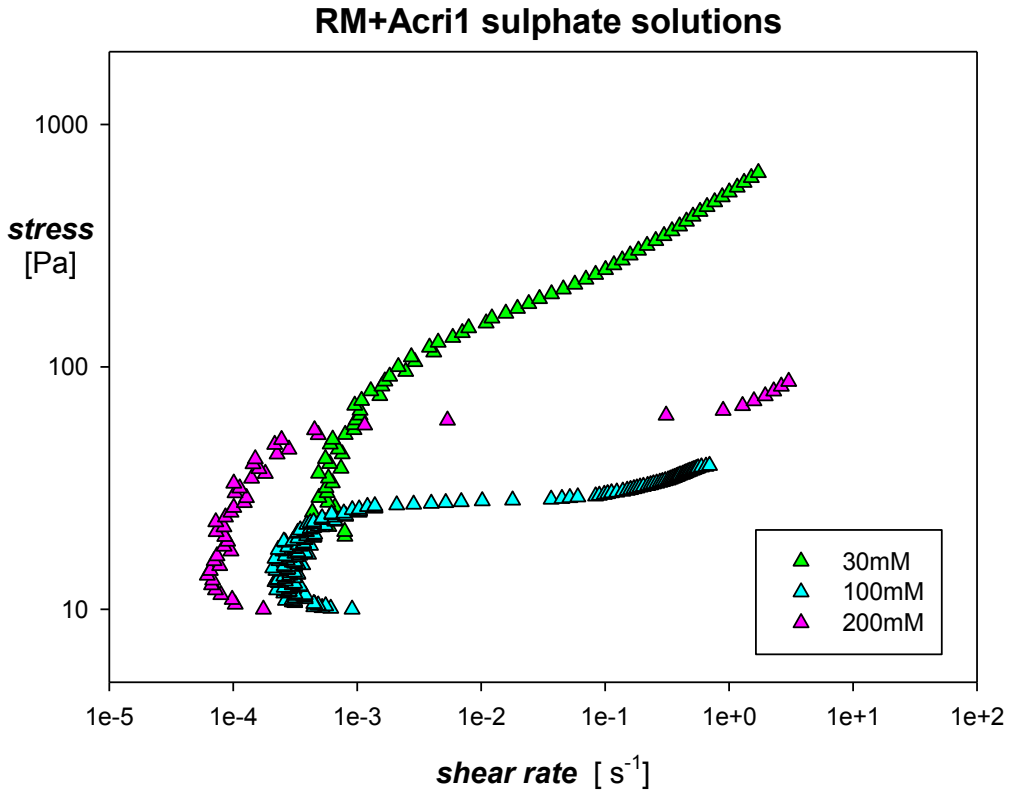


*Figure 5.39: Flow curves of the sulphate solutions with SP Acri1*

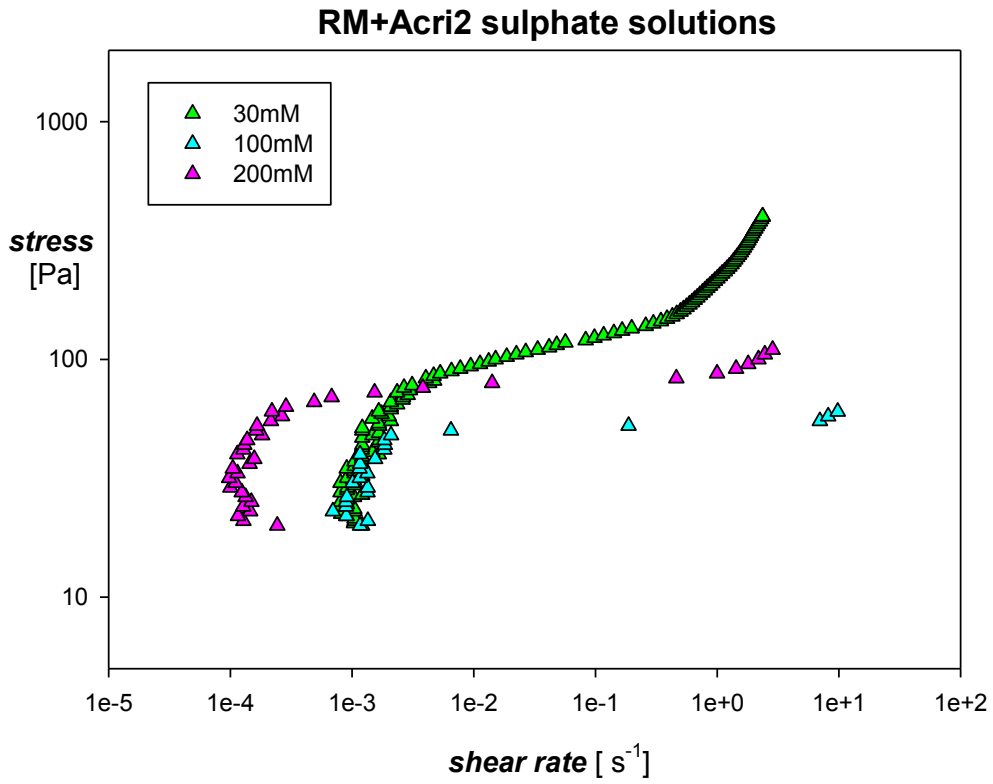


*Figure 5.40: Flow curves of the sulphate solutions with SP Acri2*

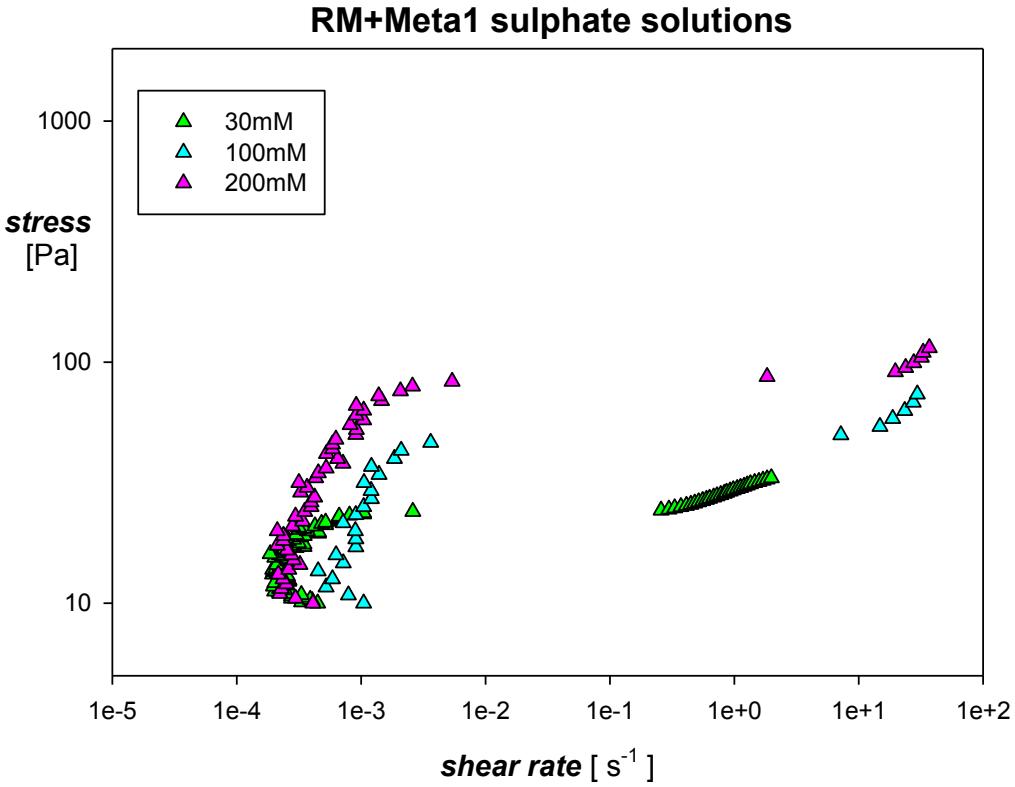


*Figure 5.41: Flow curves of the sulphate solutions with SP Meta1*

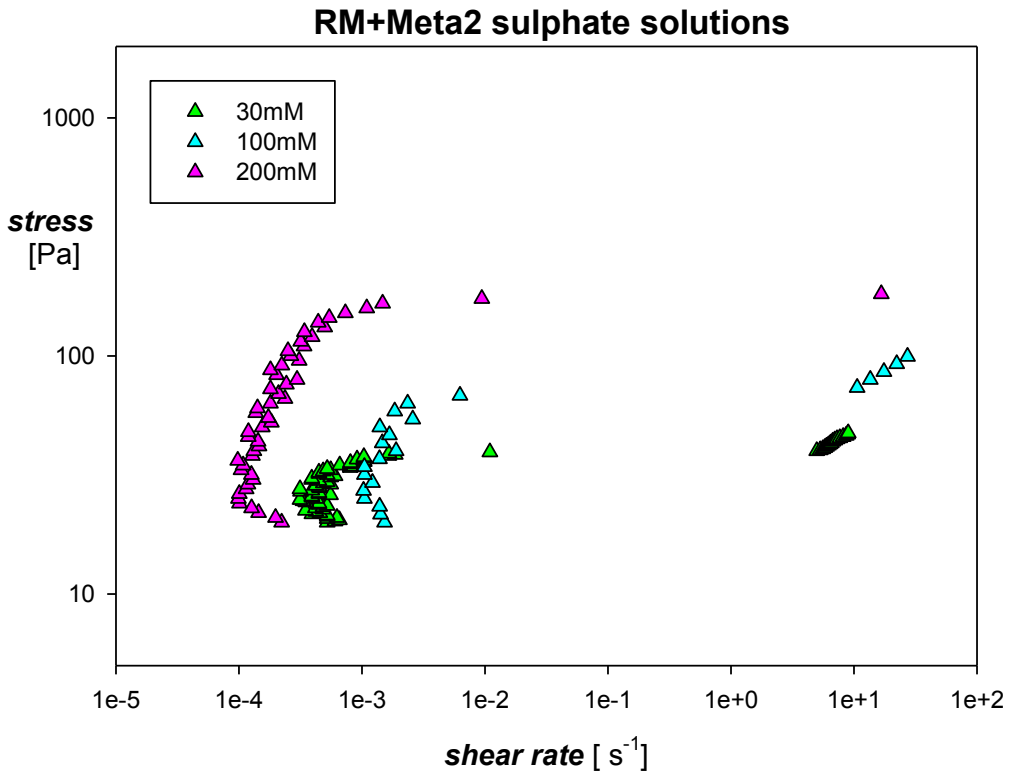


*Figure 5.42: Flow curves of the sulphate solutions with SP Meta2*

The samples have been finally tested with temperature ramp tests in the same conditions of the previous experiments. The figures from 5.43 to 5.50 illustrate the obtained results (for better clarity the G' curves are plotted separately from the G" curves).

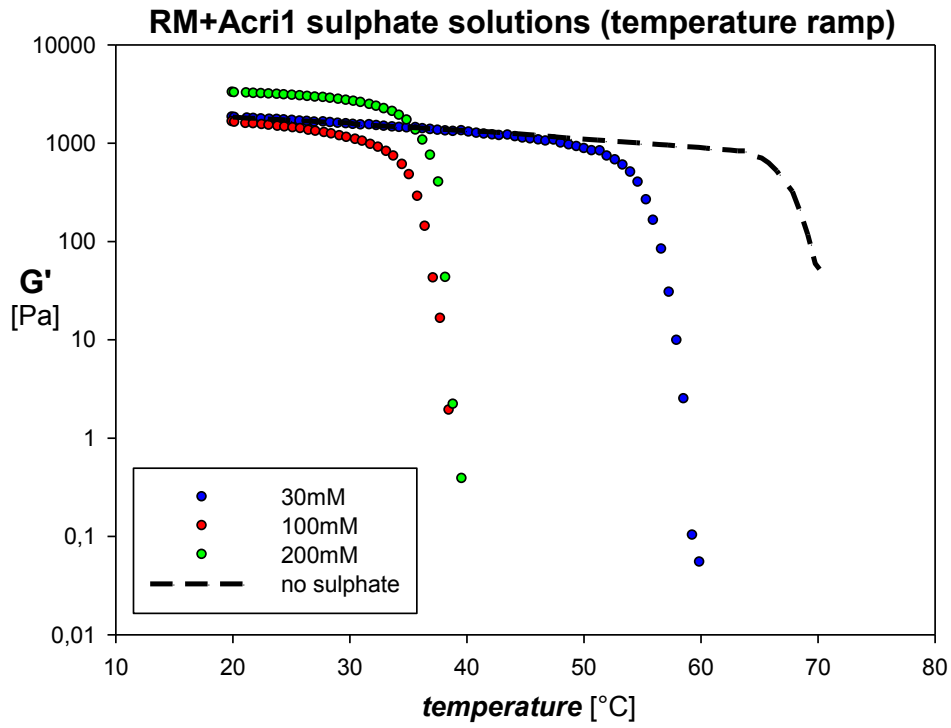


*Figure 5.43: Temperature ramp test of the sulphate solutions with Acri1 (G' curve)*

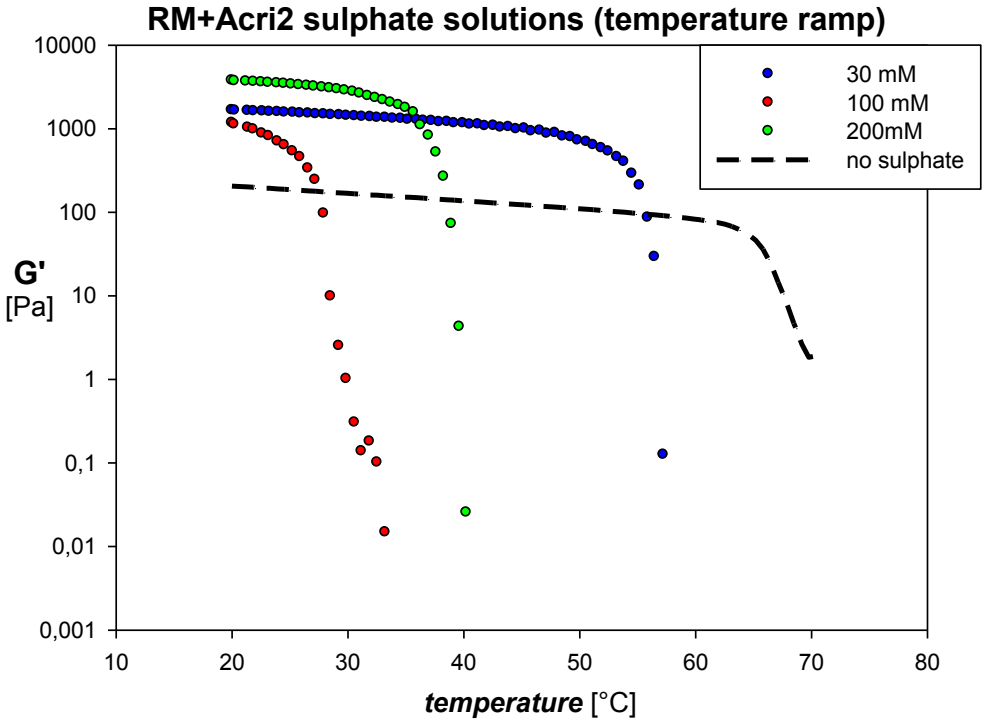


*Figure 5.44: Temperature ramp test of the sulphate solutions with Acri2 (G' curve)*

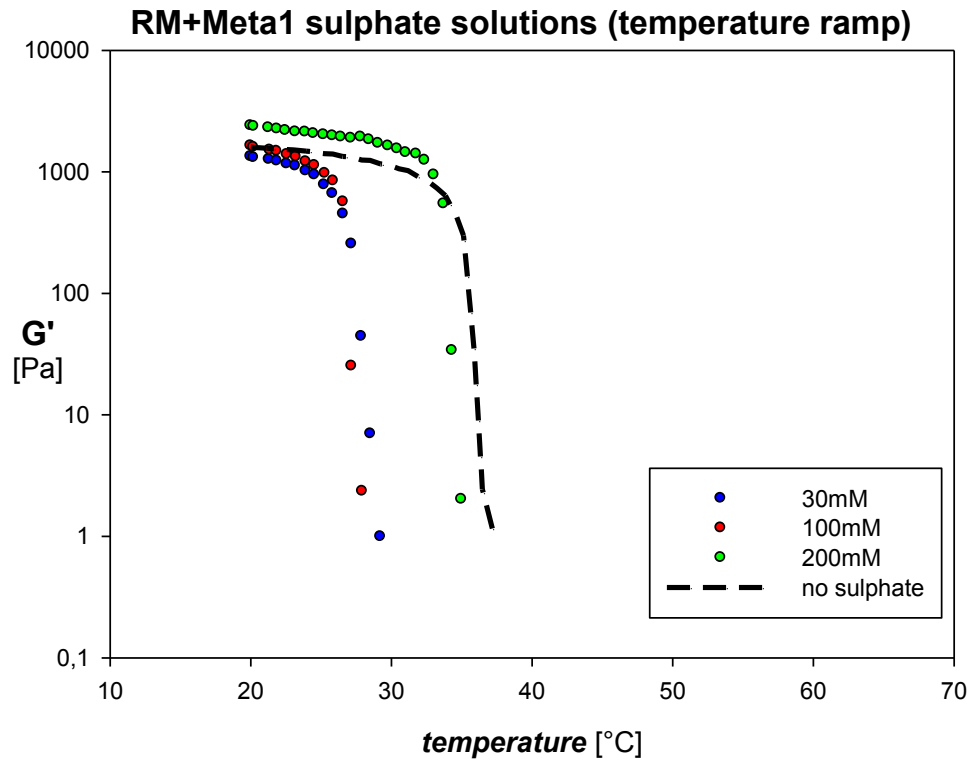


*Figure 5.45: Temperature ramp test of the sulphate solutions with Meta1 (G' curve)*

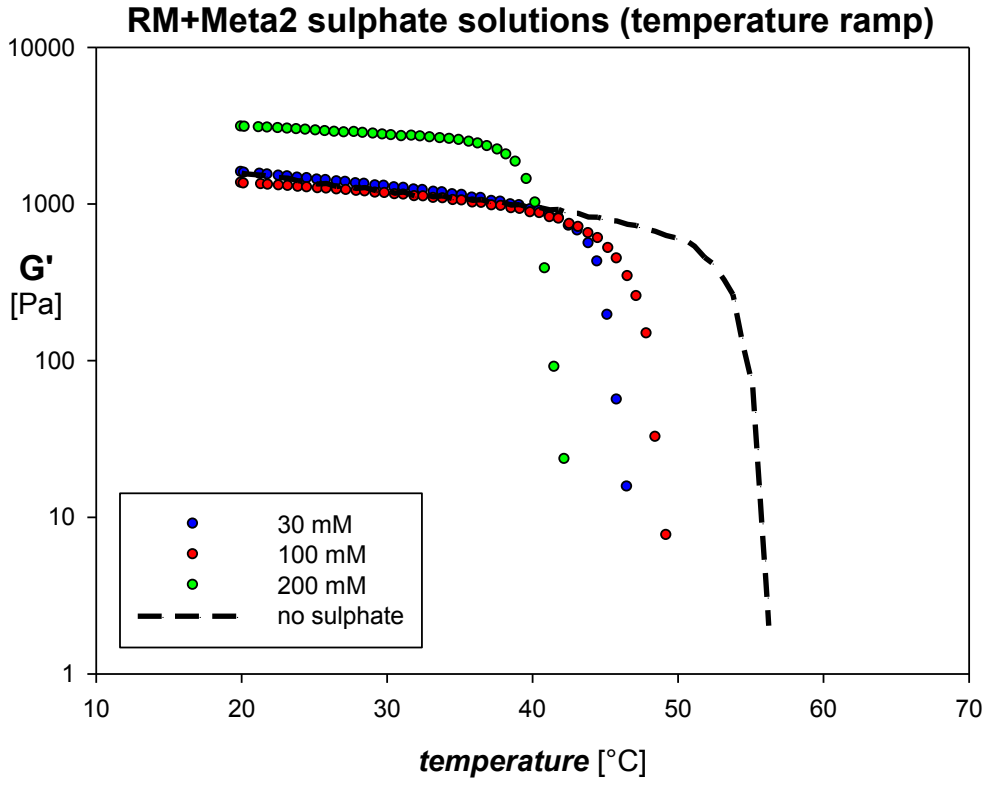


*Figure 5.46: Temperature ramp test of the sulphate solutions with Meta2 (G' curve)*

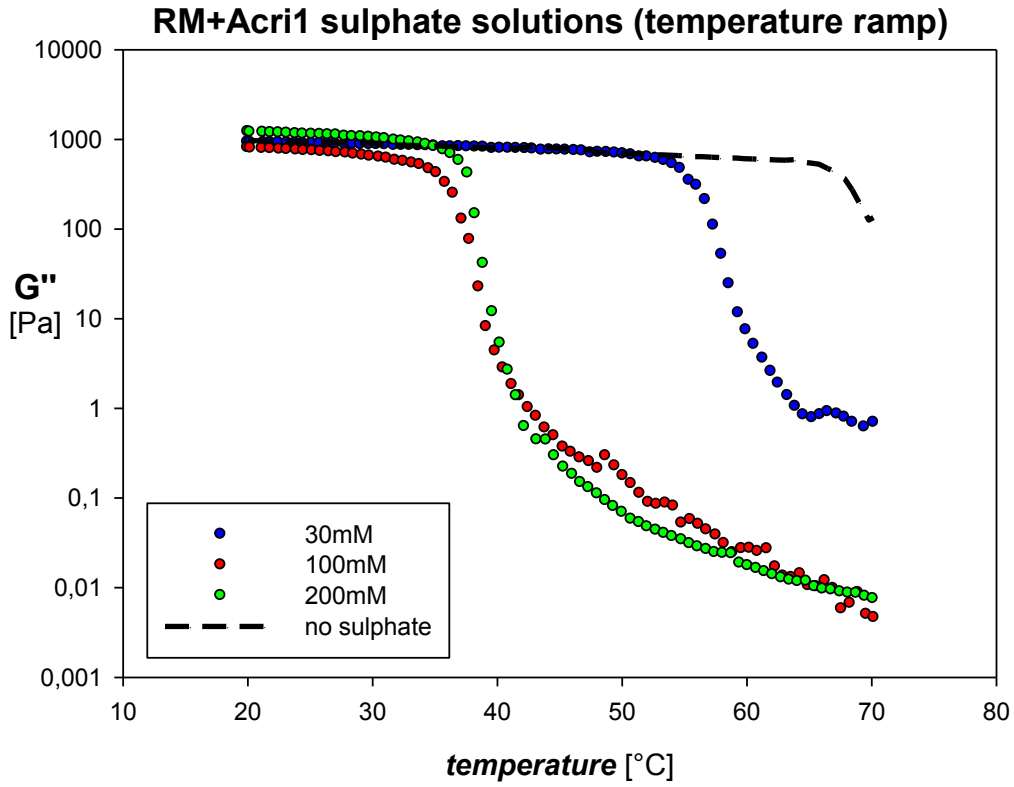


*Figure 5.47: Temperature ramp test of the sulphate solutions with Acri1 (G" curve)*

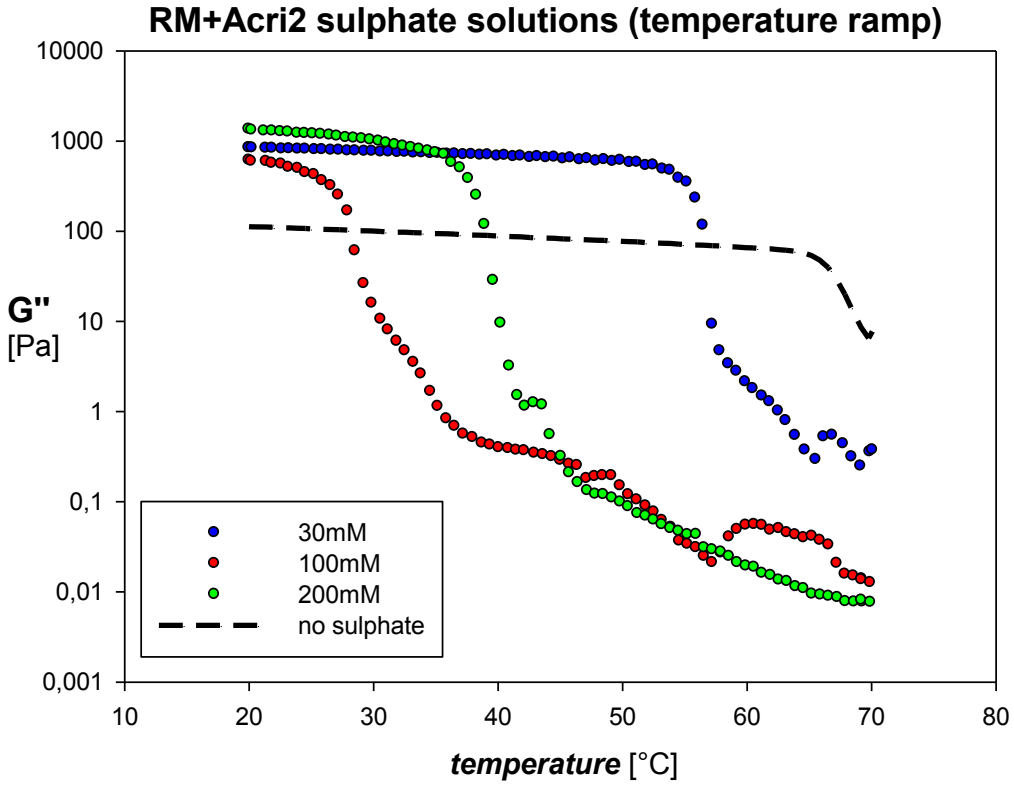


*Figure 5.48: Temperature ramp test of the sulphate solutions with Acri2 (G" curve)*

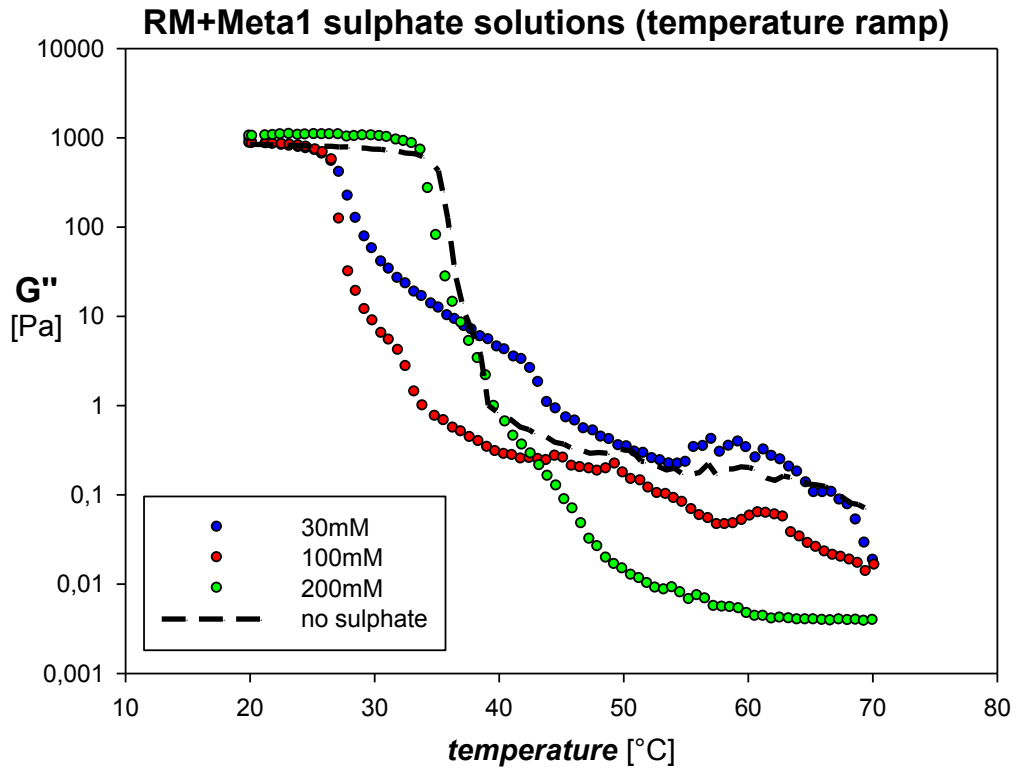


*Figure 5.49: Temperature ramp test of the sulphate solutions with Meta1 (G" curve)*

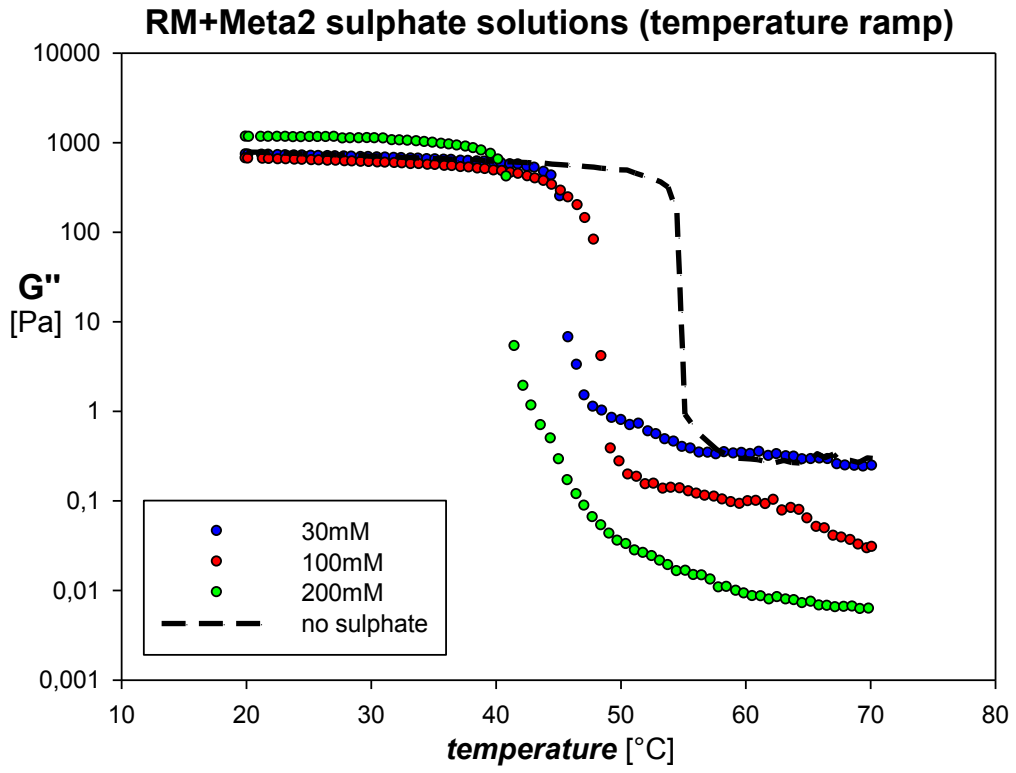


*Figure 5.50: Temperature ramp test of the sulphate solutions with Meta2 (G" curve)*

With the addition of methacrylic SP the drastic G' and G" fall occurs once again for temperatures which are very close to room temperature. This fall does not follow a particular order dependent on the sulphate concentration. On the contrary, very interesting is the fall order which characterises the solutions containing the acrylic SPs (see table 5.4).

| **SP** | G',G" fall order |
|---|---|
| ***Acri1*** | 100mM→200mM→30mM |
| ***Acri2*** | 100mM→200mM→30mM |
| ***Meta1*** | 100mM→30mM→200mM |
| ***Meta2*** | 200mM→30mM→100mM |

*Table 5.4*

The order 100mM→200mM→30mM is again respected also in the temperature ramp test and this is a further proof that this order is not random.

In order to quantitatively correlate data relative to the three different concentrations, tables 5.5, 5.6 and 5.7 are below reported. The parameters used in the comparison are the same used for the solutions prepared with neutral water and limewater.

| **Parameters** | Acri1 + RM (30 mM) | Acri2 + RM (30 mM) | Meta1 + RM (30 mM) | Meta2 + RM (30 mM) |
|---|---|---|---|---|
| $\boldsymbol{\tau_p}$ [Pa] | 120 | 84 | 69 | 72 |
| $\boldsymbol{\overline{\eta}_i}$ [Pa*s] | $\mathbf{2 \cdot 10^4}$ | $\mathbf{3 \cdot 10^4}$ | $\mathbf{1.5 \cdot 10^4}$ | $\mathbf{2 \cdot 10^4}$ |
| $\frac{\boldsymbol{\eta_s}}{\boldsymbol{\eta_c}}$ | 1.3 | 2 | 1 | 1.3 |
| $\dot{\gamma}_{cr,i}$<br>$\dot{\gamma}_{cr,s}$<br>$[\boldsymbol{s^{-1}}]$ | 0.06<br>40 | 0.017<br>0.5 | 0.016<br>4 | 0.002<br>0.25 |
| $\boldsymbol{T_p}$ [°C] | 57 | 55 | 27 | 45 |
| $\boldsymbol{\overline{G}'_i}$ [Pa]<br>$\boldsymbol{\overline{G}''_i}$ [Pa] | 1510<br>850 | 1163<br>701 | 1022<br>987 | 1085<br>867 |

*Table 5.5*

| **Parameters** | Acri1 + RM (100 mM) | Acri2 + RM (100 mM) | Meta1 + RM (100 mM) | Meta2 + RM (100 mM) |
|---|---|---|---|---|
| $\boldsymbol{\tau_p}$ [Pa] | 30 | 54 | 74 | 72 |
| $\boldsymbol{\overline{\eta}_i}$ [Pa*s] | $\mathbf{2 \cdot 10^4}$ | $\mathbf{2 \cdot 10^4}$ | $\mathbf{1.4 \cdot 10^4}$ | $\mathbf{2 \cdot 10^4}$ |
| $\frac{\boldsymbol{\eta_s}}{\boldsymbol{\eta_c}}$ | 1.4 | 1.4 | 1 | 1.4 |
| $\dot{\gamma}_{cr,i}$<br>$\dot{\gamma}_{cr,s}$<br>$[\boldsymbol{s^{-1}}]$ | 0.008<br>0.34 | 0.065<br>0.15 | 0.0036<br>6 | 0.0063<br>9 |
| $\boldsymbol{T_p}$ [°C] | 37 | 29 | 27 | 48 |
| $\boldsymbol{\overline{G}'_i}$ [Pa]<br>$\boldsymbol{\overline{G}''_i}$ [Pa] | 1620<br>980 | 1073<br>911 | 1043<br>958 | 1048<br>887 |

*Table 5.6*

| **Parameters** | Acri1 + RM (200 mM) | Acri2 + RM (200 mM) | Meta1 + RM (200 mM) | Meta2 + RM (200 mM) |
|---|---|---|---|---|
| $\boldsymbol{\tau_p}$ [Pa] | 100 | 94 | 74 | 72 |
| $\boldsymbol{\bar{\eta}_i}$ [Pa*s] | $\mathbf{2.5 \cdot 10^4}$ | $\mathbf{2 \cdot 10^5}$ | $\mathbf{1.4 \cdot 10^4}$ | $\mathbf{2 \cdot 10^4}$ |
| $\frac{\boldsymbol{\eta_s}}{\boldsymbol{\eta_c}}$ | 2 | 16 | 1 | 1.4 |
| $\dot{\gamma}_{cr,i}$<br>$\dot{\gamma}_{cr,s}$<br>$[\boldsymbol{s^{-1}}]$ | 0.001<br>0.19 | 0.014<br>0.45 | 0.0054<br>1.8 | 0.008<br>0.25 |
| $\boldsymbol{T_p}$ [°C] | 38 | 39 | 34 | 41 |
| $\boldsymbol{\bar{G}'_i}$ [Pa]<br>$\boldsymbol{\bar{G}''_i}$ [Pa] | 1620<br>980 | 1073<br>911 | 2759<br>998 | 3030<br>1180 |

*Table 5.7*

## 5.4 *Comparison between solutions and real systems*

As done in the chapter dedicated to paints, a comparison between the aqueous solutions and the correspondent cement mixtures has been operated. For this purpose, some cement mixtures for extrusion with the same additives in the same proportions have been first prepared (according to the procedure exposed in the paragraph 2.10) and tested with the die rheometer. The experimental procedure used is the following: after loading the rheometer with the material, the piston moves with a fixed constant velocity, obtaining a graph similar to that reported in figure 5.51. In this way the pressure of the material at the entrance is obtained as a function of time. The signal, except for an initial peak of transient, is essentially constant. In this phase the stationary point has been calculated as the average of the pressures in the range between the beginning of the flattening of the curve and the final point.

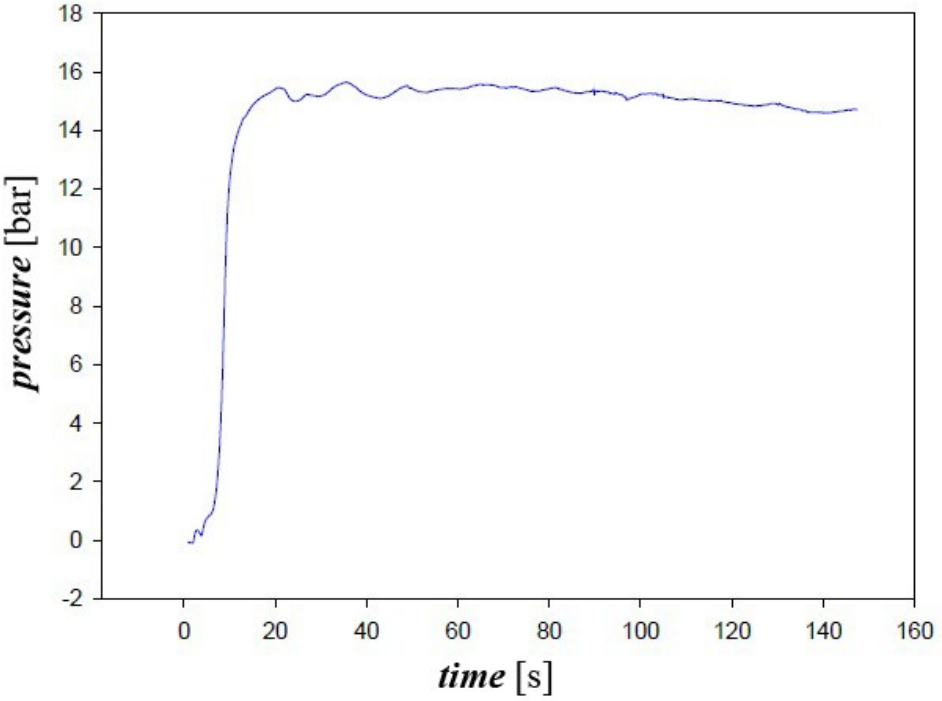


*Figure 5.51: Example of the output graph for the die rheometer*

For each material the pressure value has been calculated for all the velocities and is reported in table 5.8.

| Velocity [mm/min] | Apparent shear rate [1/s] |
|---|---|
| 6,9 | 1,95 |
| 13,2 | 3,73 |
| 25,2 | 7,12 |
| 48,6 | 13,73 |
| 93,6 | 26,45 |
| 180 | 50,86 |
| 250 | 70,65 |

*Table 5.8*

From the pressure drop data the diagram $\boldsymbol{\sigma}_{\mathrm{p}}$ vs. $\dot{\gamma}_a$ can be obtained. From this curve the real shear rate is calculated from the slope of the curve and used to obtain the final graph $\eta$ vs. $\dot{\gamma}$.

The results have been plotted in comparison with that obtained by the analysis with the rotational rheometer of the aqueous solutions (figures 5.52-5.53).

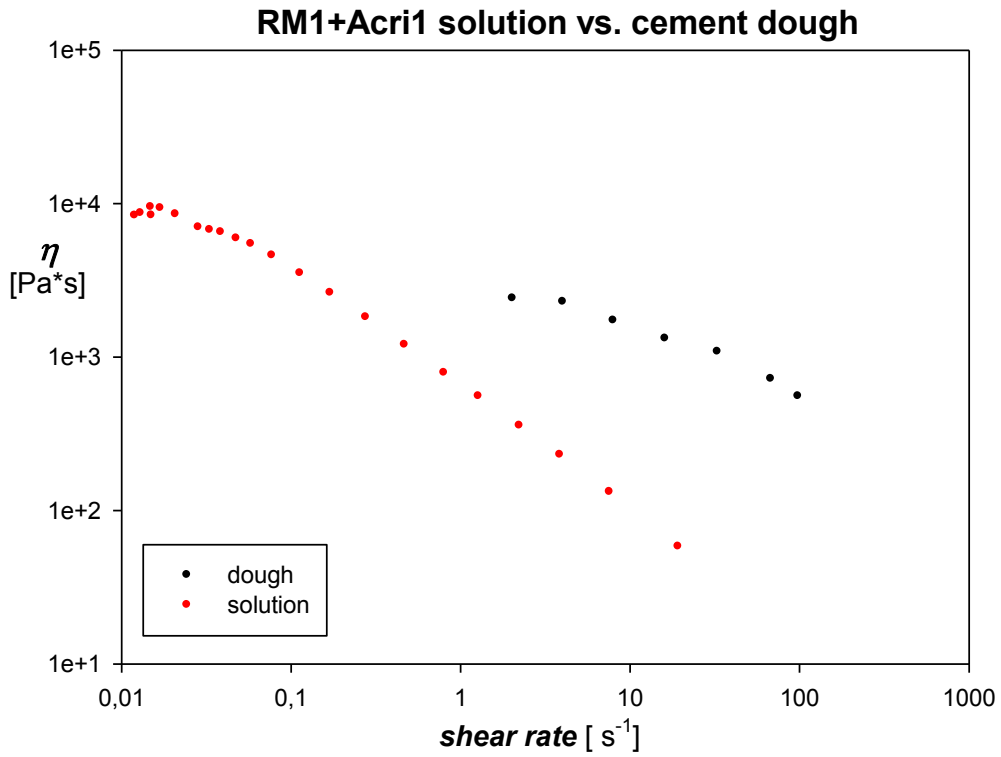


*Figure 5.52: Comparison between the solution and the correspondent cement dough (RM1+Acri2)*

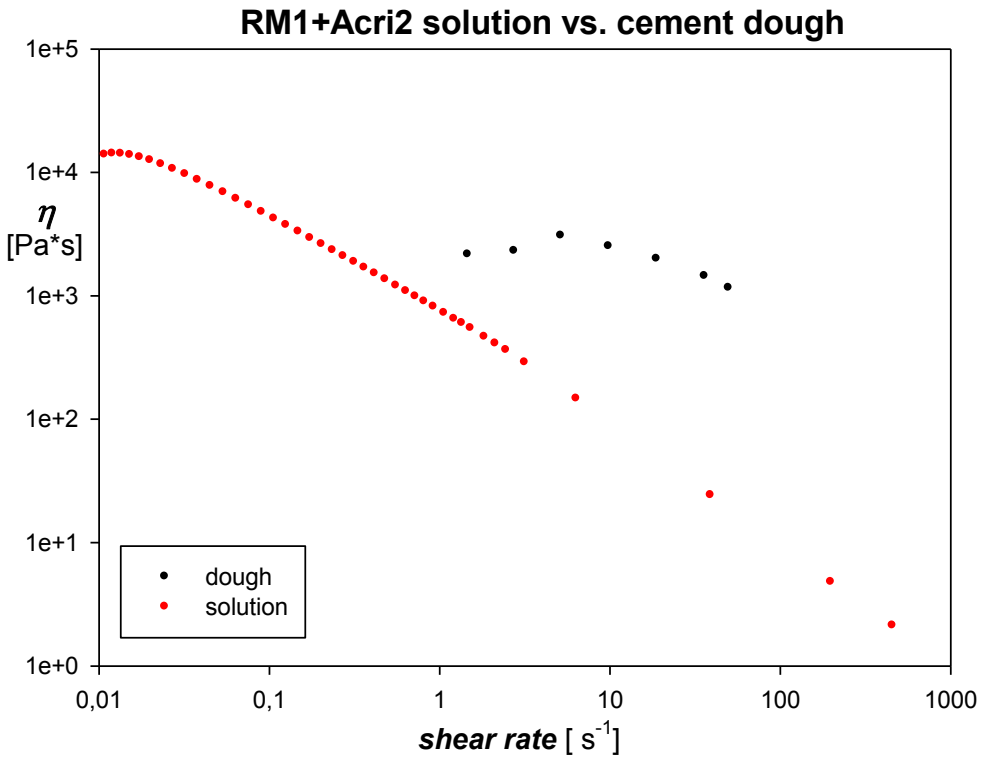


*Figure 5.53: Comparison between the solution and the correspondent cement dough (RM1+Acri1)*

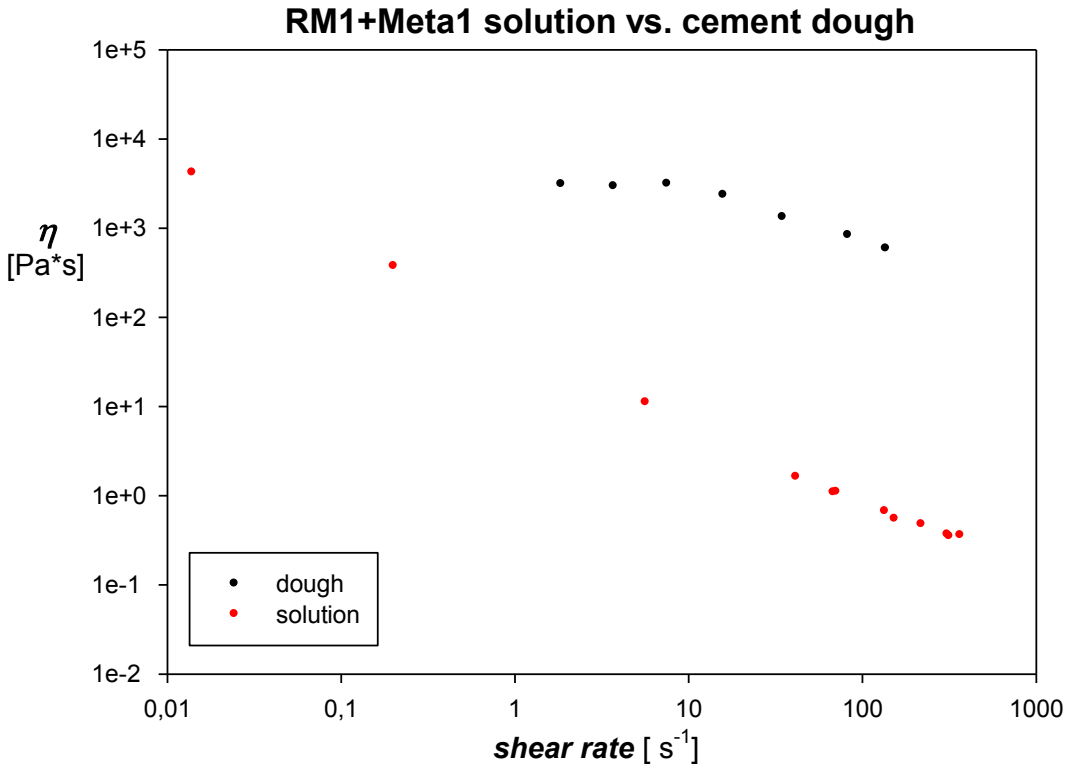


*Figure 5.54: Comparison between the solution and the correspondent cement dough (RM1+Meta1)*

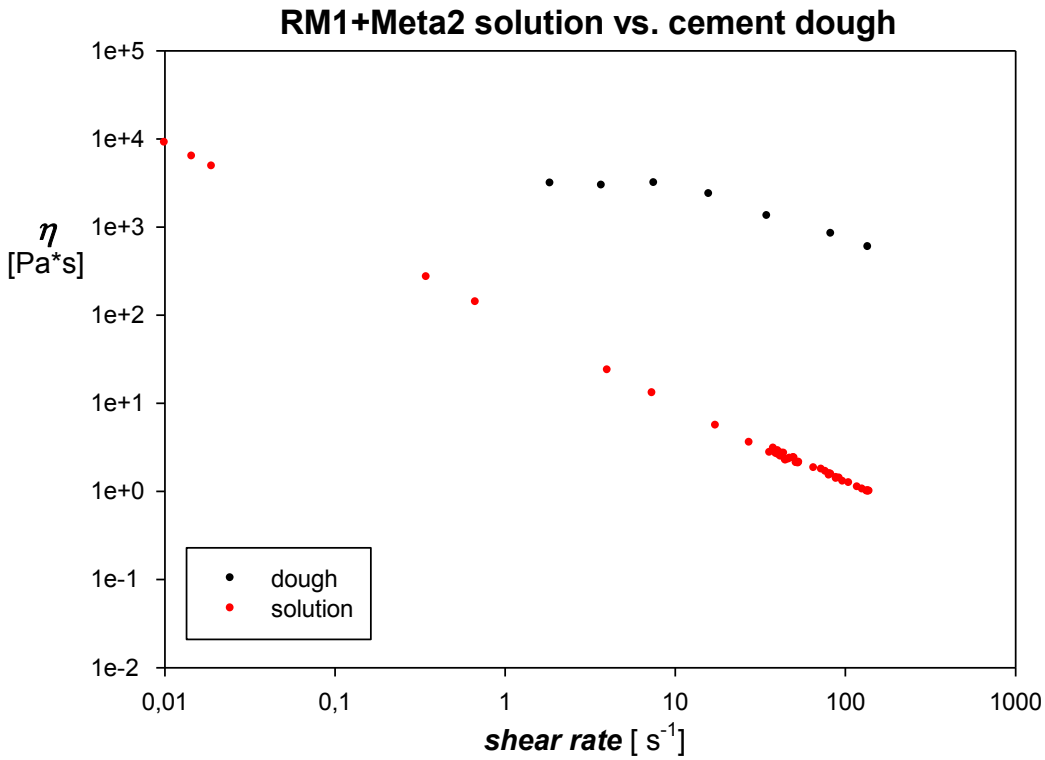


*Figure 5.55: Comparison between the solution and the correspondent cement dough (RM1+Meta2)*

Also in this case there is no a well-defined correlation between the rheological behaviour of the solutions and that of the corresponding cement formulation. The two kinds of behaviour are once again qualitatively similar. Also in the case of the cement dough there is a viscosity decrease after a plateau but it is always a light decrease which is located in a different shear rate zone of that of the solutions viscosity fall. Probably also in this systems for extrusion the contribution to the viscosity of the cement powder and of the other substances present in the mixture is not so unimportant as thought before. Another important consideration regards the fact that the additives can very probably work in a different way according to the different chemical environment. For example, the paragraph 1.7 has explained the action mechanism of the SP and its anti-flocculating effect essentially due to its adsorption on the cement particles, but it is still not very clear how it works in the aqueous solution where it is in combination essentially with cellulose and not with cement.

This study have allowed to optimize a measurement method that can be exploited, mainly in the case of cement mixture for extrusion, to rheologically characterize different compositions searching for the best formulation for this innovative application. In the following paragraph, a rheological study of some cement-based formulations is reported with a special focus on the possibility to mix a

Portland cement with a calcium-sulfoaluminate cement to obtain more eco-compatible extruded materials.

## 5.5 *Rheological study of formulations for extrusion application*

The experimental method optimized during the previous work has given the possibility to test some mixed formulation to be used for extrusion application. In particular, these formulations have been obtained by mixing two kinds of cement: a Portland cement 52,5R and a calcium-sulfoaluminate cement. These two cements have a similar granulometry but the hydration process is quite different and for this reason the rheological behaviour of the hybrid formulations is not so obvious. To understand the effect of a partial substitution of cement Portland on the rheology, the first system characterised were the two standard systems: a formulation with 100% Portland cement (A) and a formulation with 100% calcium-sulfoaluminate cement (B). The velocity of the piston used for these experiments are reported in table 5.9 (the velocity 13,2 mm/min was not possible for the 100% calcium-sulfoaluminate cement formulation because of a too fast setting) and the comparisons between the two kinds of formulation is shown in figure 5.56.

| **Velocity [mm/min]** | **Apparent shear rate [1/s]** |
|---|---|
| 13,2 | 3,73 |
| 25,2 | 7,12 |
| 48,6 | 13,73 |
| 93,6 | 26,45 |
| 120 | 33,91 |
| 180 | 50,86 |
| 250 | 70,65 |
| 380 | 107,38 |
| 480 | 135,64 |

*Table 5.9*

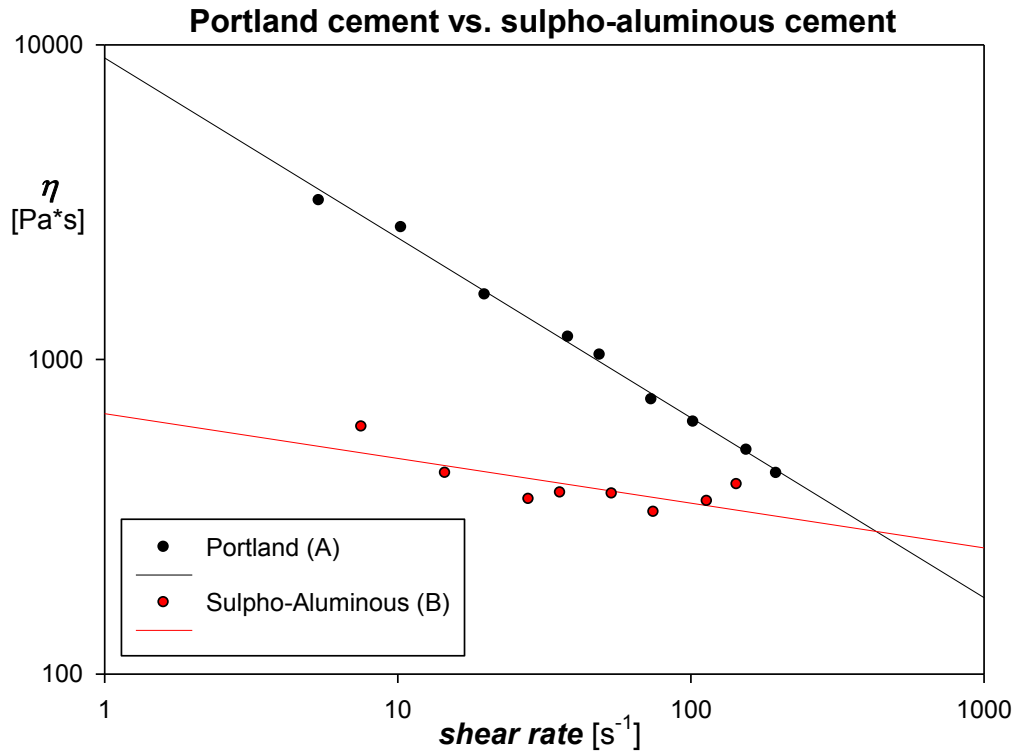


*Figure 5.56: Comparison between the two standard formulations with interpolating curves*

From the comparison main difference suddenly emerges: despite the two formulations have the same cement amount and the same quantity of water, filler and additives, in the entire shear rate range the viscosity values of the formulation A are always higher than that of the formulation B. Another important aspect is represented by the difference between the slopes of the interpolating straight lines, which is equal to n-1. The *flow index* n and consequently the slope of the lines can be used to measure how the behaviour of a certain material moves away from the Newtonian behaviour. In fact, the Newtonian fluids are characterised by a constant viscosity which is independent from the shear rate: this is represented by an horizontal straight line with null slope. Analysing the slope of these curves in figure 5.57, a slope n-1= 0,55 is observed for the formulation A while a slope n-1=0,14 is observed for the formulation B. This means that the behaviour of the formulation B is much closer to the Newtonian behaviour. To understand how the substitution of a Portland fraction with the calcium-sulfoaluminate cement can modify the rheology of the formulation A four different hybrid formulations were analysed: 5%, 10%, 15% and 30%. The percentage value refers to the amount of calcium-sulfoaluminate present on the total. A fifth composition at 50% was also prepared but its hardening was so rapid that it resulted impossible to

work this dough with the calander and consequently to test it in the rheometer. The results are shown in figure 5.57.

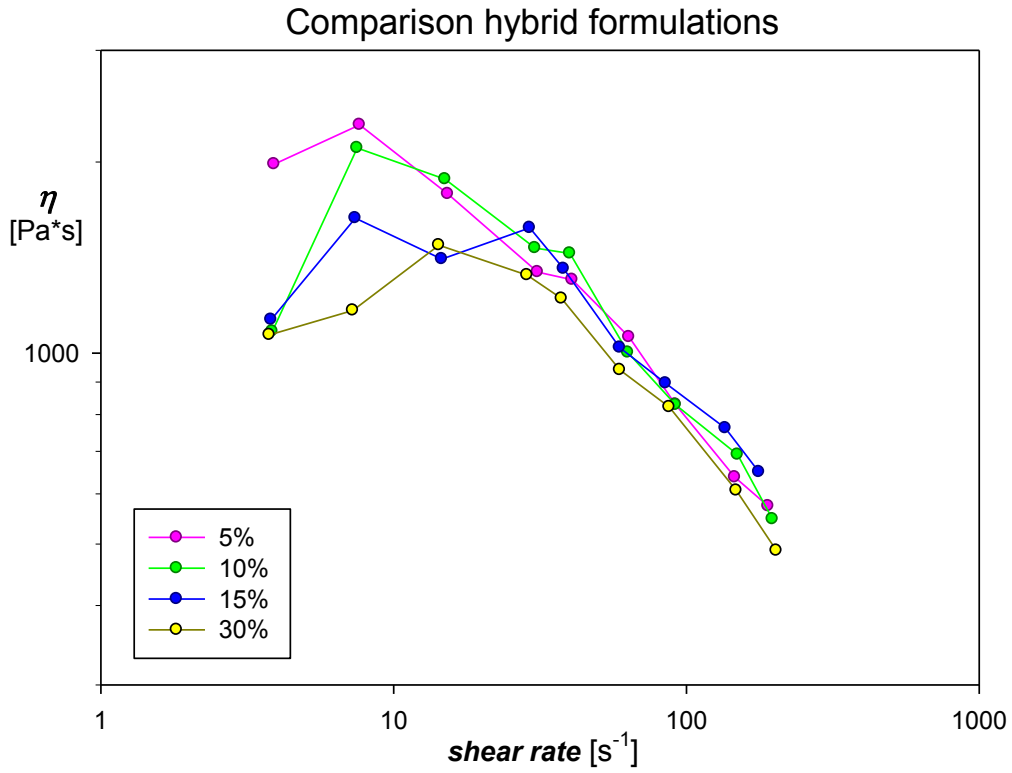


*Figure 5.57: Comparison between the hybrid formulations*

Figure 5.57 shows the experimental points gathered for the four hybrid formulations that present a substantial oscillation due to the intrinsic difficulty of the measurement method. The experimental results have been fitted according to the Ellis model (see paragraph 1.10) which uses three parameters to describe the relation between stress and shear rate (equation 5.1).

$$\sigma = \frac{\eta_0 \dot{\gamma}}{1 + a(\dot{\gamma})^{1-n}} \tag{5.1}$$

The three parameters have then been used to calculate the real shear rate according to the Mooney-Rabinowitsch method. Figures 5.58-5.61 show the interpolating curves of the four hybrid formulations.

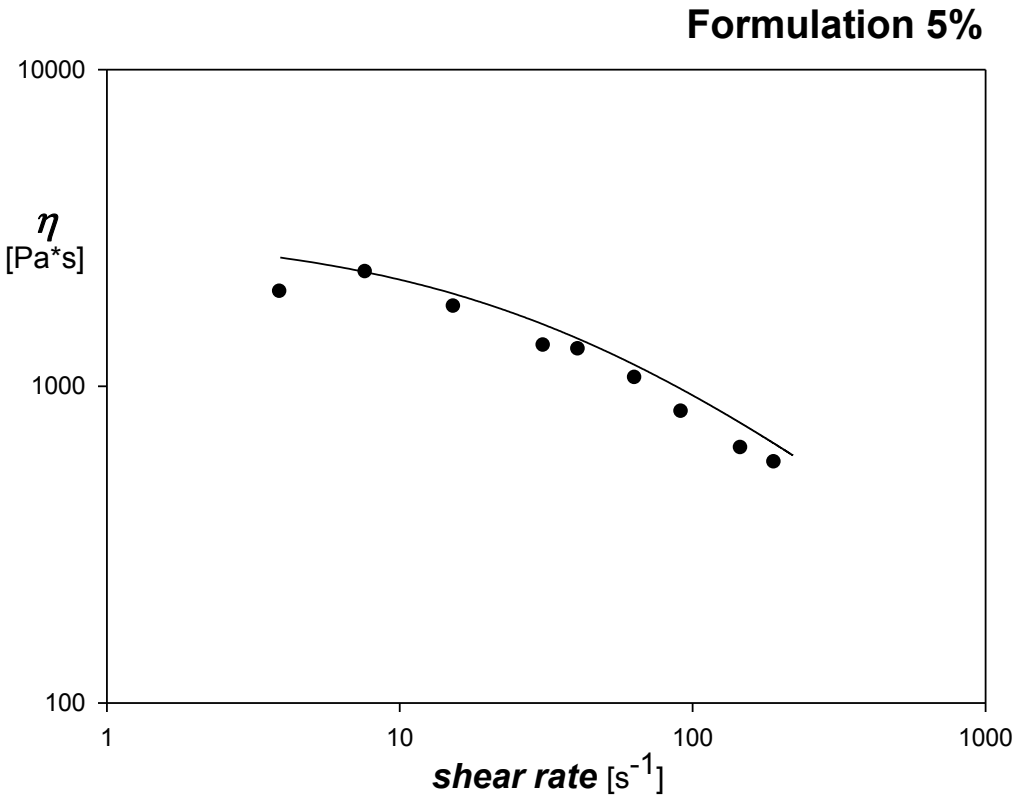


*Figure 5.58: Interpolating curve for the 5% formulation*

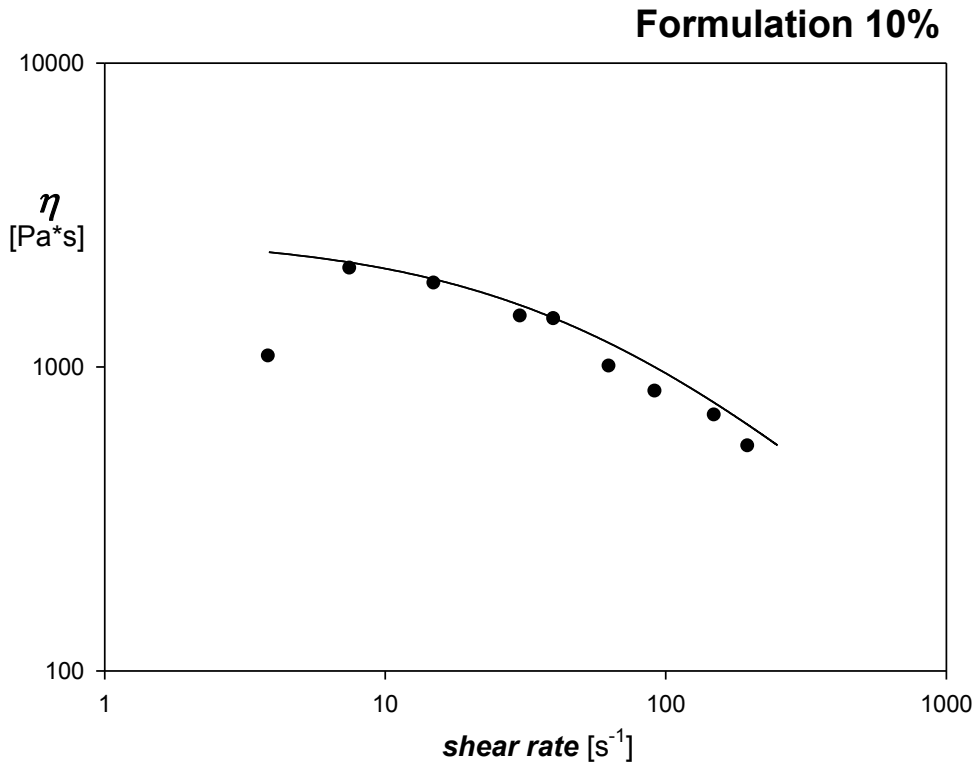


*Figure 5.59: Interpolating curve for the 10% formulation*

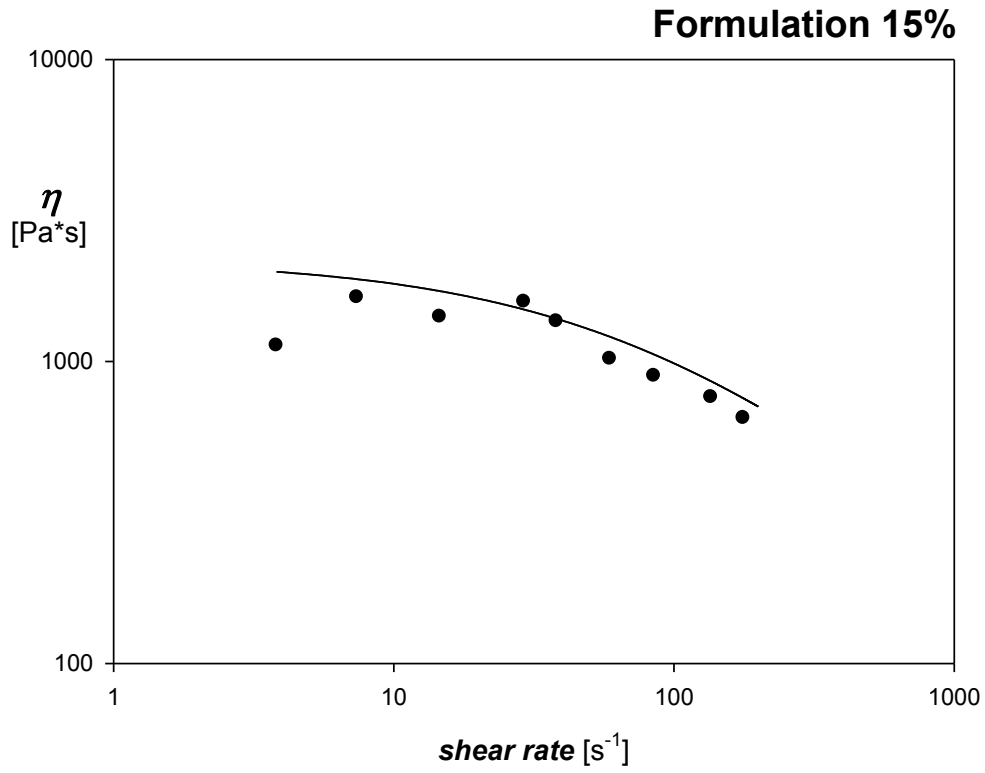


*Figure 5.60: Interpolating curve for the 15% formulation*

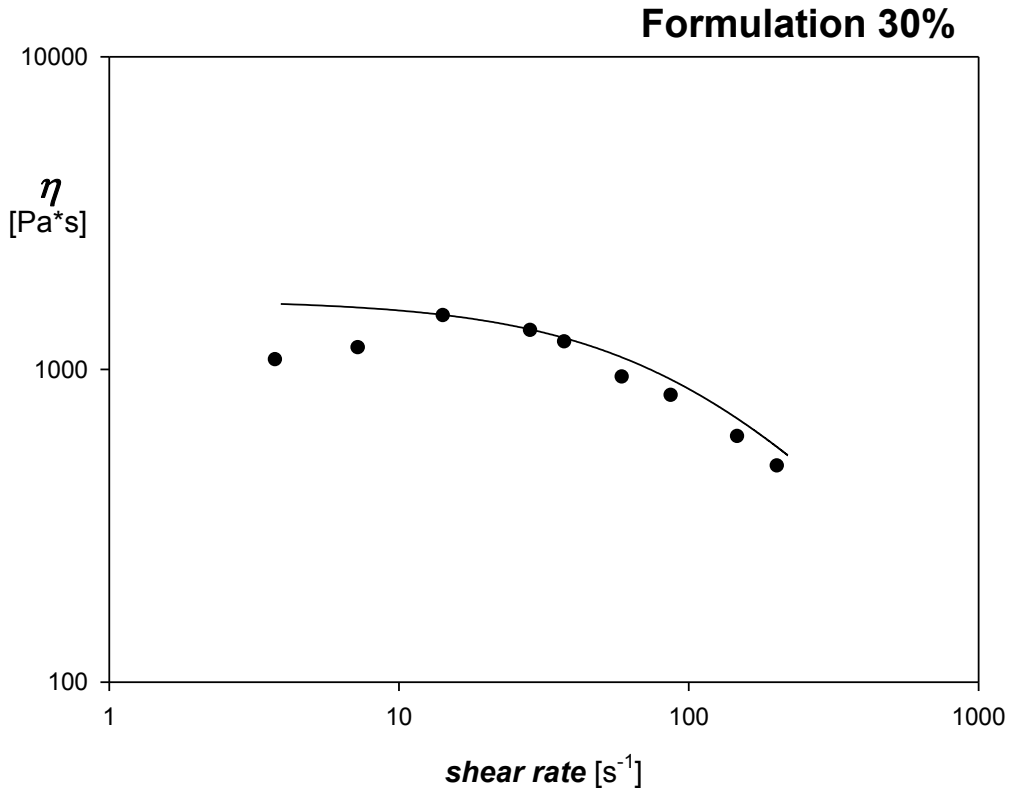


*Figure 5.61: Interpolating curve for the 30% formulation*

In figure 5.62 all interpolation curves are shown; the curve of the two standard formulations are also reported for comparison.

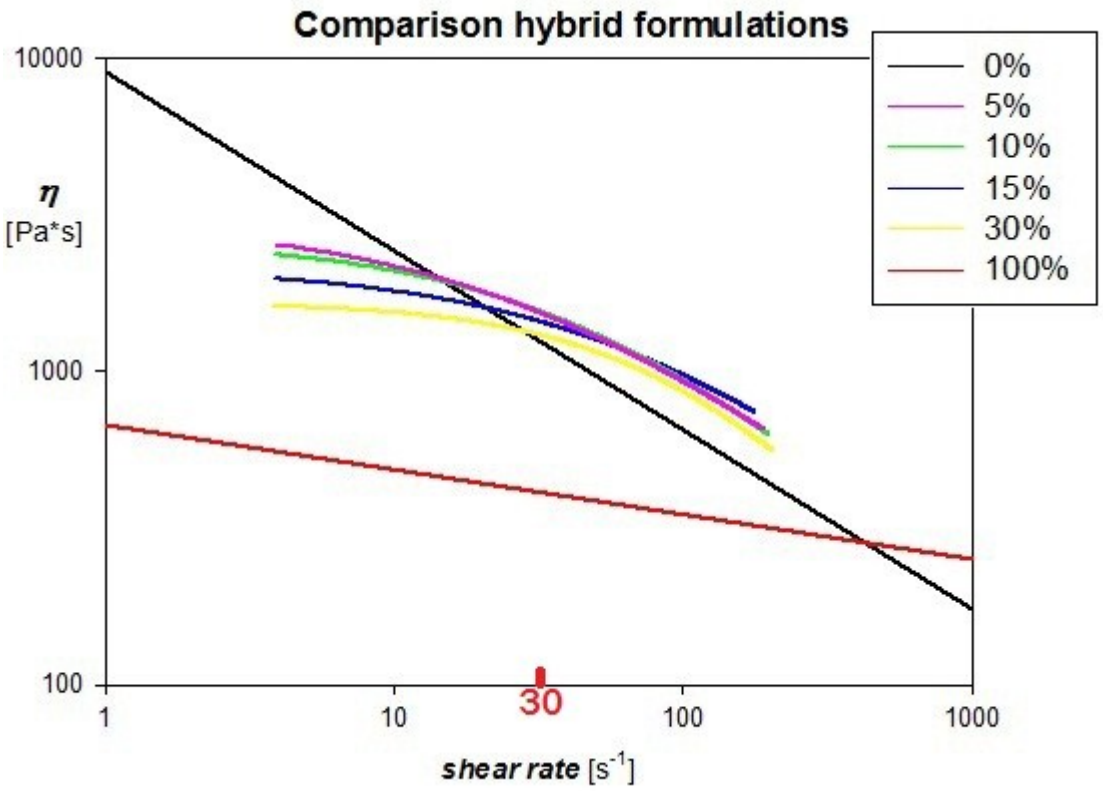


*Figure 5.62: Comparison between the hybrid and standard formulations*

The addition of calcium-sulfoaluminate cement clearly modifies the rheological behaviour of this kind of formulations. In particular, the graph in figure 5.59 can be divided in two regions: the zone with $\dot{\gamma}$ <30$s^{-1}$ shows a synergic effect between the two cement. Apart from a viscosity decrease, the presence of calcium-sulfoaluminate cement determine the appearance of a plateau. In the second region, with $\dot{\gamma}$ >30$s^{-1}$, an increase of viscosity is visible with respect to the formulation A (all Portland cement). The change in the curve slope observable in this region is typical of a pseudo-plastic behaviour. Another important consideration regards the fact that in the first region (low shear rate) the calcium-sulfoaluminate cement strongly influences the viscosity value of the formulation: the viscosity decreases with the increase of the calcium-sulfoaluminate cement content. The latter seems to act like a "lubricant" in the formulation. This is an important score

because during the extrusion process, which involves shear rates in the range of 4-5 $s^{-1}$ to 35-40 $s^{-1}$, a viscosity decrease can lead to a decrease of the strength necessary to push the mixture through the die. This results in a lowering of the process costs.

## 5.6 *Conclusions*

Some rheological experiments have been performed on two extremely different kinds of samples: the first category is represented by some aqueous solutions containing RMs and SPs, while the second category is represented by the cement doughs obtained mixing cement and other materials to the same RMs and SPs. The SPs used in these experiments belonged to two different classifications: metacrylics and acrylics. A rheological study on the neutral water and limewater solution has been first performed evidencing a drastic decrease of viscosity trespassing a stress threshold in the stress sweep tests when the SPs are added to the solution. In this case the only exception seems to be represented by the acrylic SPs when they are added to the limewater solutions. As explained above, this effect is very probably due to a sort of instability introduced in the solution by the addition of the SPs. The temperature ramp tests have instead evidenced another peculiar behaviour of these solutions: a sharp decrease of G' and G" values have been noted trespassing a certain value of temperature when the SPs is added to the solutions. This effect can be due to a micro-precipitation of the cellulose derivatives induced by a lower affinity of this latter with water at high temperatures in presence of the SP. Also in this case, some exceptions are represented by few solutions containing acrylic SPs in alkaline environment. Further experiments with a pHmeter on these solutions have evidenced that the carboxylic groups of the acrylic SPs are more acid than in the methacrylic SPs (with the same esterification rate) for inductive effect, so they are more available to establish interactions with the positive charged ions present in the solution. This ionic interaction is probably responsible for the different rheological behaviour of solutions containing acrylic SPs in limewater. The neutral water and the limewater solutions without SPs show in any case very similar rheological behaviours.

The situation seemed to change instead in the following experiments when a sulphate ion addition has been operated on the same solutions. This addition is aimed to better simulate the chemical environment of the cement formulations: three different sulphate concentrations (30 mM, 100 mM and 200 mM) have been prepared in order to simulate, respectively, low-sulphated cement,

medium-sulphated cement and high-sulphated cement. With this modification, in the temperature ramp test a drastic G' and G" value decrease has been observed also for the solution without SPs. The fall phenomenon is any case visible also for all the other solutions, either in the stress sweep tests than in the dynamical temperature ramp tests. The fall order 100 mM→200 mM→30 mM (considering the stress/temperature increasing) was the same in most of the performed experiments and for this reason it seems more than a randomness, but the data collected are not enough to suggest an exhaustive explanation. The clear concept is that the addition of sulphate ions leads to some visible changes in the aqueous solution rheological behaviour.

A clear interpretation for all these phenomena has not been found yet but further investigations (also involving complementary experimental methods or analysis different from a rheological investigation) could be aimed at better understanding the causes of the observed behaviours.

Some tests have also been performed in the CTG-Italcementi Group laboratories to study the rheology of the cement-based mixtures prepared with the same additives. For these tests a die rheometer has been used and the results obtained have been plotted in comparison with the rheological curves obtained from the aqueous solutions. The comparison has evidenced that to make a full forecast of the rheological behaviour of the cement doughs is not completely possible starting from the study of the aqueous solutions. This can be due essentially to two reasons: 1) the cement powder presence and its hydration reactions, together with the presence of other materials, has an effect on the viscosity of the formulation which is not negligible; 2) the interaction RM-SP can differ substantially from the interaction RM-SP-Cement and can lead to unexpected phenomena.

Anyway all the preliminary work about these systems can be effectively used to better formulate the mixtures for the extrusion process. Some experiments have been performed finally on several formulations mixing two different cements: a 52,5R Portland cement and a calcium-sulfoaluminate cement. With this aim, five different substitution concentrations (of calcium-sulfoaluminate cement on the total cement amount) have been experimented: 5%, 10%, 15%, 30% and 50%. The latter has not been tested because its hardening time was too short to allow a perfect mixing and accurate measurements. To have standards for comparison, two formulations have been also prepared with, respectively, 100% Portland cement (which obviously corresponds to 0% calcium-sulfoaluminate cement) and 100% calcium-sulfoaluminate cement. Both standard formulations have shown a typical pseudo-plastic behaviour, which can be modelled according to a power law. Moreover, in the range of shear rate explored, the formulation with calcium-sulfoaluminate cement tends to

behave like a Newtonian fluid. The study of the hybrid formulations, modelled according to the Ellis model, has revealed that their rheological properties are strongly influenced by the presence of the calcium-sulfoaluminate cement. The viscosity values at low shear rates are radically different from the viscosity of the 0% formulation and they tends to be lower and lower with increasing the calcium-sulfoaluminate cement content. The presence of the latter leads also to a change in the qualitative trend of the curve: the appearance of a Newtonian plateau is visible for all hybrid formulations. A sort of “lubricant effect” has so been observed for the calcium-sulfoaluminate cement at low-medium shear rates. This is very important from a practical point of view because it allows to optimize the hybrid formulations in order to lower the cost of the extrusion process.

# *Appendix I*

## APPENDIX I: MEASURE METHOD WITH DIE RHEOMETER

The die rheometer used for the experiments is characterised by a rectangular section of depth $2\delta$ and width $W$. $L$ is the length of the die. If the width is much larger than the depth ($W>>\delta$), it is possible to ignore the tangential stresses in the transversal direction, because the stresses on the surfaces of sides $W$ and $L$ are dominant. Considering $y$ the vertical axis, the control volume is in this case a parallelepiped with base $W$x$L$ and height $dy$. The force balance in the motion direction is so given by equation a.

$$W dy\,(P_0 - P_L) + WL\boldsymbol{\sigma}|_{\boldsymbol{y}} - WL\boldsymbol{\sigma}|_{\boldsymbol{y+dy}} = 0 \qquad (a)$$

Dividing equation a by W, L and dy and taking the limit dy→0

$$\frac{d\sigma}{dy} - \frac{(P_0 - P_L)}{L} = 0 \qquad (b)$$

Integration of equation b gives:

$$\sigma = \frac{\Delta P}{L} y + C_1 \qquad (c)$$

with $C_1$ null for symmetry. Introducing the Newton law it becomes

$$-\frac{dv}{dy} = \frac{\Delta P}{L}\frac{y}{\eta} \qquad (d)$$

which integrated with the condition of adherence at the wall gives a parabolic profile of velocity (equation e)

$$v = \frac{\Delta P}{2\eta L}\delta^2\left(1 - \frac{y^2}{\delta^2}\right) \qquad (e)$$

The flow rate is obtained from the following integration (equation f)

$$Q = 2\int_0^{\delta} vW dy = \frac{2W\delta^3}{3L}\frac{\Delta P}{\eta} \qquad (f)$$

In the case of the rectangular section, the apparent shear rate can be obtained by combining together equations d and f

$$\dot{\gamma}_a = -\left.\frac{dv}{dy}\right|_{\delta} = \frac{\Delta P}{L}\frac{\delta}{\eta} = \frac{3Q}{2W\delta^2} \qquad (g)$$

and the wall stress on the side is given by equation h

$$\sigma_w = \frac{\Delta P\delta}{L} \qquad (h)$$

So, finally, the viscosity for a Newtonian fluid is obtainable simply through the ratio between $\sigma_w/\dot{\gamma}_a$. In the die rheometer the stress, and also the shear rate, vary along the direction perpendicular to the motion. So for non-Newtonian fluids, which exhibit a viscosity dependent upon the shear rate, the fluid will respond to the flow changing its viscosity continuously. In this case, the evaluation of the viscosity can still be possible according to the "Mooney-Rabinowitsch method". This method takes origin from the consideration that, if it is possible to determine the correspondent value of shear rate for each value of the stress on the pipe wall, the viscosity can be calculated as

the ratio of these two variables. To perform many measurements on different values of flow is so necessary.

Considering the rectangular section, the flow Q is defined by equation i

$$Q = \int_0^{\delta} 2Wv(y)dy \qquad (i)$$

Integrating and exploiting the adherence condition on the pipe side, equation l is obtained

$$Q = -2W\int_0^{\delta} y\frac{dv}{dy}dy = 2W\int_0^{\delta} y\dot{\gamma}(y)dy \qquad (l)$$

Assuming a one-to-one correspondence between the tangential stress and the shear rate, equation l can be write also as

$$Q = \frac{2W\delta}{\sigma_w}\int_0^{\sigma_w} \sigma\dot{\gamma}(\sigma)d\sigma \qquad (m)$$

On the base of definition of the apparent shear rate, is now possible to write equation n

$$\frac{3Q}{2W\delta^2} = \dot{\gamma}_a = \frac{3}{\delta\sigma_w}\int_0^{\sigma_w} \sigma\,\dot{\gamma}(\boldsymbol{\sigma})\boldsymbol{d\sigma} \qquad (\boldsymbol{n})$$

The result obtained can be suddenly used to calculate the viscosity of the fluid. Rewriting equation n as

$$\dot{\gamma}_a \sigma_w = \frac{3}{\delta} \int_0^{\sigma_w} \sigma \dot{\gamma}(\sigma) d\sigma \qquad (o)$$

and deriving respect to $\boldsymbol{\sigma}$ equation p is obtained

$$\dot{\gamma}_w = \frac{2}{3} \dot{\gamma}_a + \frac{1}{3} \sigma_w \frac{d\dot{\gamma}_a}{d\sigma_w} \qquad (p)$$

Placing

$$n = \frac{d\ ln\sigma_w}{d\ ln\dot{\gamma}_a} \qquad (q)$$

Equation p can be rewritten as

$$\dot{\gamma}_w = \dot{\gamma}_a \frac{2n+1}{3n} \qquad (r)$$

Apart from the mathematical complexity, the practical procedure to determine the viscosity with the Mooney-Rabinowitsch correction is the following:

- Several measures of **Δ**P with different flow rates should be performed. This procedure allows to determine the stress on the pipe wall for different values of the apparent shear rate;
- On a log-log graph the values so obtained must be plotted as a function of $\dot{\gamma}_a$; in this way for a given value of the apparent shear rate the slope of the line corresponds to the parameter *n*;
- From the value of *n* and of the apparent shear rate the value of the effective shear rate can be calculated using the equation r and, accordingly, the viscosity from the ratio $\sigma_w/\dot{\gamma}_a$.

- Repeating the last two steps for different values of $\dot{\gamma}_a$ the curve of viscosity vs. shear rate can be finally obtained.

As mentioned in the paragraph 3.3, there is a way to consider the entrance losses according to equation s.

$$\Delta P_{tot} = \Delta P_{ent} + \left(\frac{\Delta P}{L}\right)_{cap} L \qquad (s)$$

where the ratio $(\Delta P/L)_{cap}$ is the pressure drop for unit length of the pipe. Equation t expresses mathematically the known fact that the pressure drop increases linearly with the pipe length, but also that when this length tends to zero it is any case necessary to spend a certain quantity of energy which is equal to the entrance losses. Equation t is valid either for Newtonian than for non-Newtonian fluids. In any case, fixing the flow and the geometry of the system, the pressure drop at the entrance will be independent on the length of the pipe. The "Bagley method" consists then in performing, for each fixed flow, different measures with pipes of different lengths. Then, plotting the $\Delta P$ as a function of the pipe length, data should be interpolated by a straight line. Extrapolating to length zero, the ordinate at the origin gives the value of $\Delta P_{ent}$. The slope of the curve instead gives directly the value of $(\Delta P/L)_{cap}$ for each flow. The important thing to remember is that the relation expressed by equation t is valid only if the entrance effects run out rapidly inside the pipe. This may not be true when the residence time of the fluid in the capillary is lower than the characteristic time of the fluid (relaxation time). This means that the liquid suffers the conditions of transitory flow for a long part of the die. This phenomenon gives a non-linearity in the Bagley plot. For this and other complications, the application of the Bagley method is not always exploitable.

# *Appendix II*

## APPENDIX II: MEASURE METHOD WITH VISKOMAT

The appendix here described is relative to a procedure developed for the CTG-Italcementi Group laboratories.

When a Newtonian flow is used in any rotational rheometer, a linearity between the torque and the rotation speed occurs. This result, which comes from the linearity of the equation of motion at vanishing Reynolds number for a Newtonian fluid, is general, and does not depend on the particular geometry used. As a consequence, once the rheometer is calibrated by measurements of torque vs. rotation speed for a fluid of known viscosity, the viscosity of any other Newtonian fluid is immediately calculated from the knowledge of the calibration constant of the rheometer. In mathematical terms this means that the (Newtonian) universal relationship for a rotational rheometer can be written as:

$$M = K\eta\Omega \tag{a}$$

where M is the torque, Ω is the angular velocity, η is the fluid viscosity. K is the rheometer calibration constant.

The rheometer calibration is performed by the following steps:

- given a Newtonian fluid of known viscosity, $\eta_0$, the torque $M_0$ developed in the rheometer under an applied angular speed $\Omega_0$ is measured;
- The universal calibration constant is calculated as:

$$K = \frac{M_0}{\eta_0\Omega_0} \tag{b}$$

- once the calibration constant is known the viscosity of any fluid can be determined from the simultaneous measurement of torque and rotation speed:
-

$$\eta = \frac{M}{K\Omega} \tag{c}$$

In the case of a non-Newtonian fluid the above linearity is no longer satisfied. For this reason, the viscosity of the fluid cannot be simply obtained from the Newtonian calibration constant. In fact, the stress field is a non-linear function of the rotation speed and it is also strictly dependent upon the details of the rheometer geometry.

In order to overcome this problem, the first step is to approximate the complex geometry of the Viskomat rheometer to a simpler one, by a "reduction" procedure. In particular, in this section it will be shown that any rotating geometry can be reduced to a coaxial cylinder geometry. After such a reduction, the viscosity can be obtained by applying the standard relations that are available for this geometry.

The starting point of this procedure is the known formula that relates the angular velocity to the torque for a Newtonian fluid in the coaxial cylinder geometry:

$$\Omega = \frac{M}{4\pi L\eta}\left(\frac{1}{R_1^2} - \frac{1}{R_2^2}\right) \tag{d}$$

The geometry of a rheometer like the Viskomat is always constituted by an outer cup of radius $R_2$ and a complex inner propeller of height L. For this reason, the reduction procedure aims at determining the equivalent inner radius $R_1$. To this end, equation c is rewritten as:

$$R_1 = R_2\sqrt{\frac{1}{1 + \frac{4\pi L\eta\Omega R_2^2}{M}}} \tag{e}$$

From equation e it is apparent that the reduction procedure requires to find the $R_1$ value that determines, for a given angular speed and torque measured with the Viskomat complex geometry, the same (known) viscosity of a Newtonian fluid.

In order to clarify the steps of the reduction procedure, the above concepts can be applied to the case of a square propeller, whose geometry is reported in Figure A.

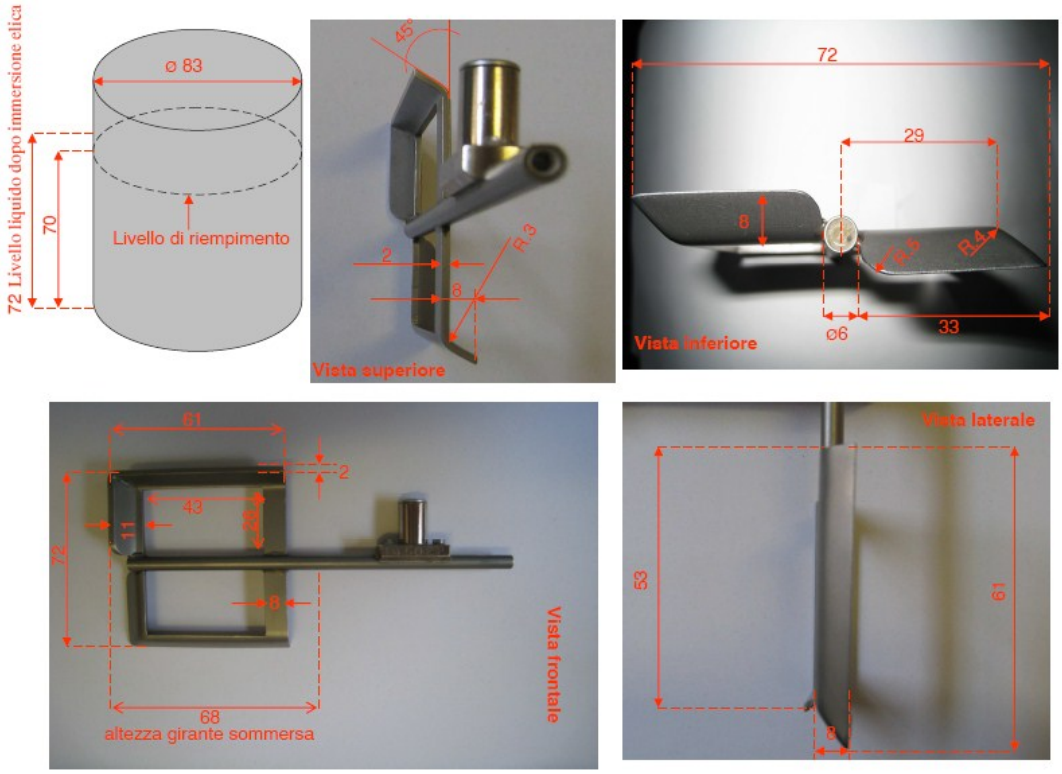


*Figure A*

In this specific case, the radius of the outer cup is $R_2$=0.0415 m and the height of the submerged part of the propeller is $L$=0.061 m. These geometrical data can be inserted in equation e to determine the equivalent inner radius $R_2$. Inserting equation a into equation e the direct relation between the rheometer constant and the equivalent inner radius is obtained as:

$$R_1 = R_2 \sqrt{\frac{1}{1+\frac{4\pi L R_2^2}{K}}} \qquad \text{(f)}$$

For the case of the square propeller of Figure A, the equivalent inner radius has been calculated from measurements performed on three Newtonian silicon oils of different viscosity. For each fluid,

first the calibration constant has been calculated from torque and angular velocity experimental data (equation b). Then, the equivalent inner radius has been obtained from equation f. The results of the procedure are reported in Table 1.

| **Oil** | $M_0$ (N·m) | $K\eta$( N·m/s) | $\eta$(N/m²s) | K(m²) | $R_1$ (m) |
|---|---|---|---|---|---|
| 12000cs test 1 | $1.37 \cdot 10^{-4}$ | $2.25 \cdot 10^{-2}$ | 13.9 | $1.62 \cdot 10^{-3}$ | 0.0308 |
| 5000cs test 1 | $5.55 \cdot 10^{-5}$ | $9.13 \cdot 10^{-3}$ | 5.70 | $1.60 \cdot 10^{-3}$ | 0.0307 |
| 1000cs test 1 | $4.75 \cdot 10^{-4}$ | $1.81 \cdot 10^{-3}$ | 1.13 | $1.61 \cdot 10^{-3}$ | 0.0308 |

*Table 1*

Two relevant comments are in order:

- the values of the inner radii obtained with different oils are very close to each other, indicating the robustness of the procedure;
- the value of the equivalent inner radius, $R_1 \cong 0.0308$ m, is slightly smaller than the actual width of the square propeller, which is 0.036 m (see Figure A). This difference, which cannot be predicted in advance, is related to the particular geometry of the propeller.

Once the inner equivalent radius is known, equation d can now be used for generating the viscosity curve of a fluid of unknown geometry. In particular, by assuming that the equation for a Newtonian fluid in a coaxial cylinder geometry can be used also for a non-Newtonian fluid, the apparent shear rate at the so-called average radius is calculated as:

$$\dot{\gamma}_{app}(\bar{R}) = \frac{2\Omega R_1^2 R_2^2}{R_2^2 - R_1^2} \frac{1}{\overline{R^2}} = \frac{2\Omega R_1 R_2}{R_2^2 - R_1^2} \qquad \text{(g)}$$

On the other hand, the shear stress at the same radius value is obtained as:

$$\sigma\left(\bar{R}\right) = \frac{M}{2\pi L R_1 R_2} \tag{h}$$

Finally, the viscosity is calculated as the ratio between equation h and equation g.

## References


[1] Harold F.W. Taylor, *Cement Chemistry*, Academic Press, **1990**

[2] Vito Alunno Rosetti, *Il calcestruzzo: Materiali e Tecnologia*, Mc Graw-Hill, **1995**

[3] J.B. Newman, B.S. Choo, *Advanced concrete technology*, Butterworth-Heinemann Editors, Oxford **2003**

[4] M. Collepardi, *Scienza e tecnologia del calcestruzzo*, 145-152, Hoepli, **1991**

[5] K. Luke, G.Luke, *Effect of sucrose on retardation of Portland cement*, Adv.Cem. Res. 12 (**2000**) 9-18

[6] A. Peschard, A. Govin, P. Grosseau, B.Guilhot, R. Guyonnet, *Effect of polysaccharides on the hydration of cement paste at early ages*, Cem. Concr. Res. 34 (**2004**) 2153-2158

[7] M. Collepardi, *Scienza e tecnologia del calcestruzzo*, 341-358, Hoepli, **1991**

[8] CM. Neubauer, M. Yang, HM. Jennings, *Interparticle potential and sedimentation behaviour of cement suspensions: Effects of admixtures*, Advanced cement based materials 8 (**1998**) 17-27

[9] C. Aldea, S. Marikunte, S.P. Shah, *Extruded fiber reinforced cement pressure pipe*, **1998**

[10] G.L. Guerrini, *Applications of high-performance fiber reinforced cement-based extrudate*, Appl. Compos. Mater. (**2002**), *35*, 530-536

[11] Stefano Turri, *Vernici: materiali, tecnologie e proprietà*, casa editrice Ambrosiana, **2007**

[12] T.C. Patton, *Paint Flow and Pigment Dispersion: A rheological Approach to Coating and Ink Technology*, sec. edition, Wiley&Sons, New York **1979**

[13] H.A. Barnes, J.F. Hutton, K. Walters, *An introduction to rheology*, Elsevier, Amsterdam **1989**

[14] C.W. Macosko, *Rheology: Principles, Measurements and Applications (advances in interfacial engineering)*, Wiley-VCH **1994**

[15] R. Gupta, *Polymer and Composite Rheology*, sec. edition, Marcel Dekker, New York **2000**

[16] Ronald G. Larson, *The structure and rheology of complex fluids*, Oxford University Press **1999**

[17] L. Lorton, B.K. Moore, M.L. Swartz, R.W. Phillips, *Rheology of luting cements*, Journal of Dental Research 59 (**1980**) 1486-1492

[18] B. Caufin, A. Papo, *The influence of the hydration process on the rheology of cement pastes*, Zement-Kalk-Gips 39 (**1986**) 389-391

[19] G.H. Tattersall, Rheology of fresh cement and concrete, British Ceramic Transactions and Journal 89 (**1990**)

[20] M.A. Schultz, L.J. Struble, *Use of oscillatory shear to study flow behaviour of fresh cement paste*, Cement and Concrete Research 23 (**1993**) 273-282

[21] B.H. Min, L. Erwin, H.M. Jennings, *Rheological behaviour of fresh cement paste as measured by squeeze flow*, Journal of Materials Science 29 (**1994**) 1374-1381

[22] M. Yang, H.M. Jennings, *Influences of mixing methods on the microstructure and rheological behaviour of cement paste*, Advanced cement Based Materials 2 (**1995**) 70-78

[23] L.J. Struble, G.K. Sun, *Viscosity of Portland-cement paste as a function of concentration*, Advanced Cement Based Materials 2 (**2005**) 62-69

[24] L.J. Struble, W.G. Lei, *Rheological changes associated with setting of cement paste*, Advanced Cement Based Materials 2 (**1995**) 224-230

[25] M.L. Allan, L.E. Kukacka, *Comparison between slag- and silica fume-modified grouts*, Aci Materials Journal 93 (**1996**) 559-568

[26] N.B. Ur'ev, R.L. Baru et al., *Rheology and thixotropy of cement-water suspensions in the presence of superplasticizers*, Colloid Journal 59 (**1997**) 773-779

[27] X. Zhang, J.H. Han, *The effect of ultra-fine admixtures on the rheological property of cement paste*, Cement and Concrete Research 30 (**2000**) 827-830

[28] S. Perret, D. Palardy, G. Ballivy, *Rheological behaviour and setting time of microfine cement-based grouts*, Aci Materials Journal 97 (**2000**) 472-478

[29] C.F. Ferraris, K.H. Obla, R. Hill, *The influence of mineral admixtures on the rheology of cement pastes and concrete*, Cement and Concrete Research 31 (**2001**) 245-255

[30] Rastoul K. et al., *A rheological study of associating polymer-particle interactions in tricalcium silicate pastes*, Polymer International 52 (**2003**) 633-637

[31] L.J. Struble, Q.Y. Jiang, *Effects of air entrainment on rheology*, Aci Materials Journal 101 (**2004**) 448-456

[32] T.H. Phan, M. Chaouche, *Rheology and stability of self-compacting concrete cement pastes*, Applied Rheology 15 (**2005**) 336-343

[33] N. Roussel, *Steady and transient flow behaviour of fresh cement pastes*, Cement and Concrete Research 35 (**2005**) 1656-1664

[34] A. Chougnet, A. Audibert, M. Moan, *Linear and non-linear rheological behaviour and silica suspensions. Effect of polymer addition*, Rheologica Acta 46 (**2007**) 793-802

[35] H. Vikan, H. Justnes, F. Winnefeld, R. Figi, *Correlating cement characteristics with rheology of paste*, Cement and Concrete Research 37 (**2007**) 1502-1511

[36] N. Roussel, *Rheology of fresh concrete: from measurements to predictions of casting processes*, Materials and Structure 40 (**2007**) 1001-1012

[37] C.F. Lu, *Latex paint rheology and performance properties*, Industrial & Engineering Chemistry Product Research and Development 24 (**1985**) 412-417

[38] K.G. Shaw, D.P. Leipold, *New cellulosic polymers for rheology control of latex paints*, Journal of Coating Technology 57 (**1985**) 63-72

[39] J.E. Hall, P. Hodgson, L. Krivanek, P. Malizia, *Influence of rheology modifiers on the performance-characteristics of latex paints*, Journal of Coatings Technology 58 (**1986**) 65-73

[40] P. Fearnleywhittingstall, *Paint rheology*, Surface Coating International 74 (**1991**) 360

[41] T.L. Maver, *Rheology modifiers – Modeling their performance in high gloss paints*, Journal of Coating Technology 64 (**1992**) 45-58

[42] J. Prideaux, *Rheology modifiers and thickeners in aqueous paints*, Surface Coating International 76 (**1993**) 177-185

[43] O. Cohu, A. Magnin, *The levelling of thixotropic coatings*, Progress in Organic Coatings 28 (**1996**) 89-96

[44] O. Cohu, A. Magnin, *Rheology and flow of paints in roll coating process*, Surface Coating International 80 (**1997**) 102-110

[45] A.J. Reuvers, *Control of rheology of water-borne paint using associative thickeners*, Progress in Organic Coatings 35 (**1999**) 171-181

[46] C. Palmonari, A. Tenaglia et al., *Rheological study to test a new formulation of silk screen paint*, Boletin de la Sociedad Espanola de Ceramica y Vidrio 39 (**2000**) 627-630

[47] F.V. Lopez, M. Rosen, *Rheological effects in roll coating of paints*, Latin American Applied Research 32 (**2002**) 247-252

[48] J. Hajas, A. Woocker, *Modified ureas: An interesting opportunity to control rheology of liquid coatings*, Macromolecular Symposia 187 (**2002**) 215-224

[49] A.J. Breugem, F. Bouchama, G.J.M. Koper, *Diffusing wave spectroscopy: A novel rheological method for drying paint films*, Surface Coating International 88 (**2005**) 135-138

[50] A. Maestro, C. Gonzalez, J.M. Gutierrez, *Interaction of surfactants with thickeners used in waterborne paints: A rheological study*, Journal of Colloids and Interface Science 288 (**2005**) 597-605

[51] D. Bhattacharya, K. Seo, L.T. Germinario et al., *Novel techniques to investigate the impact of cellulose esters on the rheological properties and appearance in automotive basecoat systems*, Journal of Coating Technology and Research 4 (**2007**) 139-150

[52] Q. Yang, X.H. Yang, P. Wang, W.L. Zhu, X.Y. Chen, *The viscosity properties of zync-rich coating from sodium silicate solution modified with aluminium chloride*, Pigment & Resin Technology 38 (**2009**) 153-158

[53] L. de Viguerie, G. Ducouret et al., *Historical evolution of oil painting media: A rheological study*, Comptes Rendus Physique 10 (**2009**) 612-621

[54] P.Dumitri, I. Jitaru, *The influence of rheology modifiers and dispersing agents on the quality of water-based decorative paints*, Revista de Chimie 61 (**2010**) 651-656

[55] T. Ueda, M. Iga, *Thin film rheology of the paint formation process and the multilayer paint film*, Nihon Reoroji Gakkaishi 39 (**2011**) 37-42

[56] B.Baldewa, Y.M. Joshi, *Thixotropy and physical aging in acrylic emulsion paints*, Polymer Engineering and Science 51 (**2011**) 2085-2092

[57] W.H. Tatton, E.W. Drew, *Industrial paint application*, 2nd ed., Newnes-Butterworths, London **1971**

[58] R. Lambourne, T.A. Strivens, *Paint and surface coating: Theory and practice*, Woodhead Publishing Cambridge (UK) **1999**

[59] E. Gutoff, E. Cohen, *Coating and Drying Defects*, Wiley&Sons, New York **1995**

[60] AAVV., *Paint and Coating Testing Manual*, J.V. Koleske, ASTM Philadelphia **1995**

[61] Vigouret M, Rinaudo M, Desbrieres J, *Thermogelation of methylcellulose in aqueous solutions*, Journal de Chimie et de Physico-Chimie Biologique 93 (**1996**) 858-869

[62] Sarkar N, *Thermal gelation of methyl and hydroxypropyl methylcellulose*, Journal of Applied Polymer Science 24 (**1979**) 1073-1087

[63] Haque A., Morris E., *Thermogelation of methylcellulose: Molecular structure and processes*, Carbohydrate Polymers 22 (**1993**), 161-173

[64] Doelker E, *Cellulose derivates,* Advances in Polymer Science 107, (1993) 199-265

[65] Owen SR, Tung MA, Paulson A, *Thermorheological studies of food polymer dispersion*, Journal of food engineering 16 (**1992**) 39-53

[66] Ford JL, *Thermal analysis of hydroxypropylmethylcellulose: powders, gels, and matrix tablets*, International Journal of Pharmaceutics 179 (**1999**) 209-228

[67] Sarkar N., Walker NC, *Hydration and Dehydration properties of MC and HPMC*, Carbohydrate Polymers 26 (1995), 195-203

[68] Sarkar N, Walker NC, *Hydration and Dehydration properties of Methylcellulose and Hydroxypropylcellulose*, Carbohydrate Polymers 27 (**1995**), 177-185

[69] Hussain S, Keary C, Craig D, *A thermorheological investigation into the gelation and phase separation of hydroxypropyl methylcellulose aqueous systems*, Polymer 43, (**2002**) 5623-5628

[70] J. Pourchez, A. Peschard, P. Grosseau, R. Guyonnet, B. Guilhot, F. Vallèe, *HPMC and HEMC: influence on cement hydration*, Cement and Concrete Research 36 (**2006**) 288-294

[71] J. Pourchez, P. Grosseau, R. Guyonnet, B. Ruot, *HEC influence on cement hydration measured by conductometry*, Cement and Concrete Research 36 (**2006**) 1777–1780

[72] M. Saric-Coric, H. Khayat, A. Tagnit-Hamou, *Performance characteristics of cement grouts made with various combinations of high-range water reducer and cellulose-based viscosity modifier*, Elsevier science 33 (**2003**) 1999-2008

[73] A. Zingg, F. Winnefeld, L. Holzer, *Adsorption of polyelectrolytes and its influence on the rheology, zeta potential, and microstructure of various cement and hydrate phases*, Journal of Colloid and Interface Science 323 (**2008**) 301-312

[74] I. Papayianni, G. Tsohos, N. Oikonomou, P. Mavria, *Influence of superplasticizer type and mix design parameters on the performance of them in concrete mixtures*, Cement and Concrete Composites 27 (**2005**) 217-222

[75] M. Palacios, F. Puertas, P. Bowen, *Effect of PCs superplasticizers on the rheological properties and hydration process of slag-blended cement pastes*, Journal of Material Science 44 (**2009**) 2714-2723

[76] Y.F. Houst et al., *Adsorption of superplasticizer admixtures on alkali-activated slag pastes* , Cement and Concrete Research 39 (**2009**) 670-677

[77] J. Golaszewski; J. Szwabowski, *Influence of superplasticizers on rheological behaviour of fresh cement mortars*, Cement and Concrete Research 34 (**2004**) 235-248

[78] Vikan H.; Justnes H.; Winnefeld F, Correlating cement characteristics with rheology of paste, Cement and Concrete Research 37 (**2007**) 1502-1511

[79] F.Winnefeld, S. Becker, J. Pakusch, *Effects of the molecular architecture of comb-shaped superplasticizers on their performance in cementitious systems*, Cement and Concrete Composite 29 (**2007**) 251-262

[80] A. Leemann, F. Winnefeld, *The effect of viscosity modifying agents on mortar and concrete*, Cement and Concrete Composite 29 (**2007**) 341-349

[81] A. Zingg, F. Winnefeld,L. Holzer, *Interaction of polycarboxylate-based superplasticizers with cements containing different $C_3A$ amounts*, Cement and Concrete Composites 31 (**2009**) 153-162

[82] C. Giraudeau, J.D.D. Lacaillaire, Z. Souguir, *Surface and Intercalation Chemistry of Polycarboxylate Copolymers in Cementitious Systems*, Journal of American Ceramic Society 92 (**2009**) 2471-2488

[83] R.J. Flatt , I. Schober, E. Raphael, *Conformation of Adsorbed Comb Copolymer Dispersants*, Langmuir 25 (**2009**) 845-855

[84] F. Ridi et al., *Hydration kinetics of tricalcium silicate in the presence of superplasticizers*, Phys. Chem. (**2003**) 1056-1071

[85] F. Ridi et. al., *Hydration process of cement in presence of a cellulosic additive. A calorimetry investigation*, Phys. Chem. (**2002**), 14727-14743

[86] F. Ridi, E. Fratini, S. Milani, P. Baglioni, *Near-infrared spectroscopy investigation of the water confined in tricalcium silicate pastes*, J. Phys. Chem. B **2006,** *110,* 16326-16331

[87] E. Fratini, S.H. Chen, P. Baglioni, M. C. Bellissent-Funel, *Quasi-elastic neutron scattering study of traslational dynamics of hydration water in tricalcium silicate*, J. Phys. Chem. B **2002,** *106,* 158-166

[88] F. Ridi et al., *Water confined in cement pastes as a probe of cement microstructure evolution*, J. Phys. Chem. B **2009,** *113,* 3080–3087

[89] J.J Thomas, H.M. Jennings, J.J. Chen, Journal of Physical Chemistry C 113 (**2009**) 4327-4334

[90] I. Pirazzoli et al., *The influence of superplasticizers on the first steps of tricalcium silicate hydration studied by NMR techniques*, Magnetic Resonance Imaging 23 (**2005**) 277–284

[91] F. Ridi, E. Fratini, P. Baglioni, *Cement: A two thousand year old nano-colloid*, Journal of Colloid and Interface Science 357 (**2011**) 255-264

[92] Z. Li, B. Mu, *Rheology behaviour of short fiber-reinforced cement-based extrudates,* Journal of Engineering Mechanics (**1999**) 530-536

[93] Z. Li, B. Mu, *Rheological properties of cement-based extrudates with fibers*, Journal of American Ceramic Society 84 (**2001**) 2343-2350

[94] J.L. White, A.B. Metzner, Journal of Applied Polymer Science 7 (**1963**) 1867-1889

[95] R. Alfani, N. Grizzuti et al., *The use of capillarity rheometer for the rheological evaluation of extrudable cement based material*, Rheology acta (**2007**), *46*, 703-799

[96] R. Alfani, Guerrini G.L., *Rheological test methods for the characterization of extrudable cement-based materials – A review*, Materials and Structures (**2005**), 38, 239-247